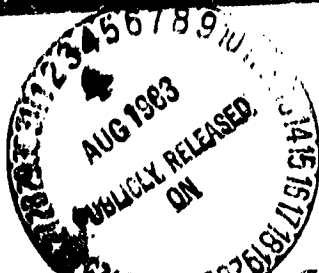


6 00167 7765

RECEIVED  
AUG 10 1983  
NASA ST FACILITY  
ASSESS

ORIGINAL PAGE IS  
OF POOR QUALITY



N83-30402

(NASA-CR-165760) NACELLE AERODYNAMIC AND  
INERTIAL LOADS (NAIL) PROJECT Test Report,  
Oct. 1979 - Nov. 1980 (Boeing Commercial  
Airplane Co., Seattle) 352 p HC A16/Mr AU1

Unclassified  
CSCL 01C G3/05 12625

## ERRATA

p. viii, line 6

change to Wing Upper Surface

p. 2, lines 1 through 4

delete; add "During the IPSA portion of the NAIL program, surface static pressures were measured as follows on both the inboard and outboard engine installations:

- Internal and external inlet surfaces
- Engine core cowling
- Pylon
- Neighboring upper and lower wing surfaces

A data base at these locations was acquired at Mach numbers 0.77, 0.80, 0.86, and 0.91 through three test flights."

p. 3, line 7

change NASI to NASI

p. 6, line 11

change 499 to 557 and 322 to 380

p. 9, line 26

change  $(W_A \sqrt{\theta_{T_2}/\delta_{T_2}})$  to  $W_A \sqrt{\theta_{T_2}/\delta_{T_2}}$

p. 10, insert

$\infty$  free stream value

$\alpha$  angle of attack

$\theta_{T_2}$  total temperature ratio at engine face,  
 $T_{T_2}/T_{SLS}$

$\rho$  air density, slug/ft<sup>3</sup>

$\theta$  circumferential position, degrees

$\delta_{T_2}$  total pressure ratio at engine face,  $P_{T_2}/P_{SLS}$

add SUBSCRIPTS after  $T_2$  and before  $\delta$

p. 10, line 20

change "pylon-core cowl intersection" to "pylon-fan cowl intersection"

p. 10, line 22

change "pylon-fan cowl intersection" to "pylon-core cowl intersection"

pp. 11 & 12, line 1

at top of photograph, obliterated callouts are  
WBL 809, 834, and 870, reading left to right

p. 16, figure 5

callouts reading from top to bottom in lower left-hand corner are  
Inboard aileron  
Trailing-edge flaps

p. 25, figure 9

In table for outboard engine (No. 4) change the Point T NAC STA value from 216.12 to 206.10

delete "Side View" from over bulleted items

In upper right hand corner, change "2°" callout to "2-deg pitch-up"

p. 28, line 2

change to "...up to 2 deg relative to the WRP (fig. 9)."

p. 28, line 10

change to "...WLT for each engine using distances given in figure 9."

p. 28, line 17

add after "...or. WBL 834.outboard."—"This reference nacelle station is labeled NAC STA in figure 9."

p. 29, table 4

In table, change 301.07 cm (118.53 in) to 301.056 cm (118.526 in)

under  $r_{EXT}/L_k$  (first part of table) change values to

0.2869

0.2859

0.2829

0.2812

0.2799

0.2781

0.2765

0.2747

0.2730

0.2708

0.2696

0.2662

0.2638

and in second column  $r_{EXT}/L_k$  change 0.2329 to 0.2330

p. 35, table 7

change callout M to G (upper left-hand corner)

change  $C_m = 206.080$  cm (81.134 in) to  $C_g = 206.080$  cm (81.134 in)

$X, Y = 0$  @ m to  $X, Y = 0$  at G

change first line of table to

$X/C_g \quad Y/C_g \quad Z/C_g$

p. 36, table 8

In INBOARD and OUTBOARD tables interchange  $Y/C_n$  and  $Z/C_n$  headings

- p. 37, table 9    in INBOARD and OUTBOARD tables interchange Y/C<sub>n</sub> and Z/C<sub>n</sub> headings
- p. 38a, b, table 10                                  replace with two new pages
- p. 39, table 11    delete 0.2750 and 0.4750 under WBL 445, UPPER and close up
- p. 41, table 13    change NAC WL 180 to NAC WL 155 and change NAC WL 155 to NAC WL 180
- p. 53, figure 21    change title to Accelerometer Installation (Thrust Link)
- p. 61, figure 33    line 14, add "Surge valve bleed position" in second column
- p. 69, line 8    change M<sub>C</sub> and V<sub>C</sub> to read M<sub>D</sub> and V<sub>D</sub>
- p. 73, table 19    replace
- p. 88, line 22    change 10 ft/s to 5 ft/s

#### APPENDIX A

- A-6, table A-2    delete Engine 4 callout and boxed data
- A-26, table A-22, line 4                                  change CONDITION 117, 1.5g to CONDITION 117, 1.6g
- A-28, table A-24, line 4                                  change CONDITION 121, 1.5g to CONDITION 121, 1.6g
- A-85, figure A-56    replace
- A-87, figure A-58    replace
- A-89, figure A-51    replace
- A-97, figure A-68    replace
- A-98, figure A-69    replace

#### APPENDIX B

- B-10, figure B-1    delete data point at 1.25 on 090-deg plot
- B-11, figure B-1    delete data point between 1.25 and 1.50 on 150-deg plot
- B-11, figure B-1    delete data points between 1.25 and 1.75

B-12, figure B-1                            delete data points between 1.25 and 1.75  
B-13, figure B-1                            delete data points between 1.00 and 1.50  
B-29, figure B-2                            delete data points between 1.25 and 1.75  
B-30, figure B-2                            delete data points between 1.25 and 1.50 on 090-deg plot  
    delete data points between 1.25 and 1.50 on 150-deg plot  
B-31, figure B-2                            delete data points between 1.50 and 1.75  
B-32, figure B-2                            delete data points between 1.00 and 1.75  
B-33, figure B-2                            delete data points between 1.00 and 1.75  
B-49, figure B-3                            delete data points between 1.25 and 1.75  
B-50; figure B-3                            delete data point at 1.25  
B-51, figure B-3                            delete data points between 1.00 and 1.50  
B-52, figure B-3                            delete data points between 1.25 and 1.75  
B-53, figure B-3                            delete data points between 1.00 and 1.75  
B-54, figure B-3                            delete data points between 1.00 and 1.75  
B-85 through B-87, figure B-5            delete local Mach = 0.0 data points  
B-89, figure B-5                            replace graph  
B-91, figure B-5                            WBL 870, replace graph  
B-101 through B-103, figure B-5        delete local Mach = 0.0 data points  
B-106, figure B-5                            WBL 870, replace graph  
B-116 through B-118, figure B-7        delete local Mach = 0.0 data points  
B-121, figure B-7                            WBL 870, replace graph  
B-135, figure B-8                            WBL 870, replace graph

MICROFICHE

Replaced entirely

# **NACELLE AERODYNAMIC AND INERTIAL LOADS (NAIL) PROJECT**

## **TEST REPORT**

**Contract NAS1-15325  
MAY 1981**

**BOEING COMMERCIAL AIRPLANE COMPANY**

## **FOREWORD**

This document constitutes the test report of work conducted under NASA contract NAS1-15325 from October 1979 through November 1980. The contract was managed by the NASA Energy Efficient Transport Office (EETPO), headed by Mr. R. V. Hood—a part of the Aircraft Energy Efficiency (ACEE) program organization at the Langley Research Center. Mr. D. B. Middleton and Mr. K. W. Heising were the technical monitors for the contract. The work was performed within the Vice-President-Engineering and the Vice-President-Flight Operations organizations of the Boeing Commercial Airplane Company. Key contractor personnel responsible for the contract work were:

**G. W. Hanks**

Program Manager

**F. J. Davenport**

Structures Technology

**R. L. Martin**

Project Manager

**F. W. McIlroy**

Flight Test Instrumentation

**K. H. Dickenson**

Structures Technology

**C. D. Beard**

Flight Test Instrumentation

**W. R. Lambert**

Propulsion Technology

**E. L. Wallace**

Flight Test Analysis

**W. F. Wilson**

Flight Test Operations

**R. D. LaBounty**

Industrial Engineering Flight Test Support

**B. W. Farquhar**

Propulsion Technology

**B. G. Skelton**

Flight Test and Crew Training Support

Results of the total program, including analysis of the test data contained in this report, will be provided in a separate NASA contractor report.

The test effort was conducted in cooperation with the Pratt and Whitney Aircraft Company, who were supported by the NASA Lewis Research Center under Contract NAS3-20632.

Principal measurements and calculations used during these studies were in customary units.

	CONTENTS	ORIGINAL DRAWINGS OR PAGES OF POOR QUALITY	Page
<b>1.0 SUMMARY . . . . .</b>			<b>1</b>
<b>2.0 INTRODUCTION. . . . .</b>			<b>3</b>
<b>2.1 Objectives . . . . .</b>			<b>3</b>
<b>2.2 Background . . . . .</b>			<b>4</b>
<b>2.3 Approach . . . . .</b>			<b>5</b>
<b>3.0 SYMBOLS AND ABBREVIATIONS . . . . .</b>			<b>7</b>
<b>4.0 TEST DESCRIPTION AND RESULTS . . . . .</b>			<b>13</b>
<b>4.1 Test Description . . . . .</b>			<b>13</b>
<b>4.1.1 Test Vehicle. . . . .</b>			<b>13</b>
<b>4.1.1.1 Flight Loads . . . . .</b>			<b>13</b>
<b>4.1.1.2 Installed Propulsion System Aerodynamics. . . . .</b>			<b>13</b>
<b>4.1.2 Instrumentation . . . . .</b>			<b>32</b>
<b>4.1.2.1 Flight Loads . . . . .</b>			<b>32</b>
<b>4.1.2.2 Installed Propulsion System Aerodynamics . . . . .</b>			<b>62</b>
<b>4.1.3 Test Conditions and Procedures . . . . .</b>			<b>65</b>
<b>4.1.3.1 Flight Loads . . . . .</b>			<b>65</b>
<b>4.1.3.2 Installed Propulsion System Aerodynamics . . . . .</b>			<b>71</b>
<b>4.1.4 Test Data Format . . . . .</b>			<b>72</b>
<b>4.2 Test Results . . . . .</b>			<b>75</b>
<b>4.2.1 Aerodynamic and Inertial Loads . . . . .</b>			<b>75</b>
<b>4.2.1.1 Aerodynamic Loads . . . . .</b>			<b>75</b>
<b>4.2.1.2 Inertial Loads . . . . .</b>			<b>88</b>
<b>4.2.2 Installed Propulsion System Aerodynamics. . . . .</b>			<b>89</b>
<b>5.0 REFERENCES. . . . .</b>			<b>91</b>
<b>APPENDIX A</b>	<b>Aerodynamic and Inertial Loads . . . . .</b>		<b>A-1</b>
<b>APPENDIX B</b>	<b>Installed Propulsion System Aerodynamics. . . . .</b>		<b>B-1</b>
<b>MICROFICHE</b>	<b>Pressure Coefficient and Mach Number Tables . . . . .</b>		<b>2</b>
	<b>Pressure Coefficient Plots . . . . .</b>		<b>80</b>
	<b>Local Mach Number Plots . . . . .</b>		<b>220</b>

## TABLES

ORIGINALLY PRINTED  
OF POOR QUALITY

	Page
1 Wing Coordinates . . . . .	18
2 Engine 3 Pylon Coordinates. . . . .	26
3 Engine 4 Pylon Coordinates. . . . .	27
4 Engines 3 and 4 Core Cowl Coordinates . . . . .	29
5 Engines 3 and 4 Inlet Coordinates . . . . .	30
6 Engines 3 and 4 Fan Cowl Coordinates . . . . .	33
7 Engines 3 and 4 Pylon-Fan Cowl Intersection . . . . .	35
8 Engine 3 Wing-Pylon Intersection . . . . .	36
9 Engine 4 Wing-Pylon Intersection . . . . .	37
10 Pylon-Core Cowl Intersection. . . . .	38
11 Wing Pressure Orifice Locations . . . . .	39
12 Engine 3 Pylon Pressure Orifice Locations . . . . .	40
13 Engine 4 Pylon Pressure Orifice Locations . . . . .	41
14 Engine 3 Inlet Pressure Orifice Locations. . . . .	42
15 Engine 4 Inlet Pressure Orifice Locations. . . . .	43
16 Engines 3 and 4 Core Cowl Pressure Orifice Locations . . . . .	44
17 Lateral Offset of Wing Pressure Belt Pressure Orifices From Wing Buttock Line . . . . .	66
18 Test Conditions Flown . . . . .	70
19 Inboard Aileron . . . . .	73
20 Pressure Coefficient . . . . .	76
21 Summary of Measurements of Engine Performance . . . . .	77
22 Engine Fuel-Flow Data . . . . .	78
23 Measurements for Engine Clearance . . . . .	79
24 Measurements of Turbine-Case Temperature . . . . .	80
25 Engine 3 A-Flange Resultants. . . . .	83
A-1 Engine 3 Pressure Port Locations . . . . .	A-3
A-2 Pressure Corrections for Instrumentation Problems . . . . .	A-6
A-3 Fourier-Bessel Coefficients for Engine 3 Pressures, Condition 101 (612K). . . . .	A-7
A-4 Fourier-Bessel Coefficients for Engine 3 Pressures, Condition 101 (538K). . . . .	A-8
A-5 Fourier-Bessel Coefficients for Engine 3 Pressures, Condition 101 (647K). . . . .	A-9

## TABLES (Concluded)

ORIGINAL EDITION  
OF FOURTH QUARTER

	Page
A-6      Fourier-Bessel Coefficients for Engine 3 Pressures, Condition 118 . .	A-10
A-7      Fourier-Bessel Coefficients for Engine 3 Pressures, Condition 102 . .	A-11
A-8      Fourier-Bessel Coefficients for Engine 3 Pressures, Condition 103 . .	A-12
A-9      Fourier-Bessel Coefficients for Engine 3 Pressures, Condition 104 . .	A-13
A-10     Fourier-Bessel Coefficients for Engine 3 Pressures, Condition 105 . .	A-14
A-11     Fourier-Bessel Coefficients for Engine 3 Pressures, Condition 106 . .	A-15
A-12     Fourier-Bessel Coefficients for Engine 3 Pressures, Condition 107 . .	A-16
A-13     Fourier-Bessel Coefficients for Engine 3 Pressures, Condition 108 . .	A-17
A-14     Fourier-Bessel Coefficients for Engine 3 Pressures, Condition 109 . .	A-18
A-15     Fourier-Bessel Coefficients for Engine 3 Pressures, Condition 110 . .	A-19
A-16     Fourier-Bessel Coefficients for Engine 3 Pressures, Condition 111 . .	A-20
A-17     Fourier-Bessel Coefficients for Engine 3 Pressures, Condition 112 . .	A-21
A-18     Fourier-Bessel Coefficients for Engine 3 Pressures, Condition 113 . .	A-22
A-19     Fourier-Bessel Coefficients for Engine 3 Pressures, Condition 114 . .	A-23
A-20     Fourier-Bessel Coefficients for Engine 3 Pressures, Condition 115 . .	A-24
A-21     Fourier-Bessel Coefficients for Engine 3 Pressures, Condition 116 . .	A-25
A-22     Fourier-Bessel Coefficients for Engine 3 Pressures, Condition 117 . .	A-26
A-23     Fourier-Bessel Coefficients for Engine 3 Pressures, Condition 120 . .	A-27
A-24     Fourier-Bessel Coefficients for Engine 3 Pressures, Condition 121 . .	A-28
A-25     Fourier-Bessel Coefficients for Engine 3 Pressures, Condition 123 . .	A-29
B-1      Summary of Selected Test Condition Averages . . . . .	B-3
B-2      Tabulated Data for Test 273-09, Condition 1.00:137.001 . . . . .	B-4

**FIGURES**ORIGINAL PAGE IS  
OF POOR QUALITY

	Page
1 RA001 Test Airplane . . . . .	14
2 Inboard Engine Buildup. . . . .	14
3 Inboard Inlet Removal . . . . .	15
4 Inboard Engine Removal . . . . .	15
5 Pressure Orifice Configuration . . . . .	16
6 Upper Wing Surface. . . . .	16
7 747 Elastic Wing Twist. . . . .	23
8 Wing Coordinate System . . . . .	24
9 Nacelle Coordinate System. . . . .	25
10 Inboard Engine Pressure Taps , . . . . .	45
11 Inboard Inlet Pressure Taps. . . . .	45.
12 Pressure Transducer. . . . .	47
13 Pressure Transducer Installation . . . . .	47
14 Pressure Transducer Box . . . . .	48
15 Cowl Door Pressure Taps. . . . .	48
16 Outboard Engine Pressure Taps . . . . .	49
17 Inertial Data Sensors . . . . .	49
18 Q-FLEX Accelerometer . . . . .	50
19 Rate Gyro . . . . .	50
20 Accelerometer and Rate Gyro . . . . .	51
21 Accelerometer Installation (Thrust Link). . . . .	53
22 Clearance Monitoring System. . . . .	53
23 Laser Generator Boxes. . . . .	54
24 Fan Video Camera Installation . . . . .	56
25 Turbine Video Camera Installation. . . . .	56
26 Fan Laser Probe . . . . .	57
27 Turbine Laser Probe. . . . .	58
28 Turbine Laser Probe Installed. . . . .	58
29 Laser Proximity Probe Locations . . . . .	59
30 Laser System Video Monitors and Controls . . . . .	60
31 Laser Video Tape Recorder . . . . .	60
32 Nitrogen System . . . . .	61
33 Expanded Engine Performance . . . . .	61

**FIGURES (Continued)**

CHARTS AND FIGURES  
OF POOR QUALITY

ORIGINATOR: DOD  
(OR R&D)

	Page
34 Typical Cross-Section of Wing Pressure Belt . . . . .	64
35 Acceptance Flight Profile . . . . .	68
36 View of Pressure Ports. . . . .	70
37 Airborne Data Analysis and Monitoring System . . . . .	74
38 Test Airplane Interior View. . . . .	74
39 Sign Convention for Steady-State Loads, Engine 3 . . . . .	82
40 Inlet Pitching Moment Time History, 538 000 lb Gross Weight Takeoff . . . . .	84
41 Inlet Airload Moment Time History, 647 000 lb Gross Weight Takeoff . . . . .	86
42 Airload Moment Time History, Stall Warning Maneuver, Flaps 10 . . . . .	87
A-1 Pressure Data Coordinate Conventions. . . . .	A-30
A-2 Engine No. 3 Inlet Pressures, Condition 101, 612K GW Takeoff (Flaps 20). . . . .	A-31
A-3 Engine No. 3 Cowl Pressures, Condition 101, 612K GW Takeoff (Flaps 20). . . . .	A-32
A-4 Engine No. 3 Inlet Pressures, Condition 101, 534K GW Takeoff (Flaps 10). . . . .	A-33
A-5 Engine No. 3 Cowl Pressures, Condition 101, 538K GW Takeoff (Flaps 10). . . . .	A-34
A-6 Engine No. 3 Inlet Pressures, Condition 101, 647K GW Takeoff (Flaps 10). . . . .	A-35
A-7 Engine No. 3 Cowl Pressures, Condition 101, 647K GW Takeoff (Flaps 10). . . . .	A-36
A-8 Engine No. 3 Inlet Pressures, Condition 118, 780K GW Simulated Takeoff (Flaps 10) . . . . .	A-37
A-9 Engine No. 3 Cowl Pressures, Condition 118, 780K GW Simulated Takeoff (Flaps 10) . . . . .	A-38
A-10 Engine No. 3 Inlet Pressures, Condition 102, Low Climb . . . . .	A-39
A-11 Engine No. 3 Cowl Pressures, Condition 102, Low Climb . . . . .	A-40
A-12 Engine No. 3 Inlet Pressures, Condition 103, Mid Climb. . . . .	A-41
A-13 Engine No. 3 Cowl Pressures, Condition 103, Mid Climb . . . . .	A-42
A-14 Engine No. 3 Inlet Pressures, Condition 104, High M Cruise . . . . .	A-43
A-15 Engine No. 3 Cowl Pressures, Condition 104, High M Cruise . . . . .	A-44
A-16 Engine No. 3 Inlet Pressures, Condition 105, Low M Cruise . . . . .	A-45
A-17 Engine No. 3 Cowl Pressures, Condition 105, Low M Cruise . . . . .	A-46

**FIGURES (Continued)**

**ORIGINAL PAGE IS  
OF POOR QUALITY**

	Page
A-18      Engine No. 3 Inlet Pressures, Condition 106, Maximum M . . . . .	A-47
A-19      Engine No. 3 Cowl Pressures, Condition 106, Maximum M. . . . .	A-48
A-20      Engine No. 3 Inlet Pressures, Condition 107, Inflight Relight . . . . .	A-49
A-21      Engine No. 3 Cowl Pressures, Condition 107, Inflight Relight . . . . .	A-50
A-22      Engine No. 3 Inlet Pressures, Condition 108, Maximum q . . . . .	A-51
A-23      Engine No. 3 Cowl Pressures, Condition 108, Maximum q. . . . .	A-52
A-24      Engine No. 3 Inlet Pressures, Condition 109, Stall Warning (Flaps Up) . . . . .	A-53
A-25      Engine No. 3 Cowl Pressures, Condition 109, Stall Warning (Flaps Up) . . . . .	A-54
A-26      Engine No. 3 Inlet Pressures, Condition 110, Stall Warning (Flaps 10) . . . . .	A-55
A-27      Engine No. 3 Cowl Pressures, Condition 110, Stall Warning (Flaps 10) . . . . .	A-56
A-28      Engine No. 3 Inlet Pressures, Condition 111, Stall Warning (Flaps 30) . . . . .	A-57
A-29      Engine No. 3 Cowl Pressures, Contition 111, Stall Warning (Flaps 30) . . . . .	A-58
A-30      Engine No. 3 Inlet Pressures, Condition 112, Idle Descent. . . . .	A-59
A-31      Engine No. 3 Cowl Pressures, Condition 112, Idle Descent . . . . .	A-60
A-32      Engine No. 3 Inlet Pressures, Condition 113, Approach . . . . .	A-61
A-33      Engine No. 3 Cowl Pressures, Condition 113, Approach . . . . .	A-62
A-34      Engine No. 3 Inlet Pressures, Condition 114, Touch and Go . . . . .	A-63
A-35      Engine No. 3 Cowl Pressures, Condition 114, Touch and Go . . . . .	A-64
A-36      Engine No. 3 Inlet Pressures, Condition 115, Thrust Reverse . . . . .	A-65
A-37      Engine No. 3 Cowl Pressures, Condition 115, Thrust Reverse . . . . .	A-66
A-38      Engine No. 3 Inlet Pressures, Condition 116, 2.0g Left Turn (Flaps Up) . . . . .	A-67
A-39      Engine No. 3 Cowl Pressures, Condition 116, 2.0g Left Turn (Flaps Up) . . . . .	A-68
A-40      Engine No. 3 Inlet Pressures, Condition 117, 1.6 Left Turn (Flaps 30) . . . . .	A-69
A-41      Engine No. 3 Cowl Pressures, Condition 117, 1.6 Left Turn (Flaps 30) . . . . .	A-70
A-42      Engine No. 3 Inlet Pressures, Condition 120, 2.0g Right Turn (Flaps Up) . . . . .	A-71

## FIGURES (Continued)

ORIGINAL PAGE IS  
OF POOR QUALITY.

	Page
A-43      Engine No. 3 Cowl Pressures, Condition 120, 2.0g Right Turn (Flaps Up) . . . . .	A-72
A-44      Engine No. 3 Inlet Pressures, Condition 121, 1.6g Right Turn (Flaps 30) . . . . .	A-73
A-45      Engine No. 3 Cowl Pressures, Condition 121, 1.6g Right Turn (Flaps 30) . . . . .	A-74
A-46      Engine No. 3 Inlet Pressures, Condition 123, Airplane Stall . . . . .	A-75
A-47      Engine No. 3 Cowl Pressures, Condition 123, Airplane Stall . . . . .	A-76
A-48      Engine No. 4 Inlet Pressures, Condition 101, 612K Gross Weight Takeoff . . . . .	A-77
A-49      Engine No. 4 Inlet Pressures, Condition 101, 538K Gross Weight Takeoff . . . . .	A-78
A-50      Engine No. 4 Inlet Pressures, Condition 101, 647K Gross Weight Takeoff . . . . .	A-79
A-51      Engine No. 4 Inlet Pressures, Condition 118, 780K Gross Weight Simulated Takeoff . . . . .	A-80
A-52      Engine No. 4 Inlet Pressures, Condition 102, Low Climb . . . . .	A-81
A-53      Engine No. 4 Inlet Pressures, Condition 103, Mid Climb. . . . .	A-82
A-54      Engine No. 4 Inlet Pressures, Condition 104, High M Cruise . . . . .	A-83
A-55      Engine No. 4 Inlet Pressures, Condition 105, Low M Cruise . . . . .	A-84
A-56      Engine No. 4 Inlet Pressures, Condition 106, Maximum M . . . . .	A-85
A-57      Engine No. 4 Inlet Pressures, Condition 107, Inflight Relight . . . . .	A-86
A-58      Engine No. 4 Inlet Pressures, Condition 108, Maximum q . . . . .	A-87
A-59      Engine No. 4 Inlet Pressures, Condition 109, Stall Warning (Flaps Up) . . . . .	A-88
A-60      Engine No. 4 Inlet Pressures, Condition 110, Stall Warning (Flaps 10) . . . . .	A-89
A-61      Engine No. 4 Inlet Pressures, Condition 111, Stall Warning (Flaps 30) . . . . .	A-90
A-62      Engine No. 4 Inlet Pressures, Condition 112, Idle Descent. . . . .	A-91
A-63      Engine No. 4 Inlet Pressures, Condition 113, Approach . . . . .	A-92
A-64      Engine No. 4 Inlet Pressures, Condition 114, Touch and Go . . . . .	A-93
A-65      Engine No. 4 Inlet Pressures, Condition 115, Thrust Reverse . . . . .	A-94
A-66      Engine No. 4 Inlet Pressures, Condition 116, 2.0g Left Turn (Flaps Up) . . . . .	A-95
A-67      Engine No. 4 Inlet Pressures, Condition 117, 1.6g Left Turn (Flaps 30) . . . . .	A-96

**FIGURES (Concluded)**

ORIGINAL PAGE IS  
OF POOR QUALITY

	Page
A-68      Engine No. 4 Inlet Pressures, Condition 120, 2.0g Right Turn (Flaps Up) . . . . .	A-97
A-69      Engine No. 4 Inlet Pressures, Condition 121, 1.6g Right Turn (Flaps Up) . . . . .	A-98
A-70      Engine No. 4 Inlet Pressures, Condition 123, Airplane Stall . . . . .	A-99
A-71      Airplane Center-of-Gravity Accelerations, Mild Gust . . . . .	A-100
A-72      Engine No. 3 Wing/Strut Accelerations, Mild Gust . . . . .	A-101
A-73      Engine No. 4 Wing/Strut Accelerations, Mild Gust . . . . .	A-102
A-74      Engine Angular Rates, Mild Gust . . . . .	A-103
A-75      Engine No. 3 Accelerations, Mild Gust . . . . .	A-104
A-76      Engine No. 4 Accelerations, Mild Gust . . . . .	A-105
A-77      Airplane Center-of-Gravity Normal Acceleration, Hard Landing . . . . .	A-106
A-78      Airplane Center-of-Gravity Angular Rates, Hard Landing . . . . .	A-107
A-79      Engine No. 3 Wing/Strut Accelerations, Hard Landing . . . . .	A-108
A-80      Engine No. 4 Wing/Strut Accelerations, Hard Landing . . . . .	A-109
A-81      Engine Angular Rates, Hard Landing . . . . .	A-110
A-82      Engine No. 3 Accelerations, Hard Landing . . . . .	A-111
A-83      Engine No. 4 Accelerations, Hard Landing . . . . .	A-112
B-1      Sample of Pressure Coefficient Data (Test 273-12, Condition 1.00.137.001.1) . . . . .	B-5
B-2      Sample of Pressure Coefficient Data (Test 273-12, Condition 1.00.137.002) . . . . .	B-25
B-3      Sample of Pressure Coefficient Data (Test 273-12, Condition 1.00.137.003) . . . . .	B-45
B-4      Sample of Pressure Coefficient Data (Test 273-12, Condition 1.00.137.004) . . . . .	B-66
B-5      Sample of Local Mach Number Data (Test 273-12, Condition 1.00.137.001.1) . . . . .	B-81
B-6      Sample of Local Mach Number Data (Test 273-12, Condition 1.00.137.002) . . . . .	B-97
B-7      Sample of Local Mach Number Data (Test 273-12, Condition 1.00.137.003) . . . . .	B-112
B-8      Sample of Local Mach Number Data (Test 273-15, Condition 1.00.137.004) . . . . .	B-127

## 1.0 SUMMARY

The Nacelle Aerodynamics and Inertial Loads (NAIL) program comprised a series of test flights that produced an in-flight measured data base of the aerodynamic and inertial loads imposed on right-hand inboard and outboard JT9D engines installed on the Boeing 747 RA001 test bed aircraft. Wing and engine installed performance data were also obtained. In this report the aerodynamic and inertial loads portion of the test program is referred to as the flight loads, and the wing and engine installed performance portion is referred to as the installed propulsion system aerodynamics (IPSA).

During the flight loads portion of the test program, surface static pressures were measured on the:

- Internal and external surfaces of the inboard inlet
- External surface of the fan cowl doors of the inboard nacelle
- External surface of the fan exhaust sleeve of the inboard nacelle
- Internal and external surfaces of the outboard inlet

Linear accelerations and pitch and yaw rates were also measured on both inboard and outboard nacelle and pylon installations.

The following measurements were made simultaneously with the surface static pressure measurements:

- Engine clearance changes on both inboard and outboard engines
- Turbine case temperature on the inboard engine
- Engine performance on both inboard and outboard engines

The resulting data were correlated with the flight loads. These measurements-

- Duplicated a portion of the airplane flight acceptance test profile
- Demonstrated the effects of variations in takeoff gross weight
- Illustrated the effects of high-g maneuvers

During the IPSA portion of the NAIL program, surface static pressures were measured on the nacelle, pylon, and neighboring wing surfaces on engines 3 and 4 (inboard and outboard). A data base was acquired at Mach numbers 0.77, 0.80, 0.86, and 0.91 through three flights of the RA001.

Pressure coefficient and local Mach number distributions were plotted for each row of pressure orifices. A geometrical description of the surfaces and pressure orifice locations on the nacelle, pylon, and wing is provided. The IPSA data base, derived from a full-scale flight vehicle, should assist in verification and development of analytical models and eventually provide the ability to predict wing-mounted propulsion system performance.

## 2.0 INTRODUCTION

The test program recommended in the feasibility study (ref. 1) describes a flight test in which flight loads and engine clearance changes can be measured simultaneously on the 747/JT9D engine installation. NASA-Langley and NASA-Lewis Research Centers authorized and jointly funded this program under separate contracts for Boeing Commercial Airplane Company (BCAC) and Pratt & Whitney Aircraft (P&WA). The BCAC effort, Nacelle Aerodynamic and Inertial Loads (NAIL) project, was funded by NASA-Langley under Task 4.3 of contract NASI-15325. The P&WA effort was funded by NASA-Lewis under Task V, JT9D Engine Diagnostic Flight Loads Test program, contract NAS3-20632. Subsequently, the BCAC contract was revised to include the installed propulsion system aerodynamics (IPSA) effort. The successful completion of this joint test program was only possible through the continuous and extensive coordination between BCAC and P&WA and the excellent cooperation of the NASA-Langley and NASA-Lewis Research Centers. This document reports the BCAC effort during the test program and represents early release of flight test data.

The testing was conducted on the Boeing-owned 747 RA001 test bed airplane during the concurrent 767/JT9D-7R4 engine development program. Following a functional check flight conducted from Boeing Field International (BFI) on 3 October 1980, the airplane and test personnel were ferried to Valley Industrial Park (GSG) near Glasgow, Montana, on 7 October 1980. The combined NAIL and 767/JT9D-7R4 test flights were conducted at the Glasgow remote test site, and the airplane was returned to Seattle on 26 October 1980.

### 2.1 OBJECTIVES

Objectives of the NAIL flight test program were to:

- o Measure flight loads (aerodynamic and inertial) typical of acceptance test and revenue service
- o Explore the effects of gross weight, sink rate, pitch rate, and various maneuvers on nacelle loads
- o Measure simultaneously engine clearance closures and engine performance changes

- Provide a data base for designing improved propulsion systems (performance retention)
- Provide a data base of pressures measured on wing, pylon, and nacelle surfaces of both inboard and outboard propulsion installations of commercial transport-sized aircraft and to gather information on airflow patterns surrounding the powerplant installations using static pressure surveys

## **2.2 BACKGROUND**

Since introduction of the jet engine into commercial transport service, historical data have indicated that deterioration of engine specific fuel consumption (SFC) occurs over the life of installed engines. Until recent shortages in fuel and the resulting high fuel costs, increases in fuel consumption were considered to be a nuisance rather than a technical problem requiring a solution. Motivated by fuel shortages and costs, the NASA Engine Component Improvement (ECI) program (part of the NASA Aircraft Energy Efficiency program) was made responsible for determining the cause of and potential solutions to installed engine SFC deterioration. As part of the ECI program, BCAC assisted P&WA under their NASA-Lewis contract NAS3-20632 during evaluation of the problem. It was found that the SFC of engines increased from 0.5% to 6% from the time of removal from the acceptance test stand followed by installation and operation on the airplane for a given period of time. Measurement of rotor blades at the outer diameter and inspection of the inner surface of engine cases indicated that definite interference occurred between the blades and the case. This interference resulted in increased clearance and gas flow leakage between the blades and the outside case. The study found that 87% of the increase in SFC was due to flight loads occurring within the first 50 flight cycles.

Factors contributing significantly to engine performance losses are divided into engine loads and flight loads, as follows:

- Engine loads (those loads not related to the flight environment)
  - Internal engine pressures
  - Thermal loads due to temperature differentials
  - Thrust loads—fore and aft
  - Centrifugal loads

- o Flight loads (those loads imposed by the flight environment)
  - o Aerodynamic pressures
  - o Inertial forces

A finite element model analysis using these factors predicted a 1% increase in SFC at sea level due to the aircraft acceptance flight test.

Aircraft fuel consumption is proportional to aircraft drag. Thus to reduce fuel consumption, drag should be minimized. Most mechanisms of drag production are understood and are predictable to some degree, with the exception of a component termed "interference drag." This drag results from disruption of the flow over the wing caused by the wing-mounted propulsion system in the vicinity of the propulsion system. This interruption interferes with the wing performance. Current techniques for estimating and minimizing interference drag rely heavily on comprehensive test programs that independently vary a set of parameters believed to significantly influence interference. Current analytical technology is sufficiently advanced so that transonic potential flows around arbitrary three-dimensional bodies can be accurately predicted. However, the development of analytical techniques depends extensively on experimental results for comparison of the predicted results. Development of analytical techniques to model the physics of flow about propulsion systems installed near wings has been initiated and some of the techniques are nearing completion. However, the comprehensive data base to which these predictions could be compared is lacking.

### **2.3 APPROACH**

Recommendations and conclusions of previous studies prescribed a feasible cost-effective approach to the NASA-funded NAIL/JT9D Flight Loads flight test program. This joint program involved BCAC and P&WA, funded by NASA-Langley and by NASA-Lewis, respectively.

A 15-hour flight test program covering portions of the acceptance flight profile, variations in takeoff and landing conditions, and high-g turns was chosen to measure simultaneously the flight loads (cause) and engine clearance changes (effect) associated with engine performance deterioration. The flight test program used the Boeing-owned 747 RA001 aircraft.

Aerodynamic loads were measured by 252 static pressure ports on the inboard nacelle (engine 3) and 45 static pressure ports on the outboard nacelle (engine 4).

Inertial loads were measured by six accelerometers and two rate gyros on both the inboard and outboard engines. The pylon and strut interface of both engines was equipped with an additional six accelerometers. The resulting engine clearance changes were measured by laser proximity probes on the fan of both engines and on the high-pressure turbine of the inboard engine. The expanded engine performance instrumentation and 20 high-pressure turbine thermocouples provided additional data on the inboard engine for resolving clearance and performance changes.

The IPSA pressure data were obtained in the neighborhood of both engines by a total of 499 static pressure orifices; 322 of these were arranged in rows above and below the wing and on each side of both pylons and core cowls. The remaining data, on both inlets and fan cowls, were acquired from part of the aerodynamic loads instrumentation.

### 3.0 SYMBOLS AND ABBREVIATIONS

OPTIONAL FORM 15  
OF FEDERAL AVIATION  
ADMINISTRATION

$A_n$	Fourier-Bessel coefficient for nth cosine harmonic
AC	axial acceleration
ACCEL	acceleration
ADAMS	airborne data analysis and monitor system
A-flange	engine front flange at nacelle station 100
$A_x$	acceleration in x-direction
$A_y$	acceleration in y-direction
$A_z$	acceleration in z-direction
$B_n$	Fourier-Bessel coefficient for nth sine harmonic
BCAC	Boeing Commercial Airplane Company
BFI	Boeing Field International, Seattle, Washington
CG	center of gravity
$C_p$	pressure coefficient
deg	degrees
ECI	engine component improvement program
EPR	engine pressure ratio
E3	engine position 3
E4	engine position 4
ft	feet
FLTRD	filtered
FS	front spar
FT	flight test
$F_x$	force in the x-direction
$F_y$	force in the y-direction
$F_z$	force in the z-direction
g	acceleration of gravity
GSG	Valley Industrial Park, northeastern Montana

<b>GW</b>	airplane gross weight
<b>H<sub>P</sub></b>	pressure altitude
<b>HPC IGV POS</b>	high-pressure compressor inlet guide vane position
<b>HPT</b>	high-pressure turbine
<b>HWLDG</b>	heavyweight landing
<b>Hz</b>	hertz (cycles per second)
<b>IGDA</b>	interactive graphics data analysis
<b>In</b>	inch
<b>In-kip</b>	1000 inch-pounds
<b>INLET STA</b>	inlet station, value increases moving aft along inlet centerline
<b>IPSA</b>	installed propulsion system aerodynamics
<b>IRIG</b>	inter-range instrumentation group master clock
<b>kn, KTS</b>	knots
<b>kcas</b>	knots calibrated airspeed, indicated airspeed corrected for position error (calibrated airspeed equals true airspeed in standard atmosphere at sea level)
<b>LAST</b>	final formatted tape produced by the flight test data system
<b>lb</b>	pound
<b>LH</b>	left hand
<b>lbn</b>	pounds mass
<b>M</b>	Mach number, ratio of true airspeed to the velocity of sound
<b>M<sub>c</sub></b>	design cruise Mach number
<b>M<sub>x</sub></b>	moment about the x-axis
<b>M<sub>y</sub></b>	moment about the y-axis
<b>M<sub>z</sub></b>	moment about the z-axis
<b>min</b>	minutes
<b>NAC BL</b>	nacelle buttock line, value increases moving outboard in the nacelle coordinate system

NAC STA	nacelle station, value increases moving aft in the nacelle coordinate system	
NAC WL	nacelle waterline, value increases moving up in the nacelle coordinate system	
NAIL	nacelle aerodynamics and inertial loads	
NASA	National Aeronautics and Space Administration	
NASTRAN	NASA structural analysis	
N1	low-pressure rotor speed	
N2	high-pressure rotor speed	
OCLK	clock position	OPTIONAL, DURING IR OR POOR QUALITY
P	pressure	
PC	pressure coefficient	
POS	position	
PSI ( $\text{lb/in}^2$ )	pounds per square inch	
$P_S$	static pressure	
PS3	low-pressure compressor discharge static pressure	
PS4	high-pressure compressor discharge static pressure	
$P_T$	total pressure	
PT2.5	fan stream total pressure at exit guide vane	
PT3	low-pressure compressor discharge total pressure	
PT7	low-pressure turbine discharge total pressure	
PWR LVR ANG	power lever angle	
P&WA	Pratt & Whitney Aircraft	
q,Q	dynamic pressure, $\frac{1}{2} \rho V^2$	
RA001	Boeing-owned 747-100 research aircraft 1	
RH	right hand	
rms	root mean square	
RWA	referred engine airflow, $(W_A \sqrt{\theta_{T_2}/\delta_{T_2}})$	
sec	seconds	
S	arc length along surface from highlight	
$S_{\text{nom}}$	nominal arc length along surface	

SFC	specific fuel consumption
SLS	sea level standard
TO	takeoff
TR	thrust reverse
T <sub>T</sub>	total temperature
TT3	low-pressure compressor discharge total temperature
TT4.5	high-pressure compressor discharge total temperature
TT6	high-pressure turbine discharge total temperature
TT7	low-pressure turbine discharge total temperature
V	true airspeed, feet per second
V <sub>C</sub>	design cruise speed
V <sub>S</sub>	stalling speed or the minimum steady flight speed at which airplane is controllable
WA	engine airflow
WBL	wing buttock line, value increases by moving outboard
W <sub>f</sub>	fuel flow rate
WFS	wing front spar
WRP	wing reference plane
WUT	windup turn, a level turn produced by increasing the angle of bank at a prescribed rate
T <sub>2</sub>	free stream value
T <sub>2</sub>	angle of attack
T <sub>2</sub>	total temperature ratio at engine face, $T_{T_2}/T_{SLS}$
T <sub>2</sub>	air density, slug/ft <sup>3</sup>
f	circumferential position, degrees
g	total pressure ratio at engine face, $P_{T_2}/P_{SLS}$
h	fan cowl
i	pylon-core cowl intersection
k	highlight
l	inlet
l	core cowl
l	engine 4 wing-pylon intersection

m  
n  
s  
w

pylon-fan cowl intersection  
engine 3 wing-pylon intersection  
pylon (strut)  
wing

## **4.0 TEST DESCRIPTION AND RESULTS**

### **4.1 TEST DESCRIPTION**

The Boeing-owned 747 RA001 test bed aircraft (fig. 1) was the basis of the Nacelle Aerodynamic and Inertial Load (NAIL) flight test program, which comprised two basic studies and data collection systems divided into the flight loads and installed propulsion system aerodynamics (IPSA) programs. Where necessary, discussion of the flight loads and IPSA portions are separated for clarity. However, airplane and performance data were used by both programs, and some of the flight loads pressure data were used by the IPSA program.

#### **4.1.1 Test Vehicle**

##### **4.1.1.1 Flight Loads**

The NAIL program required fabrication and installation effort to provide the means to collect, control, and maintain the quality and quantity of data obtained. The flight loads portion of the program required instrumentation of the inboard and outboard engines (i.e., positions 3 and 4). Highest emphasis was placed on engine 3, which is shown on the wing during the buildup period (fig. 2).

Likewise, during the postflight test phase, refurbishment was necessary to prepare the aircraft for the next program. Inlet 3 (fig. 3) was removed followed by engine 3 (fig. 4), which was shipped to Pratt and Whitney Aircraft (P&WA) for further static testing followed by an analytical teardown and refurbishment.

##### **4.1.1.2 Installed Propulsion System Aerodynamics**

Description of the basic B-747 test vehicle pertinent to the IPSA program requires a geometrical definition of the fan inlet, fan cowl, pylon, and core cowl for an inboard and an outboard engine installation and requires neighboring wing geometry for each engine. This description is provided by defining the local geometry with relative positions and contours of pressure orifice rows and wing-pylon, pylon-nacelle intersections. Figures 5 and 6 describe the location and nomenclature for the pressure orifice rows.

ORIGINAL PAGE  
BLACK AND WHITE PHOTOGRAPH

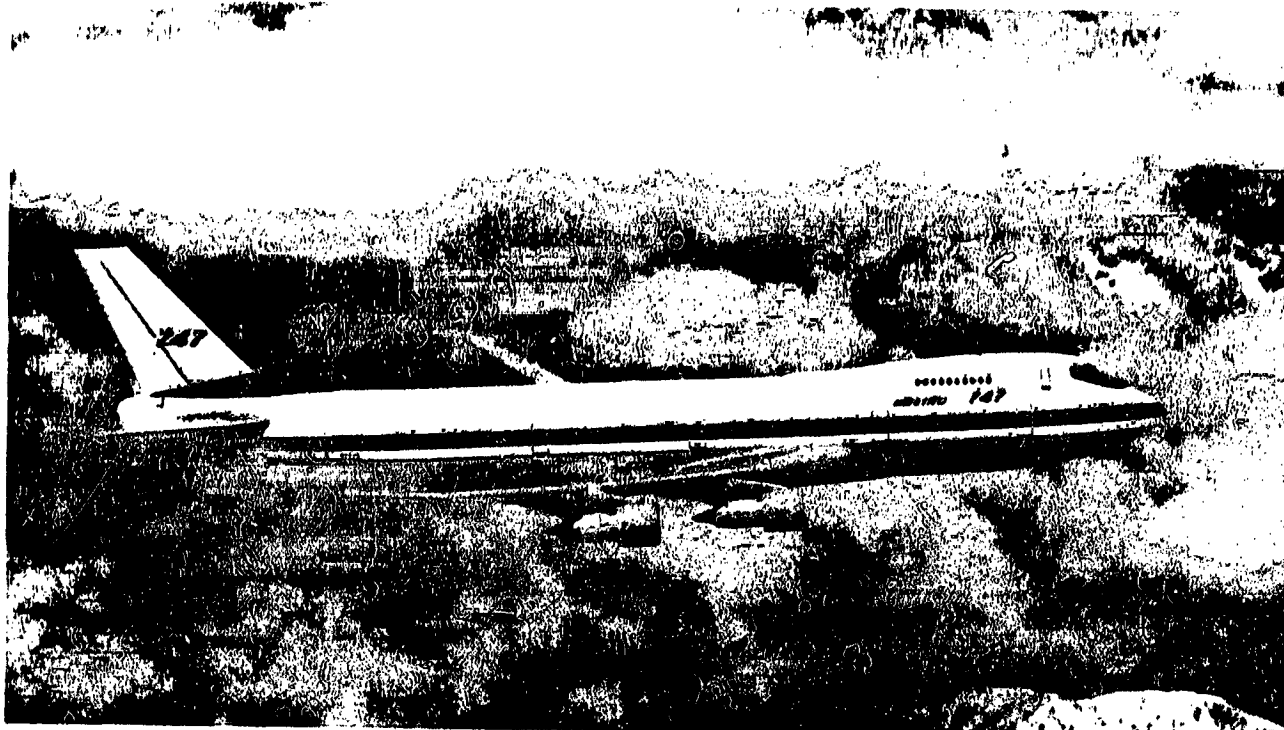


Figure 1. RA001 Test Airplane

128209-1

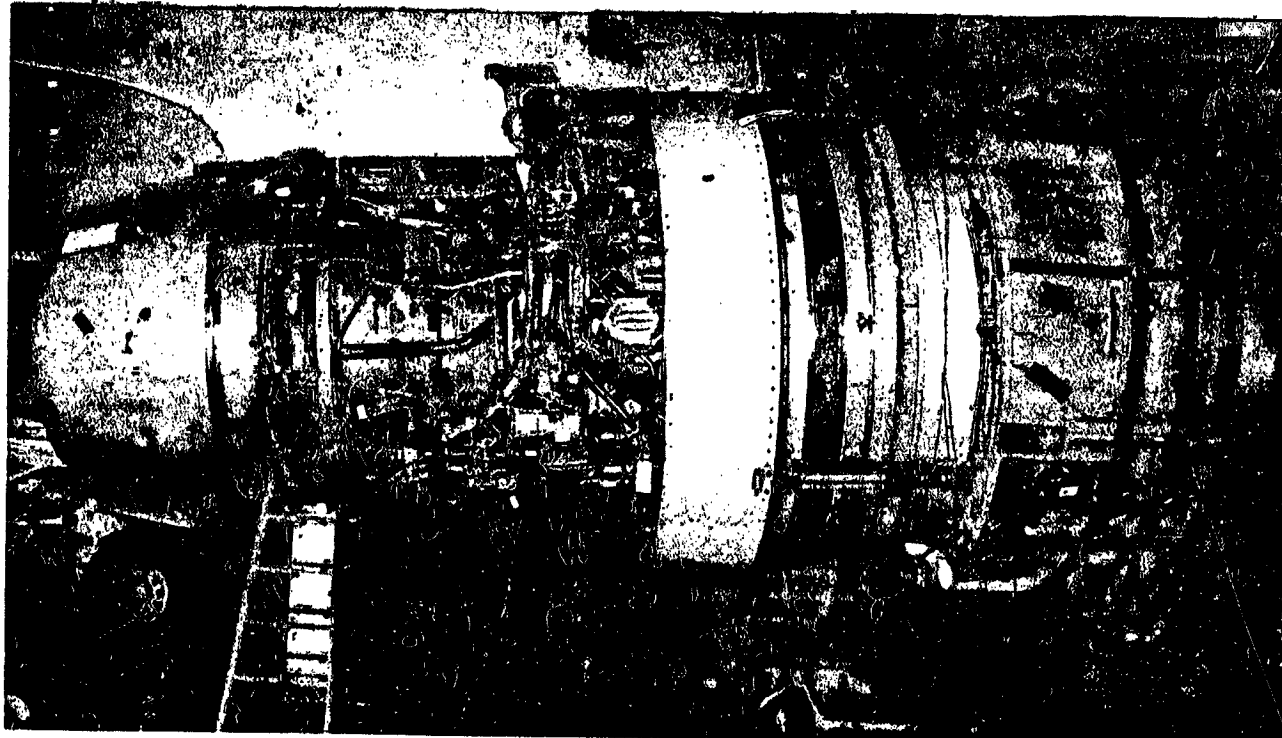


Figure 2. Inboard Engine Buildup-

128209-2

ORIGINAL PAGE  
BLACK AND WHITE PHOTOGRAPH



*Figure 3. Inboard Inlet Removal*

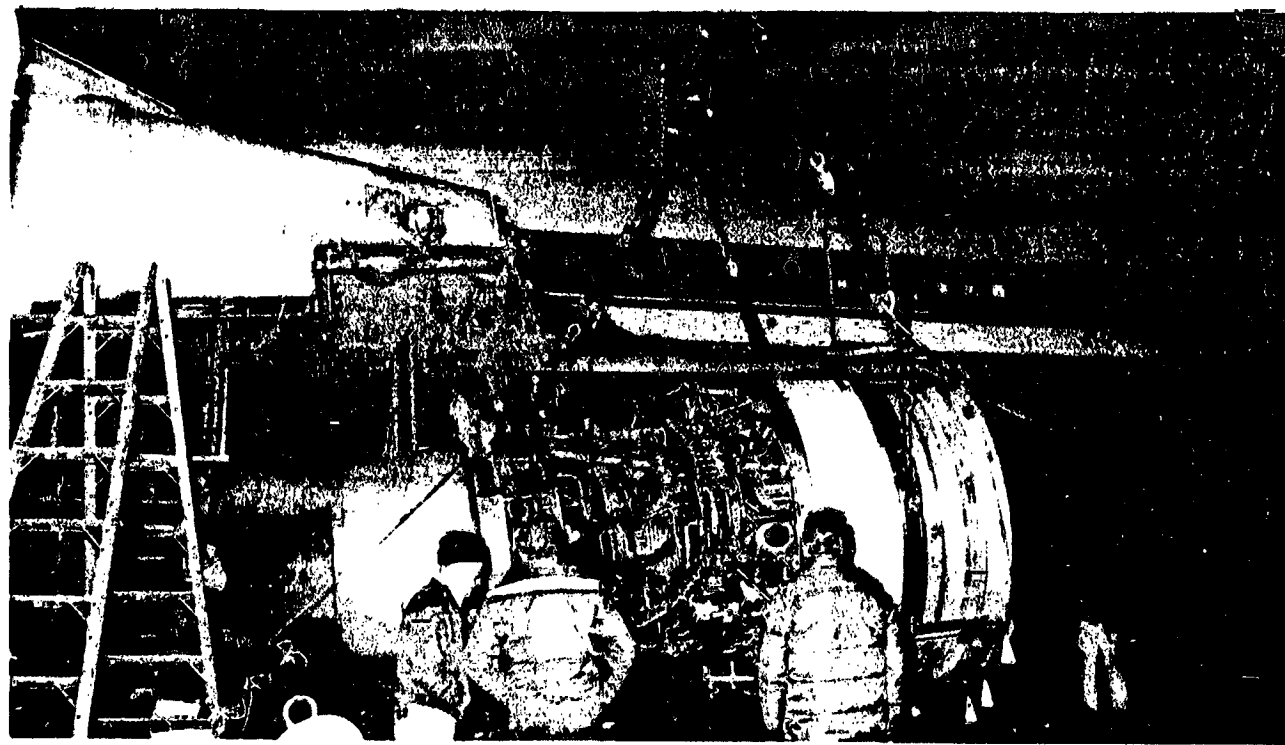


*Figure 4. Inboard Engine Removal*

ORIGINAL PAGE  
BLACK AND WHITE PHOTOGRAPH

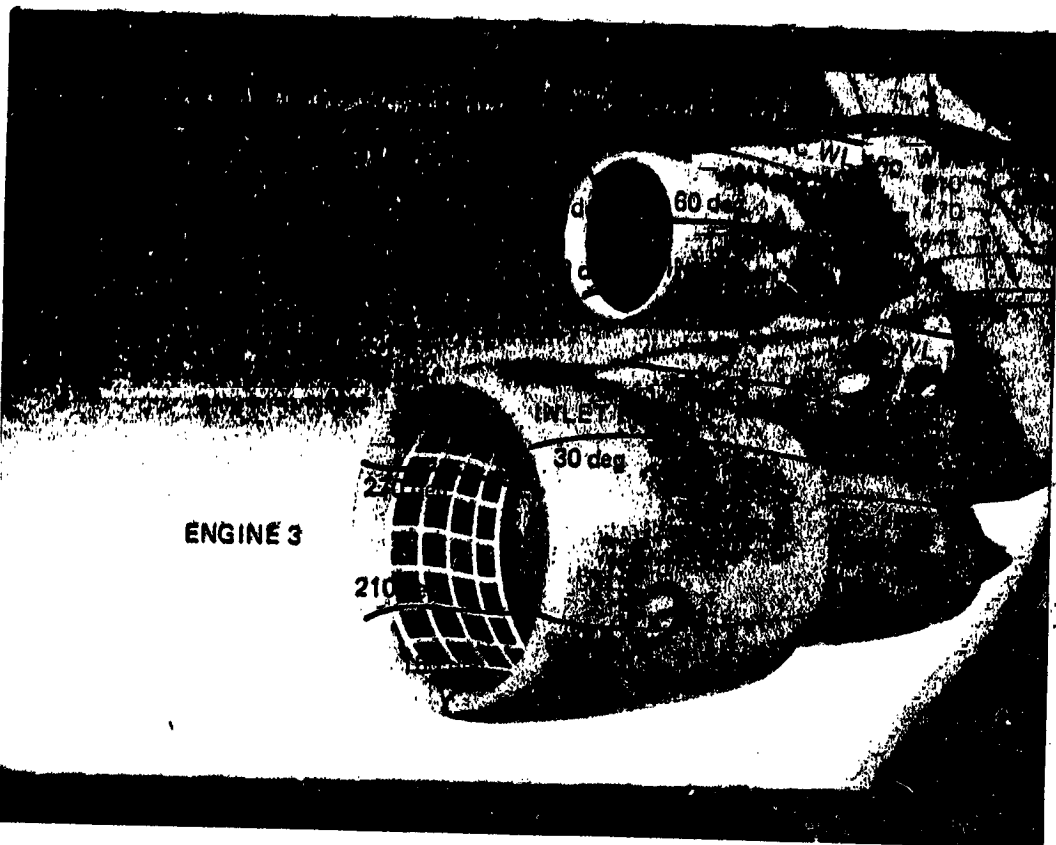


Figure 5. Pressure Orifice Configuration

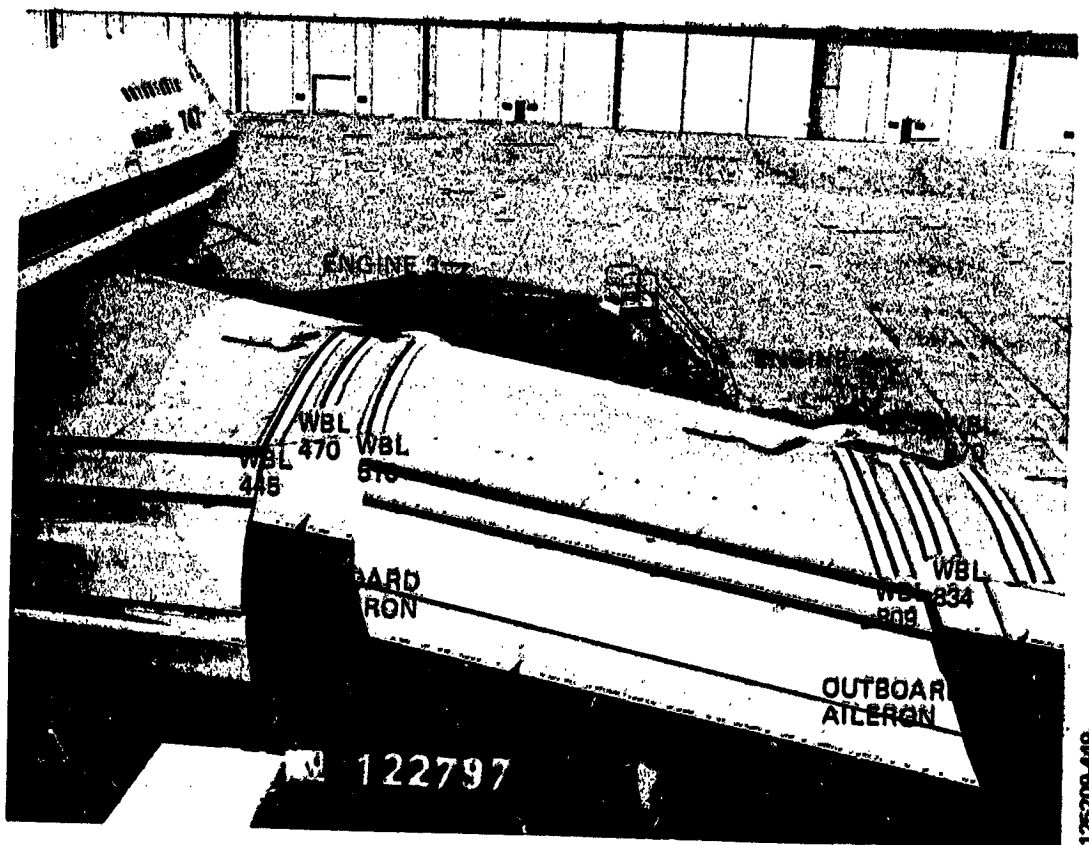


Figure 6. Upper Wing Surface

**Wing Geometry**—Coordinates defining the wing cross-sectional profiles (table 1) are measured along and perpendicular to the wing reference plane (WRP). The WRP is an untwisted plane with 7-deg dihedral and +2-deg angle of incidence to the aircraft body centerline. The coordinates given in table 1 orient the wing profiles as they are in the no-load or jig position, so that the wing leading edges are not necessarily on WRP. See figure 7 for a plot of the jig wing twist. The in-flight wing twist, measured at 50% chord, varies with airplane Mach number and gross weight. In figure 7, the elastic wing twist is plotted for a Mach number of 0.86 at two representative airplane gross weights.

The spanwise location of each wing cross-sectional profile is denoted by a wing buttock line (WBL), which defines a plane perpendicular to the WRP (fig. 8). The relative fore and aft location of the wing cross-sectional profile at each WBL due to wing sweep is also shown in figure 8. Here, the leading-edge sweep angle is identified inboard and outboard of WBL 470 (inboard engine) and WBL 834 (outboard engine).

The leading-edge sweep angle is measured in the WRP relative to a line that is perpendicular to each WBL (470 and 834) and passes through the intersection of the WBL plane and the projection of the wing leading edge in the WRP (fig. 8). The wing leading-edge sweep is constant between WBL 445 and 834. However, it changes outboard of WBL 834 (outboard engine).

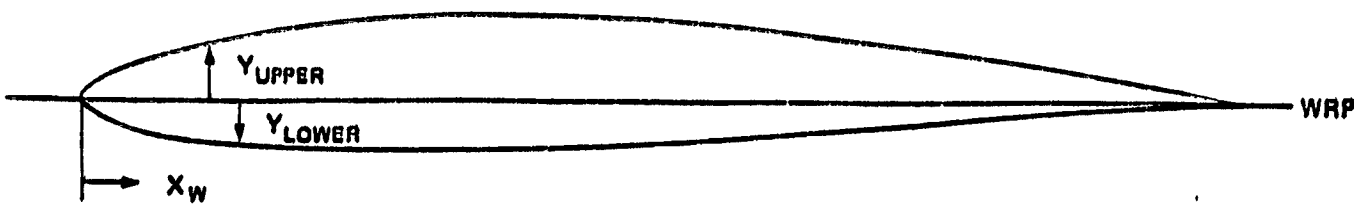
Also at WBL 834, a fairing extends from the outboard strut over the wing leading edge. Fairing coordinates given in table 1 are along the intersection of the WBL 834 plane and the fairing surface.

**Engine Nacelle and Pylon Geometry**—Coordinates defining engine nacelle and pylon geometry are given in a second coordinate system, the nacelle, which is shown in relation to the WRP in figures 8 and 9.

Pylon cross-sectional coordinates (tables 2 and 3) are measured along and perpendicular to the nacelle buttock line (NAC BL) 0.0, which defines a plane perpendicular to the WRP that is toed inboard 2-deg relative to the WBL plane (fig. 8). Depending on engine location, the origin of this 2-deg toe-in is at the intersection of the WBL 470/834 plane and the WRP at the projection of the WBL 470/834 wing profile leading edge. These profile leading edges are labeled T (figs. 8 and 9). A side view of the pylon and engine nacelle (fig. 9) shows that the pylon coordinates (tables 2 and 3) are contained in nacelle

ORIGINAL PAGE IS  
OF POOR QUALITY

Table 1. Wing Coordinates



$X_w = 0$  @ WING LEADING EDGE

WBL 445 $C_w = 989.78 \text{ cm (389.68 in)}$		
$\frac{X_w}{C_w}$	$\frac{Y_{UPPER}}{C_w}$	$\frac{Y_{LOWER}}{C_w}$
0.00	-0.00205	0.00208
0.01	0.00901	0.00695
0.02	0.01414	0.00837
0.03	0.01791	0.00965
0.05	0.02333	0.01196
0.10	0.03198	0.01665
0.15	0.03790	0.02058
0.20	0.04234	0.02393
0.25	0.04650	0.02682
0.30	0.04783	0.02910
0.35	0.04953	0.03067
0.40	0.05032	0.03103
0.45	0.05002	0.03064
0.50	0.04902	0.02951
0.55	0.04712	0.02761
0.60	0.04401	0.02533
0.65	0.03996	0.02269
0.70	0.03493	0.01987
0.75	0.02915	0.01691
0.80	0.02338	0.01398
1.00	0.0	0.0

125209-24-168

ORIGINAL PAGE IS  
OF POOR QUALITY

Table 1. Wing Coordinates (Continued)

$\frac{X_w}{C_w}$	$\frac{Y_{UPPER}}{C_w}$	$\frac{Y_{LOWER}}{C_w}$
0.00	-0.00128	0.00125
0.01	0.00928	0.00678
0.02	0.01429	0.00894
0.03	0.01798	0.00797
0.05	0.02331	0.00988
0.10	0.03210	0.01388
0.15	0.03828	0.01742
0.20	0.04289	0.02063
0.25	0.04622	0.02362
0.30	0.04870	0.02624
0.35	0.05060	0.02820
0.40	0.05180	0.02909
0.45	0.05208	0.02912
0.50	0.05164	0.02840
0.55	0.05023	0.02687
0.60	0.04779	0.02488
0.65	0.04429	0.02251
0.70	0.03999	0.01983
0.75	0.03488	0.01636
0.80	0.02877	0.01265
1.00	0.0	0.0

12500-24-102

ORIGINAL PAGE 13  
OF POOR QUALITY

Table 1. Wing Coordinates (Continued)

WBL 470		$C_w = 952\text{cm} (374.84 \text{ in})$
$X_w / C_w$	$Y_{UPPER} / C_w$	
0.00	-0.00171	
0.10	0.03190	
0.20	0.04246	
0.30	0.04803	
0.40	0.05078	
0.50	0.04990	
0.60	0.04839	
0.70	0.03889	
0.80	0.02628	
1.00	0.0	

WBL 834		$C_w = 619.49\text{cm} (243.89 \text{ in})$
$X_w / C_w$	$Y_{UPPER} / C_w$	
0.00	0.0	
0.10	0.03801	
0.20	0.04797	
0.30	0.05289	
0.40	0.05551	
0.50	0.05418	
0.60	0.04937	
0.70	0.04126	
0.80	0.03009	
1.00	0.0	

FAIRING	
-0.128	-0.029
-0.087	-0.015
-0.028	0.008
0.037	0.015

123209-24-170

ORIGINAL PAGE IS  
OF POOR QUALITY

Table 1. Wing Coordinates (Continued)

WBL 809 $C_w = 646.29 \text{ cm} (252.08 \text{ in})$		
$\frac{X_w}{C_w}$	$\frac{Y_{UPPER}}{C_w}$	$\frac{Y_{LOWER}}{C_w}$
0.00	0.0	0.0
0.01	0.01135	0.00464
0.02	0.01674	0.00536
0.03	0.02142	0.00599
0.05	0.02701	0.00722
0.10	0.03705	0.01043
0.15	0.04296	0.01377
0.20	0.04717	0.01706
0.25	0.05014	0.02011
0.30	0.05228	0.02269
0.35	0.05371	0.02440
0.40	0.05468	0.02511
0.45	0.05470	0.02491
0.50	0.05387	0.02400
0.55	0.06201	0.02249
0.60	0.04919	0.02023
0.65	0.04554	0.01817
0.70	0.04114	0.01658
0.75	0.03598	0.01297
0.80	0.03003	0.01037
1.00	0.0	0.0

125208-24-171

ORIGINAL PAGE IS  
OF POOR QUALITY

Table 1. Wing Coordinates (Concluded)

$\frac{X_w}{C_w}$	$\frac{Y_{UPPER}}{C_w}$	$\frac{Y_{LOWER}}{C_w}$
0.00	-0.00140	0.00140
0.01	0.01034	0.00617
0.02	0.01591	0.00689
0.03	0.02008	0.00763
0.05	0.02723	0.00881
0.10	0.03685	0.01204
0.15	0.04298	0.01528
0.20	0.04715	0.01842
0.25	0.05017	0.02128
0.30	0.05234	0.02366
0.35	0.05383	0.02611
0.40	0.05476	0.02657
0.45	0.05498	0.02619
0.50	0.05417	0.02404
0.55	0.05238	0.02238
0.60	0.04966	0.02026
0.65	0.04608	0.01774
0.70	0.04183	0.01499
0.75	0.03685	0.01226
0.80	0.03093	0.00963
1.00	0.00140	-0.00140

126293-24-172

ORIGINAL PAGE IS  
OF POOR QUALITY

125209-484

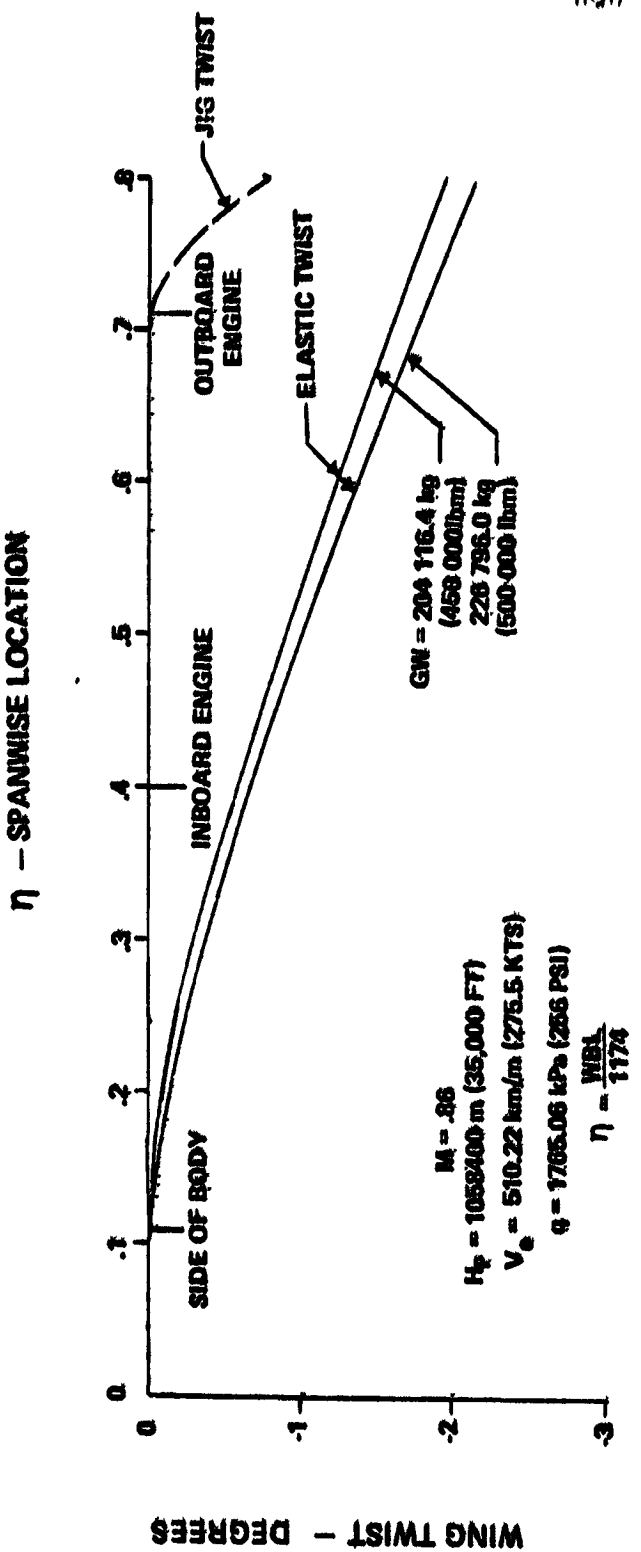


Figure 7. 747 Elastic Wing Twist

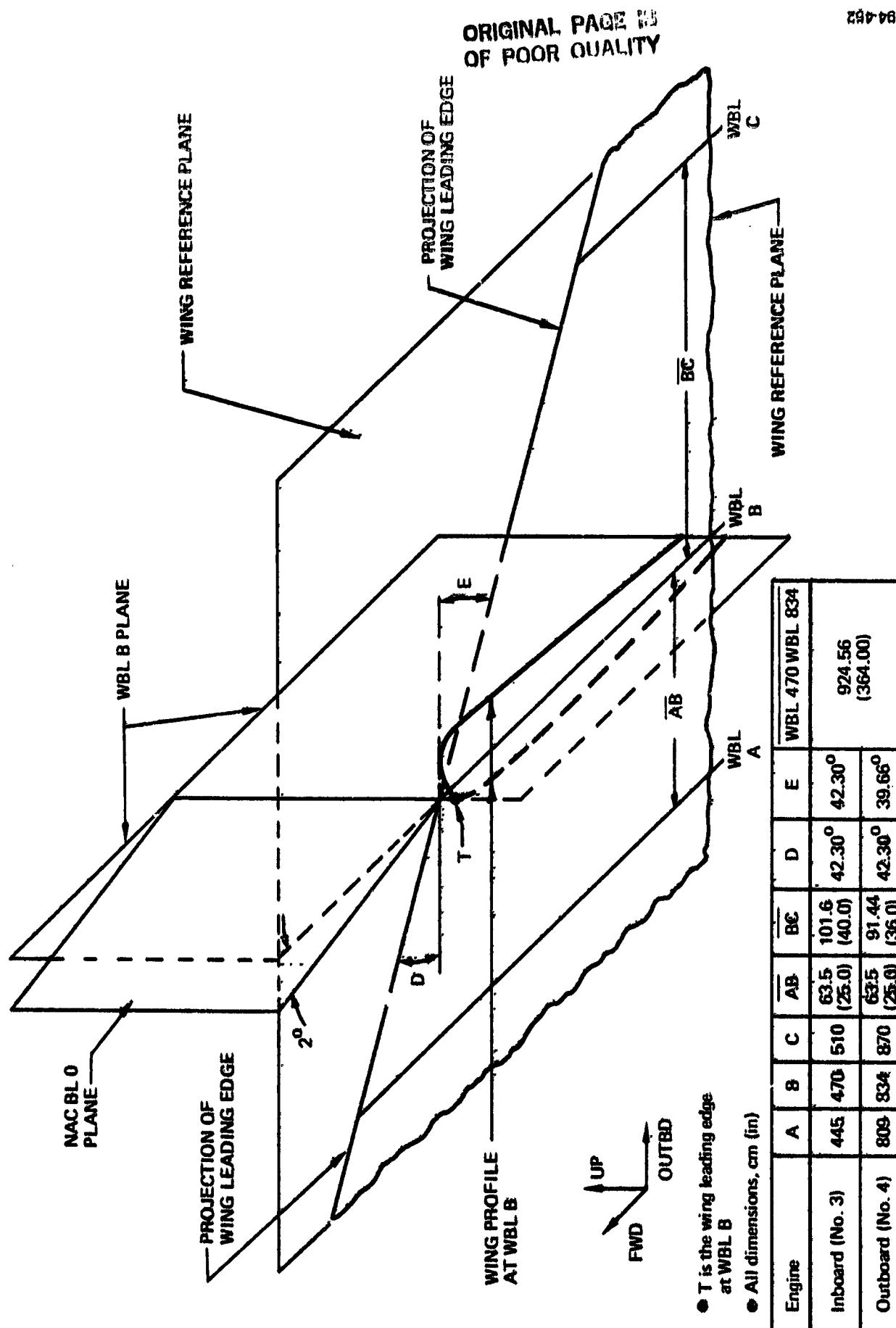
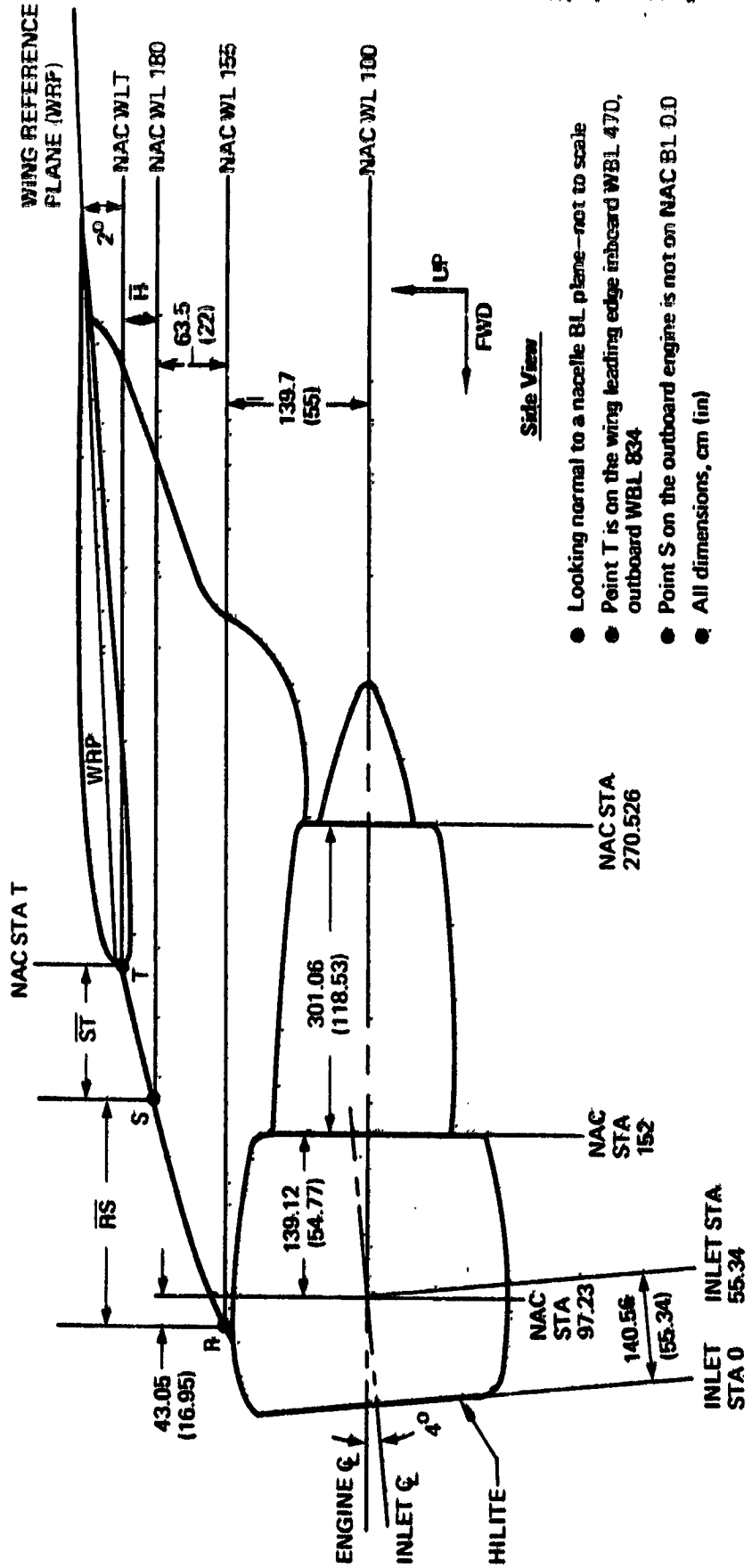


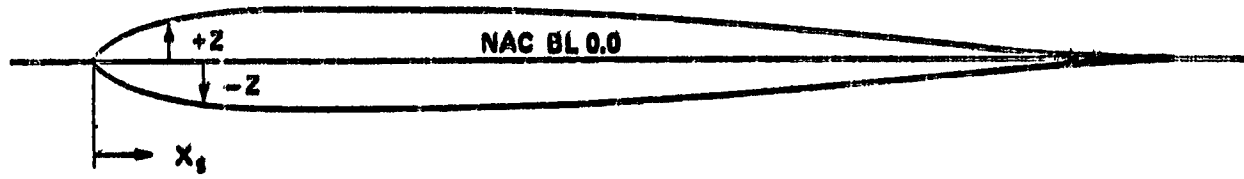
Figure 8. Wing Coordinate System



Engine	$\bar{R}\bar{S}$	$\bar{S}\bar{T}$	$\bar{H}\bar{T}$	T
Inboard (No. 3)	242.11 (95.32)	102.92 (40.52)	32.66 (12.86)	NAC STA 216.12 NAC WL 192.86 NAC BL 0.0
Outboard (No. 4)	225.45 (88.76)	94.13 (37.06)	22.86 (9.00)	NAC STA 216.10 NAC WL 189.00 NAC BL 0.0

Figure 9. Nacelle Coordinate System

Table 2. Engine 3 Pylon Coordinates



NAC WL 155 C<sub>s</sub> = 735.43cm (289.54 in)

$\frac{X_s}{C_s}$	$\frac{\pm Z}{C_s}$
0.0	0.0
0.0163	0.01160
0.0336	0.01696
0.0508	0.01889
0.0681	0.02110
0.1199	0.02549
0.2063	0.03046
0.3099	0.03447
0.3962	0.03658
0.4826	0.03768
0.5344	0.03786
0.5689	0.03782
0.6725	0.03271
0.7589	0.02601
0.8970	0.01140
1.0	0.0

NAC WL 180 C<sub>s</sub> = 722.91cm (284.61 in)

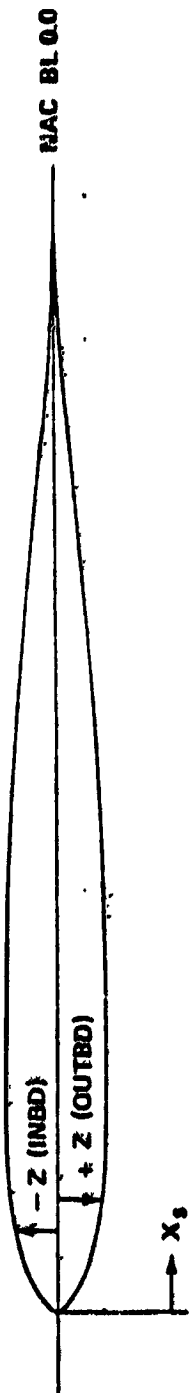
$\frac{X_s}{C_s}$	$\frac{\pm Z}{C_s}$
0.0	0.0
0.0155	0.01511
0.0330	0.02161
0.0606	0.02582
0.0887	0.03380
0.1033	0.03672
0.1209	0.03926
0.1560	0.04343
0.2087	0.04778
0.2614	0.05036
0.2966	0.05109
0.3493	0.05119
0.4722	0.05036
0.5074	0.04887
0.6479	0.03738
0.7886	0.02245
1.0	0.0

125-39-24-173

ORIGINAL PAGE IS  
OF POOR QUALITY

125209-24-17A

Table 3. Engine 4 Pylon Coordinates



$\frac{X_s}{C_s}$	$\frac{\pm Z}{C_s}$	MAC WL 155 $C_s = 684.30\text{cm} (269.41\text{ in})$	
		$\frac{-Z}{C_s}$	$\frac{+Z}{C_s}$
0.0	0.0	0.0	0.0
0.0361	0.011715	0.0459	-0.015336
0.0546	0.022939	0.0693	0.02150
0.0732	0.022268	0.0875	0.02818
0.1289	0.02739	0.1084	0.03323
0.2217	0.03274	0.1151	0.03720
0.3330	0.03704	0.1171	0.04396
0.4258	0.03891	0.12754	0.04671
0.5186	0.04650	0.2754	0.05677
0.6939	0.03983	0.3399	0.05982
0.8971	0.03015	0.3797	0.06070
0.7728	0.03062	0.5984	0.04959
0.8156	0.02153	0.6302	0.04483
0.8898	0.01734	0.8189	0.02204
1.0	0.00	0.9612	0.00434
		0.9999	0.0

$\frac{X_s}{C_s}$	$\frac{\pm Z}{C_s}$	NAC WL 180 $C_s = 602.46\text{cm} (239.55\text{ in})$	
		$\frac{-Z}{C_s}$	$\frac{+Z}{C_s}$
0.0	0.0	0.01538	0.01538
0.0361	0.0459	0.03615	0.03615
0.0546	0.0693	0.03707	0.03707
0.0732	0.0875	0.03893	0.03893
0.1289	0.1084	0.04098	0.04098
0.2217	0.1151	0.04513	0.04513
0.3330	0.1171	0.04721	0.04721
0.4258	0.12754	0.05677	0.05677
0.5186	0.2754	0.05982	0.05982
0.6939	0.3399	0.06070	0.06070
0.8971	0.3797	0.04959	0.04959
0.7728	0.5984	0.04483	0.04483
0.8156	0.6302	0.02204	0.02204
0.8898	0.8189	0.00434	0.00434
1.0	0.9612	0.0	0.0

water line (NAC WL) planes, which are perpendicular to the NAC BL 0.0 plane and pitched up to 2 deg relative to the WRP.

The proper orientation of each NAC WL plane containing the coordinates in tables 2 and 3 is achieved by first locating the reference NAC WL T plane (fig. 9) which passes through the wing leading edge at WBL 470/834. The leading-edge point may be located relative to the WRP by using coordinates given in table 1. This reference NAC WL corresponds to NAC WL 192.86 for the inboard engine and NAC WL 189.00 for the outboard engine. Coordinates defining the pylon cross-sectional profile are given for both engine pylons at NAC WL 155 and NAC WL 180. These NAC WLs can be located from the reference NAC WL for each engine (fig. 9).

Each nacelle coordinate system is an isolated coordinate system. To provide for the proper position of each engine NAC WL relative to the other, the reference NAC WL plane must be positioned to account for the difference in elevation between the inboard and outboard engine installations due to WRP dihedral.

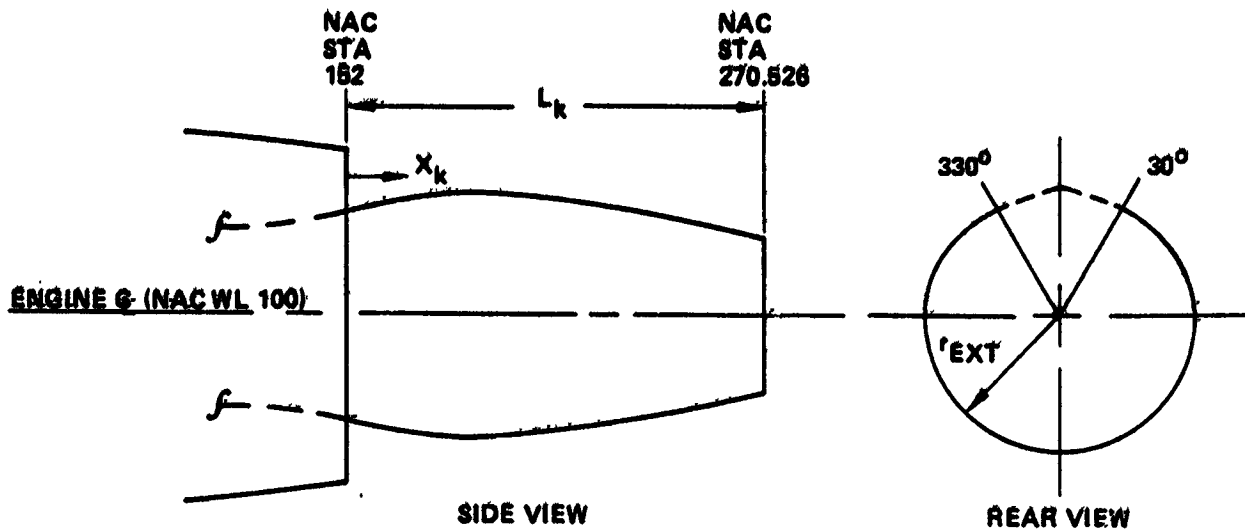
The fore and aft positions of NAC WL 155 and 180 profiles on each pylon are found by locating a reference nacelle station (NAC STA) passing through the wing leading-edge point at WBL 470 (inboard) or WBL 834 (outboard). Lines representing NAC STA are perpendicular to the intersection of a NAC WL plane and NAC BL 0.0 plane; distances between NAC STA are measured parallel to the intersection. At point T, the NAC STA reference for the inboard pylon is 216.12; for the outboard pylon, 206.10 (fig. 9).

The outboard pylon pressure port row at NAC WL 180 has an unsymmetric profile (table 3). The contour of the fairing at WBL 834 shifts the pylon leading edge to the inboard side of NAC BL 0.0.

The inlet, fan cowl, and core cowl surface geometries are the same on both engines. Each engine centerline is coincident with NAC WL 100. The core cowl is a body of revolution between 30 and 330 deg. (table 4). This cowl is defined by radii measured from NAC WL 100 at points between NAC STA 152 and NAC STA 270.526. The inlet and fan cowl profiles are given along constant inlet angles measured about the inlet centerline, which lies in the NAC BL 0.0 plane, pitched down (drooped) 4 deg relative to the engine centerline at NAC STA 97.23 (fig. 9). The fan inlet cross-sectional profile coordinates (table 5) are measured along and perpendicular to the inlet axis for five circumferential

ORIGINAL PAGE IS  
OF POOR QUALITY

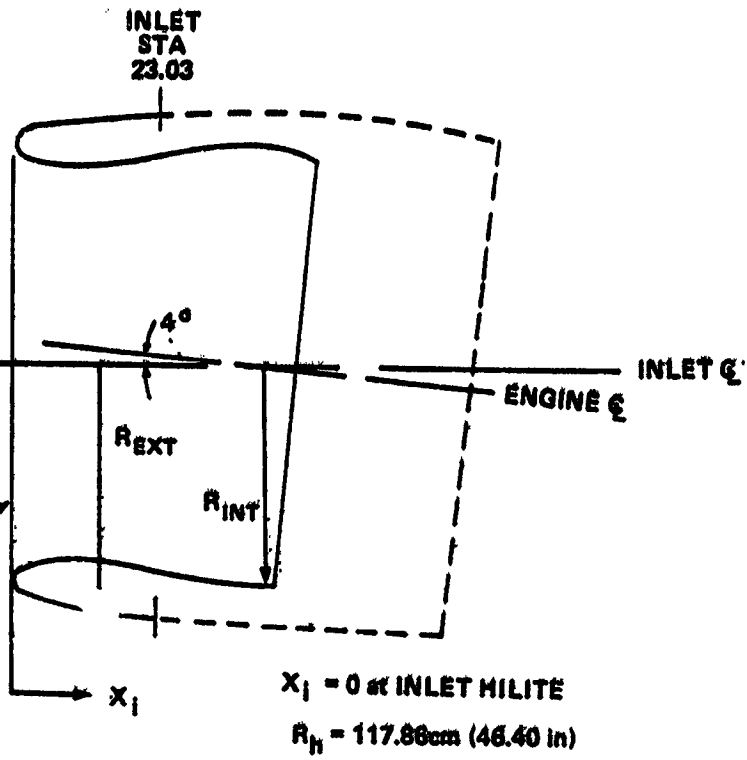
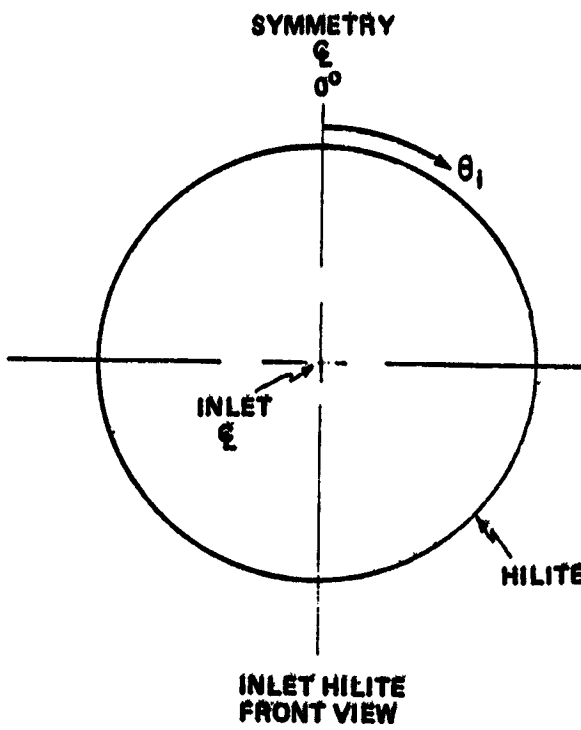
Table 4. Engines 3 and 4 Core Cowl Coordinates



$x_k = 0$ at NAC STA 152, $L_k = 301.07$ cm (118.53 in)			
$x_k / L_k$	$r_{EXT} / L_k$	$x_k / L_k$	$r_{EXT} / L_k$
0.0	0.2867	0.6834	0.2602
0.0338	0.2868	0.6918	0.2592
0.1519	0.2829	0.7003	0.2582
0.2362	0.2811	0.7425	0.2528
0.2953	0.2799	0.7762	0.2481
0.3797	0.2782	0.8100	0.2429
0.4472	0.2764	0.8353	0.2388
0.4978	0.2746	0.8690	0.2329
0.5315	0.2708	0.9028	0.2257
0.5653	0.2696	0.9196	0.2236
0.5822	0.2697	0.9634	0.2158
0.6243	0.2696	0.9966	0.2080
0.6497	0.2638	1.0000	0.2070

Table 5. Engines 3 and 4 Inlet Coordinates

ORIGINAL PAGE IS  
OF POOR QUALITY



$\theta_i = 30$

$X_i / R_h$	$R_{EXT} / R_h$	$R_{INT} / R_h$
0.2651		0.8957
0.1853		0.8991
0.1196		0.9094
0.0776		0.9217
0.0302		0.9461
0.0037		0.9786
0.0	1.0000	1.0000
0.0069	1.0158	
0.0248	1.0303	
0.0647	1.0493	
0.1379	1.0714	
0.2185	1.0877	
0.3448	1.1061	
0.4963	1.1200	

$\theta_i = 60$

$X_i / R_h$	$R_{EXT} / R_h$	$R_{INT} / R_h$
1.2874		1.0000
1.1222		1.0072
0.7813		0.9645
0.5563		0.9158
0.4019		0.8998
0.2651		0.8957
0.1196		0.9094
0.0302		0.9461
0.0	1.0000	1.0000
0.0647	1.0493	
0.1379	1.0714	
0.3448	1.1061	
0.4963	1.1200	

125209-24-175

Table 5. Engines 3 and 4 Inlet Coordinates (Concluded)

$\theta_i = 90$			$\theta_i = 150$		
$x_i / R_h$	$R_{EXT} / R_h$	$R_{INT} / R_h$	$x_i / R_h$	$R_{EXT} / R_h$	$R_{INT} / R_h$
0.2651		0.8957	0.2651		0.8957
0.1853		0.8991	0.1853		0.9004
0.1198		0.9094	0.1198		0.9126
0.0778		0.9217	0.0778		0.9261
0.0302		0.9461	0.0302		0.9518
0.0037		0.9788	0.0037		0.9829
0.0	1.0000	1.0000	0.0	1.0000	1.0000
0.0069	1.0158		0.0069	1.0158	
0.0248	1.0303		0.0248	1.0303	
0.0647	1.0493		0.0647	1.0493	
0.1379	1.0714		0.1379	1.0714	
0.2155	1.0877		0.2155	1.0877	
0.3448	1.1061		0.3448	1.1061	
0.4963	1.1200		0.4963	1.1200	

$\theta_i = 180$		
$x_i / R_h$	$R_{EXT} / R_h$	$R_{INT} / R_h$
1.1822		1.0044
1.1222		1.0072
0.7813		0.9546
0.8563		0.9158
0.4019		0.8998
0.2651		0.8957
0.1198		0.9126
0.0302		0.9518
0.0	1.0000	1.0000
0.0647	1.0493	
0.1379	1.0714	
0.3448	1.1061	
0.4963	1.1200	

ORIGINAL PAGE IS  
OF POOR QUALITY

angles measured about the inlet centerline. At these same inlet angles, the fan cowl cross-sectional profiles are defined relative to the engine centerline. Coordinates in table 6 give the angle about the engine centerline for each point with the distance to the surface measured along and perpendicular to NAC WL 100.

Pylon-fan cowl, pylon-core cowl, and wing-pylon intersections are defined along axes of the nacelle coordinate system (tables 7 through 10). These tables include the information necessary to locate these intersections. The pylon-core cowl intersection is separated into three sections between NAC STA 220 and 270.526 to define a pylon-core cowl fairing surface (table 10).

The pressure orifice positions on the defined profiles are given in tables 11 through 16. A pressure orifice is found in the profile plane at the intersection of the aircraft surface and a line normal to the X direction at the nondimensional position given by X/C or X/L.

#### 4.1.2 Instrumentation

The NAIL program was an ambitious undertaking in terms of number of measurements obtained. There were 693 pressure measurements, 30 accelerometers, 7 rate gyros, 12 blade clearance measurements, and 20 thermocouples for required test data. Numerous thermocouples were used to provide temperature information on heat-sensitive instrumentation. Finally, expanded engine performance data were provided by an additional 68 measurement channels. The quantity and quality of the data obtained were excellent.

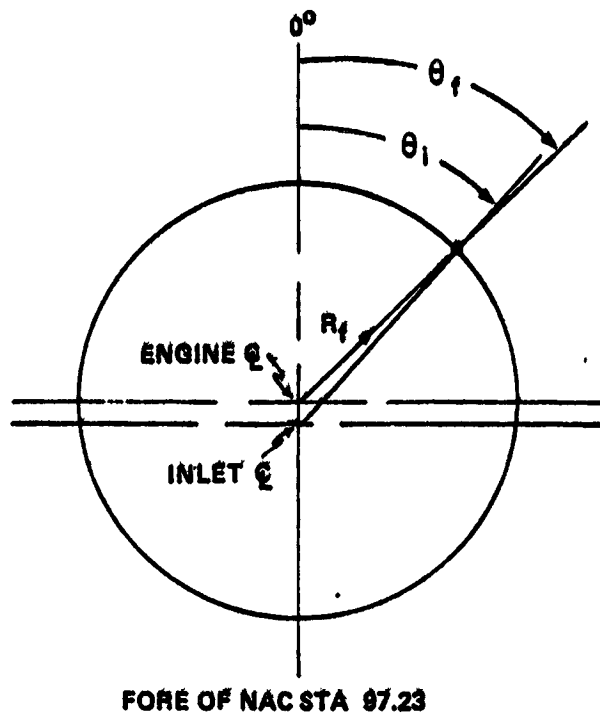
Instrumentation placed on or near the numbers 3 and 4 engine and pylon was designed to further the understanding of the flight loads (cause) and engine clearance changes (effect) associated with engine deterioration and to provide information on the flight environment of the engine and wing interface.

##### 4.1.2.1 Flight Loads

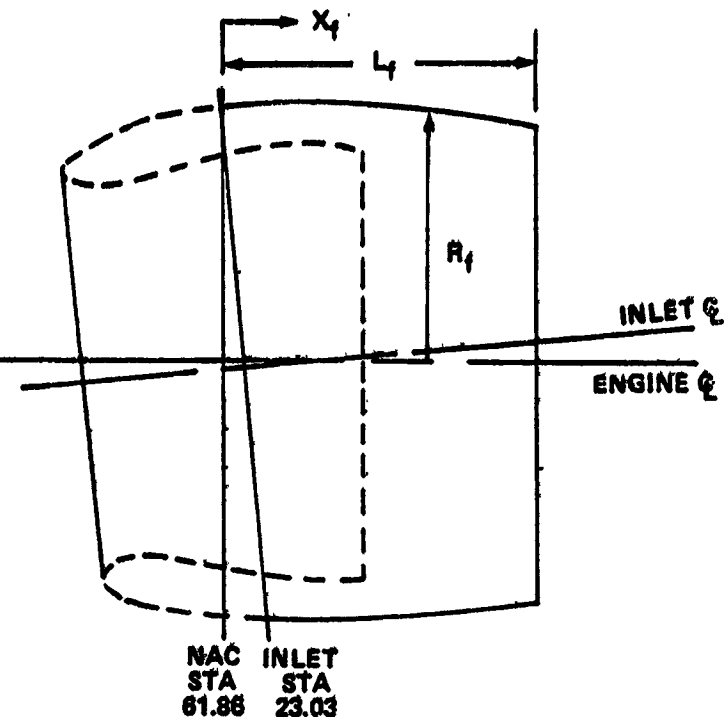
**Pressure Instrumentation**—Most of the pressure instrumentation was placed on the inlet of engine 3 (figs. 10 and 11). It was believed that the inboard engine was subject to higher angles of attack than the outboard engine because wing bending reduced the incidence of the outboard nacelle and because the outboard nacelle was less affected by upflow induced by the wing flaps. Therefore, the inboard nacelle sustained greater loads and was chosen for a more detailed survey using 252 pressure taps.

ORIGINAL PAGE IS  
OF POOR QUALITY

Table 6. Engines 3 and 4 Fan Cowl Coordinates



FORE OF NAC STA 97.23



$x_f = 0$  at NAC STA 61.86

$L_f = 228.96\text{cm}$  (90.14 in)

$\theta_i = 30$

$\theta_f$	$\frac{x_f}{L_f}$	$\frac{R_f}{L_f}$
31.356	0.0	0.5640
30.928	0.1126	0.5663
30.568	0.2123	0.5732
29.976	0.3821	0.5771
29.261	0.5851	0.5875
28.483	0.7892	0.5447
28.168	0.8669	0.5358
27.579	1.0000	0.5148

$\theta_i = 60$

$\theta_f$	$\frac{x_f}{L_f}$	$\frac{R_f}{L_f}$
62.262	0.0147	0.5641
61.634	0.1126	0.5727
60.020	0.2123	0.5781
60.001	0.3821	0.5802
58.843	1.0000	0.5148

ORIGINAL PAGE IS  
OF POOR QUALITY

Table 6. Engines 3 and 4 Fan Cowl Coordinates (Concluded)

$\theta_i = 90$

$\theta_f$	$\frac{X_f}{L_f}$	$\frac{R_f}{L_f}$
92.483	0.0349	0.5771
91.929	0.1125	0.5816
91.234	0.2123	0.5846
90.071	0.3821	0.5835
88.642	0.5851	0.5885
87.080	0.7892	0.8446
86.449	0.8669	0.5358
85.265	1.0000	0.5148

$\theta_i = 150$

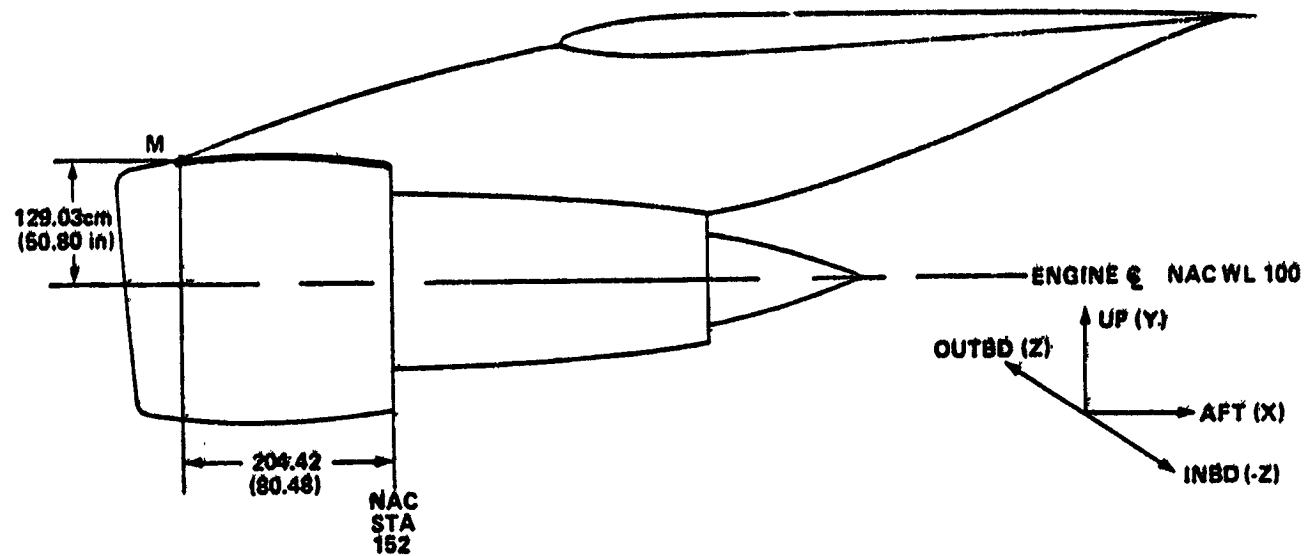
$\theta_f$	$\frac{X_f}{L_f}$	$\frac{R_f}{L_f}$
151.141	0.0697	0.5873
150.997	0.1125	0.5874
150.665	0.2123	0.5857
150.096	0.3821	0.5865
149.383	0.5851	0.5887
148.603	0.7892	0.5446
148.289	0.8669	0.5358
147.700	1.0000	0.5148

$\theta_i = 180$

$\theta_f$	$\frac{X_f}{L_f}$	$\frac{R_f}{L_f}$
180.000	0.0771	0.6001
180.000	0.1125	0.6000
180.000	0.2123	0.5978
180.000	0.3821	0.5867
180.000	1.0000	0.5148

ORIGINAL PAGE IS  
OF POOR QUALITY

Table 7. Engines 3 and 4 Pylon-Fan Cowl Intersection



$$C_m = 206.080 \text{ cm (81.134 in)}$$

$$X, Y = 0 @ m$$

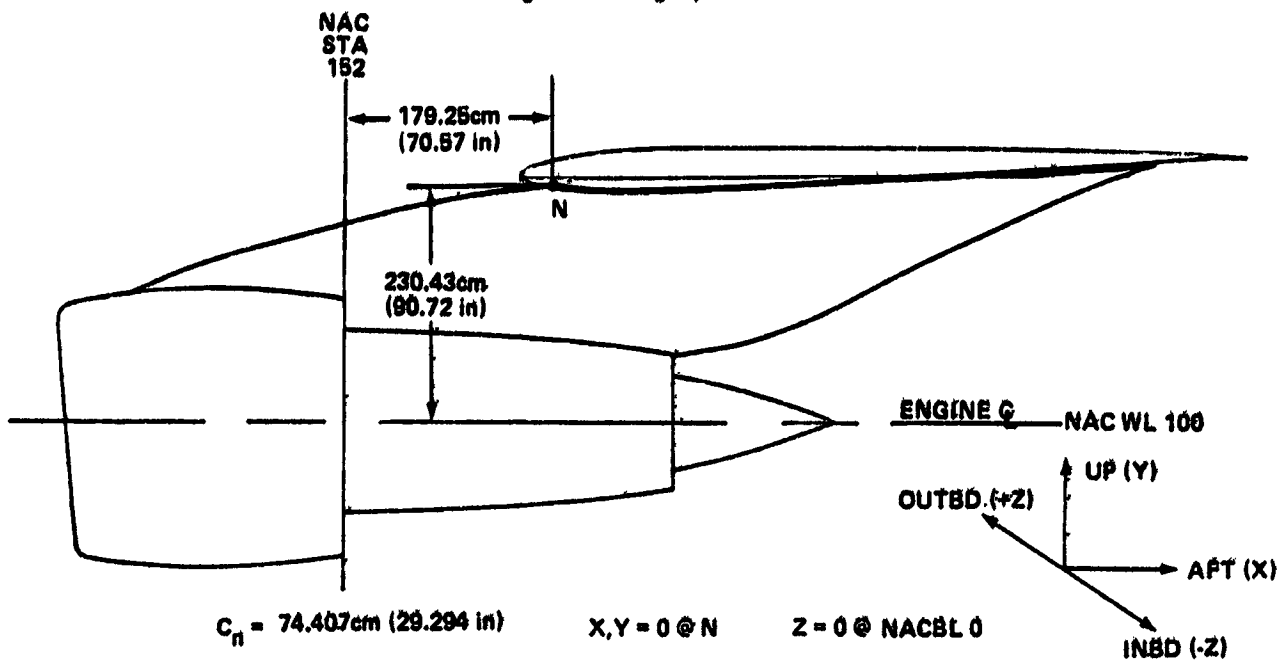
$$Z = 0 @ NAC BL 0$$

X/C <sub>m</sub>	Y/C <sub>m</sub>	$\pm Z/C_m$
0.0	0.0	0.0
0.1661	0.00801	0.0620
0.2894	0.00900	0.0779
0.4127	0.00579	0.0886
0.5369	-0.00345	0.0959
0.6715	-0.02305	0.1019
0.8437	-0.04055	0.1071
0.9919	-0.06471	0.1090

125208-26-181

ORIGINAL PAGE IS  
OF POOR QUALITY

Table 8. Engine 3 Wing-Pylon Intersection

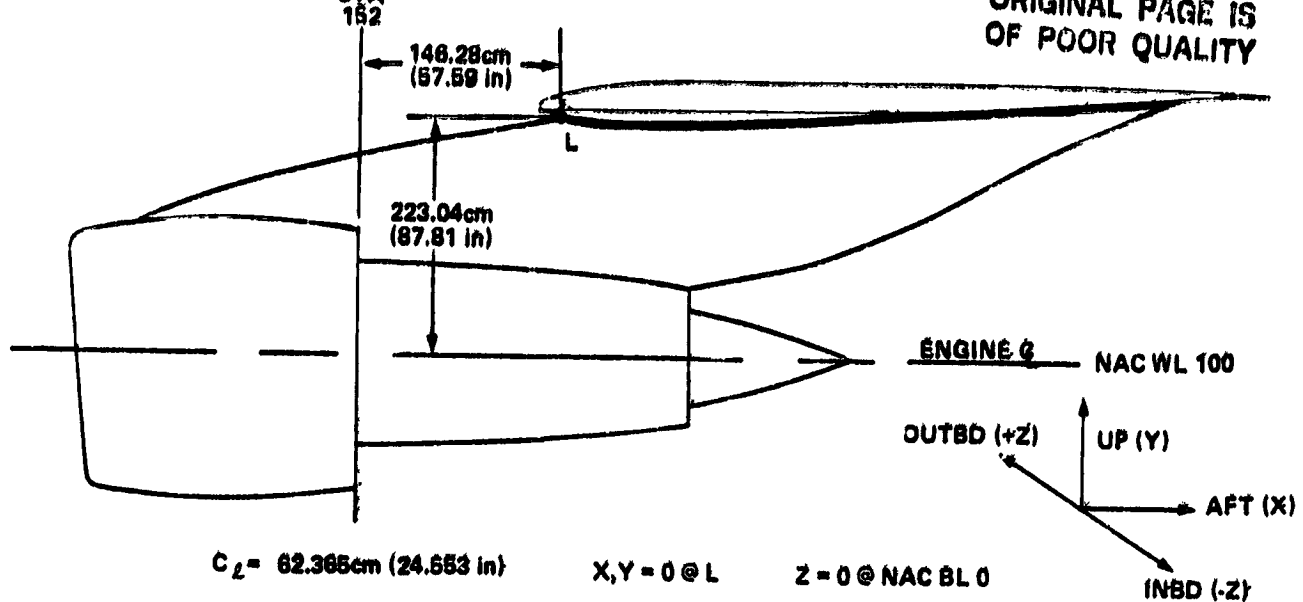


OUTBOARD		
$X/C_n$	$Y/C_n$	$Z/C_n$
0.0000	-0.0751	0.0000
0.0075	-0.0297	0.0051
0.0553	0.0703	0.0133
0.1167	0.1369	0.0187
0.2195	0.2123	0.0181
0.3304	0.2762	0.0171
0.4809	0.3451	0.0133
0.6923	0.4117	0.0068
1.0077	0.4813	-0.0038
1.8171	0.6456	-0.0324
4.5412	0.4772	-0.0922
5.3294	0.4120	-0.0802
6.1500	0.3400	-0.0486
6.9789	0.2748	0.0024
8.0122	0.2014	0.0830
8.9316	0.1369	0.1648
9.8572	0.0679	0.2284
10.0000	0.0000	0.2745

INBOARD		
$X/C_n$	$Y/C_n$	$Z/C_n$
0.0000	-0.0751	0.0000
0.0109	-0.1375	-0.0089
0.0536	-0.2048	-0.0205
0.1403	-0.2751	-0.0348
0.2823	-0.3458	-0.0509
0.4909	-0.4120	-0.0690
0.8462	-0.4793	-0.0915
1.7044	-0.5318	-0.1260
3.6137	-0.5179	-0.1526
4.2818	-0.4803	-0.1417
5.2533	-0.4100	-0.1048
6.0623	-0.3441	-0.0608
6.9789	-0.2758	0.0048
8.0122	-0.2038	0.0884
8.9316	-0.1379	0.1703
9.8572	-0.0690	0.2311
10.0000	0.0000	0.2745

Table 9. Engine 4 Wing-Pylon Intersection

ORIGINAL PAGE IS  
OF POOR QUALITY



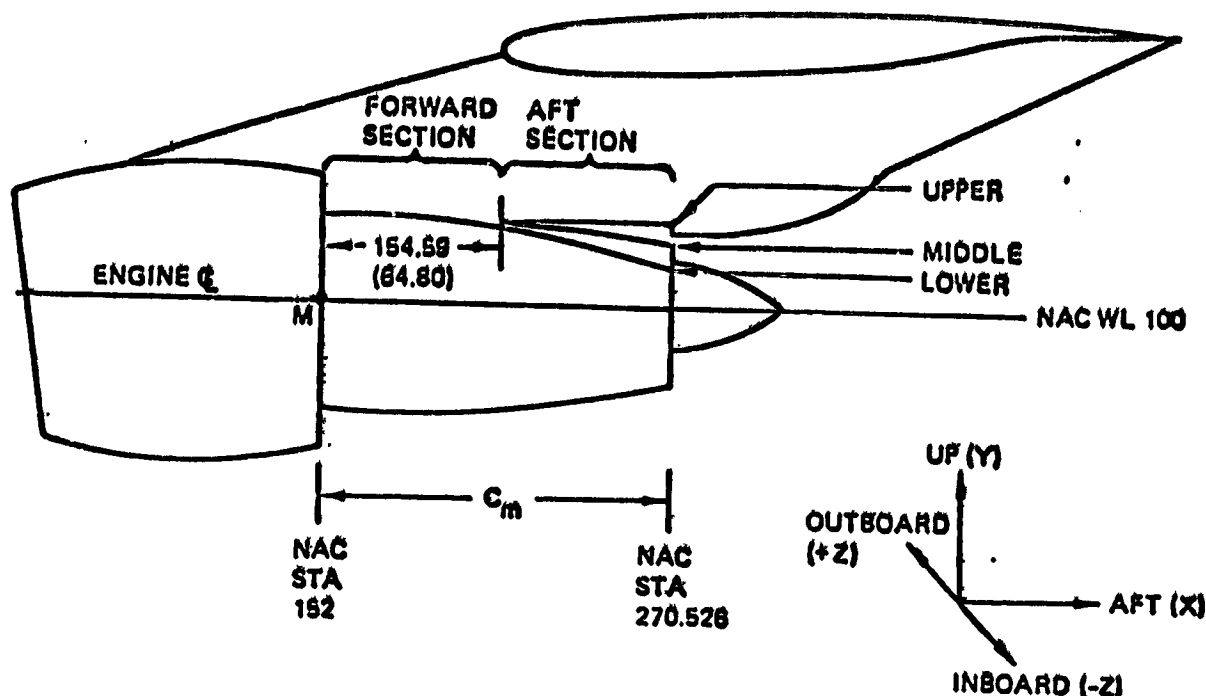
CUTBOARD		
$X/C_L$	$Y/C_L$	$Z/C_L$
0.0000	-0.0411	0.0000
0.0049	0.0000	0.0024
0.0468	0.0855	0.0065
0.1275	0.1654	0.0086
0.2366	0.2342	0.0094
0.4411	0.3275	0.0081
0.6920	0.4114	0.0049
1.0048	0.4891	-0.0004
1.5318	0.5747	-0.0118
2.5910	0.6337	-0.0391
3.5804	0.5967	-0.0546
4.0138	0.5653	-0.0509
4.8597	0.4883	-0.0216
5.6688	0.4077	-0.0209
6.4273	0.3340	0.0863
7.3498	0.2484	0.1682
8.2727	0.1637	0.2501
9.1962	0.0786	0.3319
10.0000	0.0045	0.4036

INBOARD		
$X/C_L$	$Y/C_L$	$Z/C_L$
0.0000	-0.0411	0.0000
0.0053	-0.0819	-0.0029
0.0525	-0.1637	-0.0090
0.1592	-0.2484	-0.0171
0.3063	-0.3234	-0.0261
0.5441	-0.4086	-0.0383
0.8590	-0.4863	-0.0521
1.4096	-0.5698	-0.0729
2.5093	-0.6256	-0.0949
3.8724	-0.6735	-0.0644
4.9143	-0.4863	-0.0069
5.6585	-0.4134	0.0482
6.5813	-0.3268	0.1197
7.5038	-0.2391	0.1959
8.2727	-0.1686	0.2598
9.1952	-0.0823	0.3364
9.9943	-0.0063	0.4032

12509-26-183

*Table 10: Pylon-Core Cowl Intersection (To Be Submitted in Final Report)*

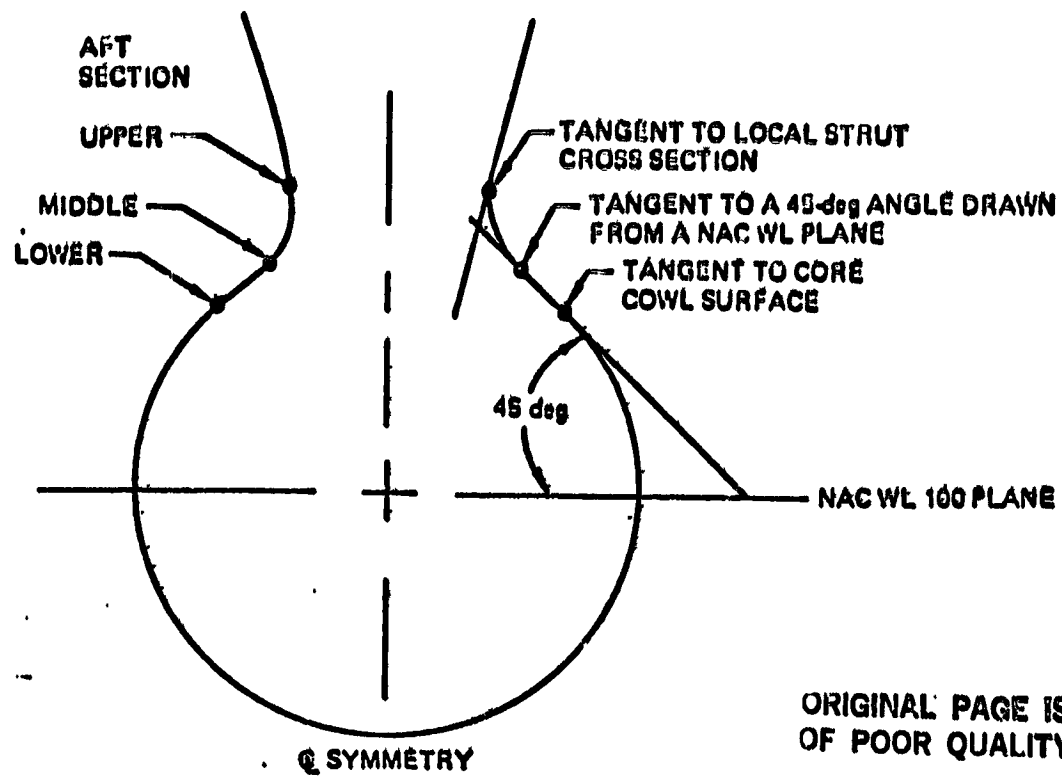
*Table 10. Pylon-Core Cowl Intersection*



$$C_m = 301.056 \text{ cm (118.526 in)} \quad X, Y = 0 \text{ at } M \quad Z = 0 \text{ at NAC BL 0}$$

FORWARD SECTION		
$X_m/C_m$	$Y_m/C_m$	$\pm Z_m/C_m$
0.0000	0.2797	0.0638
0.0377	0.2786	0.0638
0.0697	0.2780	0.0640
0.1336	0.2773	0.0643
0.1976	0.2771	0.0647
0.2296	0.2771	0.0649
0.2935	0.2771	0.0651
0.3575	0.2770	0.0653
0.3894	0.2769	0.0653
0.4454	0.2764	0.0653
0.4909	0.2754	0.0650
0.5402	0.2738	0.0631

Table 10. Pylon-Core Cowl Intersection (Concluded)

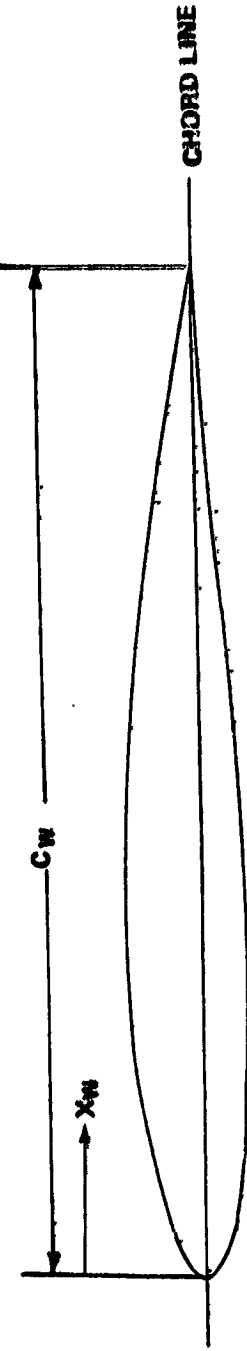


TYPICAL CROSS SECTION IN AFT SECTION  
OF STRUT-CORE COWL INTERSECTION

$C_m = 301.056 \text{ cm (118.526 in)}$   $X, Y = 0 \text{ at M}$   $Z = 0 \text{ at NAC BL0}$

AFT SECTION							
UPPER			MIDDLE		LOWER		
$X_m/C_m$	$Y_m/C_m$	$\pm Z_m/C_m$	$Y_m/C_m$	$\pm Z_m/C_m$	$Y_m/C_m$	$\pm Z_m/C_m$	
0.6737	0.2775	0.0621	0.2724	0.0639	0.2685	0.0709	
0.6159	0.2834	0.0604	0.2696	0.0657	0.2618	0.0782	
0.6581	0.2895	0.0582	0.2652	0.0672	0.2551	0.0827	
0.7003	0.2955	0.0555	0.2594	0.0683	0.2484	0.0849	
0.7159	0.2972	0.0543	0.2574	0.0681	0.2459	0.0861	
0.7333	0.2980	0.0534	0.2550	0.0676	0.2432	0.0854	
0.7425	0.2985	0.0532	0.2540	0.0672	0.2418	0.0852	
0.7845	0.2939	0.0495	0.2480	0.0641	0.2348	0.0837	
0.8268	0.2887	0.0458	0.2415	0.0597	0.2284	0.0807	
0.8690	0.2786	0.0475	0.2349	0.0540	0.2218	0.0756	
0.9112	0.2663	0.0384	0.2276	0.0473	0.2151	0.0690	
0.9534	0.2542	0.0300	0.2194	0.0406	0.2082	0.0611	
0.9956	0.2410	0.0247	0.2109	0.0337	0.2012	0.0528	
1.0000	0.2394	0.0240	0.2096	0.0332	0.2013	0.0485	

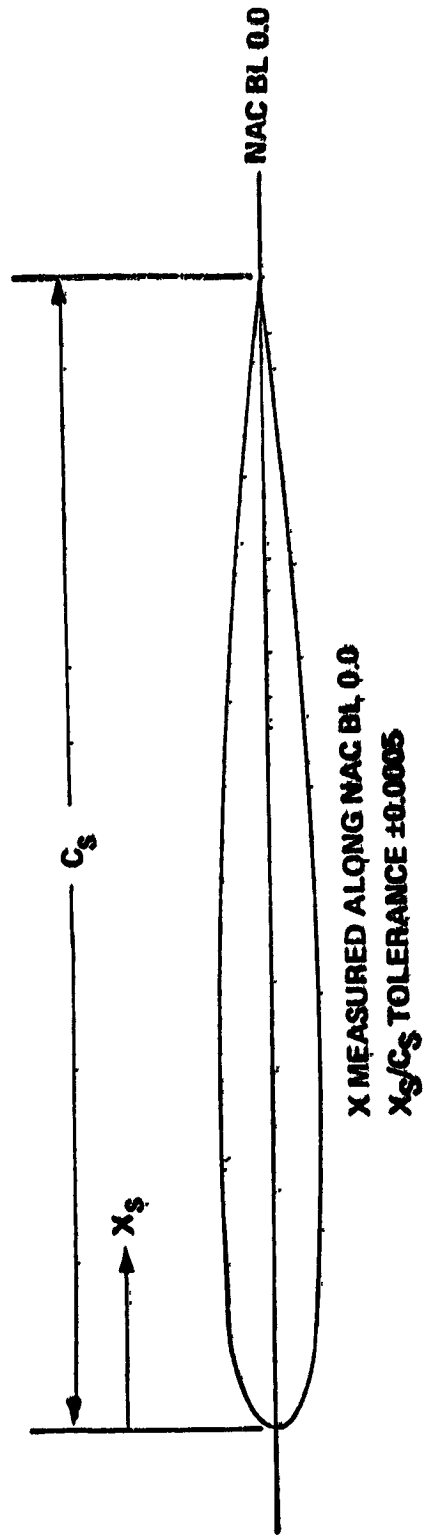
Table 11. Wing Pressure Orifice Locations



X MEASURED ALONG CHORD LINE  
 $X_W/C_W$  TOLERANCE  $\pm 0.0005$

WBL 445	WBL 470		WBL 510		WBL 834		WBL 870	
	X_W / C_W							
UPPER	LOWER	UPPER	LOWER	UPPER	LOWER	UPPER	LOWER	UPPER
FLUSH	FLUSH	FLUSH	FLUSH	FLUSH	FLUSH	FLUSH	FLUSH	FLUSH
0.0100	0.0090	0.0100	0.0090	0.0100	0.0090	0.0100	0.0090	0.0100
0.0200	0.0223	0.0200	0.0207	0.0198	0.0165	0.0200	0.0189	0.0200
0.0300	0.0320	BELT	0.0303	0.0308	0.0300	0.0300	0.0300	0.0294
0.0500	0.0492		0.0500	0.0500	0.0500	0.0500	0.0500	0.0489
0.0750	0.1000		0.0750	0.1000	0.0750	0.1015	0.1015	0.0723
0.1000	0.1500		0.1000	0.1472	0.1000	0.1500	0.1500	0.1000
0.1500	0.2000		0.1500	0.1500	0.1500	0.1500	0.1500	0.1500
0.1500	0.1500	BELT	0.1500	BELT	BELT	BELT	BELT	BELT
0.2000	0.1950		0.2000	0.1972	0.2000	0.2000	0.2000	0.2000
0.2250	0.2453		0.2250	0.2472	0.2250	0.2250	0.2250	0.2250
0.2500	0.2953		0.2500	0.2672	0.2465	0.3010	0.2500	0.3043
0.2750	0.3453		0.2750	0.3472	0.3050	0.3500	0.3100	0.3563
0.3000	0.3853		0.3000	0.3872	0.3500	0.4000	0.3510	0.4043
0.3500	0.4453		0.3500	0.4472	0.4010	0.4500	0.4000	0.4543
0.4037	0.4954		0.4037	0.4972	0.4500	0.5000	0.4500	0.5043
0.4538	0.5455		0.4538	0.4750	0.5472	0.5000	0.4750	0.5543
0.4750	0.5855		0.4750	0.5972	0.5250	0.6000	0.5000	0.6043
0.5000	0.6455		0.5000	0.5000	0.5500	0.6000	0.5250	0.6543
0.5250	0.5250		0.5250	0.5250	0.5500	0.6000	0.5500	0.6000
0.5554	0.5554		0.5554	0.6800	0.6500	0.7000	0.6500	0.6500
0.6049	0.7049		0.6049	0.6500	0.7500	0.8000	0.7000	0.7000
0.6554	0.7552		0.6554	0.7000				
0.6949	0.6949		0.6949					

Table 12. Engine 3 Pylon Pressure Office Locations



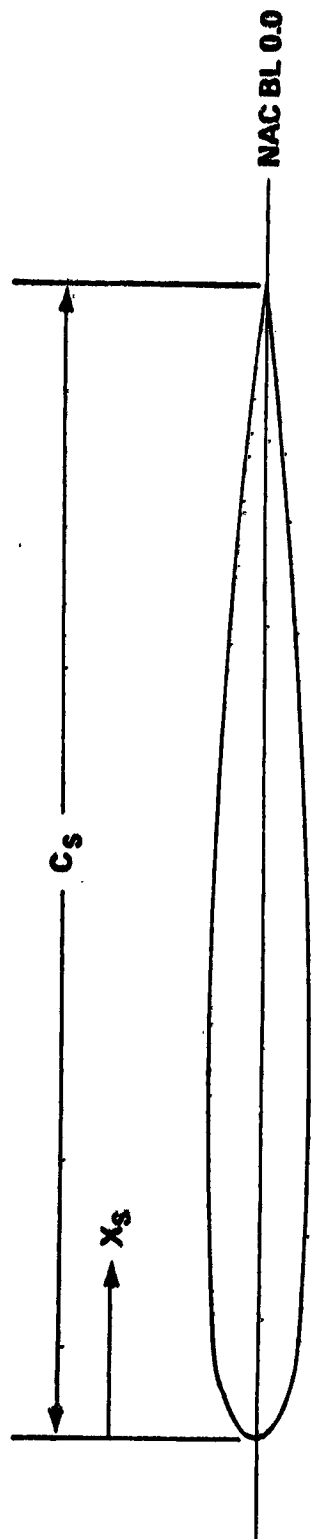
ORIGINAL PAGE IS  
OF POOR QUALITY

128292-1-188

NAC WL 155	NAC WL 180	$X_s / C_s$	$X_s / C_s$	INBD AND OUTBD	INBD AND OUTBD
0.0163	0.0168				
0.0349	0.0330				
0.0508	0.0506				
0.0750	0.0752				
0.1234	0.9898				
0.2146	0.1279				
0.3043	0.1609				
0.3938	0.2136				
0.4865	0.2614				
0.6392	0.2886				
0.5724	0.3493				
0.6207	0.4757				
0.6725	0.6514				
0.7589	0.7885				
0.8279					
0.9005					

ORIGINAL PAGE IS  
OF POOR QUALITY

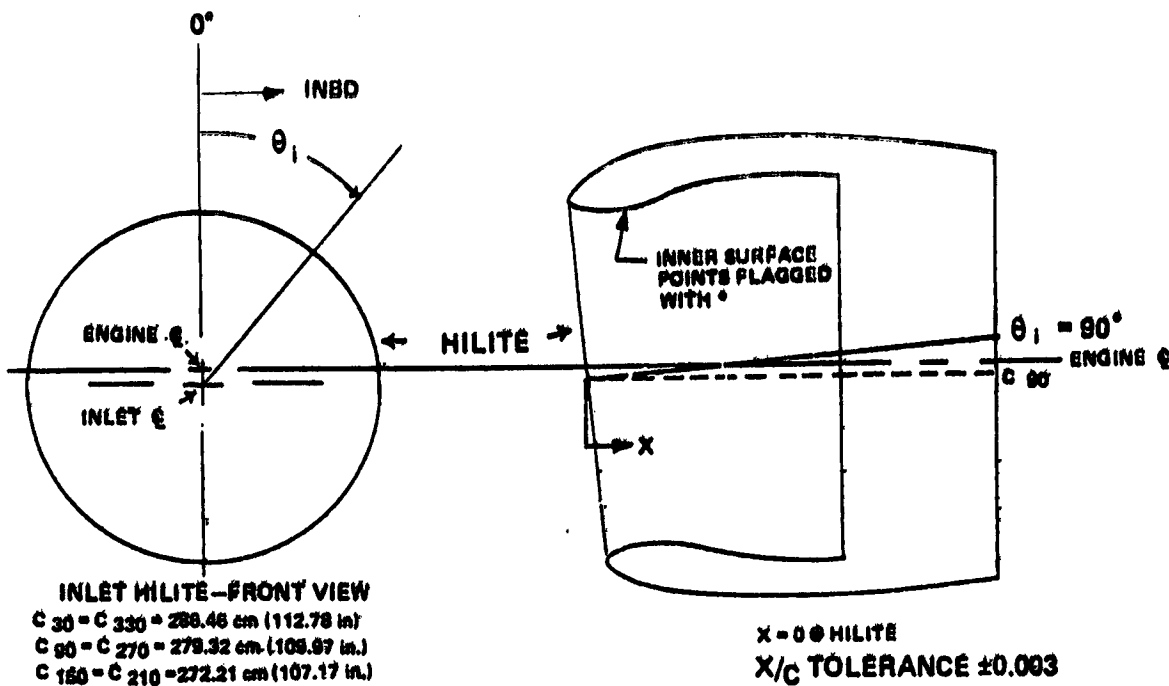
Table 13. Engine 4 Pylon Pressure Orifice Locations



X MEASURED ALONG NAC BL 0.0  
 $X_s/C_s$  TOLERANCE  $\pm 0.0005$

NAC WL 180	NAC WL 155
$X_s / C_s$	$X_s / C_s$
INBD AND OUTBD	INBD AND OUTBD
0.0175	0.0474
0.0375	0.0666
0.0546	0.0875
0.0896	0.1092
0.1326	0.1460
0.2306	0.1793
0.3321	0.2169
0.4295	0.2837
0.5229	0.3371
0.5762	0.3785
0.6237	0.4423
0.6671	0.5991
0.7228	0.8158
0.8156	0.9641
0.8998	0.9677

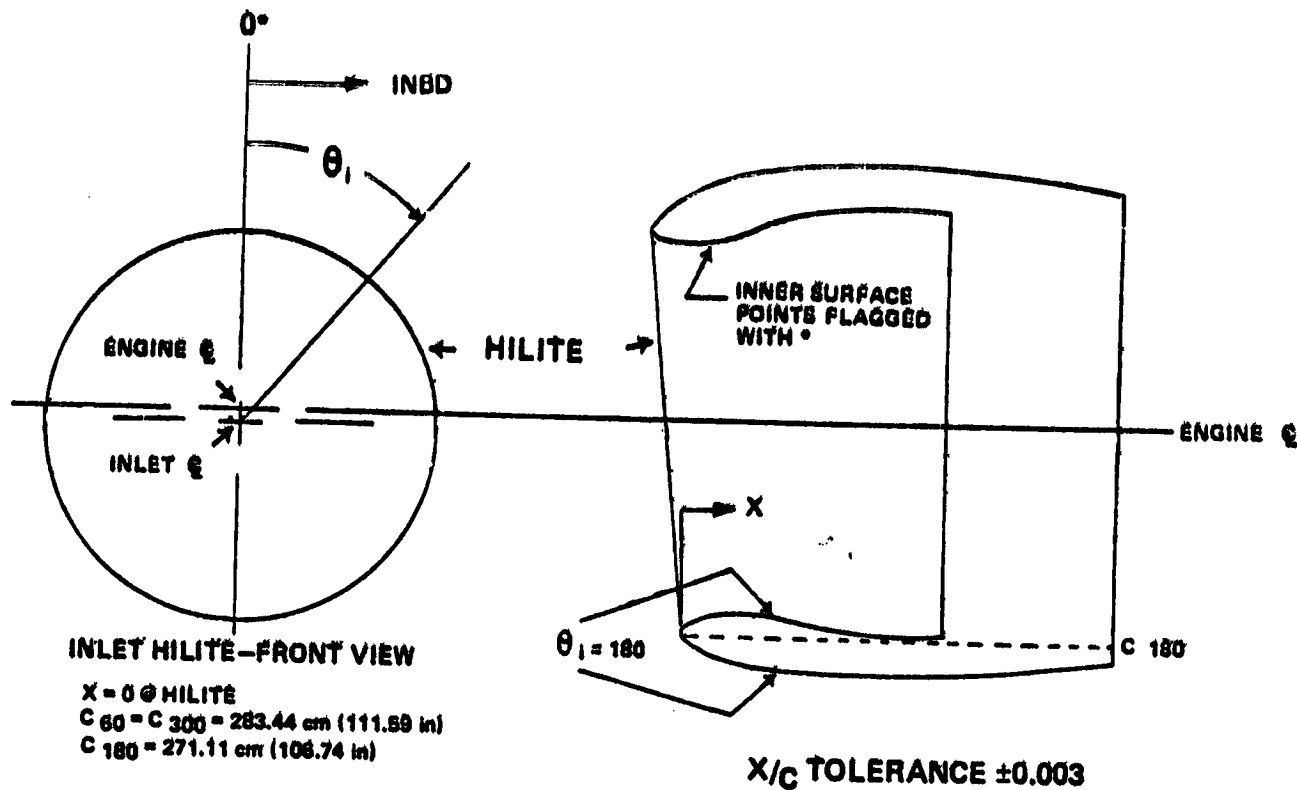
Table 14. Engine 3 Inlet Pressure Orifice Locations



$\theta_1 = 30^\circ$	$\theta_1 = 90^\circ$	$\theta_1 = 180^\circ$	$\theta_1 = 210^\circ$	$\theta_1 = 270^\circ$	$\theta_1 = 330^\circ$
$X/C$	$X/C$	$X/C$	$X/C$	$X/C$	$X/C$
0.079°	0.077°	0.080°	0.080°	0.081°	0.079°
0.051°	0.053°	0.050°	0.050°	0.055°	0.051°
0.034°	0.033°	0.034°	0.034°	0.037°	0.034°
0.014°	0.014°	0.014°	0.014°	0.014°	0.014°
0.002°	0.002°	0.002°	0.002°	0.002°	0.002°
0.000	0.000	0.000	0.000	0.000	0.000
0.004	0.004	0.005	0.005	0.004	0.004
0.010	0.011	0.012	0.012	0.011	0.010
0.025	0.028	0.030	0.030	0.028	0.026
0.056	0.061	0.063	0.062	0.062	0.056
0.086	0.091	0.095	0.095	0.090	0.086
0.122	0.128	0.146	0.146	0.128	0.122
0.168	0.174	0.183	0.181	0.172	0.178
0.212	0.227	0.227	0.224	0.218	0.214
0.261	0.277	0.277	0.276	0.267	0.262
0.336	0.348	0.345	0.343	0.339	0.337
0.467	0.463	0.458	0.465	0.463	0.464
0.572	0.576	0.571	0.569	0.567	0.570
0.646	0.647	0.639	0.639	0.639	0.646
0.718	0.719	0.710	0.708	0.711	0.718
0.824	0.824	0.813	0.810	0.816	0.827
0.994	0.997	0.994	0.991	0.990	0.994

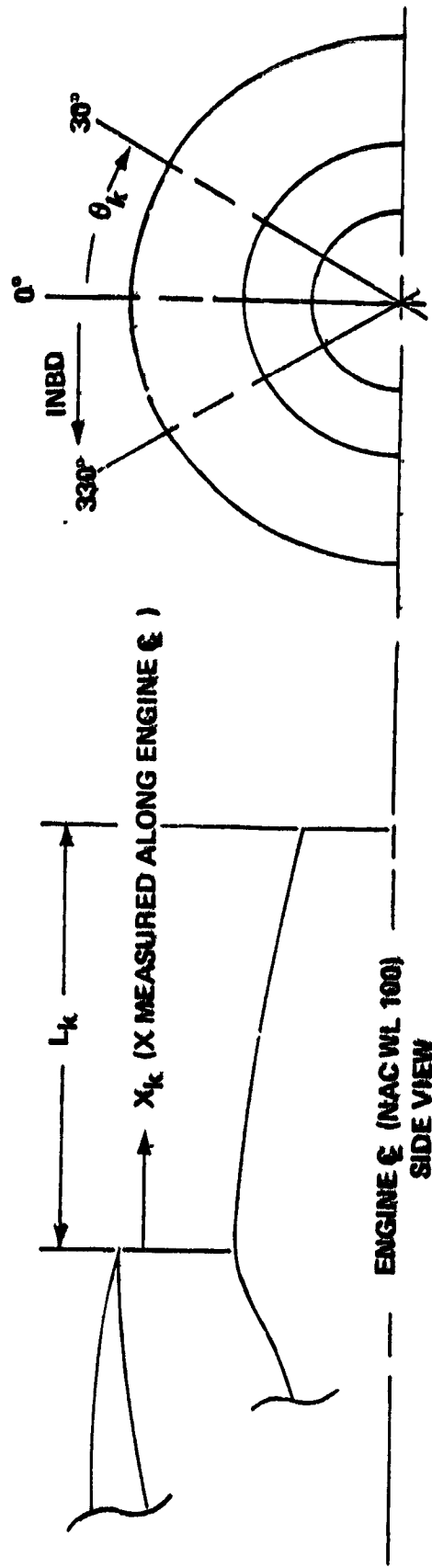
ORIGINAL PAGE IS  
OF POOR QUALITY

Table 15. Engine 4 Inlet Pressure Orifice Locations



$\theta_1 = 60^\circ$	$\theta_1 = 180^\circ$	$\theta_1 = 300^\circ$
X / C	X / C	X / C
0.441*	0.426*	0.424*
0.322*	0.318*	0.322*
0.232*	0.244*	0.228*
0.167*	0.178*	0.164*
0.104*	0.107*	0.101*
0.080*	0.052*	0.048*
0.021*	0.021*	0.021*
0.000	0.000	0.000
0.028	0.064	0.027
0.060	0.098	0.057
0.125	0.135	0.126
0.170	0.178	0.171
0.263	0.272	0.264
0.327	0.345	0.330
0.432	0.466	0.434

Table 16. Engine 3 and 4 Core Cowl Pressure Orifice Locations



ORIGINAL PAGE IS  
OF POOR QUALITY

12B209-27-1B9

CORE COWL  
REAR VIEW

$\theta_k = 30^\circ$ AND $330^\circ$	$X_k / L_k \pm 0.0007$
0.0363	0.6817
0.1552	0.6918
0.2405	0.7024
0.2928	0.7410
0.3797	0.7745
0.4472	0.8085
0.4995	0.8330
0.5315	0.8672
0.5703	0.9010
0.5822	0.9205
0.6277	0.9545
0.6497	0.9947

ORIGINAL PAGE L  
OF POOR QUALITY

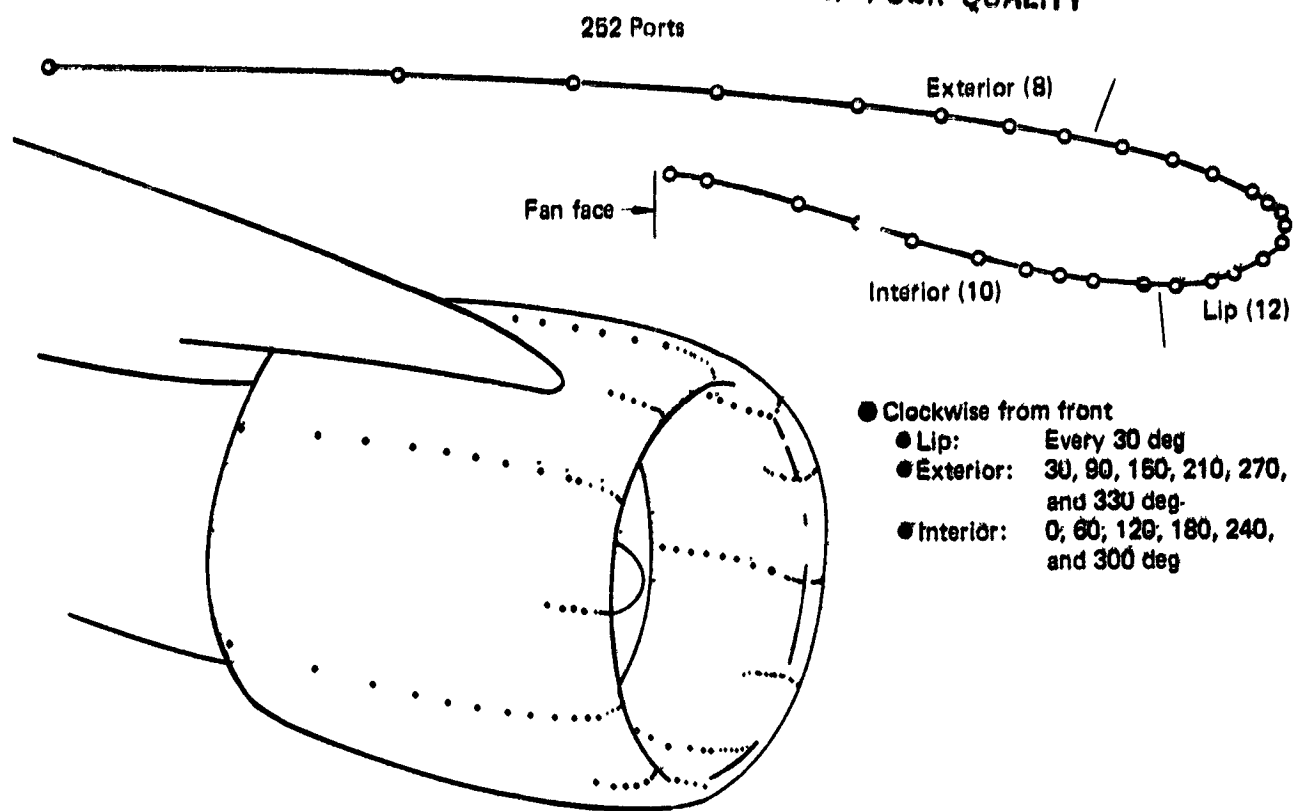
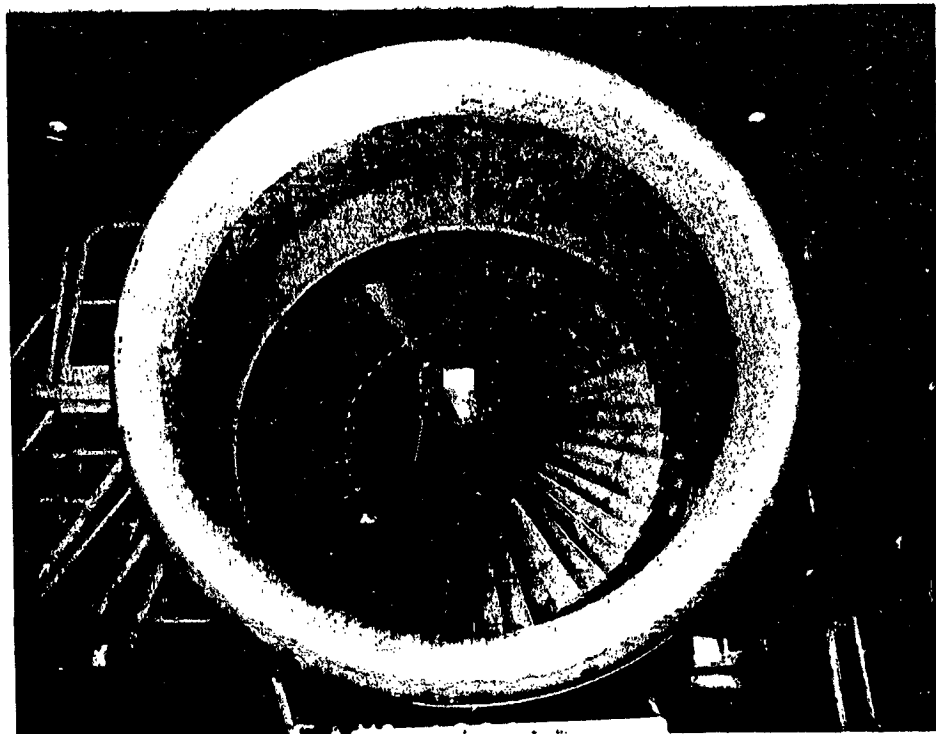


Figure 10. Inboard Engine Pressure Taps

125209-5



125209-6

Figure 11. Inboard Inlet Pressure Taps

The greatest deviations from ambient pressure and most rapid variations of pressure with distance occur near the inlet lip. Contribution of the lip area to the overall force and moment is very large. Because of this contribution, 144 taps in 12 rows, 30 deg apart, were located in the lip area. Aft of the lip, 60-deg circumferential spacing of the rows provided adequate definition.

Each pressure tap was connected to an Endevco pressure transducer (fig. 12) by approximately 8 ft of 0.061-in inside diameter copper tubing to ensure that lag effects were equalized. The transducers were mounted in temperature controlled boxes in groups of 22 (figs. 13 and 14). Each transducer measured differential pressure between the tap and a reference pressure.

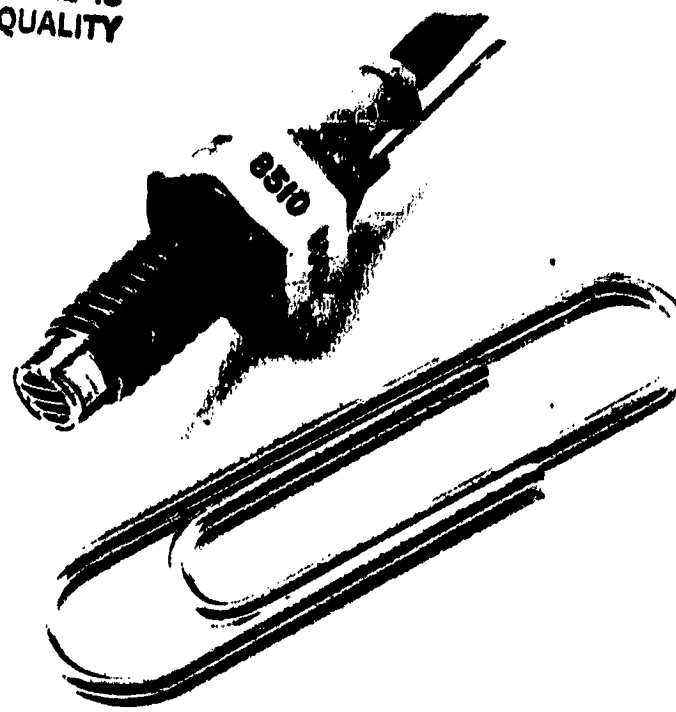
Further pressure measurements were obtained on the fan cowl doors of engine 3 (fig. 15). The arrangement was two rows of pressure taps, one on each side of both cowl doors, 30 deg from the top. Each pressure tap was connected to its individual transducer by copper tubing except at the hinges of the fan cowl doors, where a small section of copper tubing was replaced by a piece of flexible clear polymer. This flexible section enabled the doors to function throughout the test program.

The pressure instrumentation on engine 4 was designed to substantiate a finding of the feasibility study (ref. 1), which suggested that engine deterioration was independent of position. Therefore, engine 4 inlet was instrumented with three rows of 15 pressure taps each spaced 120 deg apart (fig. 16) for a total of 45 measurements. These measurements were sufficient to indicate relative load levels between inboard and outboard inlets.

**Inertial Loads Instrumentation**—Instrumentation for inertial loads consisted of accelerometers and rate gyros located on the engine and pylon (fig. 17) and the aircraft center of gravity. Linear accelerations were measured by Q-FLEX accelerometers (fig. 18). These instruments were used on both test engines and at their fore and aft wing and pylon interface. For angular accelerations two axes of a three-axis Northrop rate gyro mounted on the two test engines (figs. 19 and 20) were used.

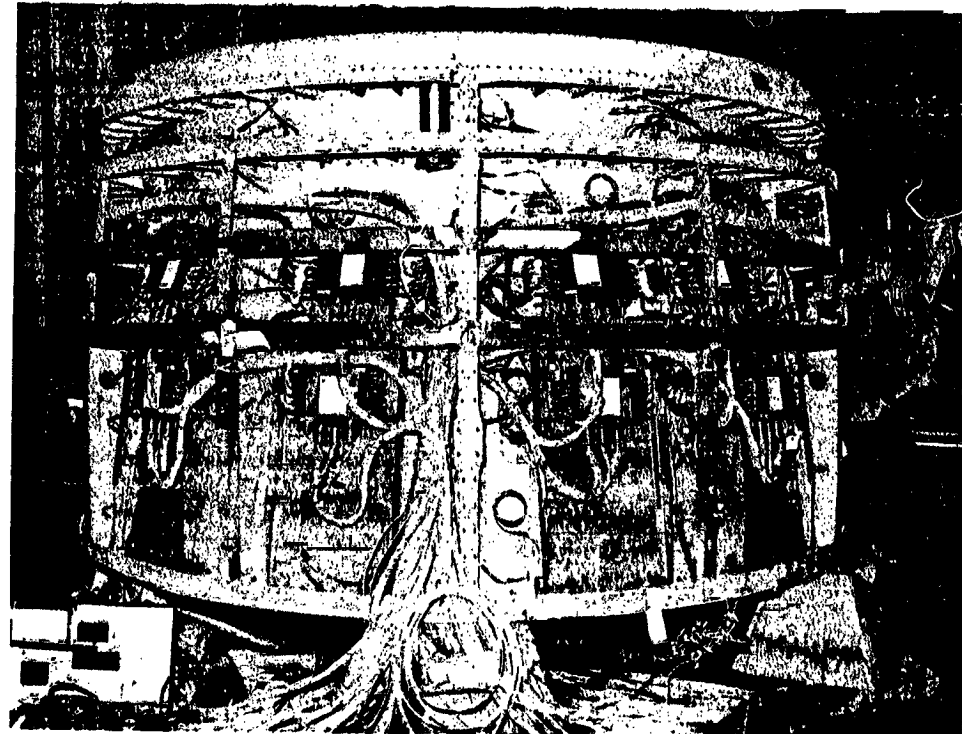
Location of accelerometers and rate gyros is referenced by clock position, looking aft. Accelerometers were placed on the engines so that lateral accelerations were measured in the lateral direction at NAC STA 46 at 3 o'clock and at NAC STA 100 at 6 o'clock. Vertical accelerations were measured at NAC STA 46 at 6 o'clock, NAC STA 100 at

ORIGINAL PAGE IS  
OF POOR QUALITY



125299-7

Figure 12. Pressure Transducer



125299-8

Figure 13. Pressure Transducer Installation

ORIGINAL PAGE  
BLACK AND WHITE PHOTOGRAPH



Figure 14. Pressure Transducer Box

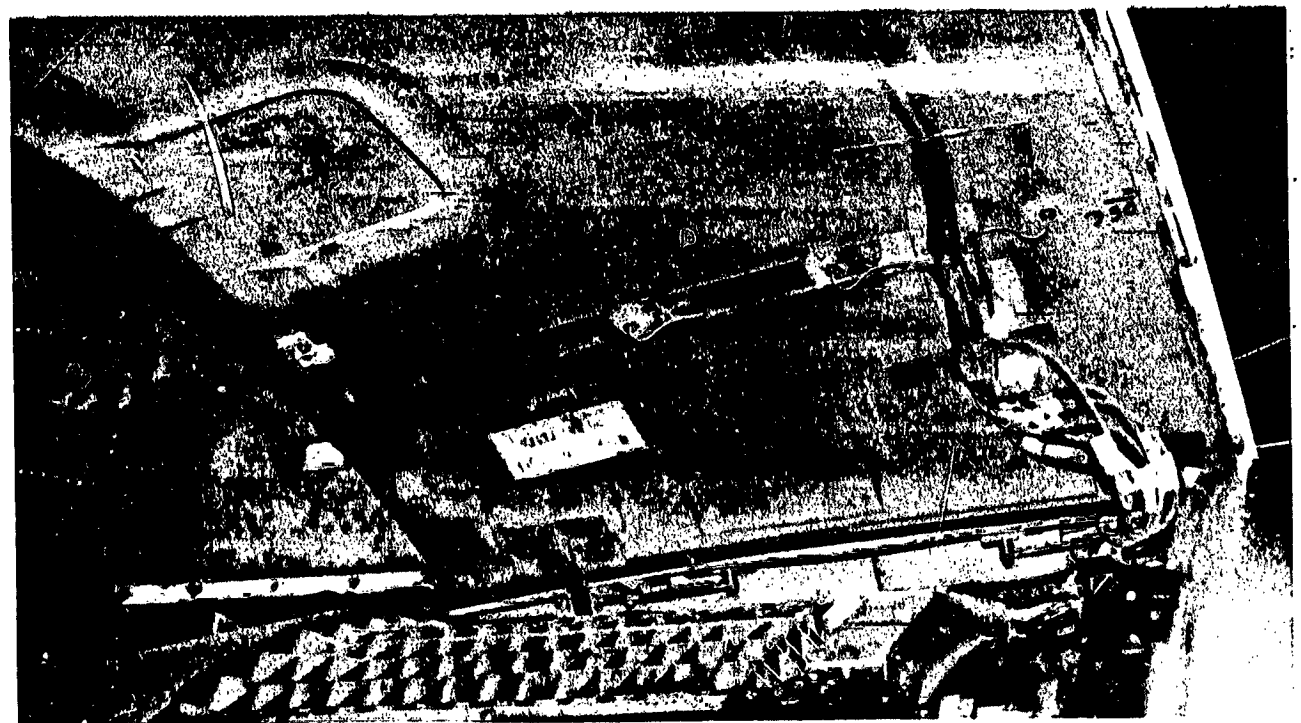
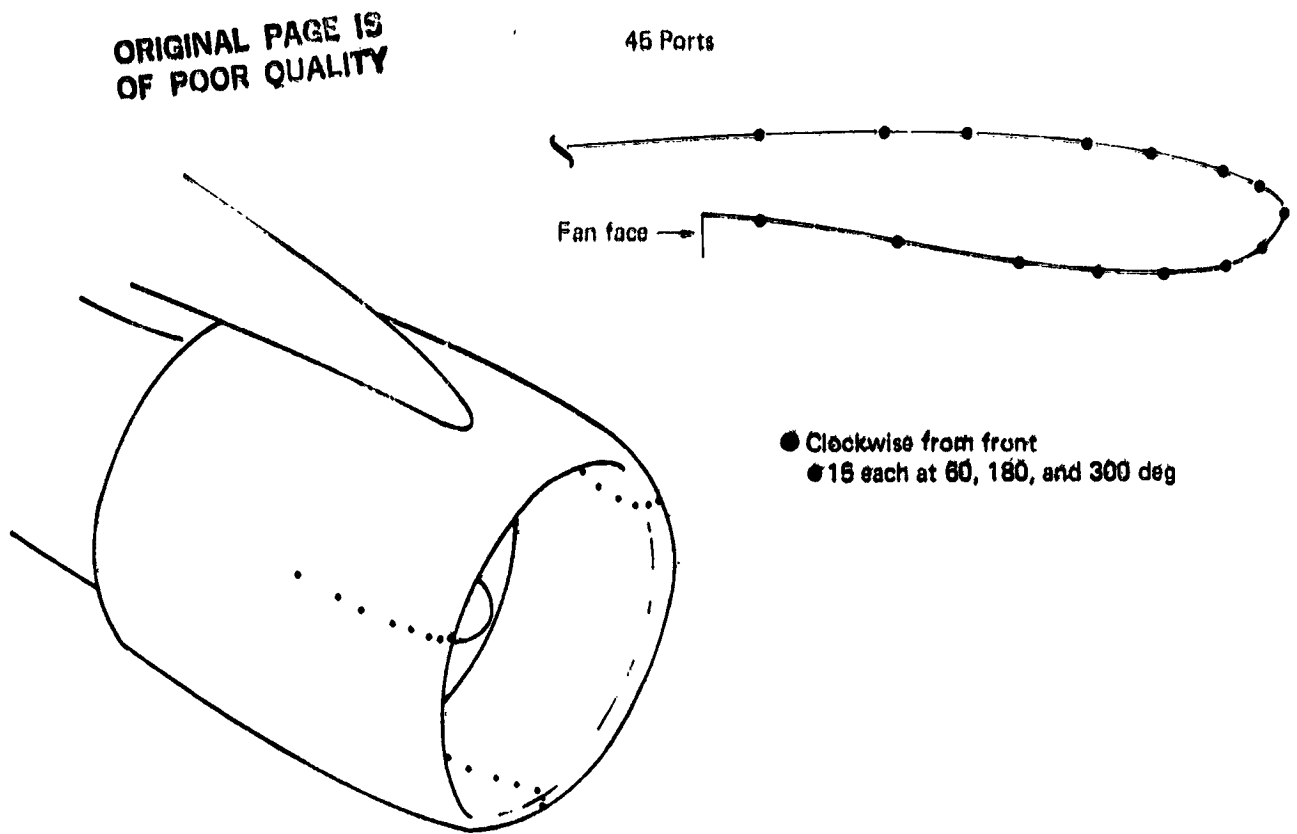
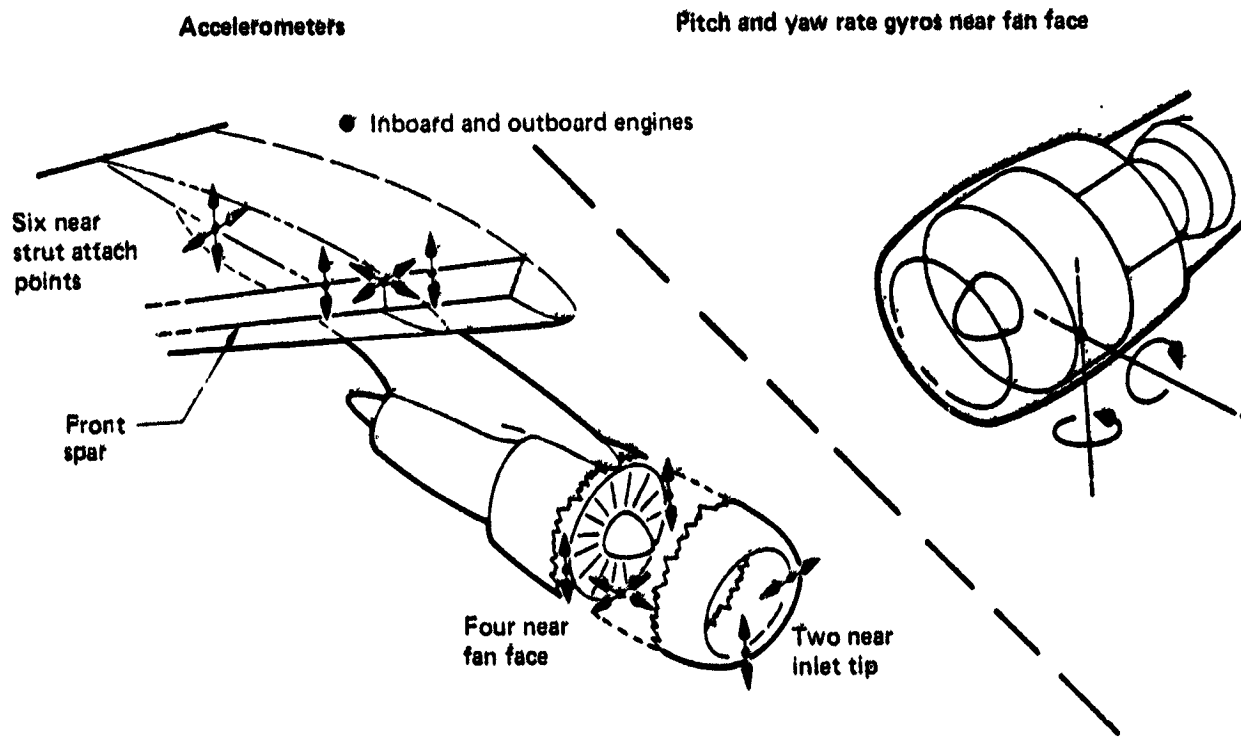


Figure 15. Cowl Door Pressure Taps



*Figure 16. Outboard Engine Pressure Taps*

126209-12



126209-11

*Figure 17. Inertial Data Sensors*

ORIGINAL PAGE  
BLACK AND WHITE PHOTOGRAPH

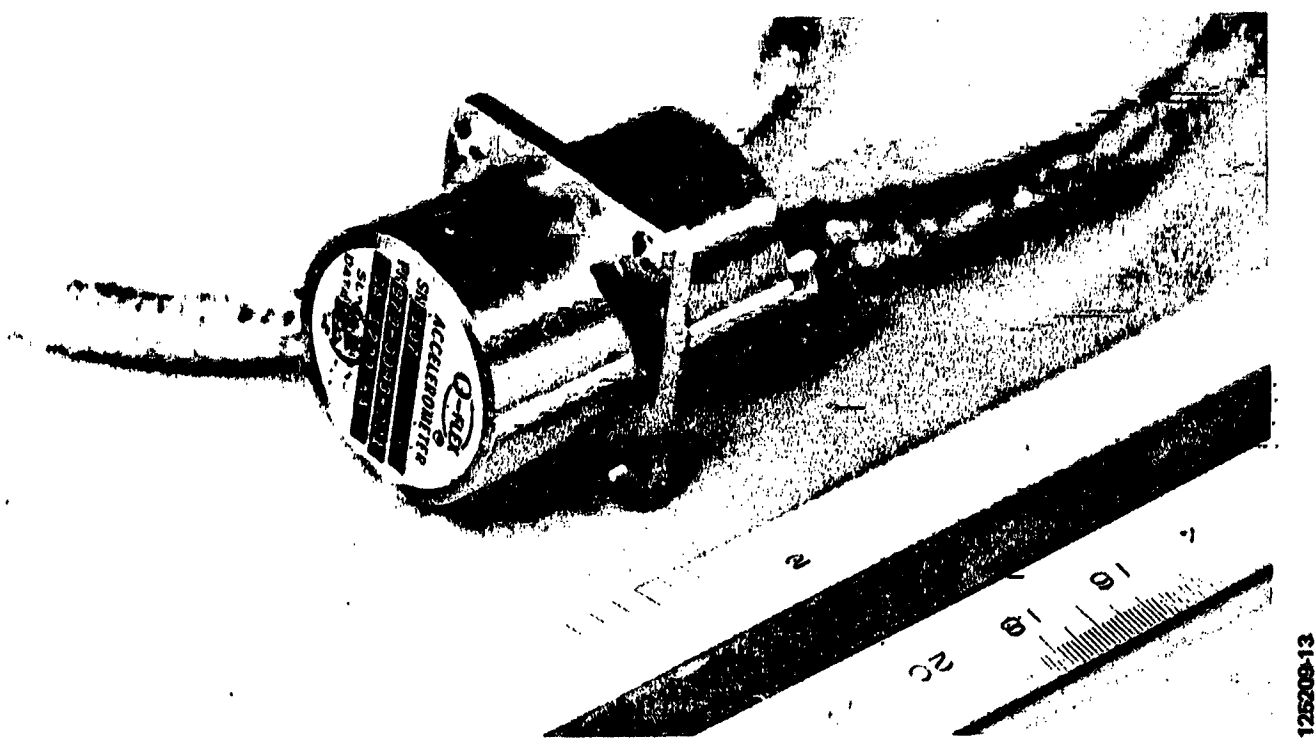


Figure 18. Q-FLEX Accelerometer

123000-13

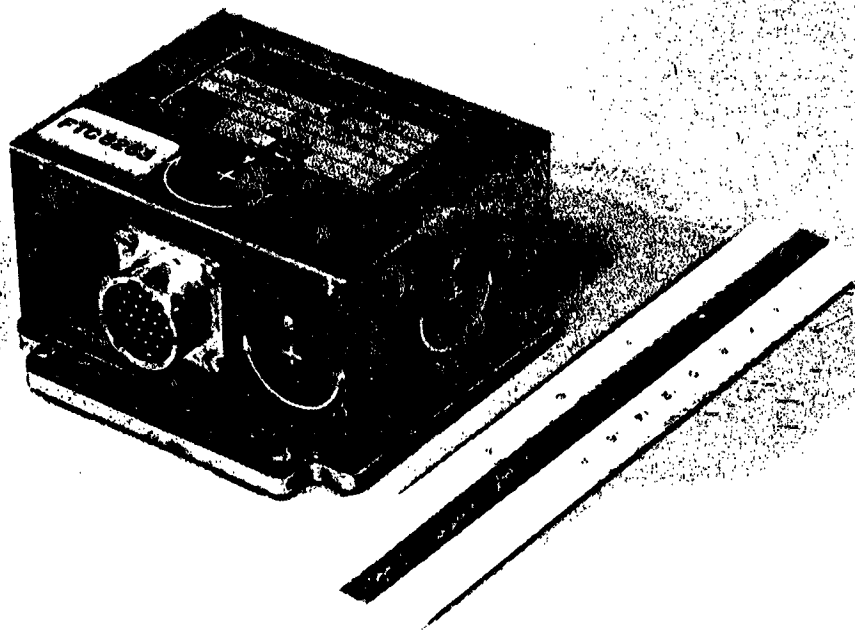


Figure 19. Rate Gyro

123000-16

ORIGINAL PAGE  
BLACK AND WHITE PHOTOGRAPH

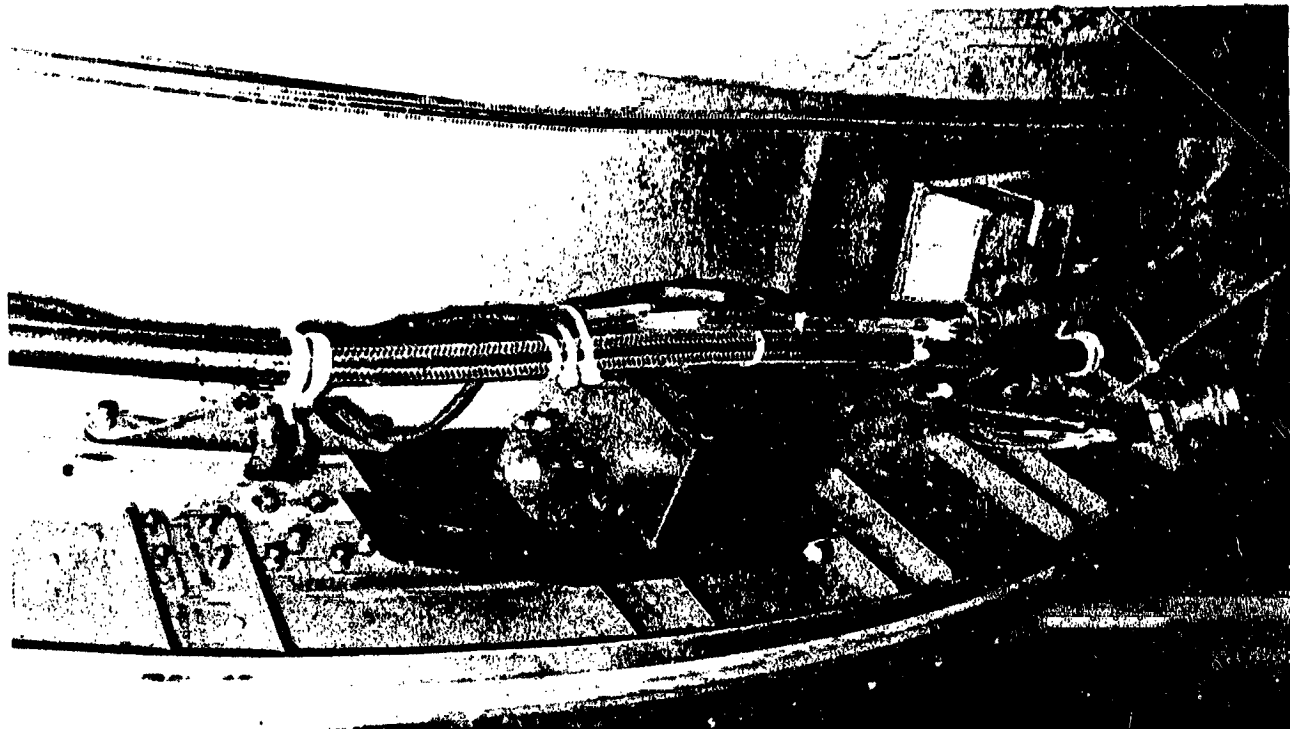


Figure 20. Accelerometer and Rate Gyro

the lateral direction at NAC STA 46 at 3 o'clock and at NAC STA 100 at 6 o'clock. Vertical accelerations were measured at NAC STA 46 at 6 o'clock, NAC STA 100 at 3 o'clock, and NAC STA 100 at 9 o'clock, and longitudinal acceleration was at NAC STA 100 at 6 o'clock. Rate gyros were placed at NAC STA 100 at 3 o'clock and were used to measure pitch and yaw rate. A total of six accelerometers and one rate gyro per engine permitted calculation of the translational and angular accelerations at the engine center of gravity.

Accelerations were also measured at the pylon/wing interfaces. The lateral accelerations were measured at the wing front spar and the rear thrust link attach point (fig. 21). The vertical accelerations were measured inboard and outboard of the front spar attach point and on the rear thrust link attach point. In the longitudinal direction, accelerations were measured only at the front spar. Each interface had a total of six linear accelerometers.

Basic airplane information was also recorded, including pitch, yaw, and roll angles, along with side-slip and angle of attack. Angular accelerations about all three axes were measured at the aircraft center of gravity.

**Clearance Measurement System**—Engine clearance change measurements were made by P&WA simultaneously with flight load application. Measurements were made on the fan and first-stage high-pressure turbine on the inboard engine and the fan stage of the outboard engine by a laser proximity system for each stage. Each clearance monitoring system consisted of: (1) the laser assembly (four lasers per box), (2) the input fiber optic assembly, (3) video camera assembly, (4) laser probe assembly (four probes per stage), (5) video monitor, and (6) video tape recorder (fig. 22).

In accordance with the interface agreement between the two companies, P&WA provided all clearance monitoring system components and made the necessary engine preparations. Operation and maintenance of the system during testing were also the responsibility of P&WA. P&WA provided to BCAC the equipment necessary for installation in the airplane during the layup period prior to testing.

Laser assemblies were installed in a rack inside the airplane cabin (fig. 23). Four laser assemblies of four laser generators per box were installed in the rack, which provided one spare box to facilitate changeover in flight should a laser generator malfunction.

ORIGINAL PAGE  
BLACK AND WHITE PHOTOGRAPH

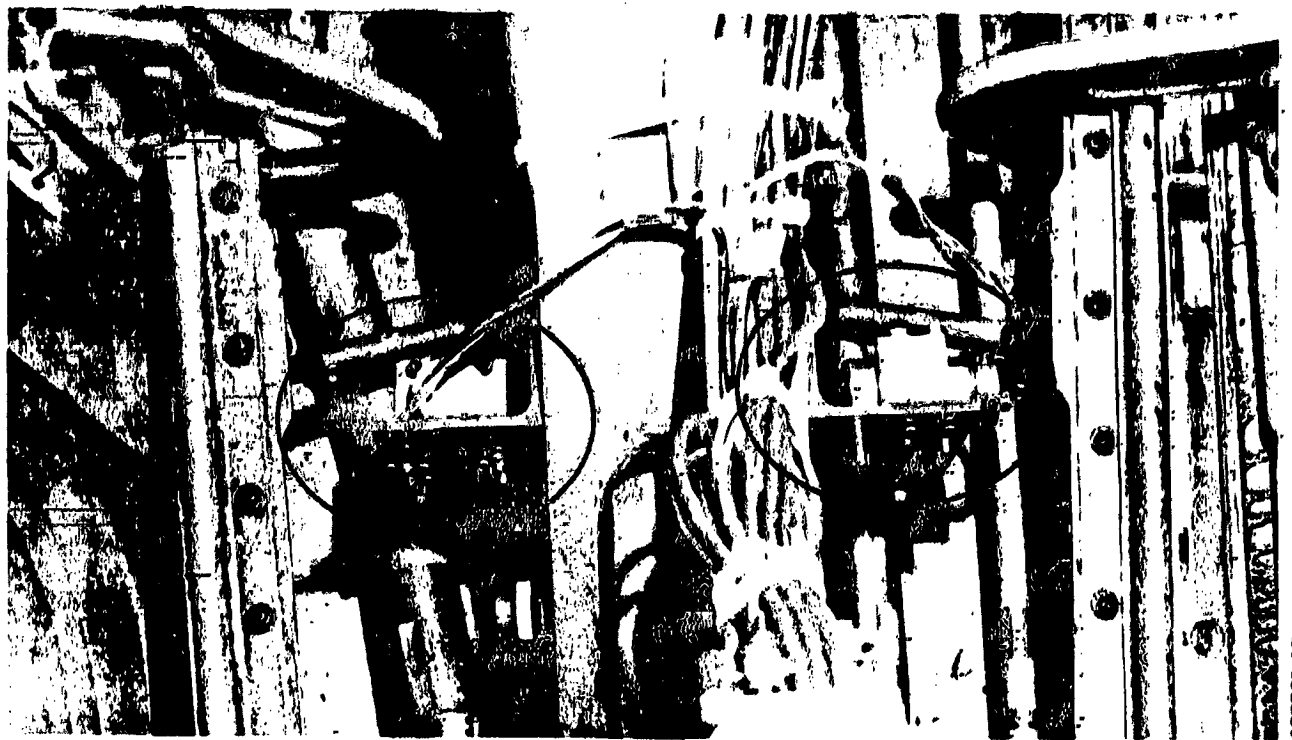


Figure 21. Acceleron Installation (Thrust Link)

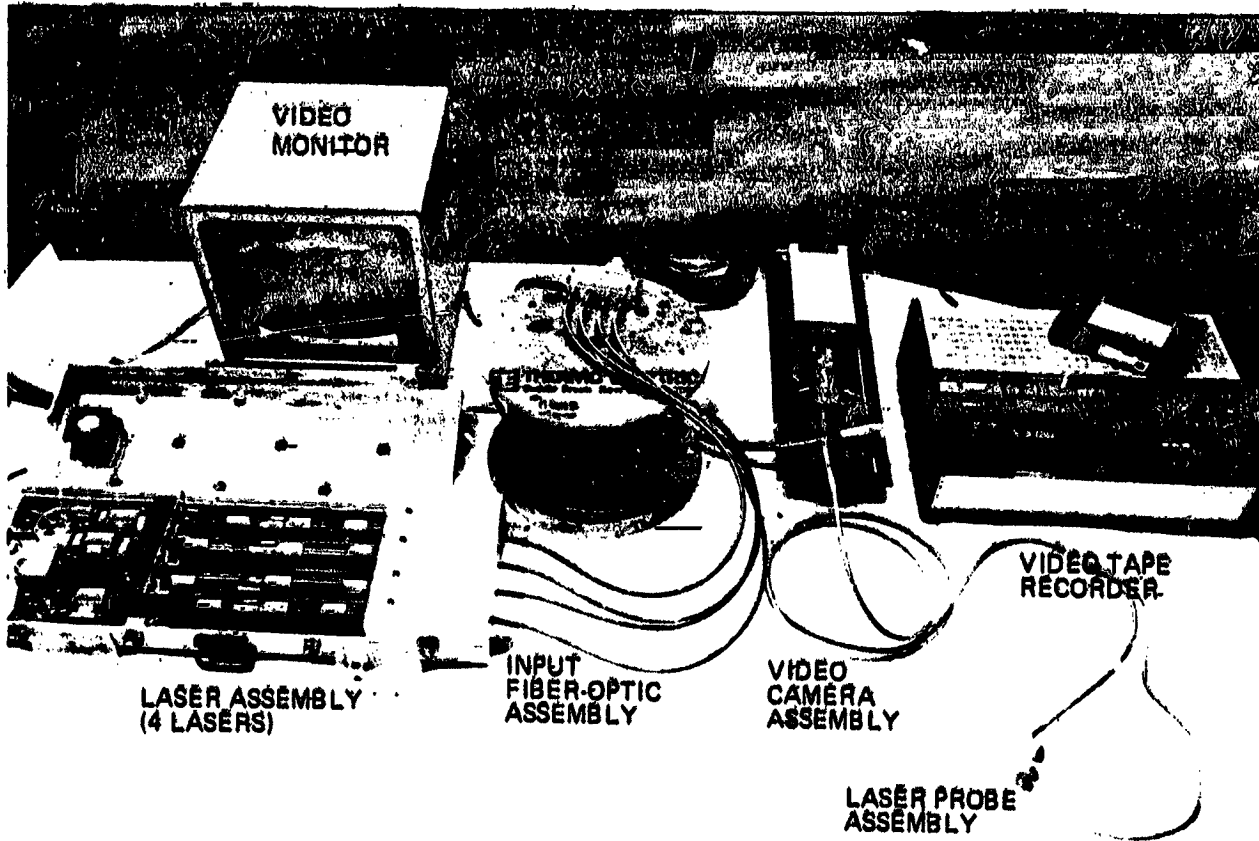


Figure 22. Clearance Monitoring System

ORIGINAL PAGE  
BLACK AND WHITE PHOTOGRAPH

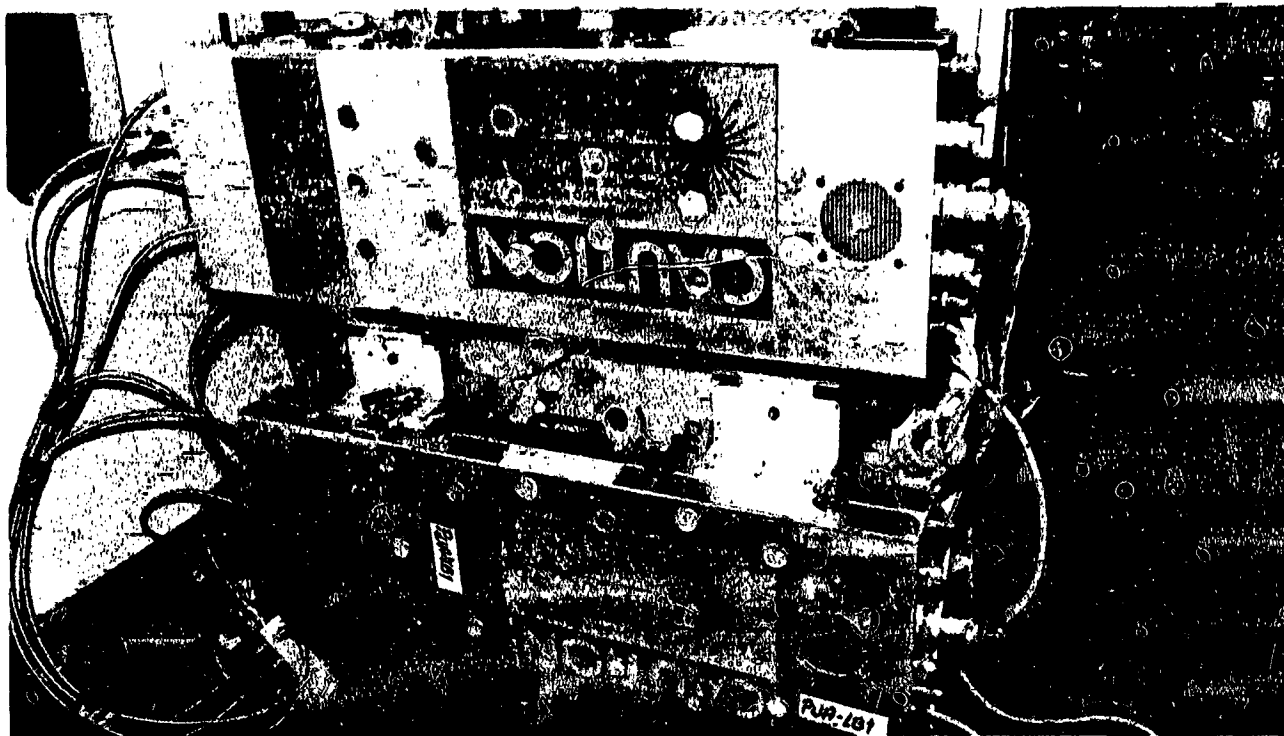


Figure 23. Laser Generator Boxes

125209-18

Video cameras were installed in the "dog house" (fig. 24) for the fans on the inboard and outboard engines and in the "kneecap" (fig. 25) of the wing and pylon intersection for the turbine of the inboard engine. The input fiber optic leads were divided in the camera box installation into four separate leads and routed to each laser probe assembly. A fan laser probe assembly is shown in figure 26 and a turbine laser probe assembly is shown in figures 27 and 28. The fan and turbine probe radial locations, which are essentially 90 deg apart, are shown in figure 29.

Reflected light from the engine blades was transmitted back through the probe and through the coherent output fiber optic to the video camera. At the video camera the reflected light was converted to a video signal and transmitted through a cable to the airplane cabin. In the cabin, clearance values were read on the video monitors (fig. 30) and were recorded on a video tape recorder (fig. 31).

In addition to the aforementioned components to the laser system, a gaseous nitrogen system was required to cool and purge the high-pressure turbine laser probes. BCAC provided the system, which was located in the forward cargo hold (fig. 32). Components of the gaseous nitrogen system included storage racks for 56 nitrogen bottles, the nitrogen bottles, the high-pressure manifolds and regulators, control valves, pressure sensors, probe temperature sensors and readout, tubing, and the flow-controlling orifice that is built into the high-pressure turbine probes. The system was configured to provide nitrogen for approximately 13 hours of operation without resupply.

**Expanded Engine Performance**—Expanded engine performance data (fig. 33) were required for the P&WA effort to correlate measured engine clearance changes or closures with performance losses. Primary emphasis was on engine 3, which had complete instrumentation (fig. 33). Minimum instrumentation to define engine speed and engine airflow and power level was provided for engine 4. Instrumentation for engine 3 was typical of that used for a performance engine test program and was compatible with that used during the pre- and postprogram base engine calibrations at the P&WA Middletown test facility. To better correlate data, the Boeing-owned flight high- and low-rotor speed tachometers (N2 and N1, respectively) and the fuel flow meter were calibrated by P&WA and were used during the pre- and postcalibration at P&WA. The tachometers and flow meter were used on this engine throughout the entire NAIL program.

ORIGINAL PAGE  
BLACK AND WHITE PHOTOGRAPH

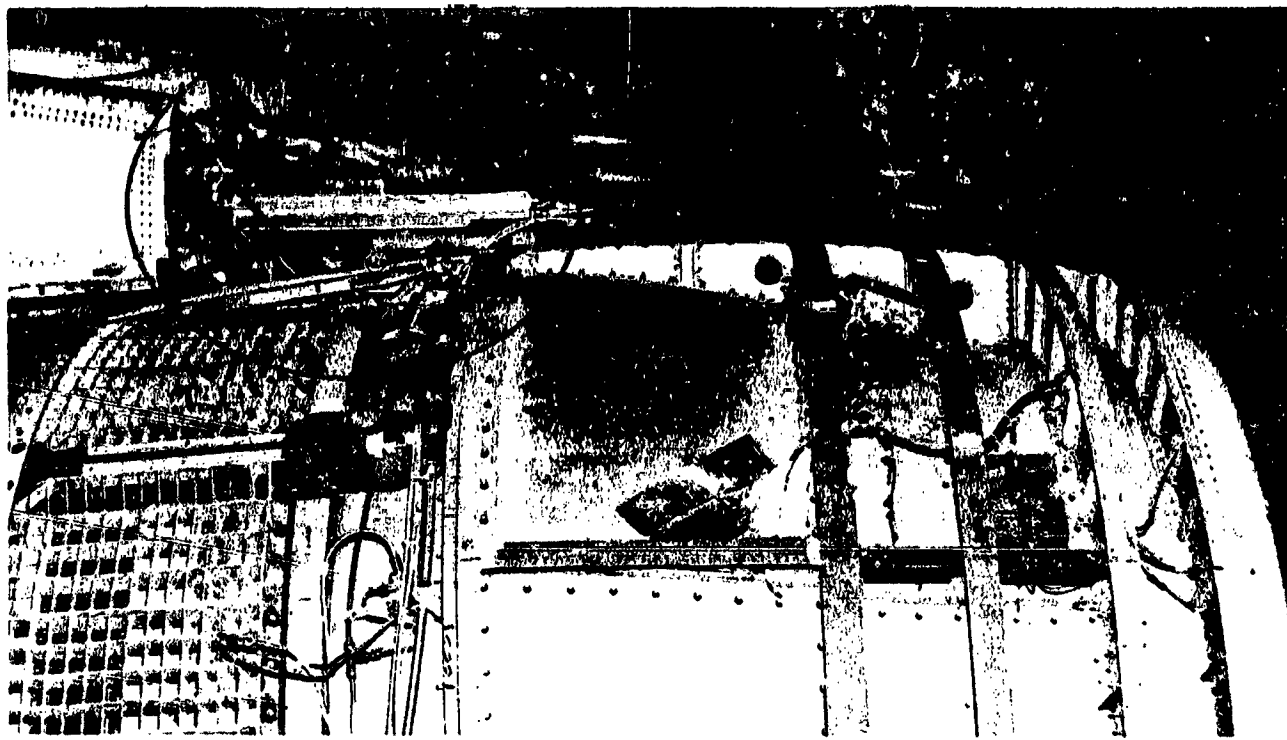


Figure 24. Fan Video Camera Installation

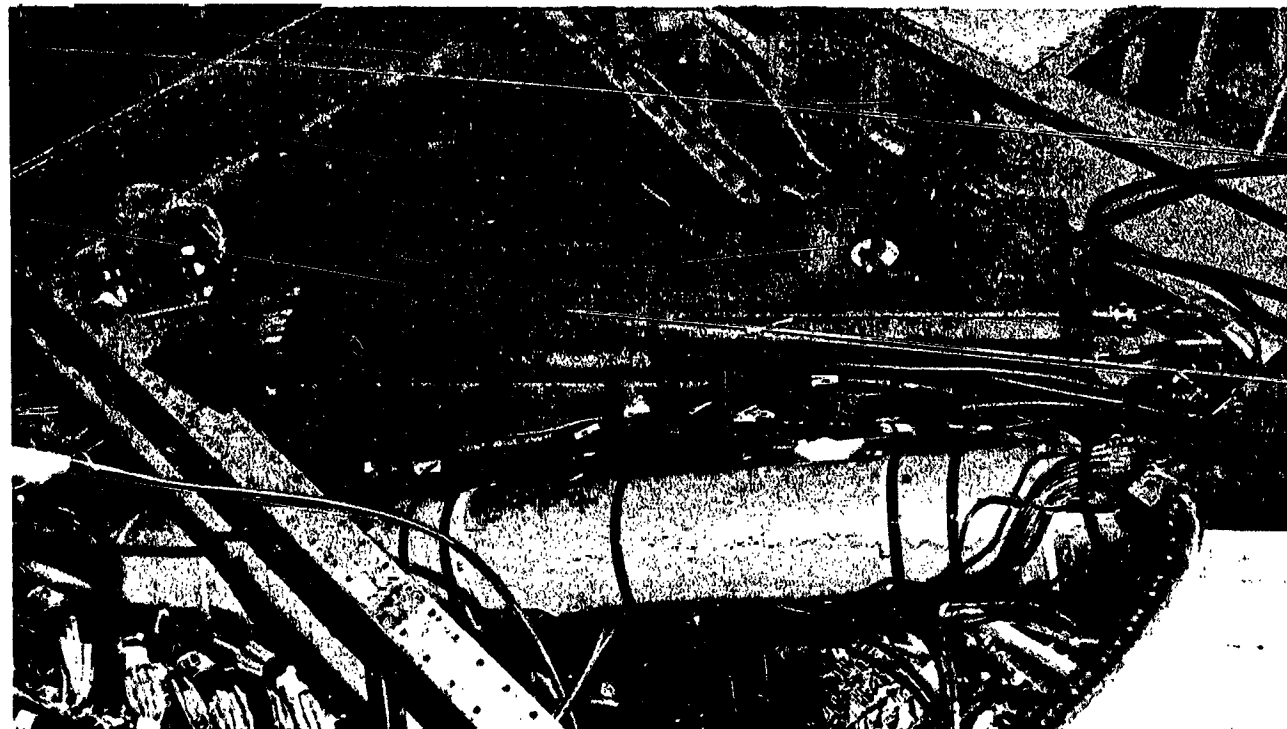


Figure 25. Turbine Video Camera Installation

ORIGINAL PAGE  
BLACK AND WHITE PHOTOGRAPH

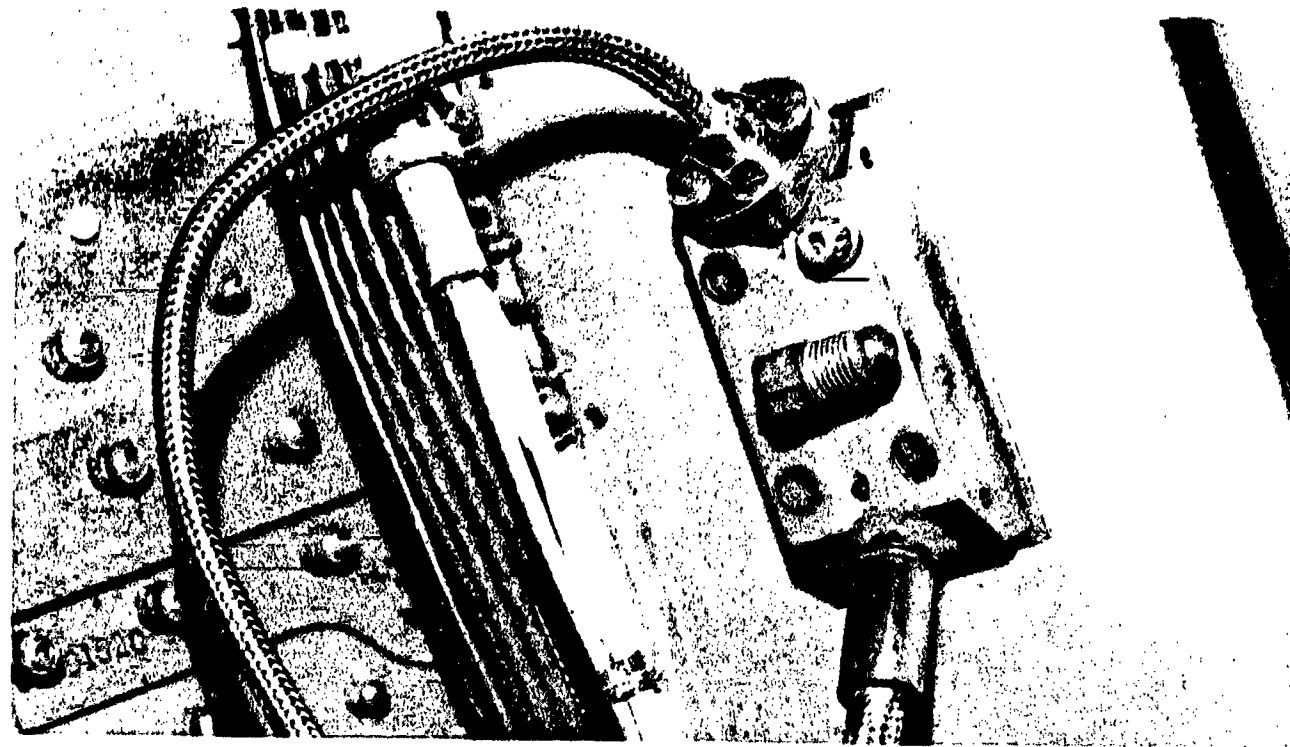


Figure 26. Fan Laser Probe

125209-21

ORIGINAL PAGE  
BLACK AND WHITE PHOTOGRAPH

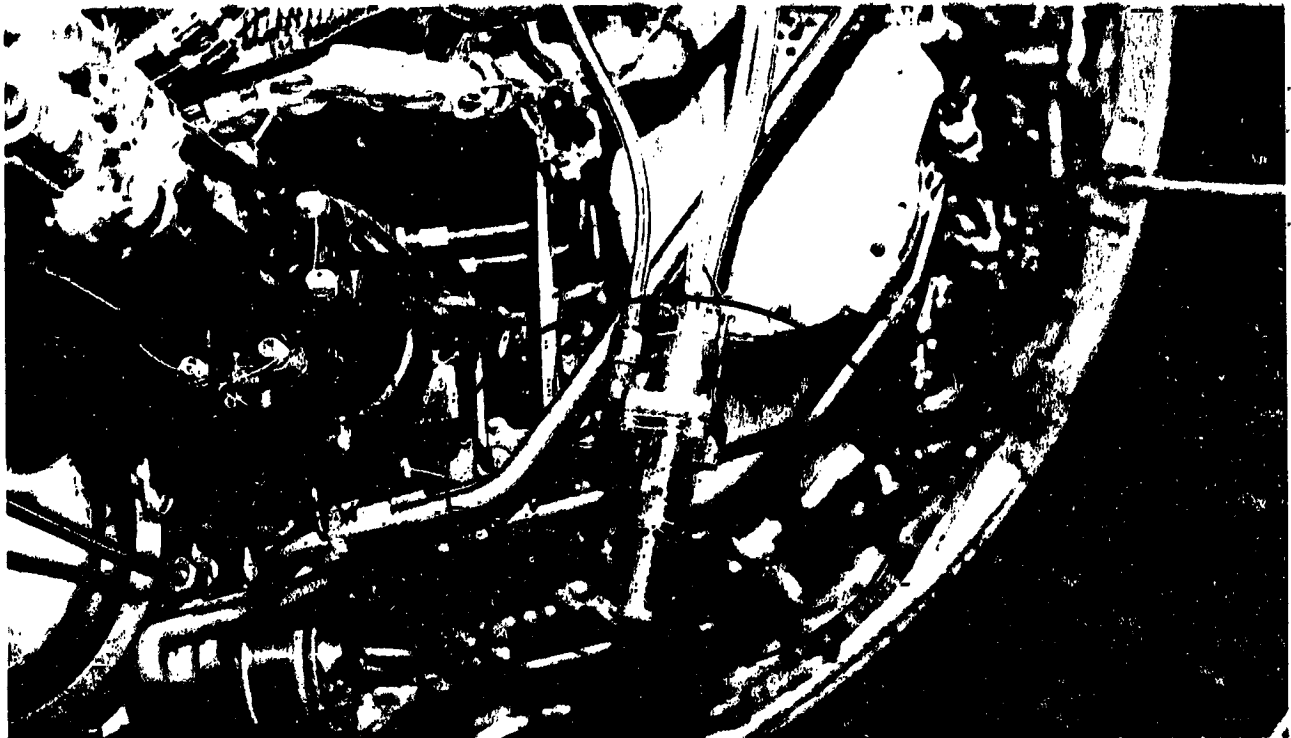


Figure 27. Turbine Laser Probe

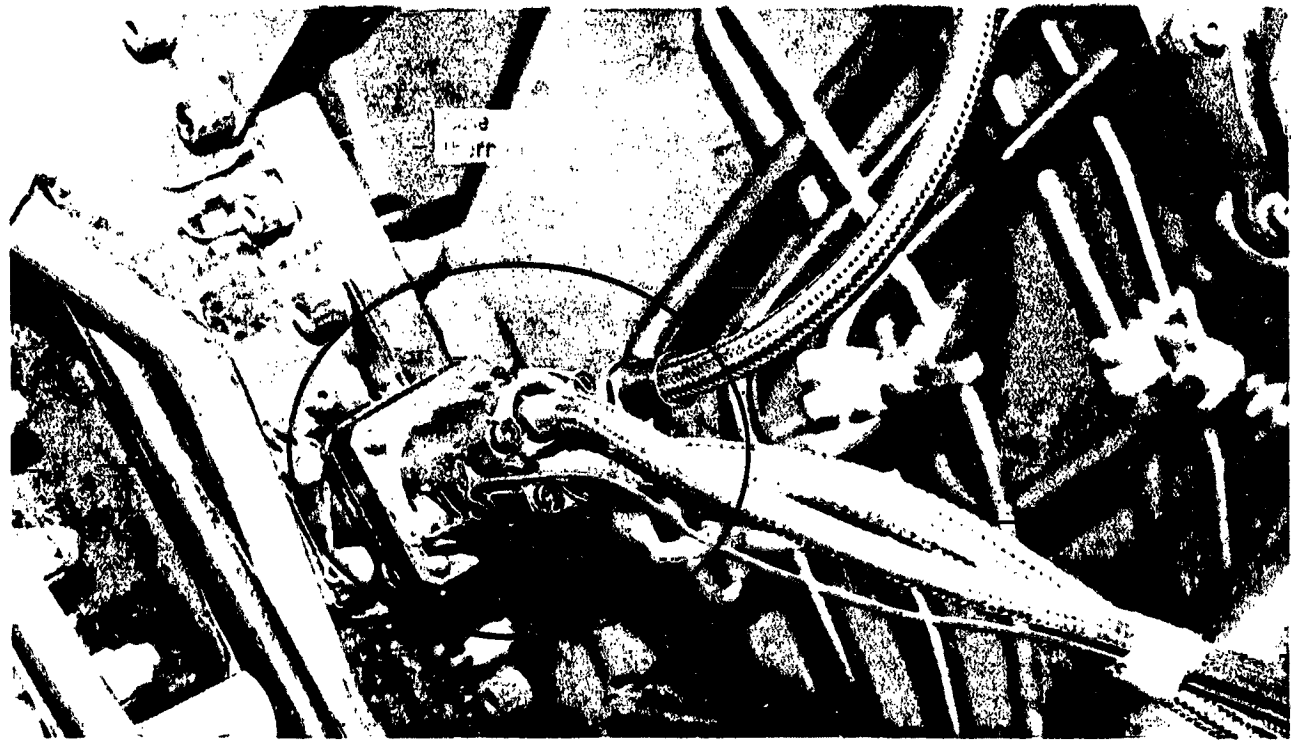


Figure 28. Turbine Laser Probe Installed

ORIGINAL PAGE IS  
OF POOR QUALITY

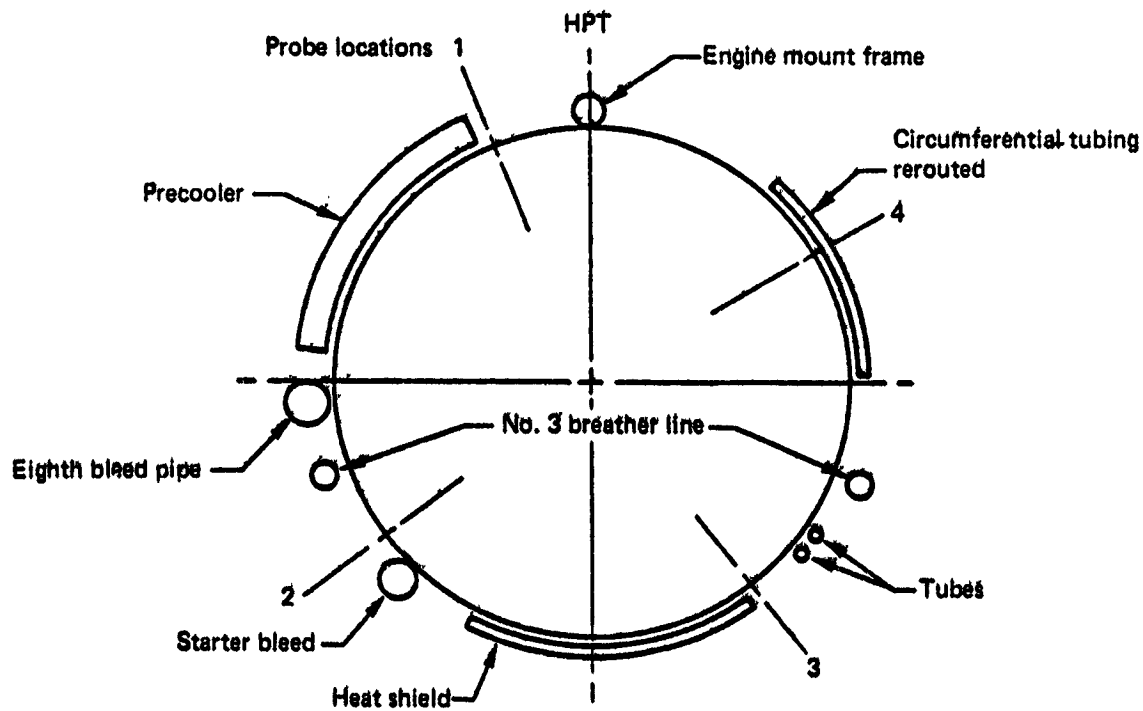
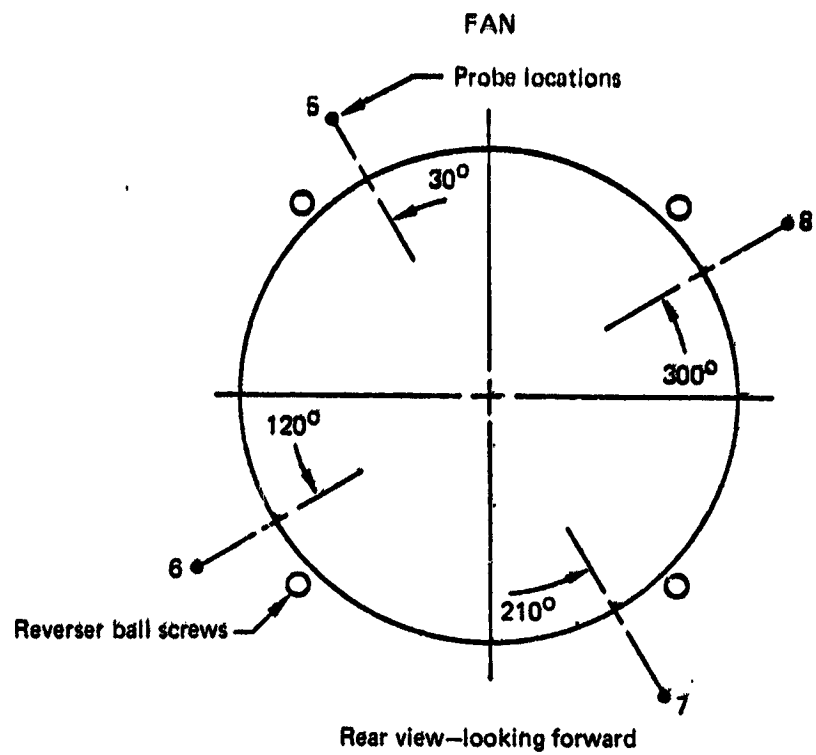


Figure 29. Laser Proximity Probe Locations

ORIGINAL PAGE  
BLACK AND WHITE PHOTOGRAPH

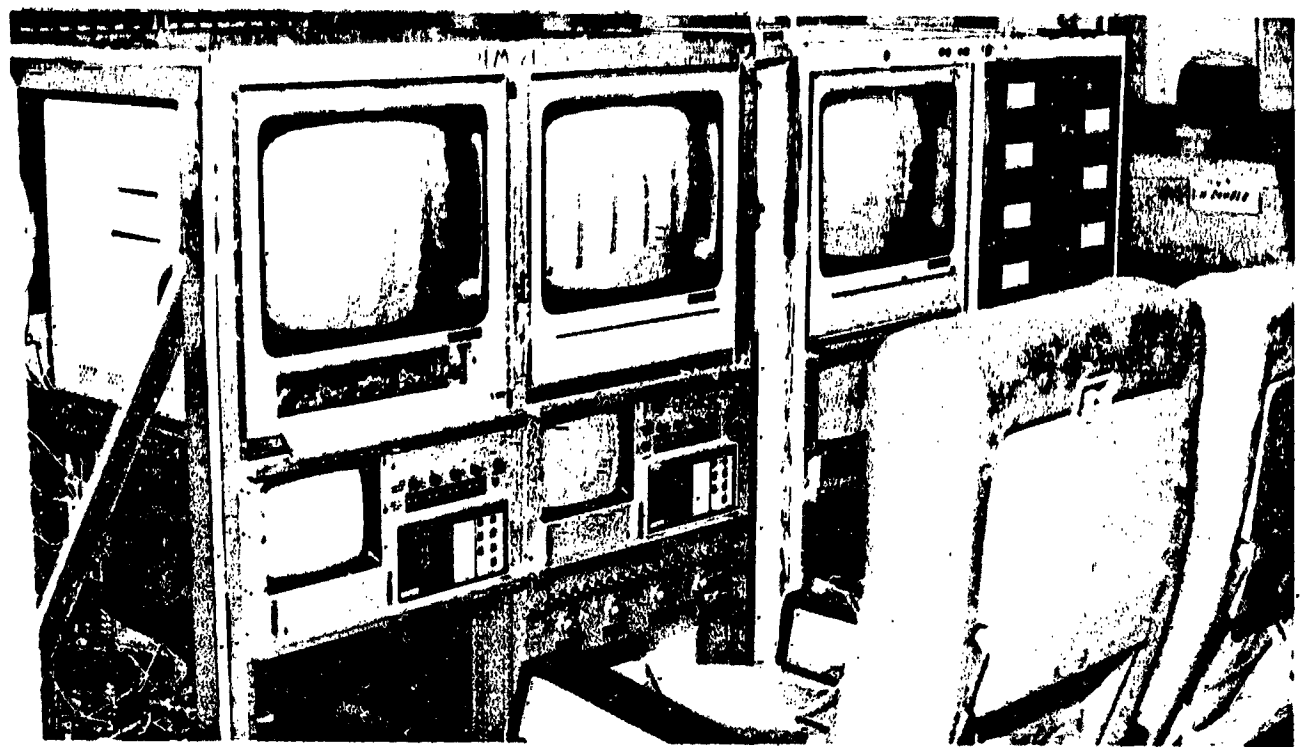


Figure 30. Laser System Video Monitors and Controls

123209-20



Figure 31. Laser Video Tape Recorder

123209-20

ORIGINAL PAGE  
BLACK AND WHITE PHOTOGRAPH



123209-36

Figure 32. Nitrogen System

N2	High-pressure (H.P.) rotor speed
N1	Low-pressure (L.P.) rotor speed
TT7	L.P. turbine discharge total temperature
TT4.5	H.P. compressor discharge total temperature
TT3	L.P. compressor discharge total temperature
TT8	H.P. turbine discharge total temperature
PT7.	L.P. turbine discharge total pressure
PT3	L.P. compressor discharge total pressure
PT2.5	Fan stream-total pressure at exit guide vane
PS3	L.P. compressor discharge static pressure
PS4	H.P. compressor discharge static pressure
HPC IGV POS	H.P. compressor inlet guide vane position
PWR LVR ANG	Power lever angle
Surge bleed valve POS	
Pylon valve POS	Pylon airbleed shut-off valve position
Air control valve, HPC	Pressure regulator
Wf	Fuel flow rate (computed)
Elapsed fuel	Total fuel burned

123209-36-108

Figure 33. Expanded Engine Performance

#### 4.1.2.2 Installed Propulsion System Aerodynamics

Instrumentation—Selection of the pressure measurement system used for this program was guided by the need to obtain pressure measurements on the wing, pylon, and core cowl only during quasi-steady-state airplane operating conditions. Accordingly, in these areas, a 24-port scanivalve pressure sampling system, which samples 12 ports per second, was compatible with the normal time frame for maintaining quasi-steady-state airplane operating conditions. The option of using individual transducers for each measurement, as on the inlet and fan cowl, thereby allowing a simultaneous sampling of each pressure, was not overlooked. Not enough transducers could be purchased from appropriate manufacturers in the time frame available to complete the test program.

A Gould Statham Model PM 131TC ( $\pm 17.2 \text{ kPa}$  [ $\pm 2.5 \text{ lb/in}^2$ ]) differential-pressure transducer was used in all scanivalve modules. Specifications for the transducer were as follows: combined nonlinearity and hysteresis of less than  $\pm 0.75\%$  full scale, thermal sensitivity shift less than  $0.01\text{/}^\circ\text{F}$  from  $-65^\circ\text{F}$  to  $+250^\circ\text{F}$  ( $-54^\circ\text{C}$  to  $+121^\circ\text{C}$ ), and thermal zero shift less than  $0.01\%$  full scale/ $^\circ\text{F}$  from  $-65^\circ\text{F}$  to  $+250^\circ\text{F}$  ( $-54^\circ\text{C}$  to  $+121^\circ\text{C}$ ). The natural frequency of the transducer diaphragm was 3500 Hz. The transducer output resulting from an acceleration stimulus applied perpendicular to the plane of the diaphragm was 0.2% of full scale per g for vibration frequencies to approximately 20% of the diaphragm natural frequency. Above the natural frequency, the response increased in accordance with the behavior of an undamped single-degree-of-freedom system.

Each scanivalve transducer housing was fitted with a thermostatically controlled heater jacket, which maintained a  $10^\circ\text{C}$  ( $50^\circ\text{F}$ ) operating environment for the transducer given ambient temperatures below  $10^\circ\text{C}$  ( $50^\circ\text{F}$ ). The heater system, however, did not maintain a  $10^\circ\text{C}$  ( $50^\circ\text{F}$ ) environment if the ambient temperatures were above  $10^\circ\text{C}$  ( $50^\circ\text{F}$ ). This condition seemed likely to occur only in the scanivalve assemblies mounted in the engine pylon where engine bleed air ducts transfer heat into the pylon bays. To monitor the temperature at each scanivalve location, a thermocouple was installed on each scanivalve assembly.

The impact of airplane- or engine-induced vibration on the installed pressure transducers was assessed during the ferry flight to the remote test site. It was assumed that the highest vibration levels would be encountered in scanivalve installation in the engine pylon. Piezoelectric accelerometers were bonded onto the installed scanivalve assembly

and g-levels were measured in a direction perpendicular to the plane of the transducer diaphragm during cruise conditions approximating the required test conditions. The highest measured acceleration level was approximately 0.9g rms at 230 Hz that would produce an output of 0.18% of full scale, based on the transducer acceleration sensitivity.

Other sources of measurement error involved signal gain, analog-to-digital conversion stability, and sampling speed. Testing transducers showed nonlinearity and hysteresis to be  $\pm 0.82\%$  at worst and  $\pm 0.30\%$  on an average. Based on pre- and postflight system calibrations and monitored in-flight operating conditions, the analog-to-digital conversion error was  $\pm 2\%$ . Scanivalve sampling speed was found to be significant only in shock areas. A 6.9 kPa ( $1 \text{ lb/in}^2$ ) pressure drop between the first 12 ports and the last 12 ports introduced a  $\pm 1\%$  error. The accuracy of measured pressures was estimated to be  $\pm 3\%$  in low-pressure gradient areas and  $\pm 4\%$  in shock areas.

Static pressure orifices were installed on the pylon and core cowl of inboard and outboard engines 3 and 4 and on the wing in the vicinity of both engines. Three rows of surface-static pressures on the upper surface of the wing and two rows on the lower surface were installed near both engines, (figs. 5 and 6). Two rows of surface static pressures on each side of the engine pylon were installed on engines 3 and 4 (fig. 6). Finally, two rows of surface static pressures were installed on each side of the engine core cowl of engines 3 and 4 (fig. 6).

Surface-static pressure orifices were installed flush to the local wing, pylon, and core cowl surface except for the wing-pressure orifices, which were located over or aft of the wing fuel tanks. In these areas, pressure belts were bonded to the wing surface and faired into the surface (fig. 34). The location of the transition from flush orifices to pressure belt orifices is documented for each wing pressure measurement row (see table 1).

To improve the accuracy of actually locating a position of the pressure orifice on the wing, pylon, or core cowl, computer-generated surface-profile templates marked with the desired orifice location were used in regions experiencing large changes in surface curvature. The actual location of installed pressure orifices deviated in some cases from the desired location because of interference with, for example, structural members and anti-icing ducts. Actual locations were checked again after installation. Orifice positions tabulated in tables 11 to 16 represent the actual installed pressure orifice position plus or minus the tolerance indicated with each group of coordinates.

ORIGINAL PAGE IS  
OF POOR QUALITY

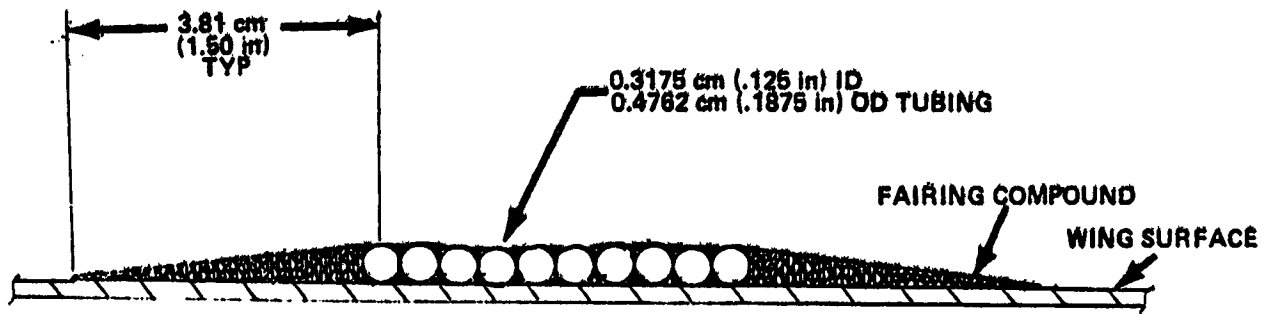


Figure 34. Typical Cross-Section of Wing Pressure Belt

125209-27-190

Orifice positions on the engine 3 fan inlet and cowl did not deviate from the angular position of the profile. Engine 4 fan inlet and cowl orifices deviated from the angular position of the profiles a maximum of  $\pm 2$  deg. The other significant deviation occurred on both engines 3 and 4 NAC WL 155 and 180 pressure orifice rows. The NAC WL values were within  $\pm 1.78$  cm (0.7 in).

Additional clarification of locations for those pressure orifices located in the upper and lower surface wing pressure belts is necessary. For belt-located pressure orifices, one pressure orifice was allocated to one belt tube. Because the belt tubes were arranged laterally to provide a low profile, the orifice locations gradually deviated laterally due to tube width, resulting in increasing orifice distance from the start of the pressure belt. Table 17 presents the manner and amount of deviation for each pressure belt orifice at a given WBL.

#### 4.1.3 Test Conditions and Procedures

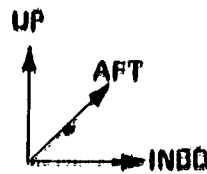
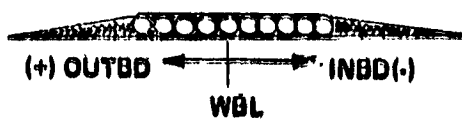
##### 4.1.3.1 Flight Loads

Testing for performance degradation was accomplished in several well defined stages. Such testing was necessary to measure engine clearance changes resulting from various flight maneuvers. Once the installation and fabrication on the test bed aircraft was completed, an engine ground calibration was performed prior to the functional check flight. This calibration enabled comparison with the test stand calibrations by P&WA and provided a data base line for the flight test program.

It was suspected that the first .1% loss in performance due to engine clearance changes occurred during the production flight test acceptance profile (fig. 35). Therefore, this profile was chosen as the basis of the first test flight and was followed by a second ground calibration. Subsequent flights contained high-g turns and variations in takeoff gross weight. Under the test plan, each series of tests required a ground calibration after the particular series. Using these calibrations, performance deterioration was determined for each series of tests. The final ground calibration was performed after completing all flight testing. In all, five ground calibrations were conducted during the NAIL flight test program.

**ORIGINAL PAGE IS  
OF POOR QUALITY**

**Table 17. Lateral Offset of Wing Pressure Belt Pressure Orifices From Wing Buttack Line**



WBL 446				WBL 610			
UPPER SURFACE		LOWER SURFACE		UPPER SURFACE		LOWER SURFACE	
X <sub>w</sub> /C <sub>w</sub>	OFFSET X 0.1688 cm (1/16")	X <sub>w</sub> /C <sub>w</sub>	OFFSET X 0.1688 cm (1/16")	X <sub>w</sub> /C <sub>w</sub>	OFFSET X 0.1688 cm (1/16")	X <sub>w</sub> /C <sub>w</sub>	OFFSET X 0.1688 cm (1/16")
0.2000	0	0.1950	0	0.2000	0	0.1972	0
0.2250	-3	0.2453	-3	0.2250	-3	0.2472	-3
0.2500	-6	0.2953	-6	0.2500	-6	0.2972	-6
0.2750	-9	0.3453	-9	0.2750	-9	0.3472	-9
0.3043	-12	0.3953	-12	0.3000	-12	0.3972	-12
0.3543	-15	0.4454	-15	0.3500	-15	0.4472	-15
0.4037	-18	0.4954	-18	0.4000	-18	0.4972	3
0.4638	-21	0.5455	3	0.4500	-21	0.5472	6
0.4750	-24	0.5955	6	0.4750	3	0.5972	9
0.5060	-27	0.6455	9	0.5000	6	0.6472	12
0.5250	3			0.5250	9		
0.5554	6			0.5800	12		
0.6049	9			0.6000	15		
0.6551	12			0.6500	18		
0.7049	15			0.7000	21		
0.7652	18						
0.8049	21						

WBL 470	
UPPER SURFACE	
X <sub>w</sub> /C <sub>w</sub>	OFFSET X 0.1688 cm (1/16")
0.2000	0
0.3000	-3
0.4000	-6
0.5000	3
0.6000	6

Table 17. Lateral Offset of Wing Pressure Belt Pressure Orifices  
From Wing Buttock Line (Concluded)

WBL 808				WBL 870			
UPPER SURFACE		LOWER SURFACE		UPPER SURFACE		LOWER SURFACE	
X <sub>w</sub> /C <sub>w</sub>	OFFSET X 0.1588 cm (1/16")	X <sub>w</sub> /C <sub>w</sub>	OFFSET X 0.1588 cm (1/16")	X <sub>w</sub> /C <sub>w</sub>	OFFSET X 0.1588 cm (1/16")	X <sub>w</sub> /C <sub>w</sub>	OFFSET X 0.1588 cm (1/16")
0.2000	0	0.2000	0	0.2000	0	0.2043	0
0.2250	-3	0.2500	-3	0.2250	-3	0.2543	-3
0.2466	-6	0.3000	-6	0.2500	-6	0.3043	-6
0.3000	-9	0.3500	-9	0.3000	-9	0.3543	-9
0.3500	-12	0.4000	-12	0.3500	-12	0.4043	-12
0.4000	-15	0.4500	-15	0.4000	-15	0.4543	-15
0.4500	-18	0.5000	-18	0.4500	-18	0.5043	3
0.5000	-21	0.5500	3	0.4750	-21	0.5543	6
0.5250	3	0.6000	6	0.5000	3	0.6043	9
0.5500	6	0.6500	9	0.5250	6	0.6543	12
0.6000	9			0.5500	9		
0.6500	12			0.6000	12		
0.7000	15			0.6500	15		
0.7500	18			0.7000	18		
0.8000	21						

WBL 834	
UPPER SURFACE	
X <sub>w</sub> /C <sub>w</sub>	OFFSET X 0.1588 cm (1/16")
0.2405	0
0.3000	-3
0.4000	-6
0.5000	3
0.6000	6

ORIGINAL PAGE IS  
OF POOR QUALITY

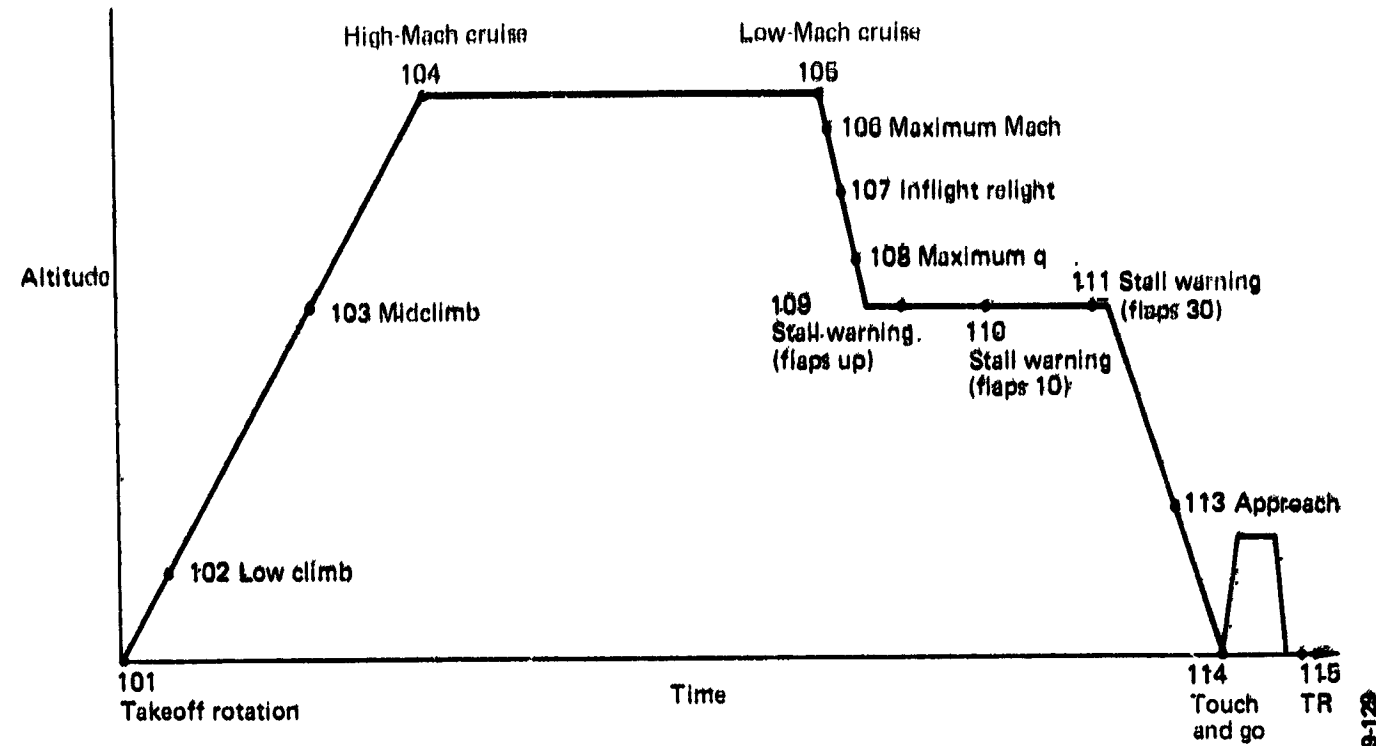


Figure 35. Acceptance Flight Profile

125309-122

The final test conditions (table 18) of the NAIL program resulted from compromise and various flight restrictions. Originally NAIL was to be a standalone flight program. However, the flight test was conducted concurrently with the 767/JT9D-7R4 test program, which imposed certain flight restrictions on RA001. The most notable restrictions were to remain within the 767 design cruise speed and Mach number ( $V_C$  and  $M_C$ ) limits of 360 kcas and  $M = 0.86$  until the completion of all JT9D-7R4 test conditions and to limit nacelle loads to 80% of the design limit. Upon completion of the JT9D-7R4 program, the 767 design envelope  $V_C$  and  $M_C$  limits of 420 kcas and  $M = 0.91$  were applied to the NAIL program.

Several restrictions were imposed on the NAIL program—not because of the NAIL flight test profile but because of inclement weather (i.e., rain, snow, hail, fog, high wind, and wide variations in temperature). Moisture caused problems for the RA001 in that only engine 1 had thermal anti-ice protection. Therefore, no flights were conducted into known or suspected icing conditions. The pressure instrumentation (fig. 36) was not to be exposed to visible moisture to ensure that water did not enter the lines and freeze.

Use of laser probes for detection of engine clearance changes dictated adherence to three conditions: that the nitrogen purge and cooling system operate whenever engine 3 was used, that nitrogen cooling be required for the camera environmental housings when ambient ground conditions dictated, and that the aircraft heading prevent sunlight from entering the inlet and interfering with laser readings.

Because a functional check flight and a ferry flight to the remote test site were required prior to any NAIL data collection effort, it was necessary to restrict the level of power to prevent performance losses in the analytically built engine 3. Therefore, all flights prior to the first data flight were limited to an engine pressure ratio (EPR) of 1.18 with no bleeds during takeoff and maintained a locked throttle climb to 10 000 ft at which time normal operation resumed.

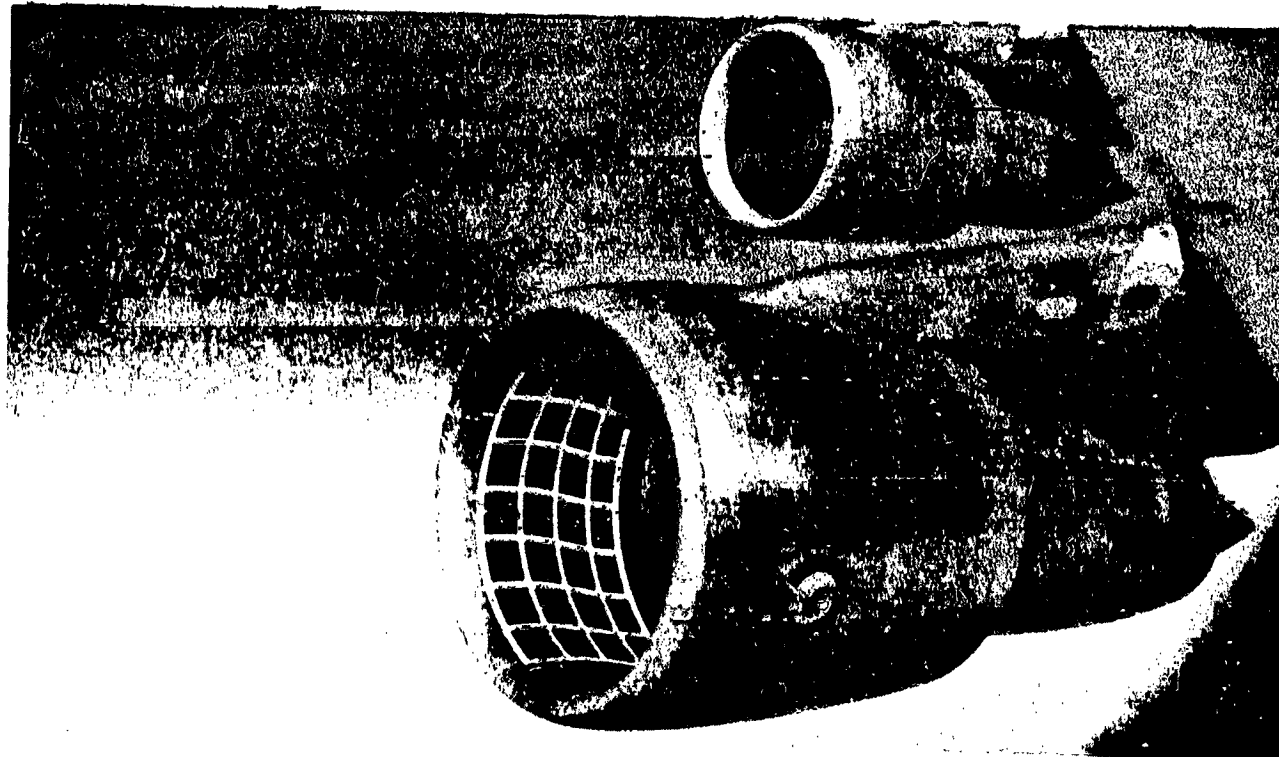
As a result of the concurrent testing programs, data were taken over approximately 33 hours of flight time instead of over the initially planned 15-hour maximum. The increased flight time resulted in a substantially larger quantity of data to survey and select from for analysis and provided additional conditions for analysis. The result of this concurrent testing was that additional data were obtained, yet flight hours charged to the NASA program were considerably fewer than planned.

ORIGINAL PAGE IS  
OF POOR QUALITY

Table 18. Test Conditions Flown

Test condition	Test no.	Event time	Pressure altitude, ft	M
101 612K gross weight takeoff (flaps 20)	273-7	6:41:44	2 663	0.260
101 638K gross weight takeoff (flaps 10)	273-10	9:44:10	2 667	0.239
101 647K gross weight takeoff (flaps 10)	273-11	10:13:52	2 634	0.264
118 780K gross weight simulated takeoff (flaps 10)	273-15	8:13:18	3 646	0.298
102 Low climb	273-10	9:46:00	5 861	0.367
103 Mid climb	273-7	7:28:44	17 187	0.899
104 High M cruise	273-7	7:49:26	36 481	0.859
105 Low M cruise	273-7	7:56:40	36 612	0.772
106 Max M.	273-15	12:09:27	36 978	0.906
107 Inflight relight	273-7	8:12:53	27 859	0.721
108 Maximum q	273-16	11:39:00	24 513	0.838
109 Stall-warning (flaps up)	273-7	8:18:58	16 964	0.391
110 Stall warning (flaps 10)	273-7	8:22:26	16 239	0.347
111 Stall warning (flaps 30)	273-7	8:24:52	17 049	0.270
112 Idle-descent	273-7	8:28:56	8 450	0.439
113 Approach	273-7	8:34:27	6 003	0.265
114 Touch and go	273-7	8:40:36	2 561	0.263
115 Thrust reverse	273-7	8:46:00	2 561	0.179
116 2.0g left turn (flaps up)	273-10	13:33:58	8 397	0.487
117 1.6g left turn (flaps 30)	273-10	13:41:07	8 202	0.260
120 2.0g right turn (flaps up)	273-15	11:04:03	8 240	0.476
121 1.6g right turn (flaps 30)	273-15	11:07:25	8 278	0.266
123 Airplane stall	273-10	13:26:17	9 000	0.207

125208-22-102



125208-22

Figure 36. View of Pressure Ports

#### 4.1.3.2 Installed Propulsion System Aerodynamics

Four test conditions were flown during the IPSA program. The test conditions included level flight at  $M = 0.77$ ,  $0.80$ , and  $0.86$  and at  $M = 0.91$ , a condition that required the airplane to be put into a shallow dive. The test conditions flown at  $M = 0.77$ ,  $0.86$ , and  $0.91$  satisfied the contract commitment and were coincident with flight load conditions. All test conditions were flown at a representative cruise altitude.

Preflight and postflight calibrations of the pressure measuring system were performed for each test flight. During a test flight, seven flight condition parameters were monitored online with a multichannel pen recorder. These parameters included flight Mach number, ambient total temperature, angle of attack, heading, pressure altitude, sideslip, and inboard aileron position. These parameters were used collectively to determine the stability of the airplane prior to and during the recording of measured pressure data. In each parameter, the deviations allowed for approximately a 30-sec period during which measured data were recorded; these deviations are:

Mach number	$\pm 0.001$
Ambient total temperature	$\pm 0.1^\circ\text{C}$
Angle of attack	$\pm 0.25 \text{ deg}$
Heading	$\pm 0.2 \text{ deg}$
Pressure altitude	$\pm 3.048 \text{ m} (\pm 10 \text{ ft})$
Sideslip	$\pm 0.25 \text{ deg}$
Aileron position	$\pm 1 \text{ deg}$

All test conditions were flown with the airplane autopilot engaged and in the altitude hold mode.

Because all measured pressure data were acquired during cruise conditions, no wing leading- or trailing-edge devices that would alter the basic wing geometry described in table 1 were deployed with the exception of the inboard aileron. In cruise, the inboard aileron provided small amounts of roll control and was combined with various amounts of midspan spoiler deployment for larger rolling moment inputs. During data recordings, some small aileron deflections, well below those levels causing limited spoiler deployment, were required to maintain level flight. Accordingly, this small amount of inboard aileron deflection effectively changed the local wing camber at WBLs 445, 470, and 510.

For reference, the geometrical arrangement of the inboard aileron at WBLs of 445 and 510 including the wing line location is presented in table 19. The outboard aileron was locked out during cruise and therefore was an inactive control surface at 0-deg deflection.

#### 4.1.4 Test Data Format

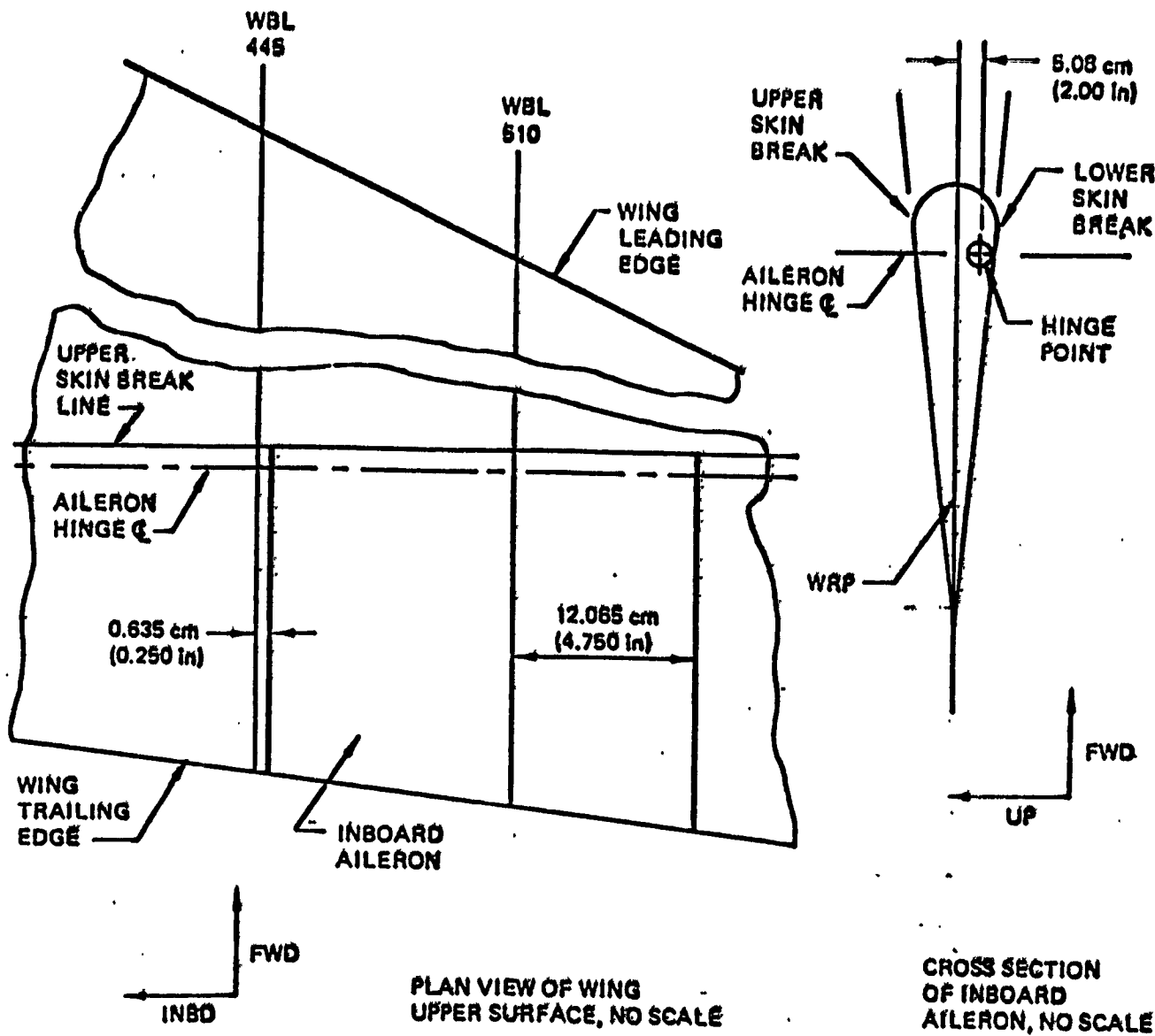
The data collected during the NAIL program required careful use of the airborne data analysis and monitor system (ADAMS) and of the final data system. Of particular concern was the ability to assess real-time data quality for flight decisions, because 1023 channels of measurements were being made during the combined test program and no ground-based analysis system was available at the remote site. It was necessary to send the flight tape to Seattle shortly after completion of the day's testing. This requirement did not allow rerunning the tape on the ADAMS. Therefore, essentially all decisions were based upon real-time data obtained from the ADAMS during flight. Further development of the onboard ADAMS and the combined use of the final data system in conjunction with the flight test interactive graphics data analysis (fGDA) site aided in coping with this problem.

The basic ADAMS (fig. 37) could not handle the volume of data required by the JT9D-7R4 and NAIL programs. The expanded data handling capabilities of the analysis groups doubled that of the basic system by using a second ADAMS on the RA001. The quantity of data collected during the program required system modification in order to minimize testing and preflight delays. These modifications to the onboard flight test system (fig. 38) provided adequate remote-base support to the flight test program. Several hardware and software changes to the basic ADAMS were implemented to accomplish this support.

Two other significant hardware changes were made to the basic ADAMS. First, a fixed head disk for program and measurement information storage was used. The fixed head disk eliminated loading of information through Cartridges each time the system was brought online. This improvement was vital because activating the system required 1 to 2 min rather than 15 min as projected, based on the number of measurements required. A 15-min delay was unacceptable in terms of cost, if the system should malfunction once airborne. Further, rapid selection of preselected data sources was also a requirement in view of the quantity of data being measured and the concurrent test program to permit

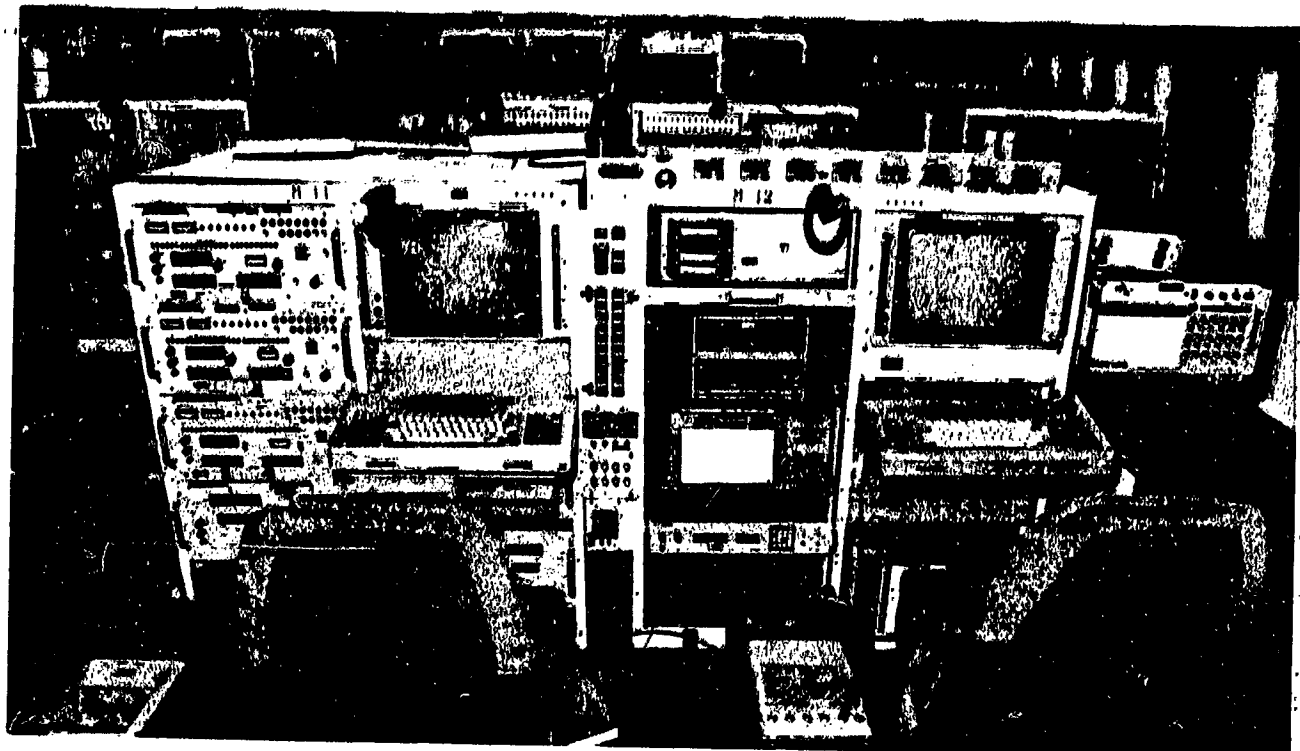
ORIGINAL PAGE IS  
OF POOR QUALITY

Table 19. Inboard Aileron



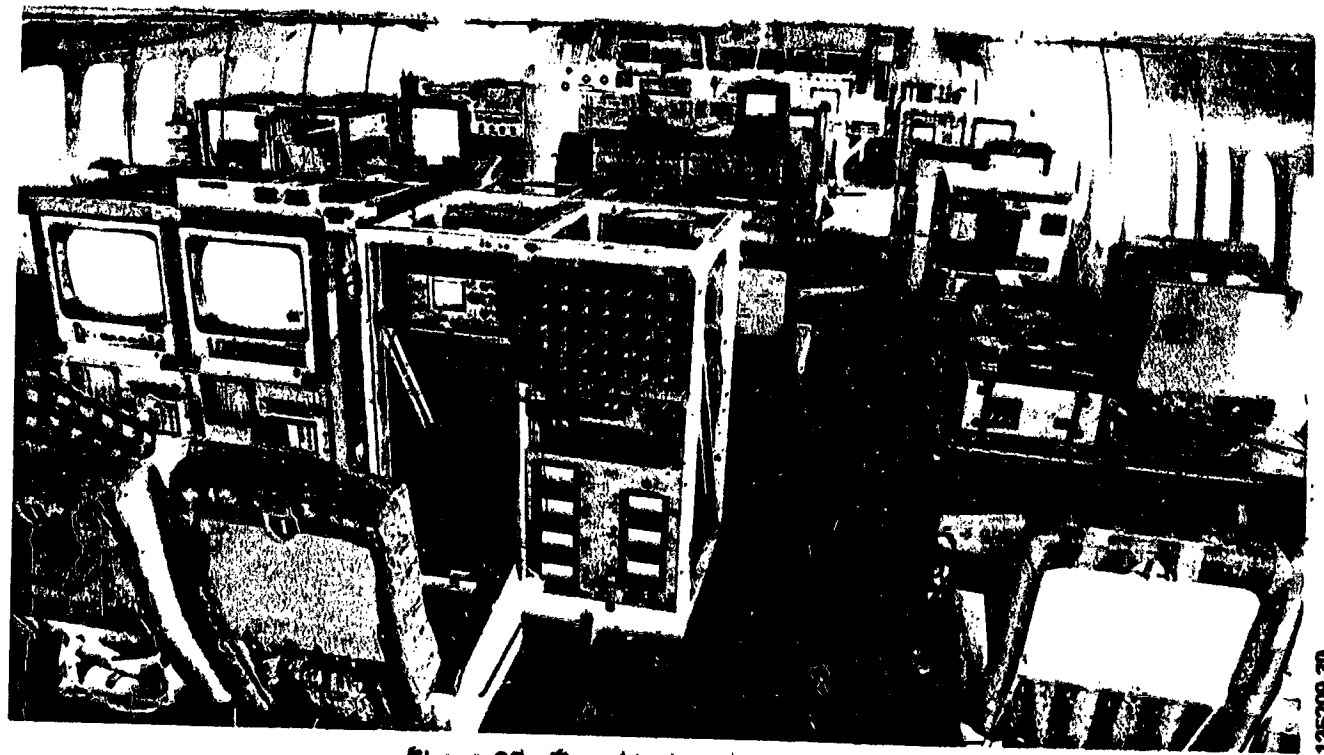
DISTANCE MEASURED IN WRP, cm (in)	WBL	
	445	610
Leading edge to aileron hinge centerline	830.78 (327.08)	680.54 (267.93)
Leading edge to upper surface skin break line	827.58 (325.82)	677.34 (266.67)
Leading edge to lower surface skin break line	828.47 (326.17)	677.77 (266.84)

ORIGINAL PAGE IS  
OF POOR QUALITY



12209-29

Figure 37. Airborne Data Analysis and Monitoring System



12209-30

Figure 38. Test Airplane Interior View

the test engineers to track their respective data. Second, a data measurement selector was incorporated into the ADAMS. This was necessary because approximately 1023 measurements were obtained during the flight test. The data measurement selector sent data preselected for output to the digital-to-analog converter.

The original ADAMS software could not support the NAIL program during remote base operation. An onboard pressure coefficient (PC) program was lacking, and thus development of an interim program that satisfied the needs of analysis was necessary. The PC program was developed to use the Brush recorder as a quasographics system and to use the line printer for summary outputs. The program could calculate pressure coefficients for up to 16 measurement groups with a maximum of 20 pressure ports each. The output of the program was displayed on the Brush recorder while a summary table of port differential pressures and pressure coefficient values was printed on the line printer. This information was output either continuously or upon keyboard command for a predetermined time interval. The program provided real-time information for determining data quality and for making decisions on subsequent test conditions.

Data were supplied in the forms of tables, computer-generated graphs, and data files on magnetic tapes. Table 20 is an example of a pressure coefficient data table. Engine performance and fuel flow examples are given in tables 21 and 22. An example of an engine clearance data table is given in table 23. Finally, table 24 is an example of a turbine case temperature table. The magnetic tape data files included all the above examples and basic airplane data for all flight conditions, plus acceleration data for the heavyweight landing.

## 4.2 TEST RESULTS

### 4.2.1 Aerodynamic and Inertial Loads

#### 4.2.1.1 Aerodynamic Loads

Pressures were measured at 252 ports in 12 rows nominally 30 deg apart on the inlet and fan cowl of engine 3. The actual spacing varied slightly for some ports because of installation and arrangement requirements. (See Appendix A for details.) Fourteen ports were found to have defective or doubtful transducers, and the indicated pressures of those ports were not used. Pressure data are presented graphically and in tabular form in Appendix A.

**ORIGINAL PAGE IS  
OF POOR QUALITY**

001-02-00221

Table 20. Pressure Coefficient

AIRPLANE MODEL		767-100		TEST 273-07		PRESSURE COEFFICIENT	
AIRPLANE NUMBER		8A001					
COORDINATION	C	ALPHA	0	PRESS-INLET	E3 PT01 240R	PRESS-INLET	E3 PT03 240R
TYPE		PSI	PSI	PS	PS	PS	PS
HR-MIN-SEC		DEG	PSI	3211	3212	3213	3214
8-33-20-016	DIA	IEC	11.152	IEC	10.994	IEC	10.627
8-33-20-064	DIA	-1.06	11.116	-1.220	10.956	-1.106	10.435
8-33-20-114	DIA	-1.182	11.152	-1.187	10.954	-1.365	10.227
8-33-20-164	DIA	-1.197	11.093	-1.188	10.954	-1.566	10.027
8-33-20-214	DIA	-1.182	11.126	-1.168	11.029	-1.435	10.512
8-33-20-264	DIA	-1.254	11.913	-1.123	10.994	-1.507	10.457
8-33-20-314	DIA	-1.254	11.069	-1.186	11.029	-1.636	10.472
8-33-20-364	DIA	-1.310	11.152	-1.155	11.053	-1.523	10.520
8-33-20-414	DIA	-1.239	11.152	-1.188	11.039	-1.436	10.492
8-33-20-464	DIA	-1.296	11.097	-1.155	11.050	-1.435	10.471
8-33-20-514	DIA	-1.353	11.086	-1.153	11.050	-1.562	10.563
8-33-20-564	DIA	-1.268	11.056	-1.123	10.995	-1.537	10.582
8-33-20-614	DIA	-1.225	11.209	-1.091	10.952	-1.507	10.532
8-33-20-664	DIA	-1.246	11.011	-1.192	11.012	-1.671	10.537
8-33-20-714	DIA	-1.246	11.048	-1.188	11.030	-1.636	10.572
8-33-20-764	DIA	-1.340	11.012	-1.188	11.022	-1.672	10.572
8-33-20-814	DIA	-1.226	11.137	-1.137	11.012	-1.672	10.572
8-33-20-864	DIA	-1.254	11.084	-1.123	10.995	-1.672	10.572
8-33-20-914	DIA	-1.211	11.070	-1.117	11.021	-1.672	10.572
8-33-20-964	DIA	-1.212	11.026	-1.185	11.013	-1.672	10.572
8-33-21-014	DIA	-1.254	11.035	-1.126	11.013	-1.672	10.572
8-33-21-064	DIA	-1.269	11.265	-0.955	11.021	-1.672	10.572
8-33-21-114	DIA	-1.325	11.325	-0.866	11.020	-1.637	10.572
8-33-21-164	DIA	-1.225	11.041	-1.169	11.030	-1.637	10.572
8-33-21-214	DIA	-1.311	11.068	-1.137	11.013	-1.692	10.572
8-33-21-264	DIA	-1.295	11.043	-1.137	11.013	-1.692	10.572
8-33-21-314	DIA	-1.283	11.092	-1.153	11.013	-1.692	10.572
8-33-21-364	DIA	-1.297	11.097	-1.137	11.013	-1.692	10.572
8-33-21-414	DIA	-1.225	11.126	-1.169	11.057	-1.637	10.572
8-33-21-464	DIA	-1.155	11.126	-1.124	11.057	-1.637	10.572
8-33-21-514	DIA	-1.212	11.069	-1.163	11.055	-1.692	10.572
8-33-21-564	DIA	-1.198	11.097	-1.163	11.055	-1.692	10.572
8-33-21-614	DIA	-1.269	11.053	-1.126	11.055	-1.692	10.572
8-33-21-664	DIA	-1.225	11.023	-1.128	11.055	-1.692	10.572
8-33-21-714	DIA	-1.283	11.023	-1.128	11.055	-1.692	10.572
8-33-21-764	DIA	-1.241	11.092	-1.174	11.055	-1.692	10.572
8-33-21-814	DIA	-1.284	11.023	-1.165	11.055	-1.692	10.572
8-33-21-864	DIA	-1.340	11.080	-1.165	11.055	-1.692	10.572
8-33-21-914	DIA	-1.213	11.069	-1.165	11.055	-1.692	10.572
8-33-21-964	DIA	-1.213	11.023	-1.165	11.055	-1.692	10.572

卷之三

CONDITION AVERAGES  
CAPTURED AIRSPEED  
CAPTURED ALTITUDE  
DYNAMIC PRESSURE  
PROGRAM LIBRARY 08/11/80 F207  
PACH NUMBER 0-245  
FLAP POSITION 0-30 DEG  
LANDING GEAR UP  
CROSS WIND 0 KIAS  
F207 08/11/80 0-245 118  
F207 08/11/80 0-245 118-1  
F207 08/11/80 0-245 118  
F207 08/11/80 0-245 118

ORIGINAL PAGE IS  
OF POOR QUALITY

152200-20-110

Table 21. Summary of Measurements of Engine Performance

AIRPLANE MODEL 747-100				TEST 273-15				JTF ENG PERF SUMMARY				REQUEST NO 1116-0191 DATE 10/31/68 TIME 0515								
AIRPLANE NUMBER 64441		V KTIS		DELTAV DEG C		TAT DEG C		T71 DEG C		P71 IN HG		P71 IN HG		DELTA DEG C		DELTA IN HG		DELTA IN HG		
24096.	0.681	364.4	2.5	-39.2	-12.7	11.56	16.75	0.3863	0.4934	0.4924	0.4945	0.4924	0.4945	NDA	NDA	NDA	NDA	NDA	NDA	
<b>AIRPLANE DATA</b>																				
ENG	F76 LBS	F80 LBS	SFC RPM	R71 RPM	R72 RPM	R73 C/K	R74 LBS	NDA	NDA	NDA	NDA	NDA	NDA	NDA	NDA	P25P71 P27P71	P25P71 P27P71	S74 P72 P73 P74 P75 P76 P77	S74 S75 S76 S77 S78 S79 S7A	
1	NDA	NDA	100	100	NDA	NDA	NDA	NDA	NDA	NDA	NDA	NDA	NDA	NDA	NDA	NDA	NDA	NDA	NDA	
2	NDA	NDA	100	100	NDA	NDA	NDA	NDA	NDA	NDA	NDA	NDA	NDA	NDA	NDA	NDA	NDA	NDA	NDA	
3	7212.	6.6975	2788.	6644.	628.	749.	10938.	5039.	628.	749.	10938.	1398.	1398.	1398.	1398.	205.227	1.892	12.763	1.892	12.763
4	NDA	NDA	100	100	NDA	NDA	NDA	NDA	NDA	NDA	NDA	NDA	NDA	NDA	NDA	NDA	NDA	NDA	NDA	
5	NDA	NDA	100	100	NDA	NDA	NDA	NDA	NDA	NDA	NDA	NDA	NDA	NDA	NDA	NDA	NDA	NDA	NDA	
<b>GAS GENERATOR SUMMARY</b>																				
ENG	F76 LBS	F80 LBS	F77 LBS	F78 LBS	F79 LBS	F80 LBS	F81 LBS	NDA	NDA	NDA	NDA	NDA	NDA	NDA	NDA	P25P71 P27P71	P25P71 P27P71	S74 S75 S76 S77 S78 S79 S7A	S74 S75 S76 S77 S78 S79 S7A	
6	NDA	NDA	NDA	NDA	NDA	NDA	NDA	NDA	NDA	NDA	NDA	NDA	NDA	NDA	NDA	NDA	NDA	NDA	NDA	
<b>THRUST CALCULATION DETAIL SUMMARY</b>																				
ENG	FGF LBS	FRGF LBS	FRAT LBS	FRFP LBS	FRFP LBS	FRFP LBS	FRFP LBS	P25P71 NDA	P25P71 NDA	P25P71 NDA	P25P71 NDA	P25P71 NDA	P25P71 NDA	P25P71 NDA	CGF COP	AFAN APRT FT2 K/PFS LBS/C	R12.5 NDA NDA NDA NDA	S74 S75 S76 S77 S78 S79 S7A		
1	NDA	NDA	NDA	NDA	NDA	NDA	NDA	NDA	NDA	NDA	NDA	NDA	NDA	NDA	NDA	20.119	NDA	NDA	NDA	
2	NDA	NDA	NDA	NDA	NDA	NDA	NDA	NDA	NDA	NDA	NDA	NDA	NDA	NDA	NDA	7.226	NDA	NDA	NDA	
3	17697. <td>3386.<td>13865.<td>13562.<td>182.</td><td>1.7036.<td>1.6956.<td>1.6962.<td>1.7032.<td>1.7032.<td>1.7032.<td>1.7032.<td>1.7032.<td>1.7032.<td>1.7032.<td>20.119</td><td>0.9461</td><td>0.9461</td><td>0.9461</td><td>0.9461</td></td></td></td></td></td></td></td></td></td></td></td></td></td>	3386. <td>13865.<td>13562.<td>182.</td><td>1.7036.<td>1.6956.<td>1.6962.<td>1.7032.<td>1.7032.<td>1.7032.<td>1.7032.<td>1.7032.<td>1.7032.<td>1.7032.<td>20.119</td><td>0.9461</td><td>0.9461</td><td>0.9461</td><td>0.9461</td></td></td></td></td></td></td></td></td></td></td></td></td>	13865. <td>13562.<td>182.</td><td>1.7036.<td>1.6956.<td>1.6962.<td>1.7032.<td>1.7032.<td>1.7032.<td>1.7032.<td>1.7032.<td>1.7032.<td>1.7032.<td>20.119</td><td>0.9461</td><td>0.9461</td><td>0.9461</td><td>0.9461</td></td></td></td></td></td></td></td></td></td></td></td>	13562. <td>182.</td> <td>1.7036.<td>1.6956.<td>1.6962.<td>1.7032.<td>1.7032.<td>1.7032.<td>1.7032.<td>1.7032.<td>1.7032.<td>1.7032.<td>20.119</td><td>0.9461</td><td>0.9461</td><td>0.9461</td><td>0.9461</td></td></td></td></td></td></td></td></td></td></td>	182.	1.7036. <td>1.6956.<td>1.6962.<td>1.7032.<td>1.7032.<td>1.7032.<td>1.7032.<td>1.7032.<td>1.7032.<td>1.7032.<td>20.119</td><td>0.9461</td><td>0.9461</td><td>0.9461</td><td>0.9461</td></td></td></td></td></td></td></td></td></td>	1.6956. <td>1.6962.<td>1.7032.<td>1.7032.<td>1.7032.<td>1.7032.<td>1.7032.<td>1.7032.<td>1.7032.<td>20.119</td><td>0.9461</td><td>0.9461</td><td>0.9461</td><td>0.9461</td></td></td></td></td></td></td></td></td>	1.6962. <td>1.7032.<td>1.7032.<td>1.7032.<td>1.7032.<td>1.7032.<td>1.7032.<td>1.7032.<td>20.119</td><td>0.9461</td><td>0.9461</td><td>0.9461</td><td>0.9461</td></td></td></td></td></td></td></td>	1.7032. <td>1.7032.<td>1.7032.<td>1.7032.<td>1.7032.<td>1.7032.<td>1.7032.<td>20.119</td><td>0.9461</td><td>0.9461</td><td>0.9461</td><td>0.9461</td></td></td></td></td></td></td>	1.7032. <td>1.7032.<td>1.7032.<td>1.7032.<td>1.7032.<td>1.7032.<td>20.119</td><td>0.9461</td><td>0.9461</td><td>0.9461</td><td>0.9461</td></td></td></td></td></td>	1.7032. <td>1.7032.<td>1.7032.<td>1.7032.<td>1.7032.<td>20.119</td><td>0.9461</td><td>0.9461</td><td>0.9461</td><td>0.9461</td></td></td></td></td>	1.7032. <td>1.7032.<td>1.7032.<td>1.7032.<td>20.119</td><td>0.9461</td><td>0.9461</td><td>0.9461</td><td>0.9461</td></td></td></td>	1.7032. <td>1.7032.<td>1.7032.<td>20.119</td><td>0.9461</td><td>0.9461</td><td>0.9461</td><td>0.9461</td></td></td>	1.7032. <td>1.7032.<td>20.119</td><td>0.9461</td><td>0.9461</td><td>0.9461</td><td>0.9461</td></td>	1.7032. <td>20.119</td> <td>0.9461</td> <td>0.9461</td> <td>0.9461</td> <td>0.9461</td>	20.119	0.9461	0.9461	0.9461	0.9461
4	NDA	NDA	NDA	NDA	NDA	NDA	NDA	NDA	NDA	NDA	NDA	NDA	NDA	NDA	NDA	318.	1.395	1.395	1.395	
<b>ALL VALUES PRINTED ARE CONDITION AVERAGES</b>																				
PROGRAM LIBRARY 82/11/68 P887										CONDITION NO 4-33-315-307 DOCUMENT NO DS-22118-1 PAGE NO										

ORIGINAL PAGE IS  
OF POOR QUALITY

111-02-002821

Table 22. Engine Fuel-Flow Data

AIRPLANE MODEL 747-100		TEST 273-13		ENGINE FUEL FLOW DATA	
AIRPLANE NUMBER RA881				PAUA JT9D-3/7	
COORDINATION	CG ER	WRF	TEST VALUES		TEST VALUES
			LBS/MIN	SEC	
11-27-49.016	3	100 NDA	NDA	100	SURF ABUF APBFSC LEVEL 100A 100B 100C 10 10 10 10
11-27-49.016	3	5619 10034	698	762 8000	71 8 72
AVERAGE	3	5619 10034	698	762 8000	71 8 72
NO. OF POINTS	3	1 1 1	1 1 1	1 1 1	• • •

REQUESTED BY 111-02-002821  
DATE 10/31/88 TIME 0515  
SURF ABUF APBFSC  
LEVEL 100A 100B 100C  
10 10 10 10

PROGRAM LIBRARY 04/11/88 PWD

CONDITION NO 4-23-015-200  
EFFECTIVE NO 45-22419-1  
PAGE NO 2

ORIGINAL PAGE IS  
OF POOR QUALITY

*Table 23. Measurements for Engine Clearance*

COORDINATION TIME	AIRPLANE NUMBER 747-100		TEST 273-15		REQUEST NO 1316-0131		DATE 10/31/70 TIME 0515	
	E3 CLEARANCE HPT 128 DEG	E3 CLEARANCE HPT 300 DEG	E3 CLEARANCE FAN 300 DEG	E3 CLEARANCE FAN 300 DEG	E4 CLEARANCE FAN 128 DEG	E4 CLEARANCE FAN 128 DEG	E5 C. CLEARANCE FAN 300 DEG	TEMP H-FLANGE TIP 53 RAD
HPT 21.7 DEG	E3 CLEARANCE HPT 218 DEG	E3 CLEARANCE HPT 218 DEG	E3 CLEARANCE FAN 30 DEG	E3 CLEARANCE FAN 30 DEG	E4 CLEARANCE FAN 218 DEG	E4 CLEARANCE FAN 218 DEG	E5 C. CLEARANCE FAN 30 DEG	TEMP H-FLANGE TIP 3 RAD
TIME	MILS	MILS						
2686	2681	2682	2686	2686	2687	2688	2689	2690
0.133	0.133	0.133	0.135	0.135	0.136	0.136	0.132	0.132
-3	-3	-3	-3	-3	-3	-3	-3	-3
MM MIN SEC	10	10	10	10	10	10	10	10
11-33-00 .094	122330	479168	26711	95729	510666	116197	88566	26670
11-33-01 .094	56532	LP	20544	68165	513695	110081	97832	40917
11-33-02 .094	67861	517338	81184	71025	522960	169189	118629	57459
11-33-03 .094	89451	LP	62683	93678	71185	114318	114318	62119
11-33-04 .094	25802	LP	2268	26764	366478	93676	60758	135825
11-33-05 .094	69898	499853	183795	34999	469427	81445	91653	37964
11-33-06 .094	66251	629913	65211	29852	515253	70216	117399	137664
11-33-07 .094	28774	463855	-2067	49689	473544	126882	133877	81564
11-33-08 .094	103825	389118	65211	102934	LP	181574	136966	87215
11-33-09 .094	59617	513224	11294	57644	647807	81271	70027	9235
AVERAGE	67510	426923	61717	60217	477536	169085	102982	43718
MINIMUM	26776	522913	-2067	26764	366678	78185	60758	9235
MAXIMUM	122330	517338	183795	182956	522960	169189	136966	216291
STD DEVIATION	28927	29753	31236	27432	49921	22201	24322	20670
NO. OF POINTS	10	7	10	8	10	10	10	10

PROGRAM LIBRARY 08/11/78 PAGE 07  
CONDITION NO 1.13-315-312  
CURENT NO 08-22119-1  
PAGE 07

**ORIGINAL PAGE IS  
OF POOR QUALITY**

卷之三

**Table 24. Measurements of Turbine Case Temperature**

To compute resultant airloads from the pressure data, a previously developed computer program was used. It approximates the inlet and cowl geometry as a series of conical frustums and adjusts for the tilt of the inlet axis with respect to the nacelle centerline by insertion of wedge-shaped surfaces. This procedure was checked by comparison to a method based on a complete three-dimensional geometry definition. Resultant forces differed by less than 3%, and resultant yaw and pitching moments at the engine face differed by less than 1%. (Rolling moments differed by 3.5% but are not significant loads.)

Figure 39 shows the coordinate system for the resultant loads.

Table 25 gives resultant loads along with key airplane and engine parameters for 23 flight conditions.

**Takeoffs**—Four takeoffs—one at flaps 20 deg and 612 000 lb gross weight and three at flaps 10 deg and gross weights of 538 000, 647 000, and 780 000 lb (simulated)—were selected for detailed loads analyses. For two takeoffs, time histories of resultant loads were calculated for the purpose of correlating maximum clearance changes, whenever they occurred, with the aerodynamic loads. For the 780 000 lb takeoff, which was simulated by a pullup maneuver at 1000 ft above ground level, the analysis was done at the instant the correct airplane lift coefficient was reached.

The flaps 20 deg, 612 000 lb gross weight takeoff was the initial takeoff for the entire test program. Peak load was reached at inter-range instrumentation group master clock (IRIG) time 6:41:44. The pitching moment at the A-flange was 329 000 in-lb.

The 538 000 lb takeoff occurred during test 273-10, and the time history covers the IRIG span of 9:44:00 to 9:44:11. Time histories of A-flange pitching moment and airflow sensor vane angle\* during the takeoff rotation are given in figure 40. The direct relationship of load to flow angle is evident. Also note that the maximum moment for this condition (401 000 in-lb) is considerably higher than the maximum for the flaps 20-deg takeoff, table 25.

---

\*The airflow sensor vanes are mounted on both sides of the fuselage near the flight deck. The flow angles indicated by the vanes are influenced by flap setting, wing upwash, body crossflow, and other factors and should not be construed as airplane angle of attack.

ORIGINAL PAGE VI  
OF POOR QUALITY

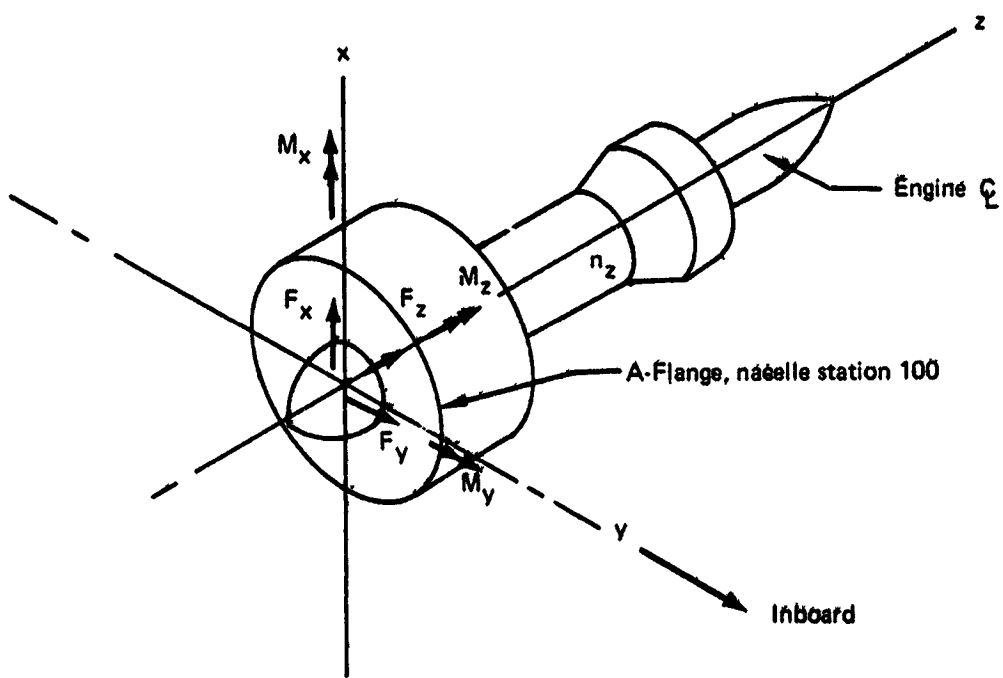


Figure 39. Sign Convention for Steady-State Loads, Engine 3

123200-55-447

Table 25. Engine 3 A-Flange Resultants

Condition	Air-speed, KCAS	Pressure altitude, ft	Mach number	Referred airflow, lb/s	Load factor, g	$F_x$ , lb	$F_y$ , lb	$M_{x'}$ , in-lb	$M_{y'}$ , in-lb
101 612K gross weight takeoff (flaps 20)	157.8	2 663	0.250	1549	1.14	6001	-2754	-147 736	-328 780
101 536K gross weight takeoff (flaps 10)	151.0	2 687	0.239	1527	1.26	7197	-2916	-152 292	-400 756
101 647K gross weight takeoff (flaps 10)	160.1	2 634	0.254	1524	1.17	7921	-3112	-159 326	-424 987
118 780K gross weight simulated takeoff (flaps 10)	183.8	3 846	0.296	1673	1.20	8344	-2787	-134 046	-430 154
102 Low climb	218.8	5 861	0.387	1639		4870	-1067	- 45 361	-206 043
103 Mid climb	290.4	17 187	0.599	1622		4084	- 588	- 25 756	-125 891
104 High M cruise	291.3	35 481	0.859	1633		2469	-1023	- 36 317	- 59 441
105 Low M cruise	288.3	35 512	0.772	1604		3478	-1131	- 42 237	-106 150
106 Max M	299.0	36 978	0.906	1642		302	- 464	- 15 779	+ 15 317
107 Inflight relight	286.7	27 859	0.721	1365		3277	-736	- 25 639	- 84 847
108 Maximum q	357.8	24 513	0.836	1617		-1410	+ 984	29 060	98 411
109 Stall warning (flaps up)	188.4	16 984	0.391	1591		5437	-1384	- 63 775	-243 214
110 Stall warning (flaps 10)	169.2	16 239	0.347	1621		6229	-2142	- 97 024	-304 770
111 Stall warning (flaps 30)	129.3	17 049	0.270	1633		3927	-1292	- 72 893	-220 730
112 Idle descent	249.7	8 450	0.439	748		4130	-1124	- 29 669	- 97 234
113 Approach	157.4	6 003	0.265	1547		3707	-1411	- 71 807	-201 854
114 Touch and go	168.5	2 581	0.263	1589		4388	-2321	-125 622	-241 654
115 Thrust reverse	113.2	2 561	0.179	1369		44	- 10	- 17 298	- 40 963
116 2.0g left turn (flaps up)	277.5	8 397	0.487	1562	1.99	7212	-3459	-133 292	-264 186
117 1.6g left turn (flaps 30)	143.0	8 202	0.260	1539	1.61	5293	-3672	-191 221	-284 557
120 2.0g right turn (flaps up)	272.1	8 240	0.476	1196	2.04	7634	-1629	- 47 456	-239 481
121 1.6g right turn (flaps 30)	151.3	8 278	0.266	1436	1.80	5416	- 359	- 10 105	-282 023
123 Airplane stall	115.7	9 000	0.207	1661		6072	-1613	- 89 181	-366 818

12299-31

ORIGINAL PAGE IS  
OF POOR QUALITY

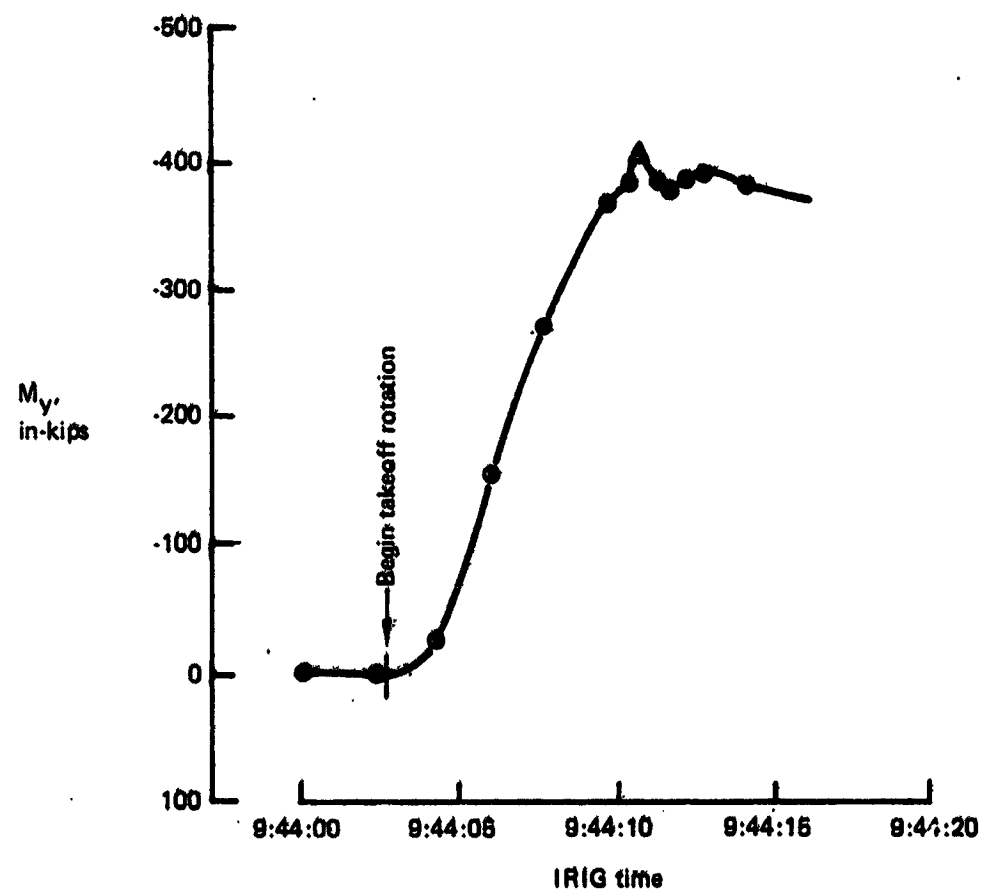
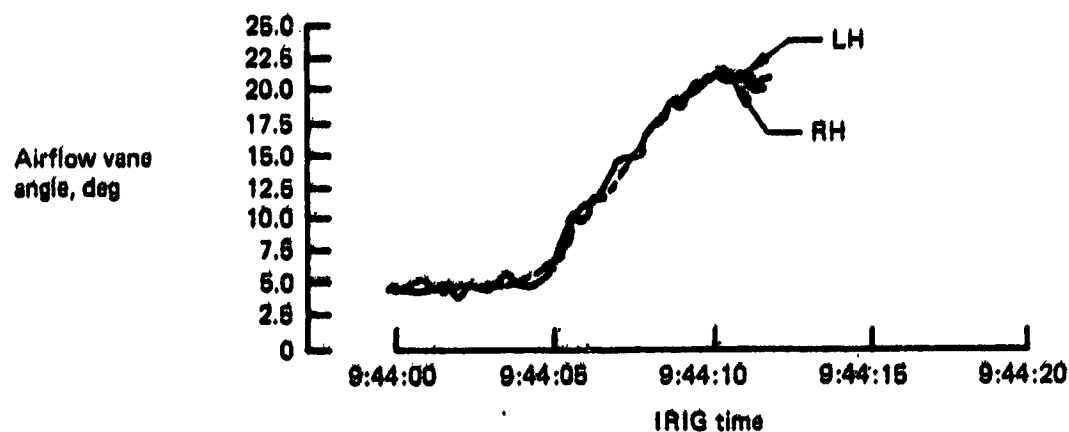


Figure 40. Inlet Pitching Moment Time History, 838 000 lb Gross Weight Takeoff

The 647 000 lb takeoff occurred during test 273-11 between IRIG time 10:13:46 and 10:13:55. The pitching moment time history (fig. 41) shows that the maximum aerodynamic load occurred at IRIG 10:13:52, with a nose-up moment of 425 000 in-lb. The load factor was 1.17g.

The simulated high gross weight takeoff occurred during test 273-15 at IRIG 8:13:18. The actual gross weight was 696 500 lb. The simulation was achieved by performing a pullup starting at 185 kn and 3646 ft altitude (about 1000 ft above ground) to produce the same airplane lift coefficient that would occur during a 780 000 lb takeoff. (The original intention was to simulate an 820 000 lb-gross weight takeoff. However, insufficient allowance was made for speed reduction due to increasing climb gradient in the pullup maneuver.) The moment at the A-flange was 430 100 in-lb.

**Other Cases**-Airloads for conditions other than takeoff were generally of substantially lesser magnitude. However, certain cases were analyzed in greater detail because of possible adverse combinations of aerodynamic loads and thermal transients in the engine. Figure 42 shows a time history of the pitching moment at the engine face, engine airflow, and body vane angle for condition 110 (stall warning 10 deg flaps). The maximum moment (305 000 in-lb) coincided with maximum engine airflow, although the maximum vane angle occurred earlier in the maneuver. The result shows that engine airflow is of comparable importance to angle of attack in determining inlet airloads.

Other cases given special attention were the turns at constant altitude to achieve a specified load factor. Engine clearance changes during these maneuvers were due to a combination of aerodynamic loads, g-loads, and gyroscopic loads. Condition 116, nominally a 2g turn to the left, was run during test 273-10 and achieved a load factor of 1.99 at IRIG 13:33:58. The A-flange moment was 264 200 in-lb. The indicated pitch rate was 4.29 deg/s and the yaw rate was about 2.9 deg/s on both engines. A 2g turn to the right was performed during test 273-15 (condition 120) at IRIG 11:04:03. The moment was 239 500 in-lb, pitch rate was 5.5 deg/s, and yaw rate was 2.8 deg/s. Turns of 1.6g at flaps 30 deg. were performed to the right and to the left. The left turn occurred during test 273-10, IRIG 13:41:07 (condition 117) with a moment of 284 600 in-lb, pitch rate of 6.5 deg/s, and yaw rate of 3.7 deg/s. The right turn occurred during test 273-15 (condition 121) at IRIG 11:07:25 with a moment of 282 000 in-lb, pitch rate of 7 deg/s, and yaw rate of 4.7 deg/s. Finally, an airplane stall occurred during test 273-10. The moment peaked at 367 000 in-lb at IRIG 13:26:16. This relatively high load level resulted from a very high angle of attack.

ORIGINAL PAGE IS  
OF POOR QUALITY

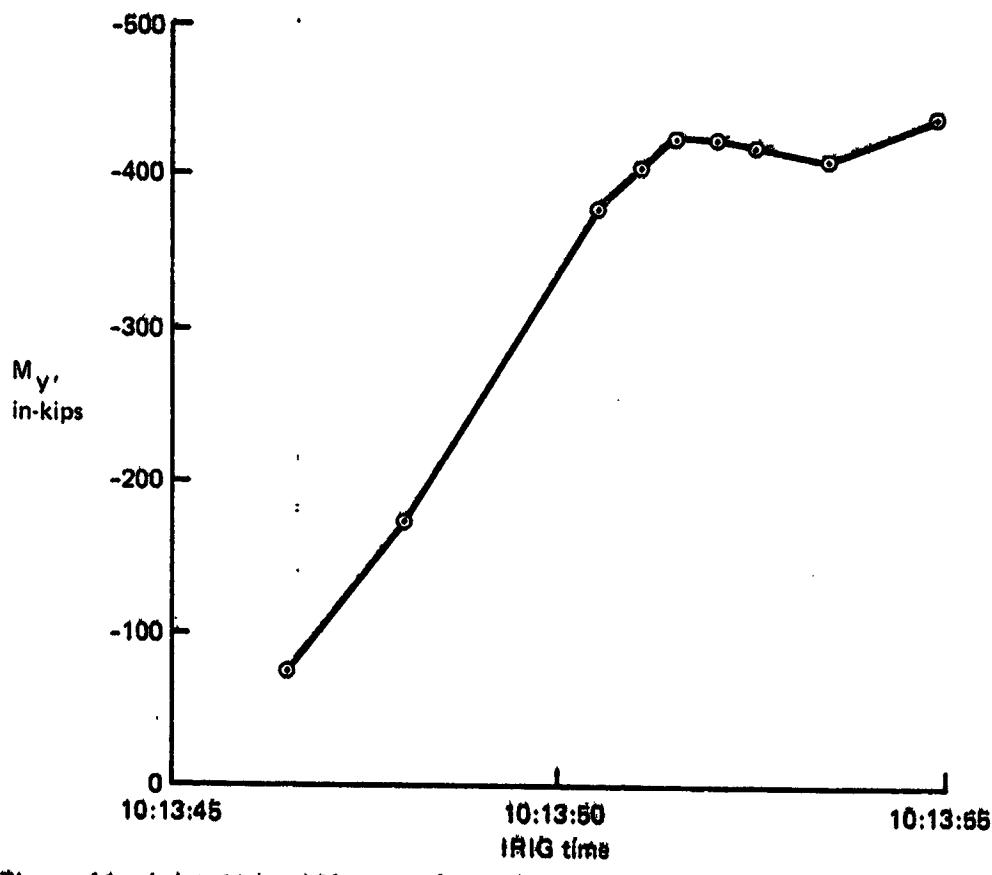


Figure 41. Inlet Airload Moment Time History, 647 000 lb Gross Weight Takeoff

125209-34

ORIGINAL PAGE IS  
OF POOR QUALITY

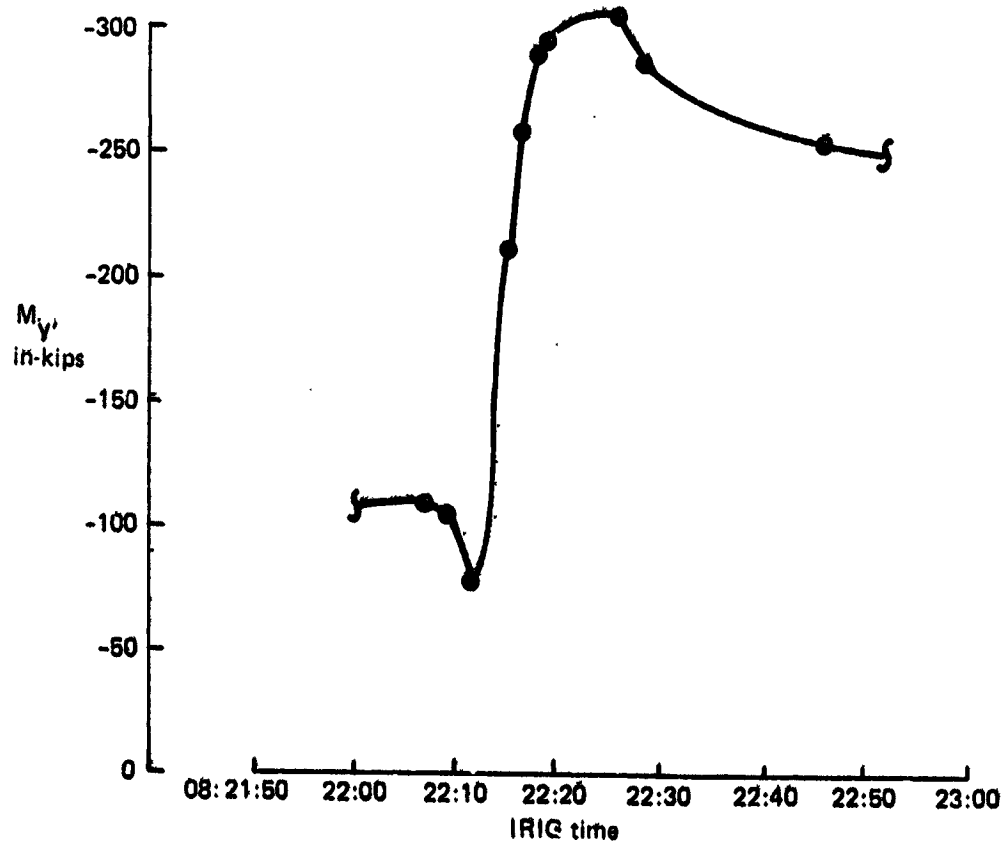
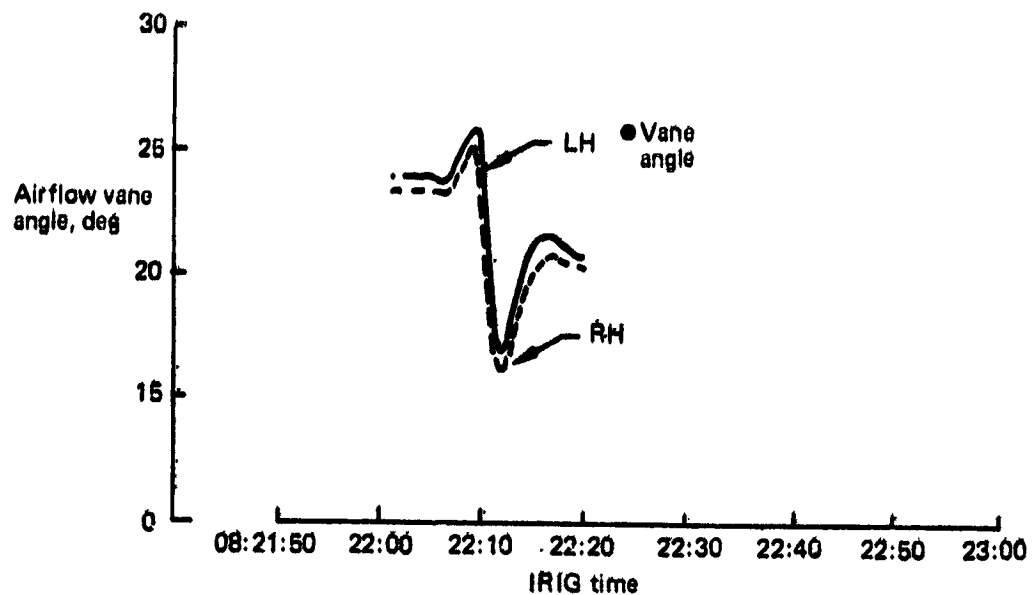


Figure 42. Airload Moment Time History, Stall Warning Maneuver, Flaps 10

125209-33

(S-2)

In this section all loads pertain to engine 3. Preliminary review of the test data indicated that the pressures on engine 4 were very close to the pressures of engine 3, implying that the loads were about equal. Comparison of the aerodynamic loads determined in the NAIL program with the loads predicted in task IIIA of the JT9D diagnostic program (ref. 2), indicate that:

- o The most critical loads were higher than predicted because of higher angles of attack than had been expected.
- o The cosine law for the circumferential pressure distribution assumed in task IIIA is only a rough approximation of the actual distribution, especially in the critical region near the highlight.
- o The phase angle of the cosine distribution is about 20 deg from the vertical near the highlight and further into the inlet approaches 0 deg.

#### 4.2.1.2 Inertial Loads

Normal accelerations measured during takeoff and flight did not exceed 1.3g except during the high-g turn maneuvers. No significant turbulence was experienced during the NAIL program. The difference between g-loads measured at the airplane center of gravity and those measured on engines 3 and 4 was within the scatter of the data. In other words, the instruments responded only to steady-state accelerations of the whole airplane, experiencing no significant contributions from wing or nacelle flexible modes.

An exception to the steady-state accelerations occurred during a hard landing in test 273-19. The airplane landed at 690 000 lb gross weight with 297 000 lb fuel and a sink rate of approximately 10 ft/s. Touchdown occurred at IRIG 8:20:49. Vertical acceleration at the airplane center of gravity was 1.53g, with peaks of 2g at engine 4 and 1.7g at engine 3. This case was selected for dynamic analysis. Another exception occurred during test 273-10 during which a mild gust was encountered at IRIG 12:11:52. Normal accelerations were 1.08g at the airplane center of gravity and 1.3g at the engines. Details of all these cases are shown in Appendix A.

Pitch rates during takeoffs did not exceed 3 deg/s, the peak value being achieved before reaching the maximum load factor.

#### **4.2.2 Installed Propulsion System Aerodynamics**

Surface static pressures were measured on the nacelle and pylon of engine 3 (inboard) and engine 4 (outboard) and on neighboring wing surfaces during three separate test flights over the span of the test period. The initial flight, test 273-09, acquired data at  $M = 0.77$ ,  $0.80$ , and  $0.86$  and revealed instrumentation problems, which were partially corrected for a second flight, test 237-12. The third flight, test 273-15, was flown primarily to fulfill the remaining NASA conditions, which included  $M = 0.91$ . The  $M = 0.91$  test was not flown until the end of the NAIL program when the speed restriction was removed concerning the other Boeing developmental programs...

Data plots of the measured pressures are presented in Appendix B.

## **5.0 REFERENCES**

- 1. NASA CR-159717 (PWA-5512-46), Expanded Study of Feasibility of Measuring In-Flight 747/JT9D Loads, Performance, Clearance, and Thermal Data—JT9D Jet Engine Diagnostics Program.**
- 2. D6-34720, Report of Task III A, Short Diagnostics Test Program, Engine Component Improvement Program, JT9D Engine Diagnostics (15 November 1978).**

## APPENDIX A

### 1.0 Pressures

The locations of pressure ports on engine 3 are shown in table A-1.

The coordinate system is shown in figure A-1. The arc length from the highlight to the port under considerations is denoted by "s." Positive values signify an external port and negative values signify an internal port.

The  $\theta$  coordinate is the azimuth angle measured from the top and clockwise looking at the inlet from the front.

A distinction was made between nominal values and actual values of  $s$  and  $\theta$ . The nominal values  $s_{nom}$  and  $\theta_{nom}$  are convenient for the computerized plotting of the data. In practice, installing the pressure taps at the nominal location was not always possible because of structural interferences. Consequently the actual  $s$  and  $\theta$  are also listed. Small discrepancies in actual pressure values resulting from these location shifts were accounted for by interpolation in the pressure integration process. The axial coordinate  $z$  (the normal distance from the highlight plane) is also listed.

Several pressure transducers gave unreliable or obviously erroneous readings. Therefore, pressures were determined by averaging values measured at adjacent ports using suitable weighting for geometric relationships. The ports for which such systematic substitutions were made are listed in table A-2. Pressures that still appeared to be erroneous after this substitution were corrected manually before they were plotted.

A complete description of the pressure distribution function  $p(s, \theta)$  at any point on the inlet is required to obtain inlet loads through integration. Because pressure was measured only at the pressure taps, an interpolation scheme was needed to determine the pressure at other locations. In the circumferential direction the Fourier-Bessel formula was used:

$$p(\theta) = A_0 + \sum A_n \cos(n\theta) + \sum B_n \sin(n\theta)$$

The use of this formula leads to a  $p(\theta)$  function that fits every measured point exactly and ensures maximum smoothness in between. In the  $s$ -direction a linear interpolation was used between measured points.

The coefficients  $A_n$  and  $B_n$  for all flight conditions are listed in tables A-3 to A-25. (Note that in the lip area, 12 coefficients are tabulated, because pressures were measured at 12  $\theta$  values. Elsewhere, only six coefficients are available, because only six  $\theta$  values were instrumented.)

The axial pressure distributions for each flight condition and value of  $\theta$  are shown graphically in figures A-2 to A-47. The pressures are plotted in terms of pressure coefficient versus nominal arc lengths. Each flight condition is covered by two pages, one (inlet pressures) pertaining to the rows of pressure ports that extend all the way into the inlet (i.e.,  $\theta = 0$  deg, 60 deg) and the other (cowl pressures) pertaining to the rows that extend to the trailing edge of the fan cowl (i.e.,  $\theta = 30$  deg, 90 deg).

On engine 4, pressure taps were installed at three circumferential locations,  $\theta = 60$  deg, 180 deg, and 300 deg. Axial pressure distributions are shown in figures A-48 to A-70. No Fourier-Bessel coefficients were calculated for this engine because no integration was carried out. The pressures were measured mainly for the purpose of comparison with engine 3 pressures. Note that for some of the test conditions the power level of engine 4 was considerably different from engine 3.

## 2.0 INERTIAL LOADS

Recorded accelerations on inlets and strut-wing intersections are presented in figures A-71 to A-83 for both engines for conditions when dynamically interesting events occurred:

- Mild gust during test 273-10
- Hard landing during test 273-15

The graphs show airplane parameters measured at airplane center of gravity and engine accelerations and angular rates. Engine accelerations were filtered to pass only frequencies below 40 Hz. Pitch and yaw rates were filtered to 5 Hz.

Table A-1. Engine 3 Pressure Port Locations

PORT NO.	NOMINAL THETA = 0. DEG	ROW NO. 1		ROW NO. 2		ROW NO. 3		ROW NO. 4		ROW NO. 5	
		Z (IN)	S (IN)								
1	-56.50	55.23	-57.68	1.64	1.54	53.60	-56.05	58.30	50.30	50.30	50.30
2	-51.21	46.99	-49.36	1.71	1.71	47.74	-50.15	61.35	50.30	50.30	50.30
3	-44.21	41.50	-43.80	1.55	1.55	42.04	-44.35	58.30	50.30	50.30	50.30
4	-36.21	36.04	-38.23	1.19	1.19	36.25	-38.45	61.42	50.30	50.30	50.30
5	-32.21	31.12	-33.23	1.15	1.15	31.14	-33.23	58.68	50.30	50.30	50.30
6	-28.21	25.69	-27.73	1.23	1.23	25.81	-27.85	61.19	50.30	50.30	50.30
7	-24.21	21.22	-23.23	1.17	1.17	21.39	-23.23	58.64	50.30	50.30	50.30
8	-20.21	18.48	-20.48	1.17	1.17	18.65	-20.65	61.10	50.30	50.30	50.30
9	-17.21	15.78	-17.78	1.24	1.24	15.95	-17.95	58.65	50.30	50.30	50.30
10	-14.21	11.29	-13.29	1.10	1.10	11.50	-13.50	60.69	50.30	50.30	50.30
11	-11.06	8.49	-10.48	1.23	1.23	8.61	-10.60	60.60	50.30	50.30	50.30
12	-8.00	5.58	-7.53	1.02	1.02	5.56	-7.50	5.48	50.30	50.30	50.30
13	-5.50	3.61	-5.48	0.00	0.00	3.63	-5.50	3.66	50.30	50.30	50.30
14	-3.00	1.41	-3.00	0.00	0.00	1.41	-3.00	1.45	50.30	50.30	50.30
15	-1.00	0.17	-1.00	0.00	0.00	0.17	-1.00	0.19	50.30	50.30	50.30
16	0.00	0.00	0.00	0.00	0.00	0.00	0.00	0.00	50.30	50.30	50.30
17	1.00	0.32	1.00	0.00	0.32	1.00	0.00	0.29	50.30	50.30	50.30
18	2.00	1.16	2.00	0.00	1.16	1.95	0.00	1.11	50.30	50.30	50.30
19	4.00	3.01	4.00	0.00	2.96	3.95	0.00	2.96	50.30	50.30	50.30
20	6.00	8.17	6.00	0.00	6.42	7.60	0.00	6.42	50.30	50.30	50.30
21	9.00	11.72	13.00	0.00	9.82	11.08	0.00	9.84	50.30	50.30	50.30
22	13.00	16.70	15.39	0.00	13.98	15.28	0.00	13.90	50.30	50.30	50.30
23	13.69	16.95	20.28	0.00	16.95	20.28	0.00	16.95	50.30	50.30	50.30
24	19.00	23.93	25.28	0.00	23.93	25.28	0.00	23.93	50.30	50.30	50.30
25	25.00	31.00	31.00	0.00	25.37	30.73	0.00	25.37	50.30	50.30	50.30
26	31.00	38.00	38.00	0.00	37.91	39.24	0.00	37.91	50.30	50.30	50.30
27	38.00	50.00	50.00	0.00	51.65	53.12	0.00	51.65	50.30	50.30	50.30
28	50.00	62.00	62.00	0.00	60.63	62.15	0.00	60.63	50.30	50.30	50.30
29	62.00	74.26	74.26	0.00	72.86	74.26	0.00	72.86	50.30	50.30	50.30
30	74.26	77.06	77.06	0.00	75.59	77.13	0.00	75.59	50.30	50.30	50.30
31	77.06	98.13	98.13	0.00	98.13	98.13	0.00	98.13	50.30	50.30	50.30
32	98.13	106.39	107.94	0.00	106.39	107.94	0.00	106.39	50.30	50.30	50.30

ORIGINAL PAGE IS  
OF POOR QUALITY

125200-20-114 (2 of 3)

Table A-1. Engine 3 Pressure Port Locations (Continued)

PORT NO.	NOM. S (IN)	ROW NO. 5 NOMINAL THETA=120. DEG			ROW NO. 6 NOMINAL THETA=150. DEG			ROW NO. 7 NOMINAL THETA=180. DEG			ROW NO. 8 NOMINAL THETA=210. DEG		
		Z (IN)	S (IN)	THETA (DEG)									
1	-56.50	53.32	-53.77	118.18				51.53	-53.97	178.17			
2	-51.21	47.61	-50.02	121.16				48.92	-51.34	180.99			
3	-44.21	41.97	-44.27	118.11				41.01	-43.39	178.10			
4	-38.21	36.32	-38.52	121.22				35.80	-37.99	181.14			
5	-32.21	31.28	-33.39	118.72				30.97	-33.08	178.68			
6	-28.21	25.85	-27.89	121.01				25.60	-27.64	181.09			
7	-24.21	21.44	-23.45	118.64				21.19	-23.20	178.63			
8	-20.21	18.70	-20.70	121.03				18.45	-20.45	181.21			
9	-17.21	15.95	-17.95	118.62				15.76	-17.70	178.62			
10	-14.21	11.64	-13.64	120.00				11.40	-13.39	180.00			
11	-11.00	8.77	-10.76	120.00				8.63	-10.62	150.00			
12	-8.00	5.92	-7.86	120.00				5.36	-7.31	150.00			
13	-5.50	3.63	-5.50	120.00				3.63	-5.50	150.00			
14	-3.00	1.41	-3.00	120.00				1.41	-3.00	150.00			
15	-1.00	.17	-1.00	120.00				-1.03	150.00				
16	0.00	0.00	0.00	120.00				0.00	0.00	180.00			
17	1.00	.32	1.00	120.00				1.00	150.00				
18	2.00	1.16	2.00	120.00				1.16	2.00	150.00			
19	4.00	3.01	4.00	120.00				3.01	4.00	150.00			
20	6.00	7.98	9.20	119.21				6.47	7.65	150.00			
21	9.00	11.06	12.33	120.51				9.89	11.15	150.00			
22	13.69	14.78	16.08	119.20				15.29	16.60	150.00			
23	19.00	25.00	25.00	19.27				23.95	25.30	150.00			
24	25.00	31.00	31.00	29.42				29.42	30.78	150.00			
25	31.00	38.00	38.00	36.71				36.71	38.08	150.00			
26	38.00	43.82	43.82	43.82				43.82	50.19	150.00			
27	50.00	60.63	62.00	60.63				60.63	62.00	150.00			
28	62.00	68.50	69.88	68.50				68.50	69.88	150.00			
29	74.26	77.00	75.59	77.00				75.59	77.00	150.00			
30	77.00	98.13	91.01	92.53				91.01	92.53	150.00			
31	98.13	107.94	106.39	107.94				106.39	107.94	150.00			
32	107.94												

**ORIGINAL PAGE IS  
OF POOR QUALITY**

(16 of 19) 11-02-002821

**Table A-1. Engine 3 Pressure Port Locations (Concluded)**

PORT NO.	ROW NO. 9 NOMINAL THETA=240. DEG			ROW NO. 10 NOMINAL THETA=270. DEG			ROW NO. 11 NOMINAL THETA=300. DEG			ROW NO. 12 NOMINAL THETA=330. DEG		
	PORT NO. (IN)	Z (IN)	S (IN)	THETA (DEG)	Z (IN)	S (IN)	THETA (DEG)	Z (IN)	S (IN)	THETA (DEG)	Z (IN)	S (IN)
1	-56.50	53.34	-55.79	238.18				53.92	-56.37	298.30		
2	-51.21	47.63	-59.04	241.08				48.45	-50.87	301.84		
3	-44.21	41.99	-44.29	238.03				42.65	-44.97	298.24		
4	-38.21	36.34	-38.54	241.22				36.86	-39.07	301.67		
5	-32.21	31.40	-33.51	238.84				31.76	-33.88	298.93		
6	-28.21	25.97	-28.01	241.13				26.39	-26.44	301.18		
7	-24.21	21.50	-23.51	238.80				21.49	-23.50	298.89		
8	-20.21	18.76	-20.76	241.21				18.75	-20.75	301.21		
9	-17.21	16.01	-18.01	238.79				16.00	-18.00	298.89		
10	-14.21	11.54	-13.54	240.69	8.95	-10.94	270.00	8.51	-10.50	300.00	3.61	-10.60
11	-11.00	8.58	-10.57	240.69	6.01	-7.97	270.00	5.55	-7.50	300.00	5.55	-7.50
12	-8.00	5.65	-7.60	240.68	4.05	-5.94	270.00	3.57	-5.44	300.00	3.58	-5.45
13	-5.50	3.60	-5.47	240.00	1.41	-3.00	270.00	1.41	-3.00	300.00	1.41	-3.00
14	-3.00	1.37	-2.94	240.00	1.17	-1.00	270.00	1.17	-1.00	300.00	1.19	-1.05
15	-1.00	0.00	-1.00	240.00	0.00	0.00	270.00	0.00	0.00	300.00	0.00	0.00
16	0.00	0.00	0.00	240.00	0.30	0.97	270.00	0.32	1.00	300.00	0.32	1.00
17	1.00	0.32	1.00	240.00	1.10	1.94	270.00	1.14	1.98	300.00	1.16	2.00
18	2.00	1.16	2.00	240.00	2.98	3.97	270.00	2.99	3.98	300.00	2.99	3.98
19	4.00	2.98	4.00	240.57	6.72	7.91	270.00	6.45	7.63	300.00	6.45	7.63
20	6.00	8.06	6.00	240.57	9.87	11.13	270.00	9.87	11.13	300.00	9.82	11.08
21	9.00	10.95	9.00	239.22	14.02	15.32	270.00	14.00	15.30	300.00	13.98	15.28
22	13.69	14.73	13.69	240.63	18.99	20.32	270.00	18.97	20.32	300.00	19.95	21.28
23	19.00	23.97	19.00	23.97	25.32	270.00	23.97	25.32	270.00	23.93	25.28	330.00
24	25.00	29.46	25.00	29.46	30.82	270.00	29.46	30.82	270.00	29.37	30.73	330.00
25	31.00	37.38	31.00	37.38	38.75	270.00	37.38	38.75	270.00	37.86	39.23	330.00
26	38.00	50.05	38.00	50.05	51.42	270.00	50.05	51.42	270.00	51.16	52.53	330.00
27	50.00	60.63	50.00	60.63	62.00	270.00	60.63	62.00	270.00	60.63	52.00	330.00
28	62.00	70.71	62.00	70.71	72.10	270.00	70.71	72.10	270.00	72.86	74.26	330.00
29	74.26	75.59	74.26	75.59	77.00	270.00	75.59	77.00	270.00	75.59	77.00	330.00
30	77.00	93.95	77.00	93.95	95.49	270.00	93.95	95.49	270.00	96.58	98.13	330.00
31	98.13	106.39	98.13	106.39	107.94	270.00	106.39	107.94	270.00	107.34	107.34	330.00

ORIGINAL PAGE IS  
OF POOR QUALITY

*Table A-2. Pressure Corrections for Instrumentation Problems*

**Engine 3**

Row No.	$\theta$ (deg)	Port No.	Averaged from:			
			Row, port	Row, port	Row, port	Row, port
1	0	None	—	—	—	—
2	30	29	2, 28	2, 30	—	—
3	60	2	3, 1	3, 3	—	—
3	60	11	3, 10	3, 12	2, 11	4, 11
3	60	14	3, 13	3, 15	2, 14	4, 14
4	90	15	4, 14	4, 16	3, 16	5, 16
4	90	29	4, 28	4, 30	—	—
5	120	None	—	—	—	—
6	150	None	—	—	—	—
7	180	12	7, 11	7, 13	6, 12	8, 12
7	180	15	7, 14	7, 16	6, 15	8, 15
7	180	22	7, 21	6, 22	8, 22	(6,23 and 8,23)
8	210	29	8, 28	8, 30	—	—
9	240	18	9, 17	9, 19	8, 18	10, 18
10	270	None	—	—	—	—
11	300	20	10, 20	12, 20	—	—
11	300	21	10, 21	12, 21	—	—
11	300	22	10, 22	12, 22	—	—
12	330	None	—	—	—	—

**Engine 4**

1	60	None	—	—	—	—
2	180	9	2, 8	2, 10	—	—
3	300	None	—	—	—	—

125389-53-423

ORIGINAL PAGE 13  
OF POOR QUALITY

125208-36

*Table A-3.*

FOURIER - BESSSEL COEFFICIENTS FOR ENGINE NUMBER THREE PRESSURES

$$P(\theta) = A(0) + \Sigma (A(n) \cos(n\theta) + B(n) \sin(n\theta))$$

CONDITION 101, 612K GROSS WEIGHT TAKEOFF (FLAPS 20) TEST 273-7 IRIG & 4-A4.1  
MACH NUMBER= 0.250 CORRECTED AIRFLOW= 1549. LB/SEC

ROW NO.	Z (IN)	A(0)				A(1)				A(2)				A(3)				A(4)				A(5)				A(6)				B(1)				B(2)				B(3)				B(4)				B(5)			
		(PSI)	(PSI)	(PSI)	(PSI)	(PSI)	(PSI)	(PSI)	(PSI)	(PSI)	(PSI)	(PSI)	(PSI)	(PSI)	(PSI)	(PSI)	(PSI)	(PSI)	(PSI)	(PSI)	(PSI)	(PSI)	(PSI)	(PSI)	(PSI)	(PSI)	(PSI)	(PSI)	(PSI)	(PSI)	(PSI)	(PSI)	(PSI)	(PSI)	(PSI)	(PSI)	(PSI)												
1	54.051	-1.2155	.3119	.0146	.0234																																												
2	48.789	-1.3906	.2381	-.0004	.0051																																												
3	41.907	-1.6120	.2576	-.0260	-.0084																																												
4	36.019	-1.9477	.2542	-.0061	.0324																																												
5	30.118	-2.2998	.2968	.0196	-.0104																																												
6	26.166	-2.6569	.3170	-.0003	-.0089																																												
7	22.196	-2.8691	.3810	-.0294	.0439																																												
8	18.211	-3.0263	.5413	-.0444	.0125																																												
9	15.214	-3.1147	.5896	-.0048	.0364																																												
10	12.215	-3.8102	1.0192	-.1093	-.0320																																												
11	9.009	-4.2116	1.4963	.0074	.0131																																												
12	6.037	-4.0698	1.5537	.1062	-.0335																																												
13	3.623	-4.3663	1.9624	.6032	-.2771																																												
14	1.413	-4.3156	2.8146	.1469	-.0137																																												
15	1.172	-2.9254	3.1801	-.2193	-.0289																																												
16	0.008	-1.4110	2.1947	.4153	-.0587																																												
17	324	-.0537	.4952	-.0949	-.0129																																												
18	1.156	.3181	.0823	.0761	-.0202																																												
19	3.007	.3003	.3196	.0635	-.0178																																												
20	4.886	.2268	.3380	-.0372	-.0167																																												
21	7.782	1.246	.3177	-.0291	-.0103																																												
22	12.404	.0544	.2180	.0113	.0082																																												
23	17.679	.0430	.2266	.0000																																													
24	23.652	.0145	.1749	.0135																																													
25	29.638	.0086	.1570	.0232																																													
26	36.633	-.0052	-.1361	.0204																																													
27	48.631	-.0309	-.1192	.0436																																													
28	60.627	-.0337	-.0807	.0618																																													
29	72.863	-.0060	.0520	.0595																																													
30	75.593	.0000	-.0304	.0592																																													
31	98.576	.0293	-.6141	.0662																																													
32	105.386	.0311	-.0079	.0888																																													

ORIGINAL PAGE IS  
OF POOR QUALITY

125209-40

Table A-4.  
FOURIER - BESSSEL COEFFICIENTS FOR ENGINE NUMBER THREE PRESSURES  
 $P_4(\theta) = A(0) + \Sigma (A(n) \cos(n\theta) + B(n) \sin(n\theta))$

ROW NO.	Z (IN)	CONDITION 101, 538K GROSS WEIGHT TAKEOFF (FLAPS 10) TEST 273-10 IRIG 9-4-10.6 ALTITUDE= 2667. FT MACH NUMBER= 0.239 CORRECTED AIRFLO= 1527. LB/SEC						B(5) (PSI)	
		A(0) (PSI)	A(1) (PSI)	A(2) (PSI)	A(3) (PSI)	A(4) (PSI)	A(5) (PSI)		
1	54.051	-1.2653	.3071	-.0549	.0249			-.0712	-.0121
2	48.789	-1.3992	.2952	-.0397	-.0062			-.0425	-.0284
3	41.907	-1.6332	.2481	-.0563	.0022			-.0177	-.0165
4	36.019	-1.9373	.2790	-.0019	.0212			-.0420	-.0289
5	30.118	-2.3164	.3508	.0058	.0195			-.0648	-.0008
6	26.166	-2.6013	.3556	.0016	.0449			-.0598	-.0293
7	22.135	-2.8568	.4149	-.0036	.0559			-.1693	.0894
8	18.211	-2.9484	.5920	-.0211	.0341			-.1832	-.0442
9	15.214	-3.1305	.7117	.0038	.0340			-.2326	.0324
10	12.215	-3.8486	1.2550	.1704	-.0939			-.4454	.0724
11	9.009	-4.1913	1.7501	-.0297	.0217	.0500	-.0423	.0927	-.0588
12	6.037	-4.0980	1.8666	.1379	-.0313	-.0405	-.0238	-.0542	-.0604
13	3.629	-4.5839	2.6442	.3778	-.2160	-.0388	-.1472	-.1629	-.0187
14	1.413	-4.7194	3.7211	.0555	-.0483	-.1750	-.1417	-.0295	.0032
15	1.172	-3.2715	3.6531	.2892	-.0954	.0708	-.1682	-.0581	.0324
16	0.000	-1.7403	2.7211	.2188	-.1229	-.0127	-.0684	-.0513	-.0231
17	1.324	-2.2774	2.7385	.2459	-.0211	-.1305	-.0225	-.0478	-.0295
18	1.156	-1.644	.0169	.1002	-.0148	.0333	-.0348	-.0127	-.0250
19	3.007	-2.374	.3167	.0641	-.0161	-.0201	-.0043	-.0064	-.0085
20	4.886	-1.857	.3403	.0980	-.0100	.0135	-.0184	-.0022	-.0174
21	7.782	-2.146	.1458	-.0147	-.0081	-.0094	-.0007	-.0048	-.0030
22	12.404	-1.0146	.2151	.0307	-.0201	-.0142	-.0512	-.0038	-.0255
23	17.679	-0.0234	.2524	.0198				-.0848	-.0154
24	23.652	-.0187	.2366	.0385				-.1302	-.0191
25	29.638	-.0355	.2049	.0758				-.0723	-.0073
26	35.633	-.0448	.1673	.0598				-.1159	-.0075
27	48.631	-.0767	.1371	.0853				-.0879	-.0075
28	60.627	-.0714	.095	.0944				-.1339	-.0540
29	72.863	-.0431	.0759	.0913				-.1568	-.0498
30	75.593	-.0441	.0493	.0956				-.1554	-.0560
31	96.576	-.0207	.0235	.0940				-.1592	-.0487
32	106.396	-.0323	.0260	.0960				-.2041	-.0532

ORIGINAL PAGE [ ]  
OF POOR QUALITY

12B20841

Table A-5.

FOURIER - BESSSEL COEFFICIENTS FOR ENGINE NUMBER THREE PRESSURES

P(THETA) = A(0) + SIGMA( A(N)COS(NTHETA) + B(N)SIN(NTHETA) )									
CONDITION 101, 647K GROSS WEIGHT TAKEOFF (FLAPS 10) TEST 273-11 IRIG 10:13:57-6									
CORRECTED AIRFLOW = 1524. LB/SEC									
ALTITUDE	MACH NUMBER	A(1)	A(2)	A(3)	A(4)	A(5)	A(6)	B(1)	B(2)
FT	0.254	(PSI)							
54.051	-1.1682	.3417	-.0027	.0336				-.0683	-.0386
48.789	-1.3738	.3132	-.0032	.0087				-.0804	.0020
41.907	-1.5479	.2544	-.0257	.0001				-.0415	-.0630
36.019	-1.8736	.3278	-.0046	.0356				-.005	.0162
30.118	-2.1989	.2315	-.0338	-.0023				-.0459	-.0346
26.166	-2.5647	.4222	-.0212	-.0037				-.0616	.0096
22.196	-2.7454	.4341	-.0656	.0762				-.1777	.0297
18.211	-2.8934	.6924	-.0494	.0088				-.1678	.0059
15.214	-3.0146	.7777	-.0082	.0631				-.2265	.0262
12.215	-3.4489	1.1173	-.1317	.1900				-.0292	-.4123
11.9.009	-4.0966	1.8516	.0094	-.0058	.0341	-.1217	.1208	-.5931	.0575
12.6.037	-3.9634	1.9817	.0920	-.0375	-.0713	-.0389	-.0367	-.6538	-.6537
13.3.623	-4.5642	2.8427	.4280	-.2135	-.0373	-.1371	-.1160	-.5411	-.0514
14.1.413	-4.4928	3.8458	.0054	-.0559	-.1744	-.1488	-.0625	-.5912	-.2022
15.1.172	-3.0392	3.7371	-.2515	-.1036	-.0934	-.1493	-.0498	-.3862	-.0513
16.0.000	-1.6151	2.6195	-.2755	-.1482	-.0318	-.0585	-.0550	-.1690	-.0469
17.324	-2.419	.6023	-.2376	-.0421	-.1072	-.0068	-.0367	-.2042	-.344
18.1.155	-1.747	.1542	-.0489	.0174	-.0197	-.0109	-.0109	-.1177	-.0475
19.3.007	-2.286	.3961	-.0913	-.0161	-.0140	-.0115	-.0056	-.1356	-.0122
20.4.866	-1.523	.4372	-.0466	.0226	-.0313	-.0223	-.0017	-.1823	-.0480
21.7.782	.0798	.4271	-.0156	-.0120	-.0156	-.0051	-.0017	-.2035	-.3218
22.12.404	.0170	.3032	-.0271	.0286	-.0062	.0471	-.0110	-.0982	-.0037
23.17.673	.0044	.2927	.0079					-.0764	-.0009
24.23.652	-.0023	-.2548	.0428					-.0186	-.0053
25.29.638	-.0135	-.2220	.0561					-.0852	-.0054
26.36.633	-.0399	-.1883	.0574					-.0192	-.0255
27.48.631	-.0203	-.1589	.0924					-.0133	
28.60.627	-.0722	-.1083	.1073					-.0130	
29.72.863	-.0359	-.0866	.1029					-.0130	
30.75.593	-.0356	-.0580	.1006					-.0130	
31.96.576	-.0399	-.0305	.0676					-.0130	
32.106.386	.0101	-.0054	-.0060					-.0130	

ORIGINAL PAGE IS  
OF POOR QUALITY

126209-42

Table A-6.  
FOURIER + BESSSEL COEFFICIENTS FOR ENGINE NUMBER THREE PRESSURES  
 $P(\theta) = A(0) + \Sigma \sin(n\theta) [A(n)\cos(n\theta) + B(n)\sin(n\theta)]$

ROW NO.	Z (IN)	CONDITION 110,780K GROSS WEIGHT SIMULATED TAKEOFF (FLAPS 10° TEST 273-45 CORRECTED AIRFLOW= 1573. LB/SEC)						TEST 273-45 CORRECTED AIRFLOW= 1573. LB/SEC					
		A(0) (PSI)	A(1) (PSI)	A(2) (PSI)	A(3) (PSI)	A(4) (PSI)	A(5) (PSI)	B(1) (PSI)	B(2) (PSI)	B(3) (PSI)	B(4) (PSI)	B(5) (PSI)	
1	54.05	-1.0638	.2357	.0467	.0049								
2	48.789	-1.2145	.2617	.0283	-.0212								
3	41.907	-1.4520	.2082	-.0414	.0112								
4	36.019	-1.7697	.2827	-.0251	.0086								
5	30.118	-2.1792	.3493	.0394	.0066								
6	26.166	-2.5309	.3831	.0135	-.0002								
7	22.196	-2.7464	.4463	.0118	.0495								
8	18.211	-2.8955	.6903	-.0743	.0268								
9	15.214	-2.9756	.7710	-.0093	.0225								
10	12.215	-3.7718	1.3369	.0804	-.0733								
11	9.009	-4.2763	2.2764	-.2362	.1502	-.0321	-.0447	.0705	-.0056	.0276			
12	6.037	-3.9914	2.1040	.0375	.0621	-.1527	.0052	-.0327	.5323				
13	3.629	-4.2421	2.7385	.3743	-.1155	-.1357	-.0054	-.0054	.0014				
14	1.413	-3.8926	3.4861	.0424	[.0391	-.1942	.1736	.1165	.127				
15	1.172	-4.2386	3.3849	[.3661	[.0934	.0689	-.1775	-.0619	.1254				
16	0.006	-8.760	2.0301	-.3551	-.0981	-.0445	.0584	-.0269	.1426				
17	1.324	.0981	.0284	-.3467	.0656	-.1547	.0054	-.0433	.3448				
18	1.156	.3123	-.1925	-.0520	-.0071	-.0173	-.0125	-.0125	.1348				
19	3.007	.2976	-.5296	.0585	.0201	-.0447	-.1132	-.0426	.1348				
20	4.986	.2613	-.4806	-.0273	-.0857	-.1029	-.1067	-.0425	.1348				
21	7.782	.1733	-.3213	.0017	-.1422	-.1659	-.1260	-.0636	.1348				
22	12.404	-.0570	-.3728	.0485	-.0482	.0072	.0559	-.0146	.1348				
23	17.679	-.1053	-.3663	.0369					.1348				
24	23.652	-.0759	-.3300	.0275					.1348				
25	29.638	-.0945	-.2570	.0934					.1348				
26	36.633	-.1000	-.2098	.0554					.1348				
27	48.631	-.1313	-.1711	.0995					.1348				
28	60.627	-.1191	-.1096	.1233					.1348				
29	72.363	-.0760	-.0836	.1066					.1348				
30	75.593	-.0597	-.0430	.1071					.1348				
31	96.576	-.0097	r.0070	.1204					.1348				
32	106.386	.0649	.0483						.1348				

ORIGINAL PAGE IS  
OF POOR QUALITY

125208-38

Table A-7.  
FOURIER - BESSSEL COEFFICIENTS FOR ENGINE NUMBER THREE PRESSURES  
 $P(\theta) = A(0) + \text{SIGNAL } A(n) \cos(n\theta) + B(n) \sin(n\theta)$ )

ALTITUDE IN FT.	Z (IN.)	CONDITION 102, LOW CLIMB TEST 273-10 (HIG 8-4589)											
		MACH NUMBER= 0.367			CORRECTED AIRFLO= 1539. LB/SEC			1000. LB/SEC					
		A(0) (PSI)	A(1) (PSI)	A(2) (PSI)	A(3) (PSI)	A(4) (PSI)	A(5) (PSI)	A(6) (PSI)	B(1) (PSI)	B(2) (PSI)	B(3) (PSI)	B(4) (PSI)	B(5) (PSI)
54. 051	-4769	-1437	.0122	.0169					.0139	.0289			
46. 769	-.6266	-.1112	.0180	-.0056					-.0251	-.0046			
41. 907	-.8567	-.1413	-.0097	.0079					-.0073	-.0211			
36. 019	-1.1651	-1.434	-.0178	.0277					-.0286	-.0187			
30. 118	-1.4941	2197	.0317	.0065					-.0059	.0092			
26. 166	-1.7984	1788	.0309	-.0002					.0009	.0899			
22. 196	-1.9869	2048	.0167	.0362					-.0754	.0745			
18. 211	-2.0864	3633	-.0114	-.0053					-.0231	-.0012			
15. 214	-2.1862	3478	.0303	-.0077					-.0273	-.0278			
12. 215	-2.6789	6373	-.0491	.0397					.0092	-.1341			
9. 009	-2.9348	9872	.0176	.0189					.0402	-.1414			
6. 037	-2.7238	9853	.0522	-.0344					-.0253	-.2150			
10	11	12	12	12	12	12	12	12	12	12	12	12	12
13	3. 629	-2. 5197	1. 0965	.2600	-.0411	-.0411	-.0965	-.0155	-.0190	-.0253	-.0236	.0349	-.0276
14	1. 4113	-1. 8334	1. 4002	.0872	-.0362	-.0362	-.1115	.0554	.0105	-.4138	-.0275	.0447	-.0239
15	1. 72	-2. 441	1. 2420	-.1469	-.0211	-.0211	-.0168	-.0304	.0464	-.3240	.0564	.0379	-.0140
16	0. 000	.7079	-.4683	-.1567	-.0014	-.0261	-.0245	-.0327	-.1434	-.3025	.0503	.0761	-.0416
17	.324	.6617	-.5627	-.0656	-.0324	-.1259	-.0043	-.0731	.2135	-.0730	.0730	.1271	-.0118
18	1. 156	4569	-.6004	-.0516	-.0014	-.0014	.0237	.0362	-.0052	.1375	.1375	.184	-.0215
19	3. 007	.2193	-.5874	-.0345	-.0116	-.0116	-.0127	.0058	-.0096	.1016	.0375	.0148	-.0074
20	4. 886	.0580	-.4357	-.0455	-.0056	-.0056	-.0119	-.0054	-.0046	.0777	.0277	.0041	-.0129
21	7. 782	-.1167	-.3472	-.0431	-.0473	-.0473	-.0183	-.0112	-.0143	-.1446	.0479	.0161	-.0165
22	12. 404	-.1783	-.2645	.0256	.0278	.0086	.0565	.0119	.0283	-.0730	.0730	.0254	-.0079
23	17. 679	-.1769	-.2411	-.0404					.0547	-.0295			
24	23. 652	-.1335	-.1965	-.0151					.0442	-.0485			
25	29. 638	-.1588	-.1558	.0262					.0726	-.0062			
26	36. 633	-.1417	-.1284	-.0076					.0325	-.0503			
27	48. 631	-.1636	-.1027	.0473					.0499	-.0163			
28	60. 627	-.1510	-.0735	.0813					.0962	-.0380			
29	72. 863	-.0964	-.0428	.0536					.1093	-.0159			
30	75. 593	-.0662	-.0161	.0535					.0993	-.0153			
31	96. 576	.0289	-.0173	.0582					.0860	-.0291			
32	106. 386	.0719	-.0484	.0149					.0839	-.0268			

ORIGINAL PAGE IS  
OF POOR QUALITY

126208-37

Table A-8.  
FOURIER - BESSSEL COEFFICIENTS FOR ENGINE NUMBER THREE PRESSURES  
 $P(\theta)$  •  $A(0)$  •  $\Sigma \sigma_n (A(n) \cos(n\theta) + B(n) \sin(n\theta))$

ROW NO.	Z (IN)	TEST 273-7 IRIG 7-28-44.5 CORRECTED AIRFLOW = 1622. LB/SEC																																				
		CONDITION 103, MID CLIMB MACH NUMBER = 0.599			ALTITUDE = 17187. FT			A(1) (PSI)			A(2) (PSI)			A(3) (PSI)			A(4) (PSI)			A(5) (PSI)			A(6) (PSI)			B(1) (PSI)			B(2) (PSI)			B(3) (PSI)			B(4) (PSI)			B(5) (PSI)
1	54.051	.6796	.1108	.0059	.0149																																	
2	46.769	.5032	.0590	.0236	.0023																																	
3	41.967	.3252	.0997	.0257	.0022																																	
4	36.019	.0586	.0927	.0003	.0053																																	
5	30.118	-	.2328	.1251	.0025																																	
6	26.166	-	.4907	.1085	.0039																																	
7	22.195	-	.6346	.1030	.0117																																	
8	18.211	-	.7180	.1969	.0174																																	
9	15.214	-	.7562	.1968	.0173																																	
10	12.215	-	.2934	.5224	.1125																																	
11	9.009	-	.1600	.5792	.0223																																	
12	6.037	-	.8481	.5046	.0567																																	
13	3.629	-	.3792	.4566	.1265																																	
14	1.413	-	.5771	.6384	.0537																																	
15	1.172	-	.7740	.2684	.0535																																	
16	0.000	1.6798	-	.3672	.0554																																	
17	1.324	-	.0110	.8984	.0712																																	
18	1.156	-	.4162	.8648	.1387																																	
19	3.007	-	.8271	.5566	.0896																																	
20	4.896	-	.4466	.4457	.1227																																	
21	7.782	-	.7982	.3256	.0854																																	
22	12.404	-	.7108	.2442	.0910																																	
23	17.679	-	.5881	.2682	.0326																																	
24	23.632	-	.4693	.1737	.0966																																	
25	29.638	-	.3996	.4457	.1227																																	
26	36.633	-	.4001	.1324	.0437																																	
27	48.631	-	.60627	.3611	.095																																	
28	72.863	-	.1889	.0103	.0018																																	
29	75.593	-	.1745	.0024	.0436																																	
30	96.576	-	.0158	.0303	.0482																																	
31	106.386	-	.1627	.0859	.0368																																	
32																																						

ORIGINAL PAGE IV  
OF POOR QUALITY

125209-4A

**Table A-9.**  
**FOURIER - BESSSEL COEFFICIENTS FOR ENGINE NUMBER THREE PRESSURES**

$$P(\theta) = A(0) + \sum_{n=1}^{\infty} [A(n) \cos(n\theta) + B(n) \sin(n\theta)]$$

CONDITION 104, HIGH-MACH CRUISE TEST 273-7 IRIG 7-82-26-6

Revolving No.	Z (IN)	MACH NUMBER = 0.859 CORRECTED AIRFLOW = 1633. LB/SEC									
		A(0) (PSI)	A(1) (PSI)	A(2) (PSI)	A(3) (PSI)	A(4) (PSI)	A(5) (PSI)	A(6) (PSI)	B(1) (PSI)	B(2) (PSI)	B(3) (PSI)
1	54.051	1.2549	.0419	.0049	.0114				.0061	.0254	
2	48.789	1.1642	-.0023	.0186	.0110				-.0114	-.0137	
3	41.907	1.0483	.0513	-.0163	-.0047				-.0182	-.0302	
4	36.019	.8918	.0273	-.0039	-.0042				-.0038	-.0057	
5	30.118	.7167	.0458	.0023	-.0062				-.0107	-.0097	
6	26.166	.5626	.0239	.0037	-.0183				-.0052	.0169	
7	22.196	.4900	.0158	.0004	.0053				.0235	.0095	
8	18.211	.4549	.0523	-.0074	-.0063				-.0114	.0112	
9	15.214	.4287	.0395	.0293	.0039				-.0029	-.0079	
10	12.215	.0382	.3054	.1780	-.1527				-.3341	.2580	
11	9.099	.2773	.1337	.0211	-.0262	.0119	.0017	-.0383	-.0751	.0155	.0129
12	6.037	.4804	.1123	.0249	-.0100	-.0036	-.0144	-.0116	-.1076	-.0187	-.0257
13	3.629	.8530	.0988	.0376	-.0107	.0318	-.0041	-.0279	-.1014	-.0030	.01
14	1.413	1.4538	.1215	.0224	-.0116	.0146	.0046	-.0002	-.0546	-.0093	.0140
15	.172	1.9564	.0396	-.0190	.0409	-.0797	.0590	.0165	-.0316	.0313	.0585
16	0.000	1.4382	-.1428	.0141	.0117	.0211	-.0166	.0015	-.0873	-.0223	-.0518
17	.324	-.3211	-.2788	.0267	.0511	.0277	-.0492	-.0537	.2317	.0850	-.0583
18	1.156	-.9313	-.5514	-.0991	.1555	-.1080	-.0617	-.1091	.2222	.0629	-.1801
19	3.007	-.8094	-.4139	-.0972	-.0242	-.0545	.0254	.0463	.0850	-.0324	-.1591
20	4.886	-.1.0264	-.3695	-.0876	-.0092	-.0444	-.0413	-.0307	.1534	.0021	-.0752
21	7.782	-.1.635	-.2509	-.1111	.0014	-.0907	-.0689	-.0001	.2235	.0568	-.0553
22	12.404	-.1.2955	-.0751	.0725	-.1358	.0405	-.0141	-.0886	-.0237	-.1513	-.0061
23	17.679	-.1.3105	-.1838	-.1854					-.0213	-.0582	-.0556
24	23.652	-.1.2673	-.2145	-.3147					-.0001	-.1679	-.0861
25	29.638	-.1.0379	-.1499	-.2650					-.2674	-.0158	-.0353
26	36.633	-.6817	-.0123	.0759					-.2456	-.0626	-.0137
27	48.631	-.4925	-.0247	-.0130					-.1280	-.0901	-.0005
28	60.627	-.4461	-.0324	.1072					-.0551	-.0699	-.0327
29	72.663	-.2016	-.0640	-.0377					1.810	-.0890	-.0266
30	75.593	-.1.883	-.0393	.0269					-.0553	.0310	-.0156
31	96.576	-.0334	.0490	.0271					.0328	.0412	-.0085
32	106.386	.2275	.1129	-.1250					-.1897	-.0485	-.1500

ORIGINAL PAGE IS  
OF POOR QUALITY

128209-43

Table A-10.

FOURIER - BESSSEL COEFFICIENTS FOR ENGINE NUMBER THREE PRESSURES

$P(\Theta/\eta) = A(0) + \text{SIGNAL } A(n)\cos(n\Theta/\eta) + B(n)\sin(n\Theta/\eta)$

CONDITION 105, LOW-MACH CRUISE TEST 273-7 IRRG 7.56-40.5

ALTITUDE = 35512. FT MACH NUMBER = 0.772 CORRECTED AIRFLW = 1604. LB/SEC

Row No.	Z (IN)	A(0) (PSI)		A(1) (PSI)		A(2) (PSI)		A(3) (PSI)		A(4) (PSI)		A(5) (PSI)		B(1) (PSI)		B(2) (PSI)		B(3) (PSI)		B(4) (PSI)		B(5) (PSI)	
		(PSI)	(PSI)	(PSI)	(PSI)	(PSI)	(PSI)	(PSI)	(PSI)	(PSI)	(PSI)	(PSI)	(PSI)	(PSI)	(PSI)	(PSI)	(PSI)	(PSI)	(PSI)	(PSI)	(PSI)	(PSI)	
1	54.051	.9171	.0449	.0039	.0037									.0046	.0200								
2	48.789	.8477	.0218	.0042	-.0022									-.0081	.0006								
3	41.907	.7400	.0550	-.0111	-.0092									-.0072	.0142								
4	36.019	.6045	.0401	.0014	-.0014									-.0098	-.0026								
5	30.118	.4582	.0632	.0027	-.0036									-.0012	-.0079								
6	26.166	.3265	.0611	.0024	-.0154									-.0140	.0095								
7	22.195	.2520	.0726	-.0038	.0162									-.0350	.0127								
8	18.211	.2295	.1285	-.0109	-.0052									-.0219	.0092								
9	15.214	.2010	.1230	.0144	-.0005									-.0279	-.0065								
10	12.215	.1745	.4389	.1660	-.1618									-.3662	.2785								
11	9.009	.0632	.3366	.0102	-.0131									-.0786	-.6062								
12	6.037	.2367	.3029	.0195	-.0094									-.0043	-.0140								
13	3.629	.5232	.2954	.0362	-.0208									-.0158	-.0137								
14	1.413	1.0399	.2920	.0233	-.0031									-.0133	-.0053								
15	1.172	1.5024	.0501	-.0284	.0448									-.0643	-.0158								
16	0.000	1.0997	.3475	-.0058	.0164									-.0237	-.0046								
17	1.324	-3.5316	.7175	-.0192	.0616									-.0010	-.1311								
18	1.156	-8790	-.0099	-.1186	.1572									-.0144	-.3094								
19	3.007	-6025	.7697	-.1784	.0598									-.0250	-.2941								
20	4.986	-3942	.8150	-.0477	.0861									-.0141	-.0231								
21	7.782	-1.0261	.6643	-.2448	-.1558									-.0501	-.1049								
22	12.404	-8653	.3685	-.1165	.1926									-.0465	-.0465								
23	17.679	-5767	-.1450	-.0887	.0558									-.0702	.0873								
24	23.652	-4215	-.0604	-.0315																			
25	29.638	-4207	-.0321	-.0230																			
26	36.633	-3731	-.0802	-.0211																			
27	46.631	-2913	-.0479	.0983																			
28	60.627	-72863	-.0191	.0054																			
29	75.593	-1149	.0266	.0418																			
30	95.576	.0414	.0429	.0412																			
31	106.386	.1689	.0771	-.0462																			
32																							

ORIGINAL PAGE IS  
OF POOR QUALITY

Table A-11.

FOURIER - BESSSEL COEFFICIENTS FOR ENGINE NUMBER THREE PRESSURES

$P(\Theta)$  +  $A(0) + \Sigma A(n) \cos(n\Theta)$

ROT. NO.	Z (IN)	CONDITION 106, MAXIMUM MACH NUMBER = 0.906			TEST 273-15 IRRIG 12-08-28.5			CORRECTED AIRFLOW = 1642. LB/SEC		
		A(0) (PSI)	A(1) (PSI)	A(2) (PSI)	A(3) (PSI)	A(4) (PSI)	A(5) (PSI)	A(6) (PSI)	B(1) (PSI)	B(2) (PSI)
1	54.05	1.3536	.0222	-.0267	.0040				-.0014	.0184
2	48.789	1.2957	-.0421	.0164	-.0159				-.0325	-.00173
3	41.907	1.1734	.0202	-.0135	.0123				-.0218	-.00194
4	36.019	.9889	-.0014	.0151	-.0123				-.0453	-.00201
5	30.118	.8559	.0592	.0257	-.0236				-.0316	.0257
6	26.166	.7210	-.0271	.0183	.0040				-.0143	-.0255
7	22.196	.6029	-.0451	-.0082	.0058				-.0420	-.0378
8	18.211	.5968	-.0065	-.0109	-.0181				-.0181	-.0055
9	15.214	.5684	-.0748	.0049	-.0390				-.0377	.0300
10	12.215	.2214	.0600	.0190	-.0214				-.2217	.0723
11	9.009	.4975	.0336	-.0065	-.0202	.0075	-.0514	-.0769	-.0738	.0074
12	6.037	.5861	-.0535	.0255	.0104	-.0087	.0102	.0232	-.1182	.0184
13	3.629	1.0293	-.1053	.0658	.0874	-.0068	-.0002	.0102	.0320	.0110
14	1.413	1.5834	-.0086	.0446	.0225	-.0103	.0266	.0378	-.0530	-.0453
15	1.172	2.0827	-.0021	-.0719	-.0281	-.1350	.0419	.0136	-.0515	-.0163
16	0.006	1.5524	-.0303	.0135	.0278	.0405	.0073	.0151	-.0701	-.0237
17	1.324	1.2614	-.0511	-.0800	.0602	.0557	-.0115	-.0577	-.1494	-.0336
18	1.156	-1.0150	.0153	-.1118	.0349	-.0137	.0228	-.0744	.2776	-.0952
19	3.007	1.7481	-.1124	.0575	-.0251	-.1382	-.0980	-.0431	.3233	-.0561
20	4.886	1.8398	-.0771	-.0371	-.0372	-.1605	-.1155	-.0908	-.0661	-.1335
21	7.782	1.8956	-.1706	-.0073	-.1383	-.1791	-.1457	-.0658	-.0526	-.0585
22	12.404	-1.1893	.0641	.0673	.1533	.0073	-.0677	-.0678	-.0271	-.1317
23	17.679	-1.2841	.0264	-.1227					-.0384	-.1212
24	23.652	-.1.2159	-.0176	-.3283					-.0079	-.1344
25	29.638	-.1.1378	-.1100	-.2093					-.0583	-.0559
26	36.633	-.1.096	.0931	-.1914					-.0587	-.1967
27	48.631	-.0564	.1249	-.1625					-.0070	-.1227
28	60.627	-.1.0564	.0032	-.1706					-.1501	-.1234
29	72.863	-.6071	.2264	-.0653					-.2271	-.1526
30	75.593	-.1555	-.0674	.0330					-.0360	-.0582
31	96.576	.0828	.0024	.0047					-.0053	-.0077
32	106.386	-.4009	-.0270	-.0135					-.0261	-.0358

ORIGINAL PAGE IS  
OF POOR QUALITY

126208-46

*Table A-12.*  
FOURIER - BESSEL COEFFICIENTS FOR ENGINE NUMBER THREE PRESSURES  
 $P(\theta\eta) = A(0) + \Sigma (A(n) \cos(n\theta) + B(n) \sin(n\theta))$

ROW NO.	$Z$ (IN)	CONDITION 107, INFIGHT RELIGHT						TEST 273? IRIG 812-535					
		MACH NUMBER= 0.721	CORRECTED AIRFLOW= 1365. LB SEC						B(1) (PSI)	B(2) (PSI)	B(3) (PSI)	B(4) (PSI)	B(5) (PSI)
		A(0) (PSI)	A(1) (PSI)	A(2) (PSI)	A(3) (PSI)	A(4) (PSI)	A(5) (PSI)	A(6) (PSI)	B(1) (PSI)	B(2) (PSI)	B(3) (PSI)	B(4) (PSI)	B(5) (PSI)
1	54.051	1.3631	.0380	.0039	.0019				-.0043	.0329			
2	48.789	1.3162	.0041	.0109	-.0031				-.0105	-.0021			
3	41.907	1.2165	.0372	-.0145	.0028				-.0048	-.0259			
4	36.019	1.0936	.0329	.0073	-.0038				-.0196	-.0063			
5	30.118	.9645	.0612	-.0064	.0066				-.0103	-.0005			
6	26.166	.8619	.0424	.0008	-.0082				-.0030	.0098			
7	22.196	.8063	.0484	.0070	.0124				-.0212	.0241			
8	18.211	.7905	.0789	-.0102	-.0052				-.0006	.0216			
9	15.214	.7794	.0511	-.0012	-.0145				-.0049	.0027			
10	12.215	.6168	.1895	.0189					-.0936	.0316			
11	9.009	.7151	.2258	.0281	-.0113	-.0200	-.0139	-.0065	-.0613	.0058	-.0293	-.0163	.0440
12	6.037	.8454	.1754	.0265	-.0129	-.0115	-.0323	-.0163	-.0992	-.0109	-.0069	-.0179	.0340
13	3.629	1.1843	.2128	.0099	-.0037	.0446	-.0112	-.0334	-.0852	.0138	-.0011	-.0169	.0305
14	1.413	1.6347	.1896	.0082	-.0090	-.0065	-.0011	.0081	-.8618	-.0133	.0163	-.0212	.0339
15	1.172	1.8213	-.0618	-.0114	.0705	-.0621	.0814	.0169	-.0172	.0451	.0572	-.0215	-.0555
16	0.096	.9195	+.3745	-.0076	.0157	.0507	.0086	.0032	.1391	.0277	.0046	-.0533	-.0532
17	-1.3076	1.3076	.6804	.0025	-.1101	.1020	-.1815	-.2560	.1476	.0549	.4912	-.1974	-.3191
18	1.156	-2.6476	1.1553	.0681	.1541	-.0102	-.0032	.0655	.5039	-.0752	-.1052	.0312	.0339
19	3.007	1.753	-.1.7517	1.1938	.3848	.1634	-.0811	-.0551	-.0108	.3537	.0234	-.1328	.0233
20	4.886	7.782	-.1.3296	-.4524	-.0766	-.0435	-.1131	-.0551	-.1609	-.0345	.3046	.0345	-.1141
21	12.404	1.9972	-.0342	-.0809	.0470	-.0320	-.0780	-.0838	-.0596	.3268	.1122	.0989	-.1052
22	17.679	8.1128	-.1238	-.0845					.1901	.0602	-.1273	-.1074	-.0878
23	23.652	6.0709	-.0864	-.0977						-.0547	-.1213	-.0933	
24	29.616	-.5605	-.0503	-.0710						.0446	.0822	-.0654	
25	36.633	-.4758	-.0348	-.0382						-.0413	-.0079	.0026	
26	48.631	-.4535	-.1103	-.0826						-.0079	-.0951	-.0152	
27	60.627	-.3824	-.0706	.1090						-.0005	-.0696	-.0127	
28	72.863	-.2378	-.0014	.0405						1087	.0696	.0295	
29	75.593	-.1724	.0121	.0367						1272	.0527	.0254	
30	96.576	.0170	.0371	.0350						.0950	.0356	.0140	
31	106.386	.2043	.0687	-.0558						.0762	.0352	.0125	
32										.2037	-.0131	.1128	

ORIGINAL PAGE IS  
OF POOR QUALITY

125209-67

Table A-13.  
FOURIER - BESSSEL COEFFICIENTS FOR ENGINE NUMBER THREE PRESSURES  
 $P(\theta) = A(0) + \Sigma [A(n) \cos(n\theta) + B(n) \sin(n\theta)]$

Row No.	Z (IN)	CONDITION 108, MAXIMUM Q TEST 273-15 IRIG 11-29-60						CORRECTED AIRFLW= 1617. LB/SEC					
		A(0) (PSI)	A(1) (PSI)	A(2) (PSI)	A(3) (PSI)	A(4) (PSI)	A(5) (PSI)	B(1) (PSI)	B(2) (PSI)	B(3) (PSI)	B(4) (PSI)	B(5) (PSI)	
1	54.051	1.8899	-0.0321	.0006	.0023			.0139	.0240				
2	48.789	1.7625	-0.0526	.0163	-.0107			-.0353	-.0006				
3	41.907	1.5896	.0257	.0105	-.0134			-.0061	-.0248				
4	36.019	1.3198	-.0157	.0296	-.0118			-.0256	.0169				
5	30.118	1.0608	.0282	.0195	-.0139			-.0372	.0012				
6	26.166	8479	-.0859	-.0035				-.0512	-.0217				
7	22.196	6978	-.1154	-.0022				-.0038	-.0369				
8	18.211	6716	-.0716	-.0269	-.0132			.0456	-.0020				
9	15.214	6181	-.1553	-.0290	-.0157			.0188	.0252				
10	12.215	2119	-.1318	-.0096	-.0492			-.0333	-.0494				
11	9.009	3716	-.1040	-.0057	-.0423			.0085	-.0783				
12	6.037	6670	-.2269	-.0276	-.0396			.0354	-.0230				
13	3.629	1.3210	-.3184	-.0065	-.0646			.0206	.0192				
14	1.413	2.1955	-.1595	-.0216	-.0171			.0542	-.0310				
15	.172	3.0088	-.0276	-.0213	-.0440			.1643	-.0979				
16	0.000	2.1532	1.499	-.0526	-.0169			.0188	-.0316				
17	.324	-.6420	-.2720	-.0005	-.0469			.0342	-.0726				
18	1.156	-1.9168	7576	-.0051	-.0801			.0802	-.0495				
19	3.007	-1.3882	7122	-.1679	-.11125			.1357	-.0211				
20	1.356	-1.6484	3827	-.1560	-.0565			.1638	-.1744				
21	7.782	-1.8445	2838	-.0624	-.1020			.2404	-.1792				
22	12.404	-2.1683	3480	-.1604	-.2299			.1212	-.1516				
23	17.679	-2.2677	3113	-.1315									
24	23.652	-2.0116	3779	-.4290									
25	29.638	-1.5213	9247	-.2902									
26	36.633	-8321	-.0708	-.0487									
27	48.631	-.9501	-.1725	.0283									
28	60.627	-.8591	-.1402	.1940									
29	72.593	-.5909	-.0854	.0192									
30	96.576	-.4531	-.0244	.0324									
31	106.386	-.0767	.0197	.0135									
32		4349	.0013	-.0147									

ORIGINAL PAGE IS  
OF POOR QUALITY

125209-4B

**Table A-14.**  
FOURIER - BESSSEL COEFFICIENTS FOR ENGINE NUMBER THREE PRESSURES  
 $P(\theta) = A(0) + \Sigma [A(n) \cos(n\theta) + B(n) \sin(n\theta)]$

ROW NO.	$Z_{IN}$	CONDITION 102, STALL WARNING (FLAPS UP)						CORRECTED AIRFLOW= 1591 LB/SEC					
		MACH NUMBER= 0.391	A(1) (PSI)	A(2) (PSI)	A(3) (PSI)	A(4) (PSI)	A(5) (PSI)	A(6) (PSI)	B(1) (PSI)	B(2) (PSI)	B(3) (PSI)	B(4) (PSI)	B(5) (PSI)
1	54.05	-2761	1449	.0074	.0232				.0150				
2	48.789	-3815	.1104	.0125	.0016				.0168				
3	41.907	-5477	.1355	.0249	.0016				.0350				
4	36.019	-7624	.1355	.0123	.0143				.0020				
5	30.118	-1.0046	.1783	.0013	.0012				.0008				
6	26.166	-1.2198	.2097	.0046	.0053				.0032				
7	22.196	-1.3409	.2406	.0212	.0372				.0578				
8	18.211	-1.4340	.3755	.0173	.0003				.0394				
9	15.214	-1.4805	.4811	.0043	.0150				.0488				
10	12.215	-1.9974	.8743	.1425	.0959				.2956				
11	9.009	-2.0706	1.1155	.0328	.0184				.0052				
12	6.037	-1.9270	1.1605	.0385	.0238				.0115				
13	3.629	-1.7872	1.2985	.2175	.0497				.0583				
14	1.413	-1.3482	1.5679	.0311	.0458				.0112				
15	1.172	-2.2912	1.3415	.1809	.0366				.0750				
16	0.009	-3666	.4574	.2659	.0140				.0041				
17	.324	.3310	.6306	.1817	.0457				.0293				
18	1.156	.2489	.7101	.1503	.0268				.1010				
19	3.007	.1350	.5792	.0782	.0041				.0131				
20	4.886	.0475	.5064	.0675	.0127				.0030				
21	7.782	.0530	.4155	.0524	.0365				.0130				
22	12.404	.1101	.2738	.0376	.0320				.0187				
23	17.679	.0724	.2702	.0162					.0564				
24	23.652	.0670	.2126	.0014					.0187				
25	29.638	.0626	.1646	.0247					.0114				
26	36.633	.0539	.1327	.0263					.0141				
27	48.631	.0708	.1052	.0516					.0131				
28	60.627	.0632	.0616	.0908					.0123				
29	72.863	.0214	.0144	.0804					.1236				
30	75.593	.0071	.0018	.0789					.1128				
31	96.576	.0504	.0263	.0869					.1042				
32	106.386	.1046	.0396	.0765					.1506				

ORIGINAL PAGE IS  
OF POOR QUALITY

125209-49

Table A-15.

FOURIER - BESSEL COEFFICIENTS FOR ENGINE NUMBER THREE PRESSURES

$P(\theta) = A(0) + \sum_{n=1}^{\infty} [A(n) \cos(n\theta) + B(n) \sin(n\theta)]$

CONDITION 110, STALL WARNING (FLAPS 10)  
ALTITUDE= 16239. FT MACH NUMBER= 0.347

TEST 273-7 IRIG 8-22-26  
CORRECTED AIRFLOW= 1621. LB/SEC

ROW NO.	Z (IN)	A(n)						B(n)					
		(PSI)	A(1) (PSI)	A(2) (PSI)	A(3) (PSI)	A(4) (PSI)	A(5) (PSI)	B(1) (PSI)	B(2) (PSI)	B(3) (PSI)	B(4) (PSI)	B(5) (PSI)	
1	54.051	-5287	1811	0114	0348			0068	0187				
2	48.789	-6518	1422	0039	0036			0170	0175				
3	41.907	-8205	1413	0018	0062			0024	0198				
4	36.019	-1.0727	1416	0010	0172			0299	0012				
5	30.118	-1.3226	2217	00357	0009			0058	0186				
6	26.166	-1.5477	2197	0416	0027			0056	0162				
7	22.196	-1.6984	2865	0014	0324			0823	0126				
8	18.211	-1.7902	4265	0089	0049			0673	0009				
9	15.214	-1.8529	5494	0422	0040			0802	0290				
10	12.215	-12.4470	9547	1486	0780			2710	0774				
11	9.003	-2.7601	16242	1442	0707	0247	-1308	1222	0517	0036	0529	0079	
12	6.037	-2.6707	17576	0789	0798	0362	-0661	0199	5312	0365	0917	0814	
13	3.629	-2.5904	19187	2102	0604	0885	-0272	0385	8151	2208	0551	0994	
14	1.413	-2.1722	2.1972	0358	0479	-1212	0774	-0090	7195	0888	1495	1003	
15	1.172	-1.0175	1.8996	2129	0786	0115	-0579	0385	5851	1632	1481	0343	
16	0.000	-1.742	1.0016	2864	0657	-0532	-0014	-0236	3785	1909	0089	-0108	
17	1.324	-1.934	3084	2250	0702	-0936	0062	0566	1357	1730	0924	0016	
18	1.156	-2.517	5329	1769	0440	0107	0066	0110	1664	0652	0019	0395	
19	3.007	-2037	5297	0960	0196	0084	0029	0225	1665	0473	0252	-0036	
20	4.886	-1.045	4816	0398	0196	-0158	-0384	0163	1680	0197	0171	0148	
21	7.782	-0.0204	4155	0385	-0264	-0031	-0120	-0043	1767	0238	0007	0287	
22	12.404	-0.0359	2977	0154	.0261	.0065	.0506	.0030	0980	0703	-00274	-0042	
23	17.679	-0.0463	2735	-0068					0671	0532	-0077		
24	23.652	-0.0262	2530	.0023					0849	0615	-0072		
25	29.638	-0.0273	2017	.0124					0910	0268	0093		
26	36.633	-0.0339	1592	.0268					0921	0722			
27	48.631	-0.0457	1215	.0554					1253	0514	0184		
28	60.627	-0.0423	.0845	.0937					410	0168	0016		
29	72.863	-0.026	-0.0493	.0891					1654	0077	0139		
30	75.593	-0.014	-0.0247	.0370					1515	0108	0078		
31	96.576	.0529	-0.035	.0885					1436	0068	0132		
32	106.386	.0853	.0043	.0976					1889	0193	.0012		

ORIGINAL PAGE IS  
OF POOR QUALITY

12B208-60

Table A-16.

FOURIER - BESSSEL COEFFICIENTS FOR ENGINE NUMBER THREE PRESSURES

$P(\theta)$   $\diamond$  SIGNAL  $A(n) \cos(n\theta)$   $\diamond$   $B(n) \sin(n\theta)$ ) ]

Row No.	Z (IN)	CONDITION 111, STALL WARNING (FLAPS 30) MACH NUMBER= 0.270						TEST 273-7 IRIG 8-24-51.9 CORRECTED AIRFLOW= 1633. LB/SEC					
		A(0) (PSI)	A(1) (PSI)	A(2) (PSI)	A(3) (PSI)	A(4) (PSI)	A(5) (PSI)	A(6) (PSI)	B(1) (PSI)	B(2) (PSI)	B(3) (PSI)	B(4) (PSI)	B(5) (PSI)
1	54.051	- .7723	.1489	.0065	.0172				.0104	.0158			
2	48.789	- .8854	.1294	.0021	.0041				.0167	.0163			
3	41.907	- 1.0550	.1283	.0229	.0025				.0322	.0176			
4	36.019	- 1.2754	.1268	.0136					.0121	.0030			
5	30.118	- 1.5261	.1569	.0093	.0004				.0015	.0226			
6	26.166	- 1.7693	.1576	.0084	.0011				.0105	.0106			
7	22.196	- 1.9176	.1947	.0185	.0388				.0504	.0399			
8	18.211	- 2.0237	.3006	.0118	.0069				.0305	.0095			
9	15.214	- 2.0874	.3601	.0167	.0242				.0383	.0072			
10	12.215	- 2.7157	.7711	.2460	.1419				.3646	.1958			
11	9.009	- 2.9698	1.2136	.1272	.0586	.0229	.0494	.0743	.2676	.0524	.0206	.0170	
12	6.037	- 2.8361	1.1916	.0207	.0508	.0019	.0107	.0492	.3878	.0281	.0557	.0333	
13	3.629	- 2.9101	1.3854	.2959	.0906	.0922	.0162	.0523	.6970	.2194	.1416	.0987	
14	1.413	- 2.7349	1.8451	.0510	.0116	.0108	.0008	.0393	.5737	.0610	.0417	.0523	
15	1.172	- 1.7020	1.8956	.1242	.0385	.0395	.1189	.0528	.5706	.1394	.0862	.0611	
16	0.006	- 1.7024	1.2416	.0694	.0351	.0304	.0262	.0067	.4445	.0818	.0450	.0053	
17	.324	.0654	.2537	.0654	.0189	.0528	.0261	.0457	.0765	.0461	.0502	.0468	
18	1.156	.2723	.0904	.0529	.0253	.0073	.0116	.0035	.0218	.0370	.0037	.0129	
19	3.007	.2404	.2027	.0471	.0077	.0101	.0061	.0092	.0525	.0116	.0017	.0013	
20	4.886	.1794	.2162	.0259	.0045	.0045	.0045	.0030	.0063	.0843	.0446	.0045	
21	7.782	.1130	.2035	.0185	.0115	.0097	.0049	.0049	.0043	.0914	.0033	.0046	
22	12.404	.0548	.1410	.0127	.0098	.0035	.0098	.0224	.0077	.0525	.0258	.0140	
23	17.679	.0547	.1458	.0089					.0077	.0476	.0438	.0009	
24	23.652	.0266	.1261	.0139						.0492	.0241		
25	29.638	.0353	.1056	.0178						.0483	.0198	.0013	
26	36.633	.0272	.0943	.0186						.0473	.0317	.0011	
27	48.631	.0099	.0764	.0346						.0556	.0302	.0043	
28	60.627	.0082	.0530	.0458						.0814	.0104	.0007	
29	72.863	.0238	.0311	.0431						.0967	.0020	.0059	
30	75.593	.0315	.0185	.0432						.0911	.0043	.0037	
31	95.576	.0502	.0112	.0498						.0859	.0090	.0053	
32	106.386	.0630	.0040	.0581						.1165	.0092	.0009	

ORIGINAL PAGE IS  
OF POOR QUALITY

126209-61

Table A-17.

FOURIER - BESSSEL COEFFICIENTS FOR ENGINE NUMBER THREE PRESSURES

$$P(\theta) = A(0) + \Sigma [A(n) \cos(n\theta) + B(n) \sin(n\theta)]$$

CONDITION 112, IDLE DESCENT TEST 273-7 IRIG 8-2B-56.4

ROW NO.	Z (IN)	TEST 273-7 CORRECTED AIRFLOW = 748. LB/SEC						B(5) (PSI)
		A(0) (PSI)	A(1) (PSI)	A(2) (PSI)	A(3) (PSI)	A(4) (PSI)	A(5) (PSI)	
1	54.051	1.2639	.0157	.0056	.0040			.0333
2	48.789	1.2300	-.0008	.0083	.0064			.0075
3	41.907	1.1914	.0344	-.0011	-.0006			.0228
4	36.019	1.1364	.0325	-.0003	-.0040			.0030
5	30.118	1.0884	.0452	-.0028	-.0073			
6	26.166	1.0491	.0584	-.0027	-.0121			
7	22.196	1.0409	.0793	.0075	.0013			
8	18.211	1.0443	.0982	-.0020	.0013			
9	15.214	1.0332	.1152	.0205	.0029			
10	12.215	1.0902	.2084	-.0098	.0222			
11	9.009	1.0727	.2361	.0117	-.0105	-.0022	-.0141	-.0435
12	6.037	1.1272	.2314	.0060	-.0151	.0046	-.0157	-.0055
13	3.629	1.2796	.2060	-.0570	-.0197	.0483	-.0082	-.0285
14	1.413	1.3977	.0371	-.0280	.0396	.0179	-.0089	-.0027
15	1.172	.82220	-.6155	-.0603	-.0673	-.0660	.0406	.0100
16	0.000	-.7917	-.14563	-.0402	.0959	.1351	-.0472	.0324
17	1.324	-2.7683	-2.1818	-.3996	.4196	.5883	-.4559	-.6023
18	1.156	-2.2738	-1.8405	-.2842	.2987	-.0044	.0093	.1758
19	3.007	-1.4961	-1.0829	-.2393	-.1418	-.0796	.0047	.0159
20	4.886	-1.2309	-.7692	-.0790	-.0327	-.1168	-.0335	.0242
21	7.782	-1.9226	-.4377	-.0436	-.0316	-.0664	-.0135	.0118
22	12.404	-.8101	-.3539	.0914	.1350	.0401	.0524	.1064
23	17.679	-.6234	-.3465	-.0879				
24	23.652	-.4811	-.2932	-.1119				
25	29.638	-.4124	-.2017	-.0459				
26	35.633	-.3266	-.1404	-.0281				
27	48.631	-.2903	-.1410	.0170				
28	60.627	-.2335	-.0617	.1045				
29	72.863	-.1294	-.0047	.0323				
30	75.593	-.0965	-.0049	.0540				
31	96.576	.0250	.0264	.0528				
32	106.386	.1516	.0701	-.0098				

ORIGINAL PAGE IS  
OF POOR QUALITY

126208-52

Table A-18.

FOURIER - BESSEL COEFFICIENTS FOR ENGINE NUMBER THREE PRESSURES									
P(THETA) = A(0) + SIGMA( A(N)COS(NTHETA) + B(N)SIN(NTHETA) )									
CONDITION 113, APPROACH TEST 2737 IRIG B-34CZ									
ALTITUDE = 6003 FT	MACH NUMBER = 0.265	CORRECTED AIRFLOW = 1547 LB/SEC					A(6)	B(1)	B(2)
Z (IN)	A(0) (PSI)	A(1) (PSI)	A(2) (PSI)	A(3) (PSI)	A(4) (PSI)	A(5) (PSI)	(PSI)	(PSI)	(PSI)
54.051	- .9824	.1956	- .0005	.0377					
48.789	-1.1374	.1467	.0344	-.0106					
41.907	-1.3859	.1597	.0027	-.0044					
36.019	-1.6508	.1058	-.0010	.0209					
30.118	-1.9705	.1965	-.0103	.0259					
26.166	-2.2215	.1914	-.0107	.0505					
22.196	-2.4542	.2377	-.0560	.0693					
18.211	-2.5446	.3324	-.0655	.0428					
15.214	-2.6340	.4313	-.0831	.0474					
10	12.215	-3.3275	.6888	.1528	-.0893	.0160	.0682	-.2242	.0178
11	9.009	-3.5093	.9366	.0280	.0208	.0073	-.0246	-.0286	-.0742
12	6.037	-3.3979	.9730	.0574	-.0241	-.0245	-.0286	-.3091	.0332
13	3.629	-3.4562	1.1390	.3777	-.0304	-.1445	-.0001	.0676	-.0430
14	1.413	-3.1806	1.6028	.1886	-.0419	-.1369	.0760	.0425	-.1309
15	1.172	-1.8572	1.8313	.0685	-.0721	-.0420	-.0420	-.0377	-.0377
16	0.000	-1.5835	1.2262	.0967	-.0242	-.0557	-.0680	-.0406	-.0520
17	1.324	2.2907	1.4633	-.0412	-.0102	-.0564	-.0496	-.0689	-.0221
18	1.156	1.4482	1.456	-.0549	-.0209	-.0128	-.0175	-.0043	-.0163
19	3.007	3.148	-2.369	-.0628	-.0133	-.0047	-.0160	-.0129	-.0163
20	4.886	2.158	-.2669	-.0366	-.0199	-.0109	-.0179	-.0122	-.0059
21	7.782	.1031	-.2219	-.0178	-.0018	-.0010	-.0027	-.0089	-.0032
22	12.404	.0367	-.1557	-.0003	-.0034	-.0168	-.0253	-.0137	-.0125
23	17.679	.0104	-.1195	.0002					
24	23.652	.0102	-.1318	-.0124					
25	29.633	-.007	-.1142	.0066					
26	36.633	-.0156	-.0937	-.0005					
27	43.531	-.0326	-.0628	.0205					
28	60.627	-.0421	-.0582	.0439					
29	72.863	-.0145	-.0387	.0376					
30	75.393	-.0033	-.0176	.0346					
31	95.576	.0385	-.0027	.0389					
32	106.336	.0624	.0138	.0430					

ORIGINAL PAGE IS  
OF POOR QUALITY

126209-63

Table A-19.

ROW NO.	Z (IN)	CONDITION 114: TOUCH AND GO						TEST 273? IRIG & 40-361						
		MACH NUMBER= 0.263	CORRECTED AIRFLOW= 1509. LB/SEC			A(0) (PSI)	A(1) (PSI)	A(2) (PSI)	A(3) (PSI)	A(4) (PSI)	B(1) (PSI)	B(2) (PSI)	B(3) (PSI)	B(4) (PSI)
1	54.051	-1.2423	.2260	.0114	.0279	-.0107	-.0333							
2	48.789	-1.3951	.2637	-.0097	-.0208	-.0329	-.0119							
3	41.907	-1.6942	.1932	-.0328	-.0924	-.0238	-.0334							
4	36.019	-2.0402	.1906	-.0274	.0245	-.0299	-.0086							
5	30.118	-2.4476	.2415	.0093	.0021	-.0347	-.0278							
6	26.166	-2.8186	.2262	-.0131	.0013	-.0269	-.0100							
7	22.196	-3.0504	.2456	-.0416	.0496	-.1412	-.0414							
8	18.211	-3.2089	.3867	-.0489	.0161	-.1026	-.0100							
9	15.214	-3.3275	.4329	-.0018	.0256	-.1242	-.0195							
10	12.215	-4.0792	.8133	-.1193	-.0816	-.3951	-.0184							
11	9.009	-4.4561	1.1894	.0149	-.0103	.0370	-.0282	.1130	-.443	-.0231	-.0699	-.0425		
12	6.037	-4.2609	1.1553	.1054	-.0295	-.0373	-.0286	-.0330	-.5649	-.0720	.0141	-.0555		
13	3.629	-4.4133	1.3605	.5531	-.1202	-.1714	.0267	-.0755	-.1412	-.3128	-.0671	-.1415		
14	1.413	-4.1699	1.9831	.2495	-.1083	-.0967	.0295	-.0620	-.1096	-.2242	-.0029	-.0055	-.0853	
15	1.172	-2.5406	2.2309	.0057	-.0629	-.1107	-.0302	-.0330	-.0498	-.1358	.0854	.0379	-.0034	
16	0.000	-1.0088	1.5795	-.0577	-.0346	-.0638	-.0689	-.0379	-.8200	-.1877	-.0942	-.0595	-.0450	
17	1.324	-2.451	.2778	-.0691	-.0017	-.0821	-.0507	-.0776	-.1448	-.0740	-.0968	-.0701	-.0680	
18	1.156	-4.9126	1.1038	-.0455	-.0347	-.0162	-.0096	-.0054	-.0675	-.0471	-.0065	-.0118	-.0243	
19	3.007	-4.0229	1.2489	-.0520	-.0068	-.0077	-.0012	-.0018	-.1206	-.0177	-.0027	-.0042	-.0106	
20	4.886	-2.8880	1.2647	-.0342	-.0017	-.0031	-.0072	-.0072	-.1511	-.0174	-.0073	.0011	.0087	
21	7.782	-1.662	.2471	-.0338	-.0168	-.0060	-.0052	-.0025	-.1581	-.0169	-.0023	-.0039	-.0094	
22	12.404	-.0812	1.6116	-.0005	-.0026	-.0063	-.0304	-.0140	-.1069	-.0224	-.0074	-.0052	-.0216	
23	17.679	-.0687	1.745	-.0089										
24	23.652	-.0498	1.405	-.0013										
25	29.638	-.0385	1.277	-.0085										
26	36.633	-.0293	1.120	-.0004										
27	48.631	-.0024	.0984	.0264										
28	60.627	-.0014	.0726	.0377										
29	72.863	-.0031	.0676	.0552										
30	75.593	.0365	-.0348	.0326										
31	96.576	.0766	-.0026	.0407										
32	106.386	.0970	.0145	.0467										

Table A-20.

FOURIER - BESSEL COEFFICIENTS FOR ENGINE NUMBER THREE PRESSURES

$P(\theta) = A(0) + \Sigma [A(n) \cos(n\theta) + B(n) \sin(n\theta)]$

Row No.	Z (IN)	CONDITION 115, THRUST REVERSE MACH NUMBER= 0.179						TEST 273-7 CORRECTED AIRFLOW= 1369. LB/SEC IRIG 845-59.4					
		A(0) (PSI)	A(1) (PSI)	A(2) (PSI)	A(3) (PSI)	A(4) (PSI)	A(5) (PSI)	A(6) (PSI)	B(1) (PSI)	B(2) (PSI)	B(3) (PSI)	B(4) (PSI)	B(5) (PSI)
1	54.051	-.8687	.1066	-.0022	.0199				.0314	-.0311			
2	48.789	-.9857	.0774	.0066	-.0071				.0352	.0045			
3	41.907	-.1.633	.0827	-.0252	-.0001				.0384	-.0216			
4	36.019	-.1.3741	.0761	-.0208	.0229				.0107	.0032			
5	30.118	-.1.6220	.0934	.0808	-.0007				.0190	-.0087			
6	26.166	-.1.8395	.0529	.0016	-.0046				.0258	.0013			
7	22.196	-.1.9762	.0370	-.0258	.0338				.0299	.0252			
8	18.211	-.2.0915	.0925	-.0263	.0043				.0127	-.0126			
9	15.214	-.2.1436	.0820	.0046	.0089				.0301	.0110			
10	12.215	-.2.6567	.2569	.1260	-.0346				.1692	.1059			
11	9.009	-.2.8212	.2523	.0170	.0129	.0199	.0133	.0655	-.0603	.0881	.0323	-.0492	-.0359
12	6.037	-.2.8874	.2861	.0495	-.0109	.0187	-.0063	-.0124	.0956	-.0364	.0294	.0015	-.0534
13	3.629	-.3.1425	.1620	.2891	-.0141	-.0186	.0041	.0694	-.2526	.0408	.1674	-.0072	-.1075
14	1.413	-.3.3882	.2734	.1837	-.0277	-.1017	.0409	.0277	.1944	.0322	.0193	.0476	-.0226
15	.172	-.2.9034	.7084	.0515	-.0238	.0634	-.1167	-.0025	.2458	-.0327	.0021	.0417	-.0094
16	0.000	-.1.9518	.5912	.0260	.0306	-.0032	.0365	-.0097	.2276	.0424	.1073	.0083	.0185
17	.324	-.3.5337	.2393	.0432	.0268	.0278	-.0432	-.0225	.1267	.0045	.1243	.0322	-.0461
18	1.156	.1747	.0377	-.0082	.0468	-.0226	-.0173	.0279	-.0755	.0403	.0086	.0236	.0444
19	3.067	.2859	.0049	-.0047	.0139	-.0079	.0161	.0032	-.0141	.0040	-.0079	.0070	.0027
20	4.886	.2717	-.0087	-.0343	.0004	-.0165	-.0130	-.0053	-.0123	.0132	.0083	-.0003	-.0004
21	7.782	.2497	-.0163	-.0184	-.0062	-.0119	-.0070	-.0043	.0022	.0047	-.0092	-.0029	.0070
22	12.404	.2022	-.0070	-.0055	-.0120	.0015	.0038	-.0238	-.0092	.0065	-.0030	-.0079	.0020
23	17.679	.1994	-.0038	-.0059					.0057	-.0022	.0107		
24	23.652	.1872	.0251	-.0208					.0105	.0275	-.0179		
25	29.638	.1845	.0366	-.0235					.0202	.0383	-.0206		
26	36.633	.1844	.0222	-.0265					.0132	.0369	-.0156		
27	48.631	.1887	.0527	-.0276					.0193	.0348	-.0237		
28	60.627	.2180	.0465	-.0269					.0120	.0262	-.0160		
29	72.863	.2228	.0393	-.0226					.0134	.0159	-.0118		
30	75.593	.2371	.0364	-.0137					.0058	.0214	-.0180		
31	96.576	.2359	.0204	-.0049					.0038	.0050	-.0076		
32	106.386	.1980	.0521	-.0227					.0352	-.0529	.0339		

ORIGINAL PAGE IS  
OF POOR QUALITY

125208-64

ORIGINAL PAGE IS  
OF POOR QUALITY

88-602921

Table A-21.

FOURIER - BESSSEL COEFFICIENTS FOR ENGINE NUMBER THREE PRESSURES

$$P(\Theta) = A(0) + \Sigma (A(n) \cos(n\Theta) + B(n) \sin(n\Theta))$$

CONDITION 116, 2.0g LEFT TURN (FLAPS UP) TEST 29340 IRIG 13:38:6  
MACH NUMBER: 0.487 CORRECTED AIRFLOW: 1562. LB/SEC

ROW NO.	Z (IN)	A(0) (PSI)	A(1) (PSI)	A(2) (PSI)	A(3) (PSI)	A(4) (PSI)	A(5) (PSI)	B(1) (PSI)		B(2) (PSI)		B(3) (PSI)		B(4) (PSI)		B(5) (PSI)	
								B(6) (PSI)	B(7) (PSI)	B(8) (PSI)	B(9) (PSI)	B(10) (PSI)	B(11) (PSI)	B(12) (PSI)	B(13) (PSI)		
1	54.051	.2640	.1281	-.0134	.0535			-.0577	-.0171								
2	46.789	.1083	.1316	.0054	.0139			-.0881	.0237								
3	41.907	-.1314	.1703	-.0038	.0334			-.0009	-.0079								
4	36.019	-.4616	.2072	.0665	.0308			-.0616	.0432								
5	31.118	-.7974	.2692	.0463	.0046			-.0240	-.0289								
6	26.166	-.10615	.1772	.0530	-.0315			-.0861	-.0051								
7	22.196	-.12836	.2457	-.0064	.0344			-.1466	-.0005								
8	18.211	-.13373	.4288	.0104	.0035			-.1260	.0081								
9	15.214	-.4437	.4468	-.0108	.0011			-.1697	.0187								
10	12.215	-.18907	.8090	-.0481	.0237			-.2491	-.0981								
11	9.009	-.2.1006	1.1932	-.0574	-.0505			-.0078	-.0172								
12	6.037	-.1.7958	1.1411	.0290	-.0436			-.0105	-.0533								
13	3.629	-.1.4055	1.2481	.2394	-.0573			-.0825	-.0005								
14	1.413	-.4567	1.4096	.0424	-.0217			-.1266	-.0790								
15	1.172	1.0349	.8838	-.1150	.0223			-.0564	.0014								
16	0.000	1.3851	-.3968	-.2134	-.0146			-.0044	.0223								
17	1.324	-.2314	1.7001	-.3180	-.0405			-.0519	-.0033								
18	1.156	-.1510	1.4350	-.1490	-.0252			-.0154	-.0117								
19	3.007	-.2599	-.1.0382	-.1289	-.0680			-.0148	.0288								
20	4.886	-.4280	-.8477	-.0774	-.0224			-.0269	-.0273								
21	7.782	-.5624	-.6215	-.1040	-.0824			-.0788	-.0345								
22	12.404	-.5198	-.4570	.0600	.0779			-.0358	.1039								
23	17.679	-.4640	-.4653	-.0906													
24	23.652	-.3679	-.3442	-.0659													
25	29.638	-.3657	-.2766	-.0067													
26	35.633	-.3076	-.1908	-.0317													
27	48.631	-.3231	-.1918	.0518													
28	60.627	-.2846	-.1157	.1245													
29	72.863	-.1849	-.0673	.0785													
30	75.593	-.1306	-.0104	.0754													
31	96.576	-.0415	.0402	.0795													
32	106.386	-.1402	-.0935	-.0118													

ORIGINAL PAGE IS  
OF POOR QUALITY

126209-66

Table A-22.

Z (ft)	CONDITION 1117.150 LEFT TURN (FLAPS 30) MACH NUMBER= 0.251						TEST 278-0 IRIG 13-41-75 CORRECTED AIRFLOW= 1539. LB/SEC					
	P(THETA)=A(0) + SIGMA( A(N)COS(NTHETA) + B(N)SIN(NTHETA) )						P(PSI)			B(1) (PSI)		
	A(0) (PSI)	A(1) (PSI)	A(2) (PSI)	A(3) (PSI)	A(4) (PSI)	A(5) (PSI)	A(6) (PSI)	B(1) (PSI)	B(2) (PSI)	B(3) (PSI)	B(4) (PSI)	B(5) (PSI)
54.05	-9.499	.2009	-.0669	.0167				-.0914				
2	49.789	-1.0971	.1845	.0061	.0082			-.0762				
3	41.907	-1.2762	.1802	-.0019	.0161			-.0353				
4	36.019	-1.5752	.1938	.0278				-.0862				
5	30.118	-1.8452	.2620	.0242	.0232			-.0557				
6	26.166	-2.1227	.2305	.0095	-.0023			-.1029				
7	22.196	-2.2870	.2815	-.0295	.0540			-.2186				
8	18.211	-2.3877	.4417	-.0353	.0101			-.2351				
9	15.214	-2.4746	.4980	-.0139	.0266			-.2313				
10	12.215	-3.0055	.8407	.0044	.0332			-.0004				
11	9.009	-3.3737	1.3271	.0286	-.0589	.0139	-.0876	.0751				
12	6.037	-3.2616	1.2591	.0868	-.0066	-.0390	-.0319	-.0118				
13	3.629	-3.5811	1.7594	.5596	-.2120	-.2344	-.0575	.1299	-.1651			
14	1.413	-3.5744	2.4727	.2308	-.0107	-.2344	-.0073	-.1879	-.4276			
15	1.172	-2.3205	2.5657	1.501	-.0112	.0807	-.1509	.0823	-.1618			
16	0.000	-1.0628	1.6854	.0412	-.0776	-.0346	-.0561	-.0567	-.1184			
17	324	-0.522	.2474	.0615	-.0162	-.1126	-.0211	.0571	-.2192			
18	1.156	.2109	.1608	.0172	-.0146	.0212	-.0027	.0034	.0493			
19	3.007	.2008	.3160	.0277	-.0064	-.0064	-.0210	.0245	-.1419			
20	4.886	.1311	.3171	.0115	-.0059	-.0020	-.0305	.0128	.1516			
21	7.782	.0572	.2791	.0068	-.0073	.0068	-.0089	-.0086	.1791			
22	12.404	.0267	.2338	-.0026	.0085	-.0145	.0322	-.0007	.1381			
23	17.679	-.0521	.2084	-.0074					.1592			
24	23.652	-.0564	.1943	-.0009					-.0419			
25	29.638	-.0696	.1714	.0277					-.0752			
26	36.633	-.0740	.1378	-.0013					.1291			
27	48.631	-.0984	.1096	.0386					-.0492			
28	60.627	-.0929	.0834	.0425					-.0039			
29	72.863	-.0544	.0701	.0422					-.0037			
30	75.593	-.0604	.0253	.0410					-.0115			
31	96.576	-.0267	-.0061	.0412					-.015			
32	106.386	-.0381	-.0232	.0245					-.0103			

ORIGINAL PAGE IS  
OF POOR QUALITY

125209-87

Table A-23.

ROW NO.	Z (IN)	ALTITUDE* FT	MACH NUMBER= 0.475	CORRECTED AIRFLOW= 1195. LB/SEC					
				P(THETA)=A(0) + SIGMA( A(N)COS(NTHETA) + B(N)SIN(NTHETA) )			TEST 273-15 IRIG 11-04-74		
				A(0) (PSI)	A(1) (PSI)	A(2) (PSI)	A(3) (PSI)	A(4) (PSI)	A(5) (PSI)
1	54.051	1.0189	.0574	.0143	.0081	.0067	.0269	.0157	.0118
2	48.789	.9301	.0580	.0141	.0281	.0201	.0157	.0118	.0024
3	41.907	.8245	.0814	.0222	.0222	.0278	.0064	.0082	.0024
4	36.019	.6528	.0963	.01745	.01745	.01745	.0171	.0146	.0146
5	30.118	.4968	.1842	.0064	.0082	.0261	.0146	.0146	.0146
6	26.166	.3763	.2579	.0171	.0171	.0171	.0171	.0171	.0171
7	22.196	.2945	.3548	.0146	.0146	.0146	.0146	.0146	.0146
8	18.211	.2881	.3611	.0014	.0184	.0184	.0184	.0184	.0184
9	15.214	.2679	.6807	.0408	.0545	.0182	.0352	.0289	.0289
10	12.215	.0287	.8385	.0075	.0311	.0589	.0270	.0437	.0223
11	9.089	.0418	.8385	.0416	.0416	.0248	.0248	.0248	.0248
12	6.037	.1711	.8619	.0115	.0356	.0356	.0205	.0332	.01640
13	3.629	.4775	.9297	.0767	.0767	.0054	.0405	.0452	.0175
14	1.413	.8816	.9405	.0151	.2531	.0187	.0512	.0486	.0406
15	1.172	1.2911	.05610	.6444	.3972	.0519	.0768	.0871	.0392
16	0.000	-1.324	-1.5881	-3.7798	-1.1996	-.02200	-.2124	-.1101	-.0218
17	1.156	-1.4182	-2.6182	-2.6182	-.5823	-.3176	-.1735	-.1039	-.0582
18	3.007	-8.137	-1.4123	-1.4123	-.1617	-.0560	-.0914	-.0878	-.0101
19	4.886	-71.98	-.9921	-.9921	-.0263	-.0917	-.1783	-.1380	-.0052
20	7.782	-.6209	-.5972	-.5972	-.0242	-.1662	-.1967	-.1386	-.0822
21	12.404	-.6654	-.5878	-.5878	-.1051	-.0438	-.0438	-.0563	-.0563
22	17.679	-.5316	-.5479	-.5479	-.0417	-.0942	-.0942	-.0357	-.1006
23	23.652	-.4077	-.4497	-.4497	-.0311	-.0311	-.0311	-.1293	-.0167
24	29.638	-.3594	-.3111	-.3111	-.2474	-.0048	-.0048	-.0661	-.0023
25	35.633	-.2991	-.2688	-.2688	-.2101	-.0749	-.0749	-.0867	-.0193
26	43.631	-.2321	-.1065	-.1065	-.1645	-.2321	-.1065	-.0523	-.0260
27	60.627	-.0513	-.1266	-.1266	-.1193	-.0513	-.1266	-.1796	-.0126
28	72.963	-.0682	-.0030	-.0030	-.1279	-.0682	-.0030	-.2041	-.0082
29	75.593	-.0415	-.1211	-.1211	-.1074	-.0415	-.1211	-.1780	-.0180
30	95.576	-.0374	-.2636	-.2636	-.1078	-.0374	-.2636	-.0107	-.0236
31	105.336	-.0323	-.0260	-.0260	-.1642	-.0323	-.0260	-.0260	-.0223
32	106.336	-.0229	-.0556	-.0556	-.1078	-.0229	-.0556	-.0556	-.0223

ORIGINAL PAGE IS  
OF POOR QUALITY

89-802921

Table A-24.

FOURIER - BESSSEL COEFFICIENTS FOR ENGINE NUMBER THREE PRESSURES		P(THETA) = A(0) + SIGMA( A(N) COS(NTHETA) + B(N) SIN(NTHETA) )	
		TEST 273-16 IRIG 11:07:27.4	
		CORRECTED AIRFLOW= 1424. LB/SEC	
ALTITUDE= 8221. FT		MACH NUMBER= 0.265	
Z (IN)	A(0) (PSI)	A(1) (PSI)	A(2) (PSI)
54.051	- .6732	.1498	-.0138
46.789	- .7798	.1857	-.0122
41.907	- .9172	.1715	-.0252
36.019	- 1.1640	.1943	-.0112
30.118	- 1.3924	.2638	-.0303
26.166	- 1.6032	.2932	-.0160
22.196	- 1.7629	.3658	-.0219
18.211	- 1.8378	.5273	-.0407
15.214	- 1.8969	.6131	-.0243
12.215	- 2.4661	1.0935	-.0316
11.909	- 2.5918	1.4074	-.0293
12.6037	- 2.5741	1.5408	-.0463
13.3629	- 2.6406	1.8284	-.2495
14.4113	- 2.7513	2.7746	-.0998
15.172	- 1.8514	2.7858	-.3798
16.0000	- 86587	1.7891	-.4421
17.324	- 0575	1.373	-.3615
18.156	- 1743	-.3116	-.1799
19.3.007	- 2564	-.3128	-.0391
20.4.886	- 2585	-.2696	-.0120
21.7.782	- 2090	-.1840	-.0207
22.12.404	- .0016	-.2832	-.0420
23.17.679	- .0482	-.2636	-.0404
24.23.652	- .0133	-.2406	-.0396
25.29.638	- .0305	-.2103	-.0755
26.36.633	- .0337	-.1704	-.0662
27.48.631	- .0501	-.1367	-.0919
28.60.627	- .0445	-.1002	-.1110
29.72.863	- .0192	-.0789	-.0964
30.75.593	- .0090	-.0598	-.1103
31.96.576	- .0195	-.0460	-.1037
32.106.386	- .0270	-.0411	-.1157

ORIGINAL PAGE IS  
OF POOR QUALITY

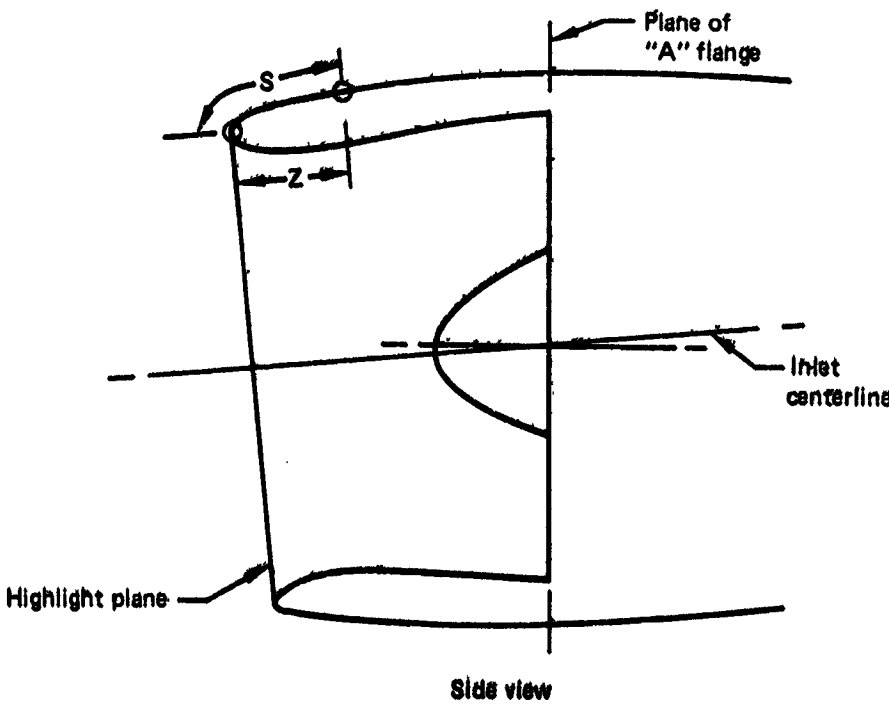
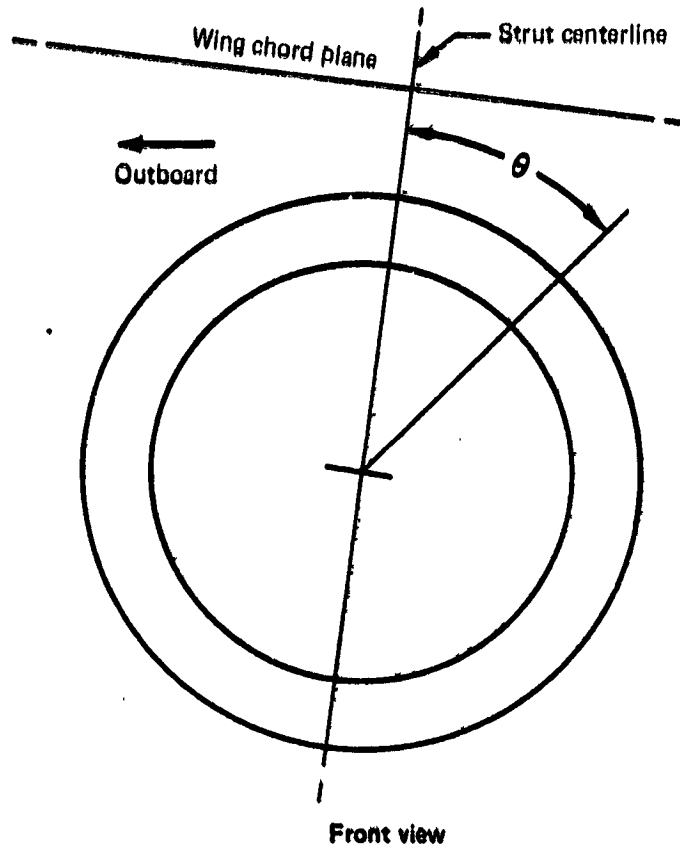
125208-69

Table A-25.

FOURIER - BESSSEL COEFFICIENTS FOR ENGINE NUMBER THREE PRESSURES

		P(THETA) = A(0) + SIGMA( A(N)COS(NTHETA) + B(N)SIN(NTHETA) )					
		TEST 273-10 IRIG 13-26-16.8					
		CORRECTED AIRFLW= 1551. LB/SEC					
ALTITUDE= 9000. FT		MACH NUMBER= 0.207					
Z (IN)	A(0) (PSI)	A(1) (PSI)	A(2) (PSI)	A(3) (PSI)	A(4) (PSI)	A(5) (PSI)	B(1) (PSI)
54.051	-1.1607	.2974	-.0420	.0230			-.0452
1 2	.2851	.2406	-.0367	.0046			-.0587
3 4	-1.4541	.2422	-.0234	.0035			-.0285
36.019	-1.7063	.2241	-.0220	.0239			-.0459
4 5	-1.9749	.3137	-.0244	.0158			-.0059
26.166	-2.2512	.2655	-.0079	-.0059			-.0303
6 7	22.196	-2.4336	.3446	-.0141			-.0136
8	16.211	-2.5427	.5000	-.0067	.0085		-.0192
9	15.214	-2.6330	.5854	-.0341	-.0201		-.0139
10	12.215	-3.1906	.9593	.1327	-.0541		-.0996
11	9.009	-3.5562	1.4117	.1436	-.0893	.0605	-.0686
12	6.037	-3.6103	1.7308	.0173	-.0802	-.0565	-.0226
13	3.629	-4.4217	2.9746	.0351	-.0340	.0176	-.0623
14	1.413	-4.5503	3.6060	.1008	-.1247	-.1533	-.0378
15	1.172	-3.4679	3.7221	.1680	-.1958	.1032	-.0681
16	0.000	-2.0984	2.6943	-.1430	-.1516	-.0877	-.1575
17	.324	.5955	1.0157	-.2368	-.0647	.0123	-.1130
18	1.156	-.0488	.1940	-.0660	-.0655	-.0052	-.2487
19	3.007	-.1212	-.1471	-.0427	-.0279	-.0143	-.0483
20	4.886	-.1013	-.2110	-.0679	-.0173	-.0110	-.0330
21	7.782	-.0936	-.2154	-.0072	-.0088	-.0155	-.0622
22	12.404	-.0177	-.1910	-.0367	-.0256	-.0076	-.0001
23	17.679	-.0027	-.1839	.0281			-.0001
24	23.652	-.0021	-.1743	.0516			-.0001
25	29.638	-.0097	-.1536	.0866			-.0001
26	36.633	-.0239	-.1245	.0826			-.0001
27	43.631	-.0489	-.1088	.1024			-.0001
28	60.627	-.0416	-.0903	.1058			-.0001
29	72.863	-.0311	-.0797	.0982			-.0001
30	75.593	-.0312	-.0690	.1009			-.0001
31	96.576	-.0238	-.0578	.0929			-.0001
32	106.386	-.0262	-.0250	.1196			-.0001

ORIGINAL PAGE IS  
OF POOR QUALITY



125009-53-422

Figure A-1. Pressure Data Coordinate Conventions

ORIGINAL PAGE IS  
OF POOR QUALITY

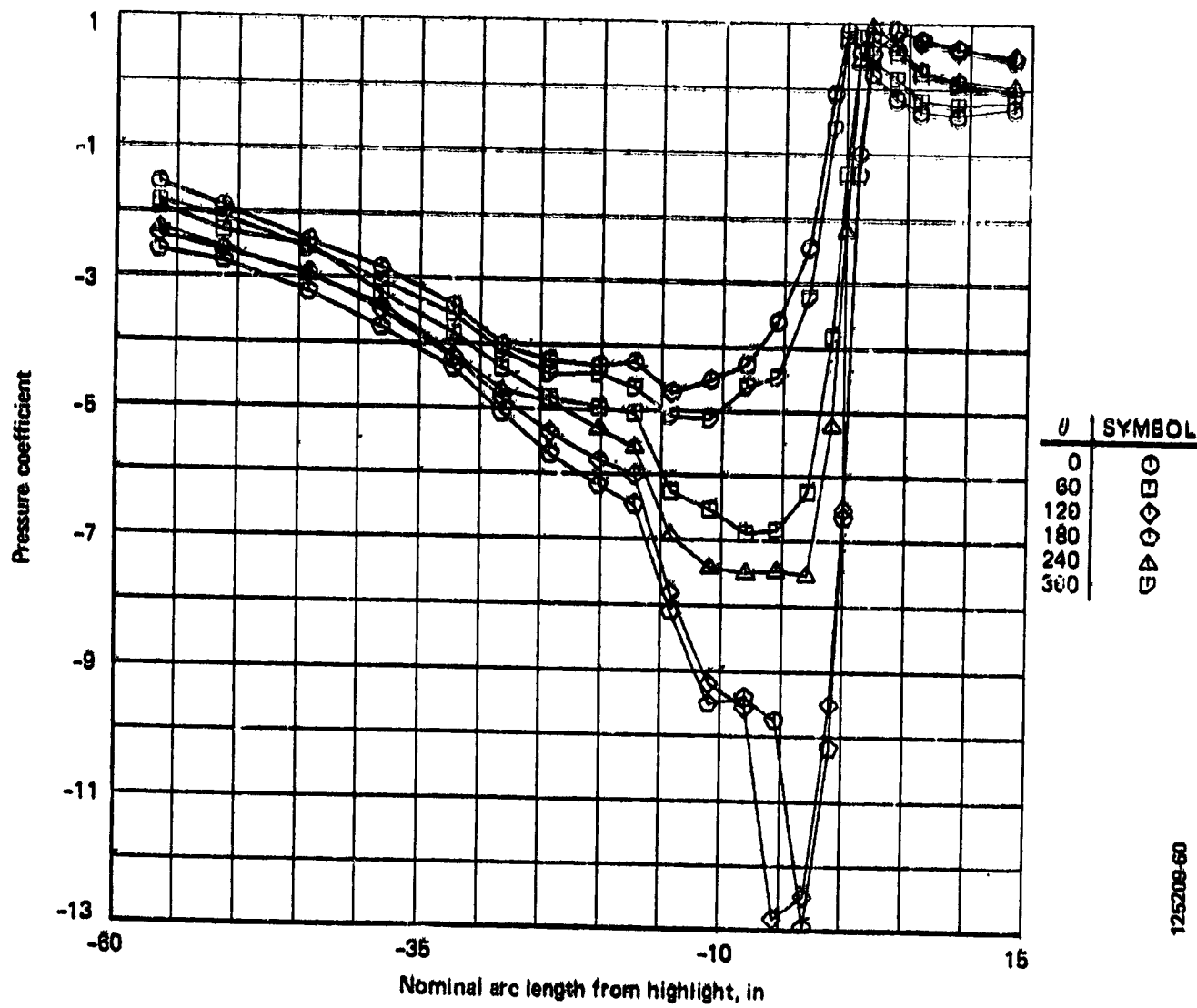


Figure A-2. Engine No. 3 Inlet Pressures, Condition 101, 612K GW Takeoff (Flaps 20)

ORIGINAL PAGE IS  
OF POOR QUALITY

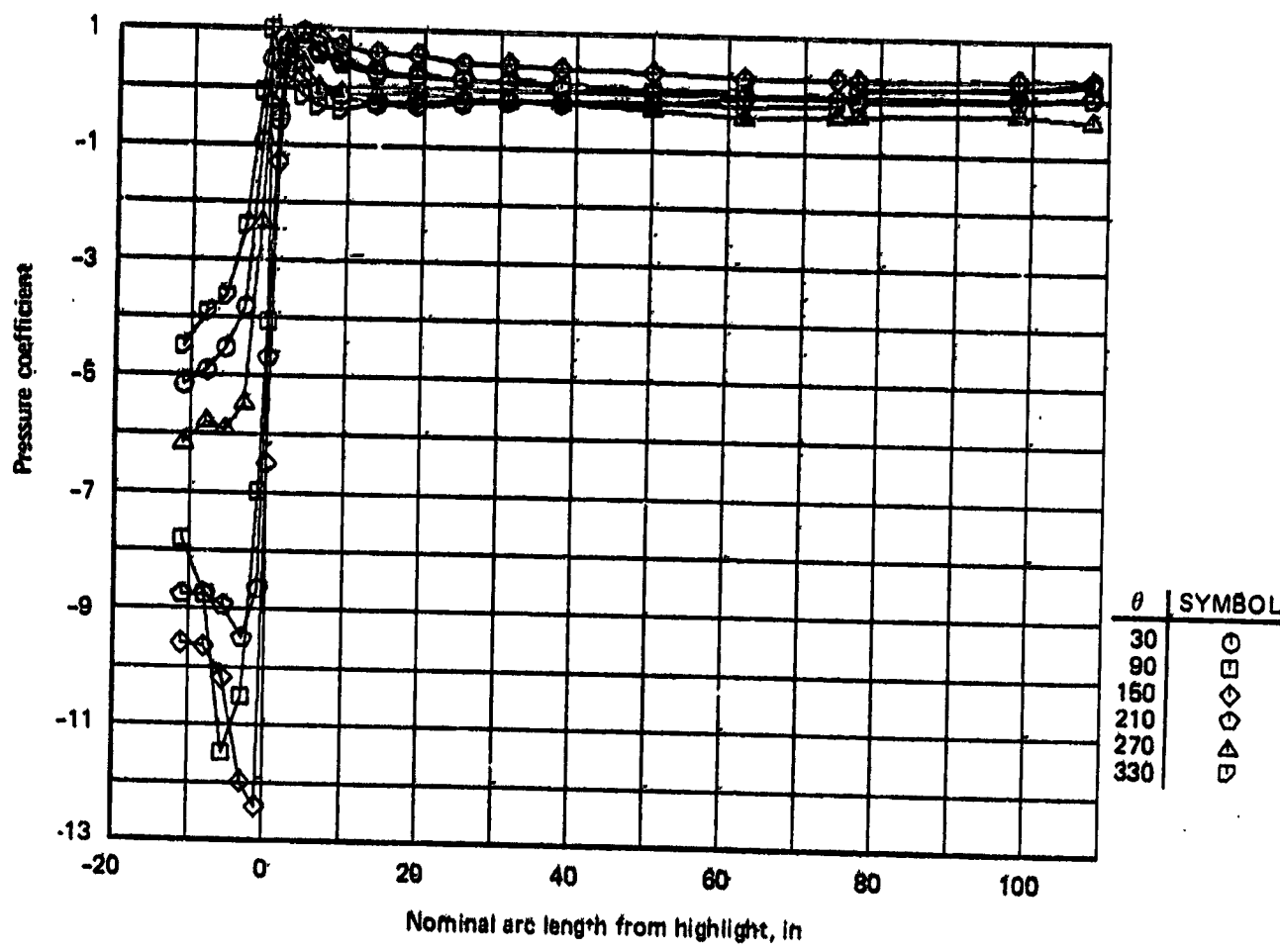


Figure A-3. Engine No. 3 Cowl Pressures, Condition 101, 612K GW Takeoff (Flaps 20)

125209-61

ORIGINAL PAGE IS  
OF POOR QUALITY

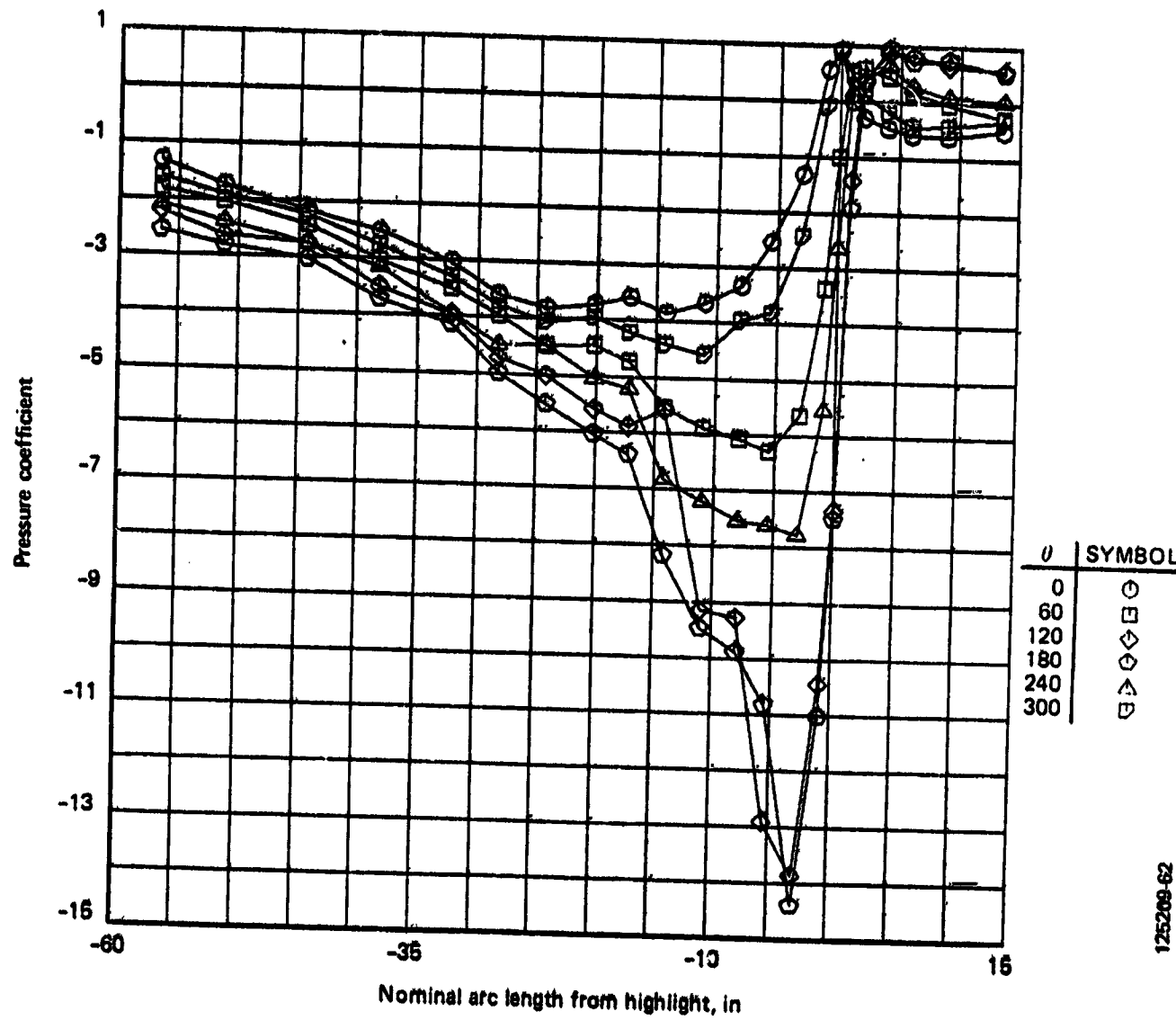


Figure A-4. Engine No. 3 Inlet Pressures, Condition 101, 538K GW Takeoff (Flaps 10)

ORIGINAL PAGE IS  
OF POOR QUALITY

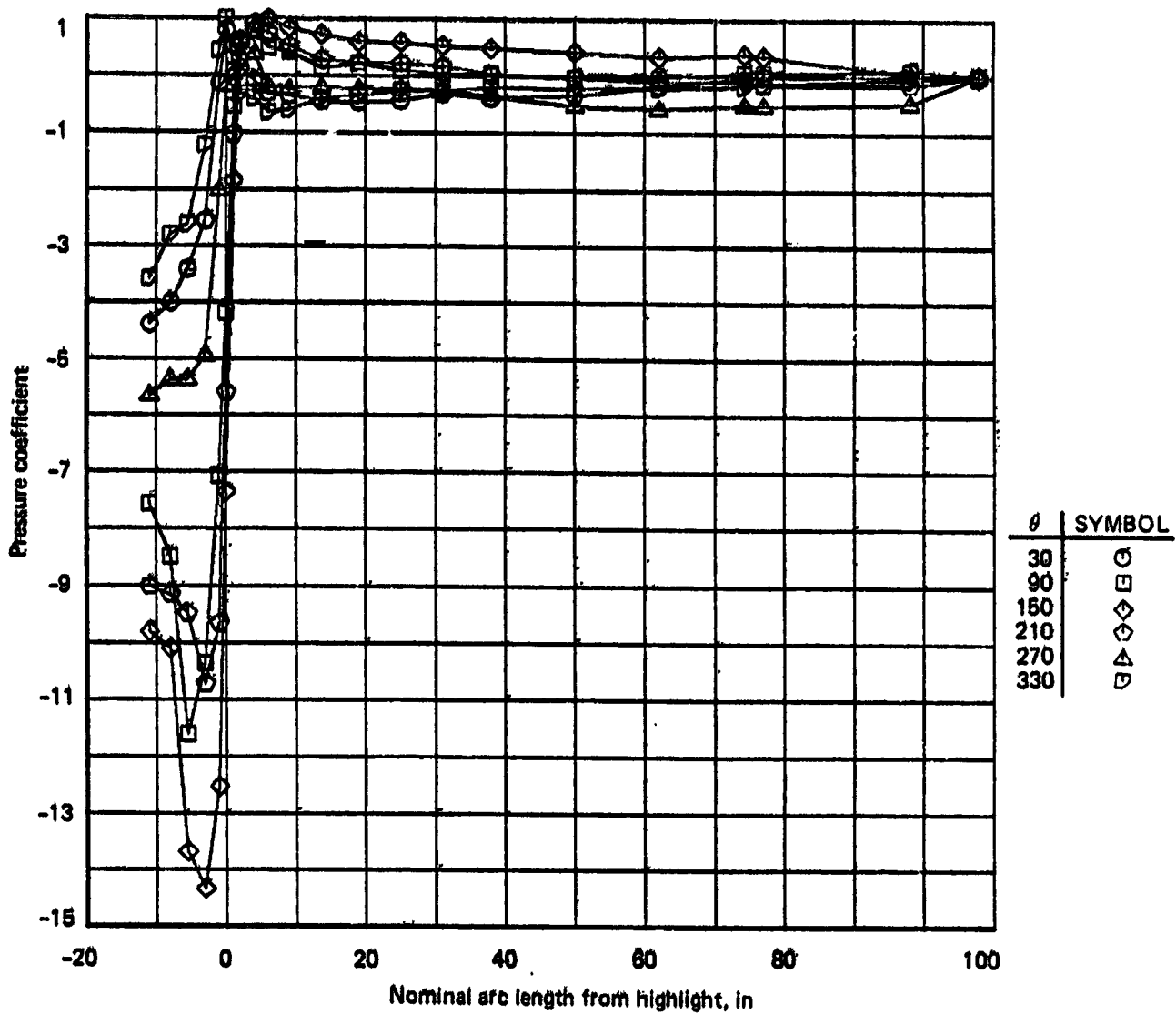


Figure A-5. Engine No. 3 Cowl Pressures, Condition 101, 538K GW Takeoff (Flaps 10)

ORIGINAL PAGE IS  
OF POOR QUALITY

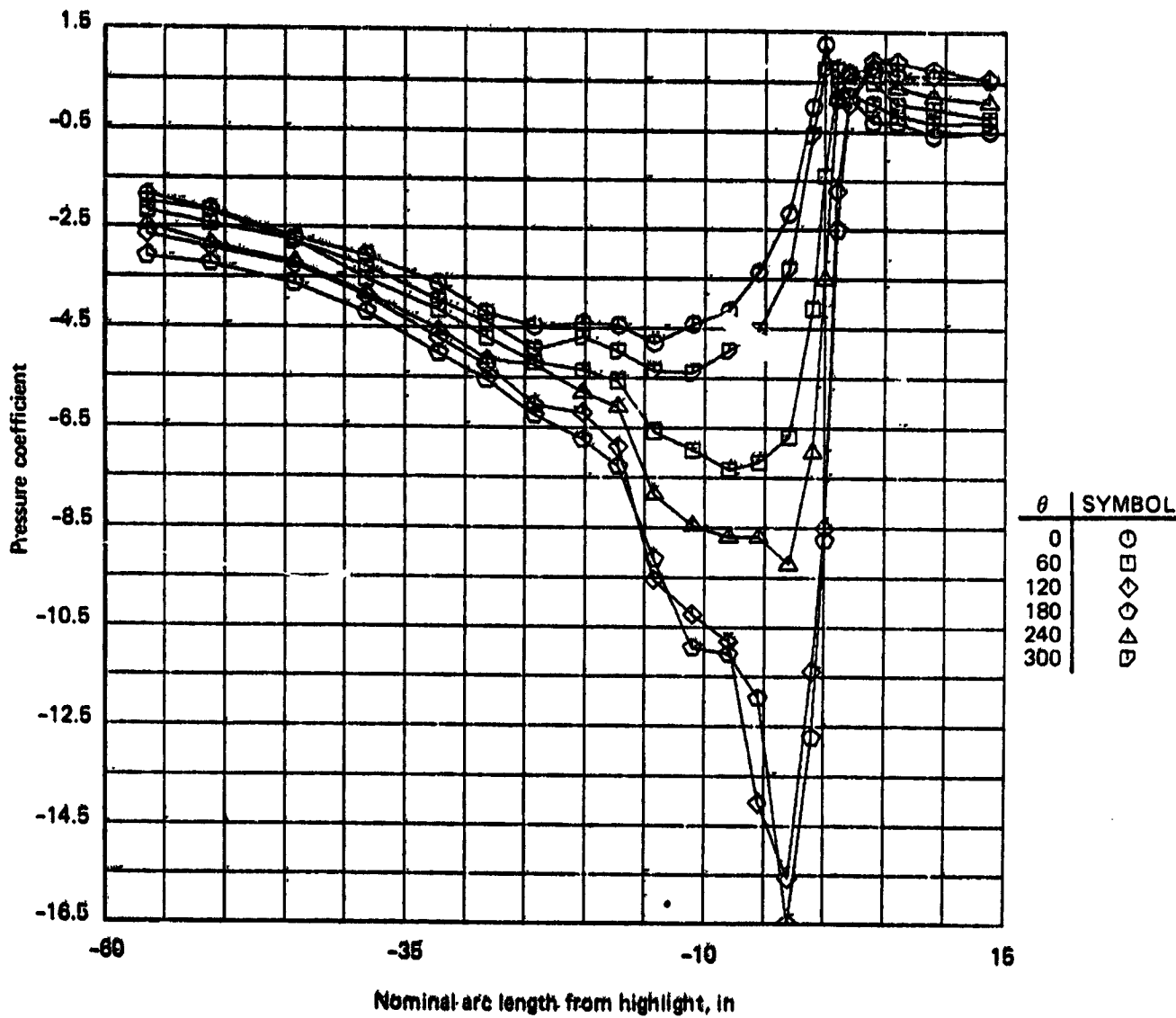
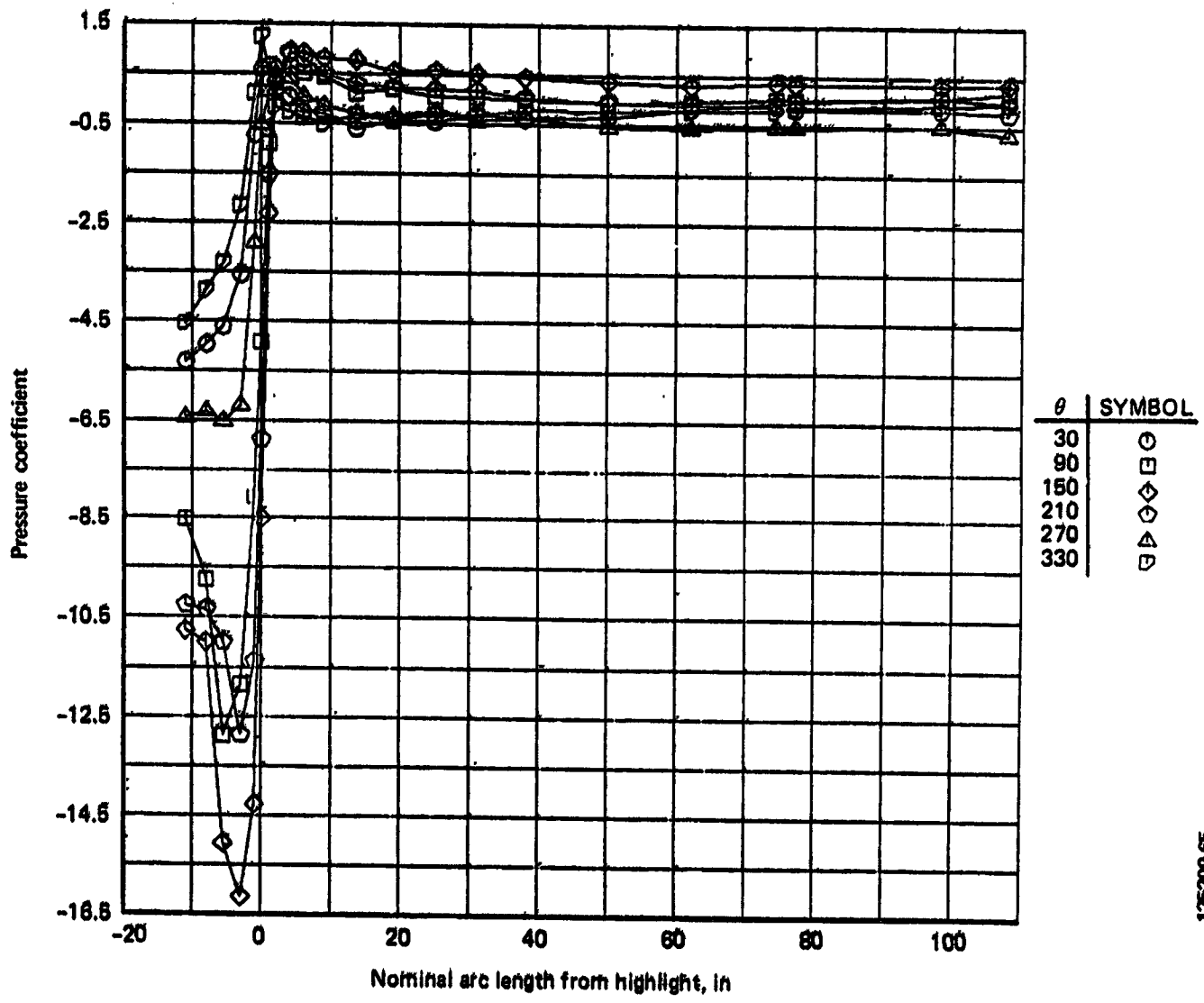


Figure A-6. Engine No. 3 Inlet Pressures, Condition 101, 647K GW Takeoff (Flaps 10)

ORIGINAL PAGE IS  
OF POOR QUALITY



125209-65

Figure A-7. Engine No. 3 Cowl Pressures, Condition 101, 647K GW Takeoff (Flaps 10)

ORIGINAL PAGE IS  
OF POOR QUALITY

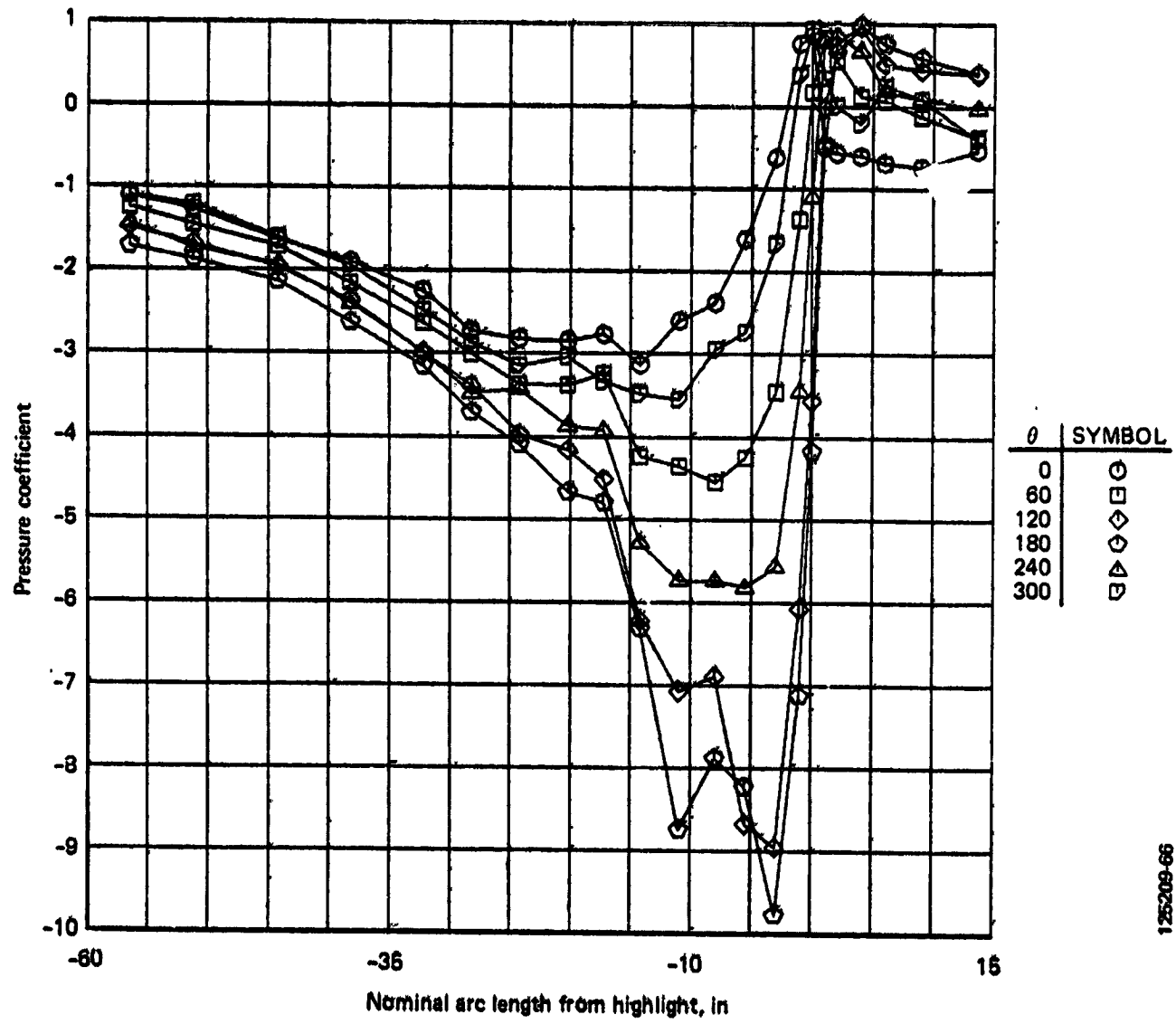


Figure A-8. Engine No. 3 Inlet Pressures, Condition 118, 780K GW Simulated Takeoff (Flaps 10)

ORIGINAL PAGE IS  
OF POOR QUALITY

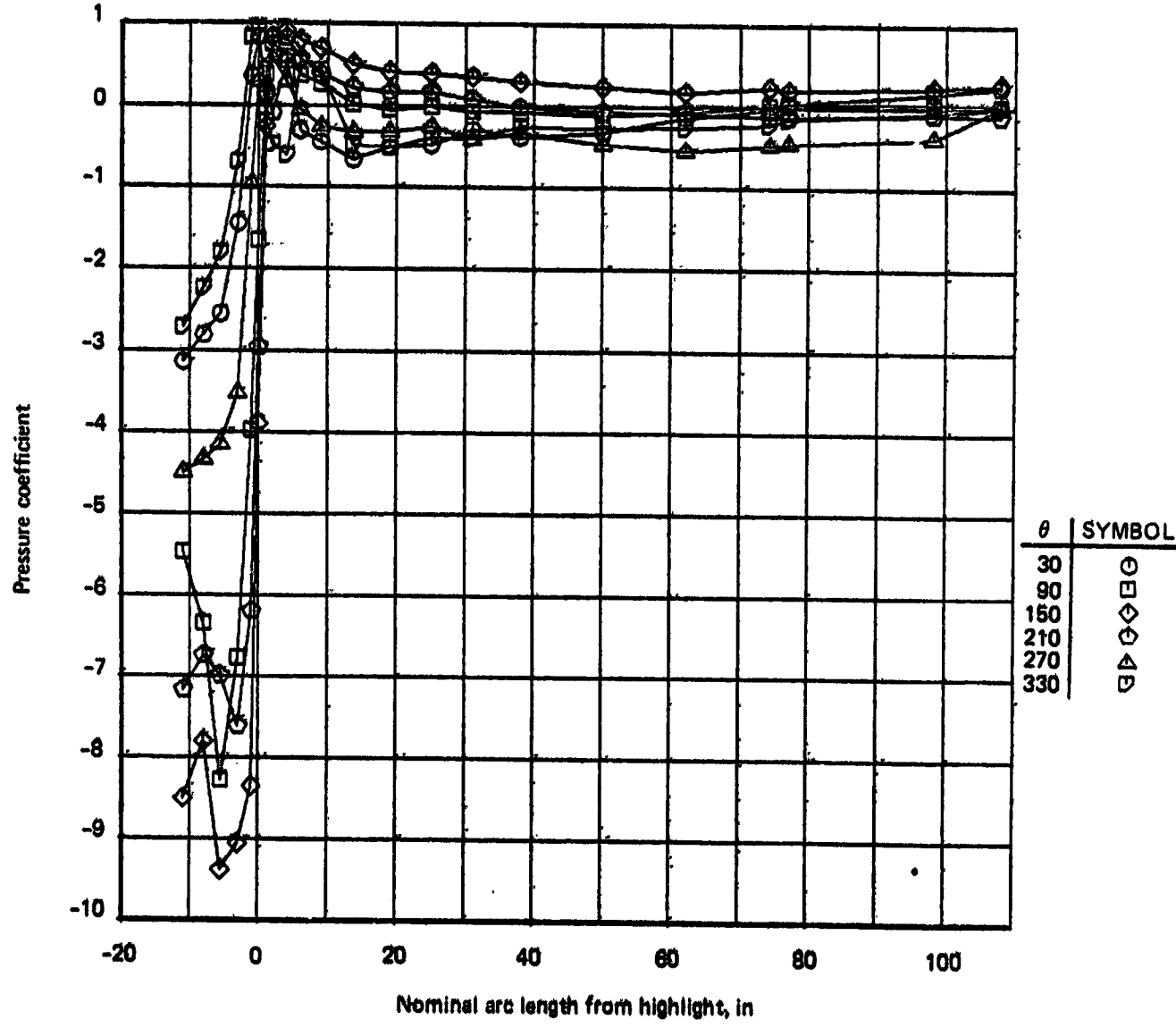


Figure A-9. Engine No. 3 Cowl Pressures, Condition 118, 780K GW Simulated Takeoff (Flaps 10)

ORIGINAL PAGE IS  
OF POOR QUALITY

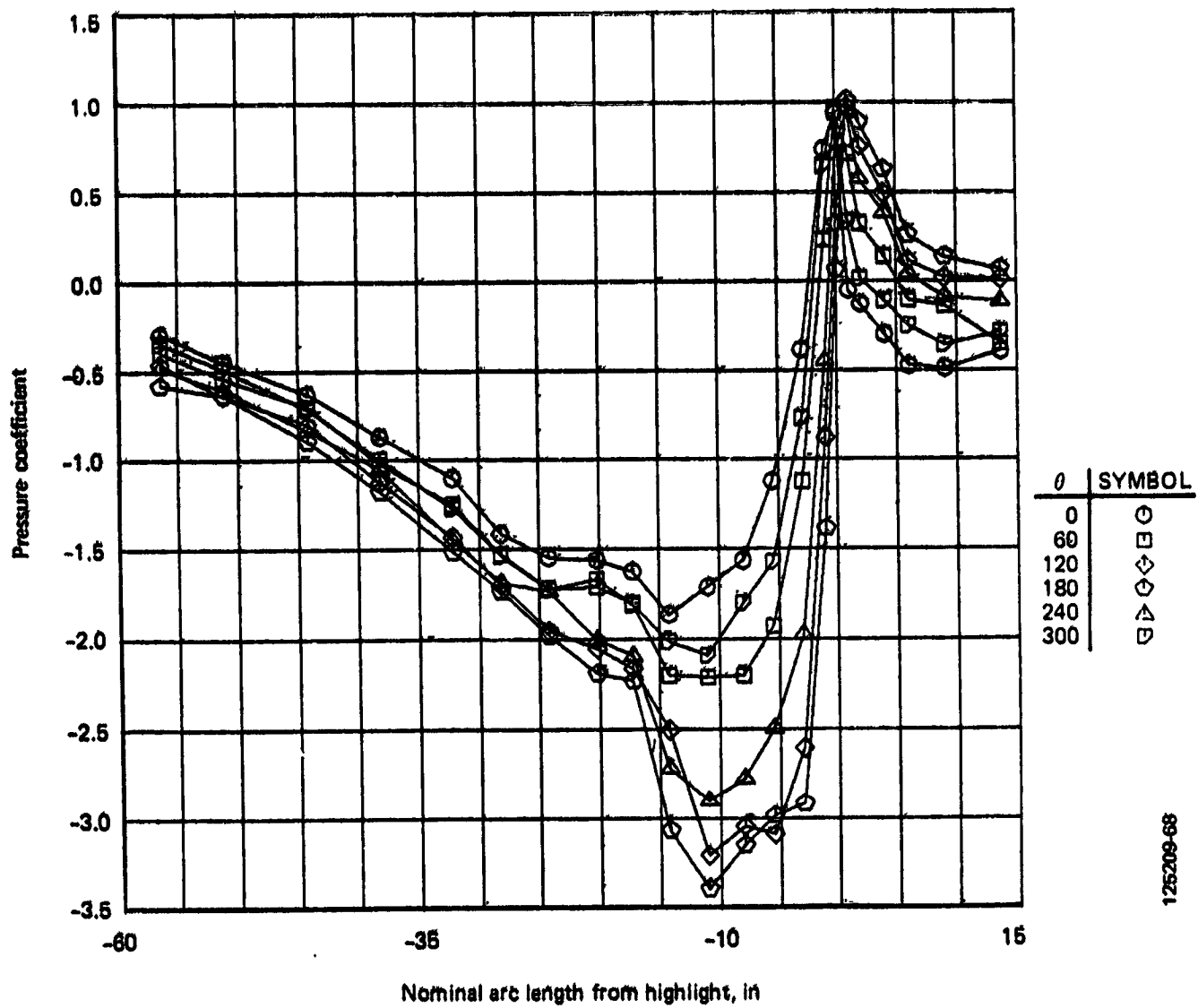


Figure A-10. Engine No. 3 Inlet Pressures, Condition 102, Low Climb

ORIGINAL PAGE IS  
OF POOR QUALITY

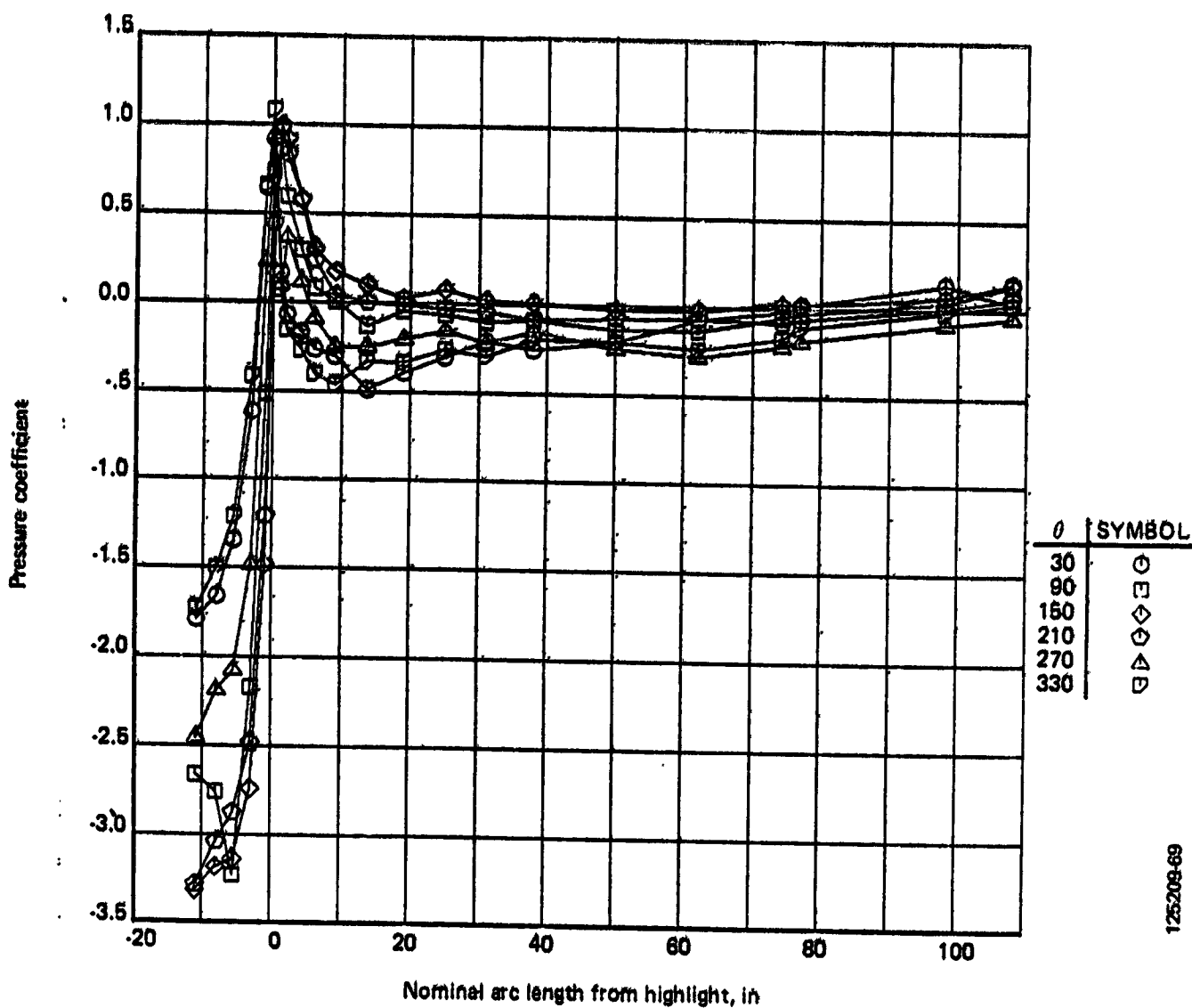


Figure A-11. Engine No. 3 Cowl Pressures, Condition 102, Low Climb

ORIGINAL PAGE IS  
OF POOR QUALITY

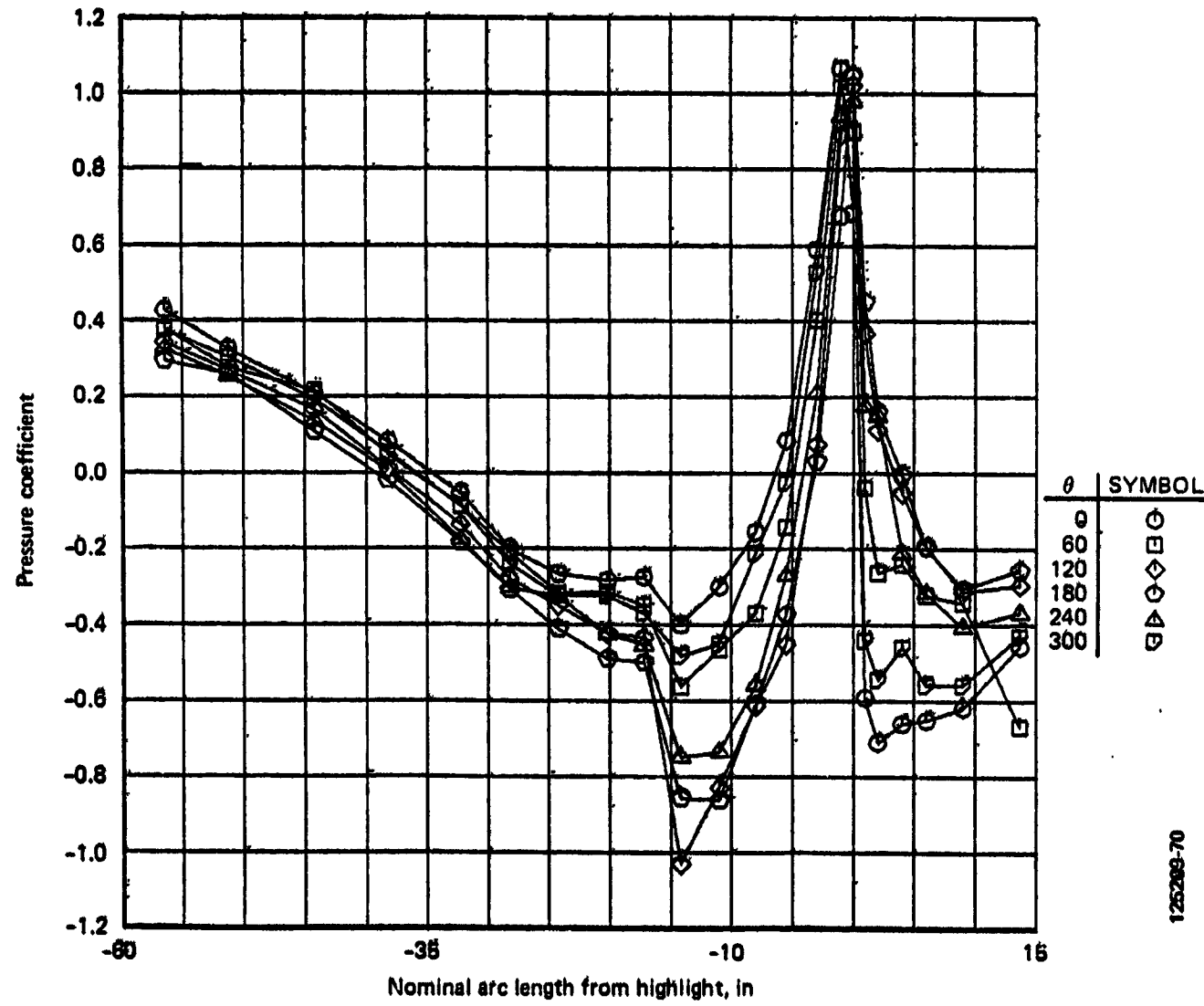


Figure A-12. Engine No. 3 Inlet Pressures, Condition 103, Mid Climb

ORIGINAL PAGE IS  
OF POOR QUALITY

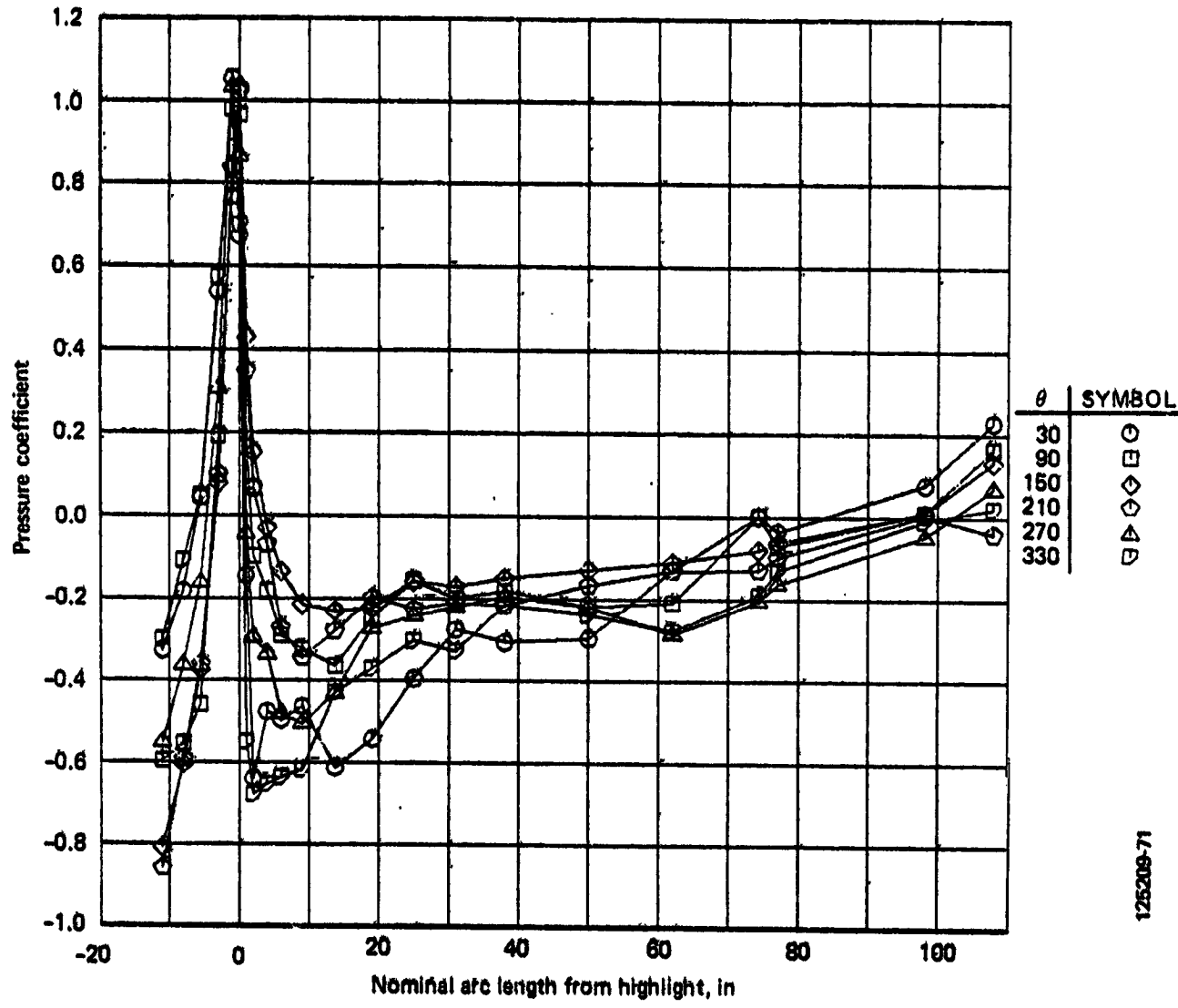


Figure A-13. Engine No. 3 Cowl Pressures, Condition 103, Mid Climb

ORIGINAL PAGE IS  
OF POOR QUALITY

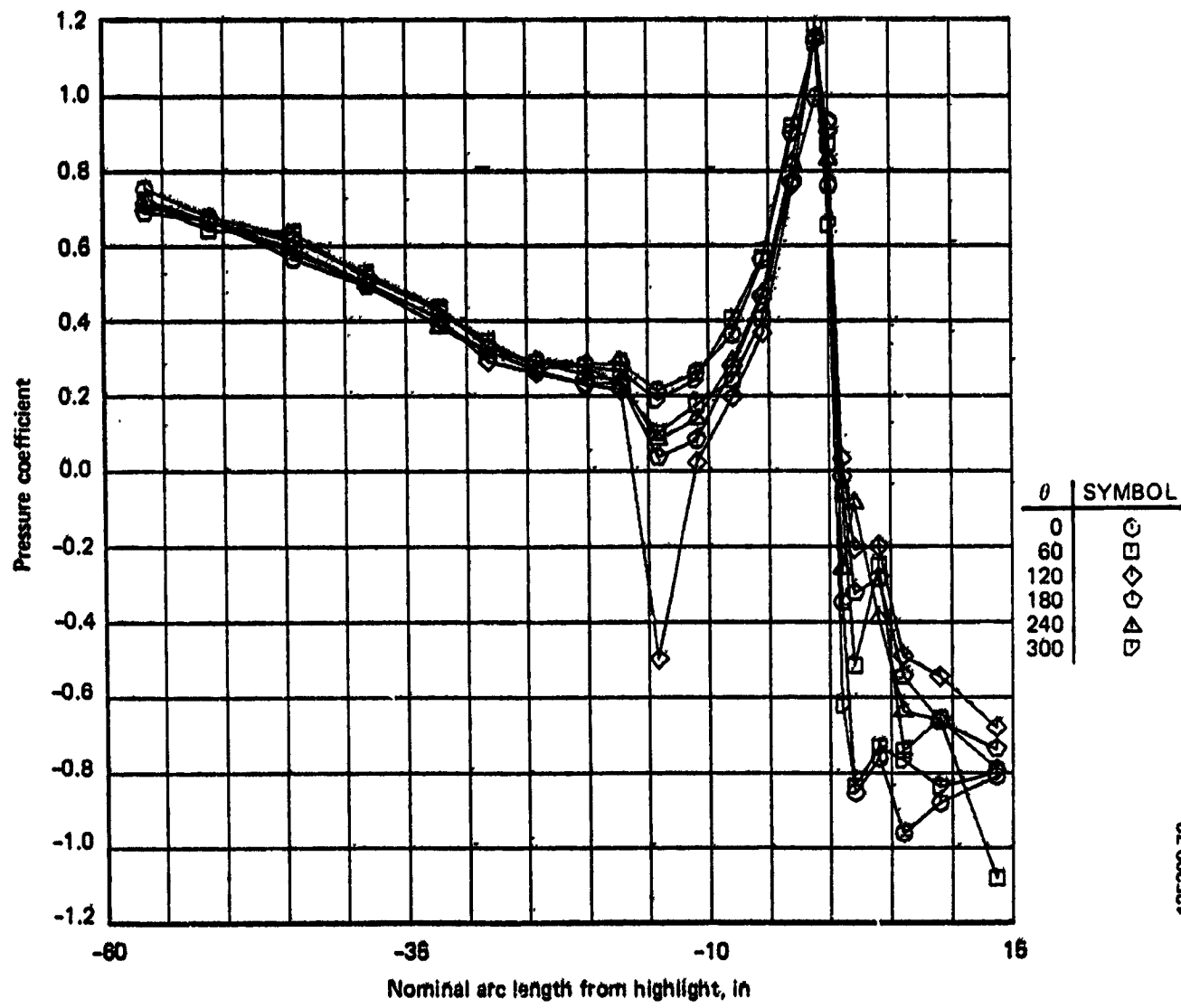


Figure A-14. Engine No. 3 Inlet Pressures, Condition 104, High M Cruise

ORIGINAL PAGE IS  
OF POOR QUALITY

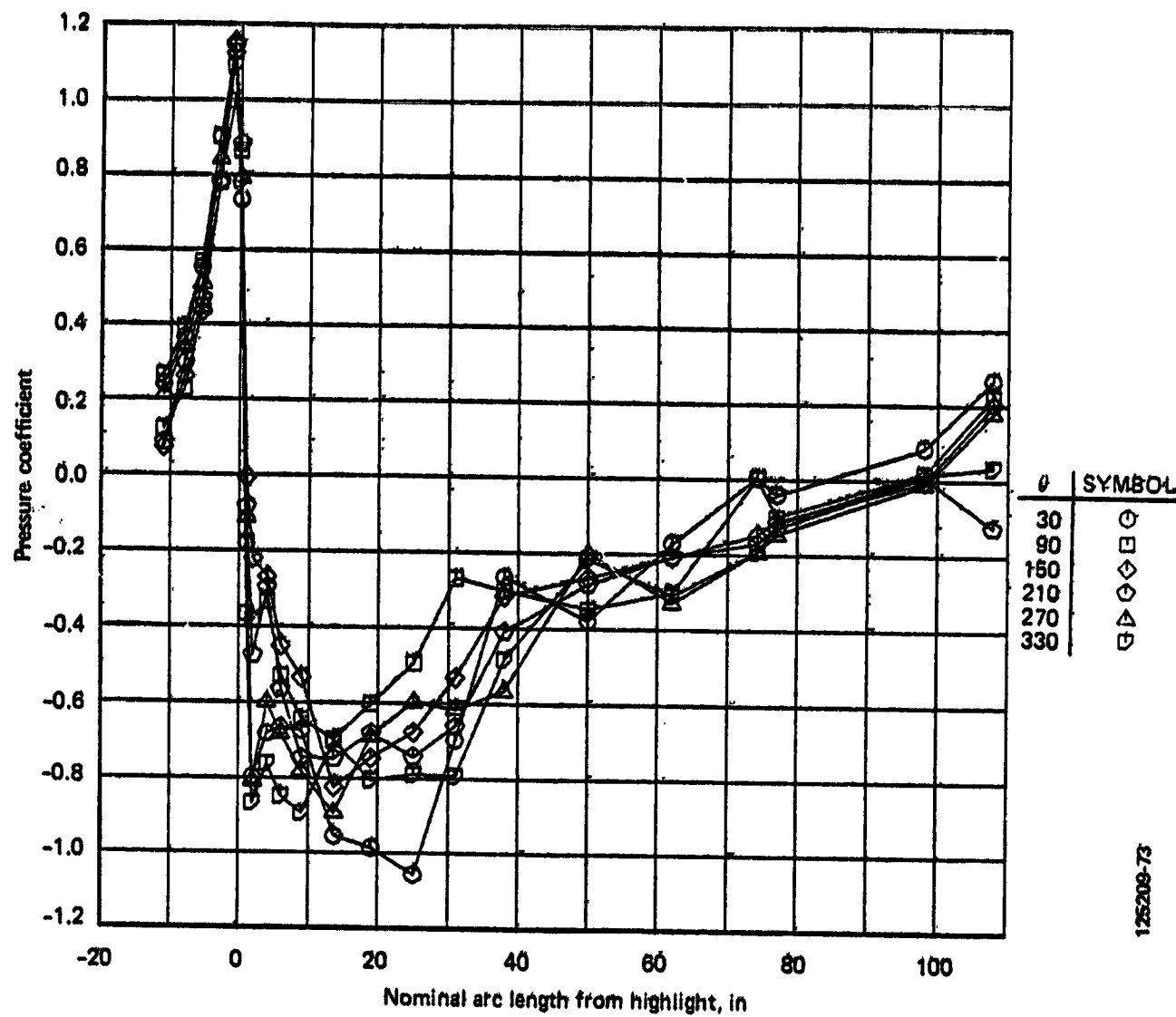


Figure A-15. Engine No. 3 Cowl Pressures, Condition 104, High M Cruise

ORIGINAL PAGE IS  
OF POOR QUALITY

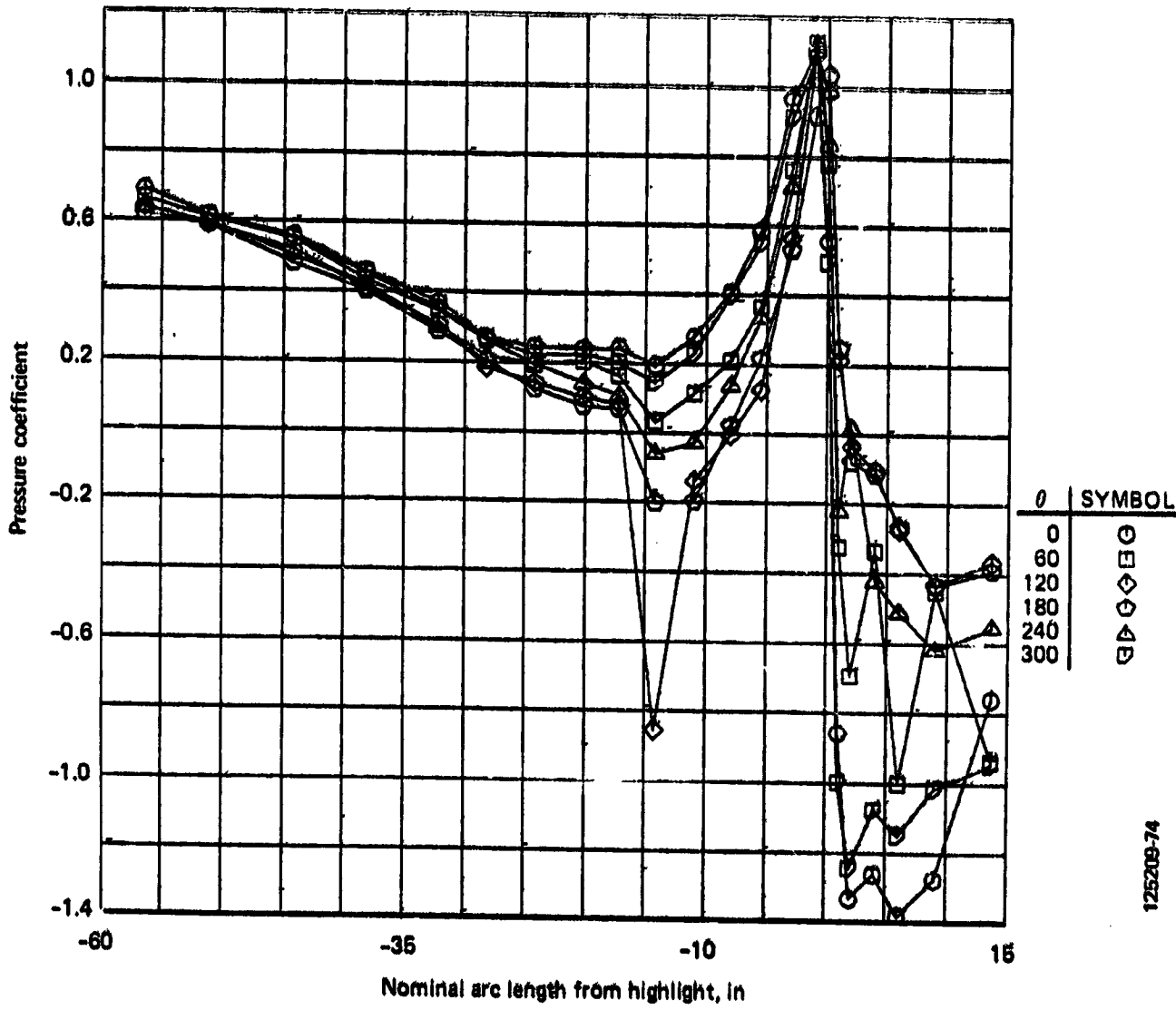


Figure A-16. Engine No. 3 Inlet Pressures, Condition 105, Low M Cruise

ORIGINAL PAGE IS  
OF POOR QUALITY

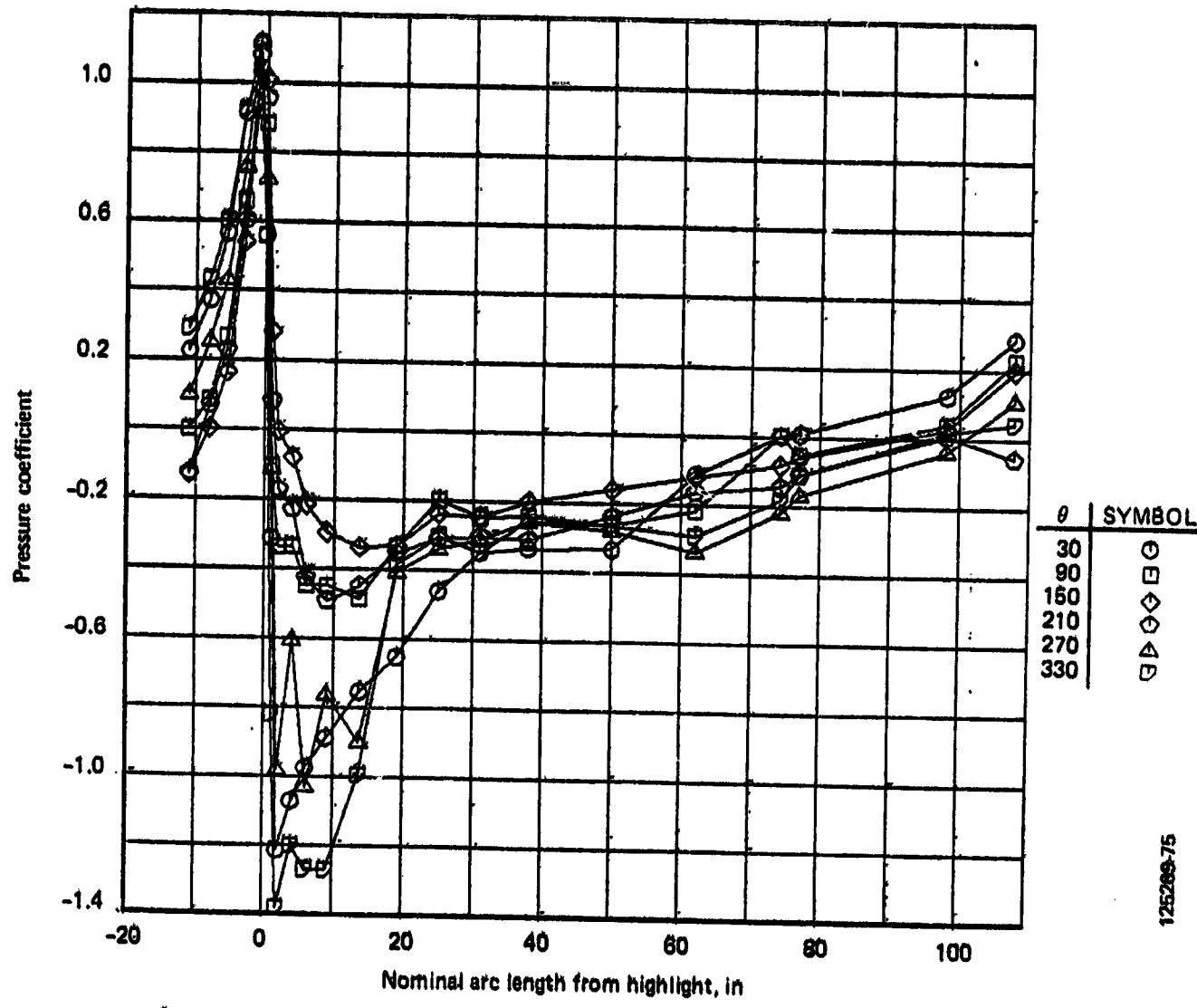


Figure A-17. Engine No. 3 Cowl Pressures, Condition 105, Low M Cruise

ORIGINAL PAGE IS  
OF POOR QUALITY

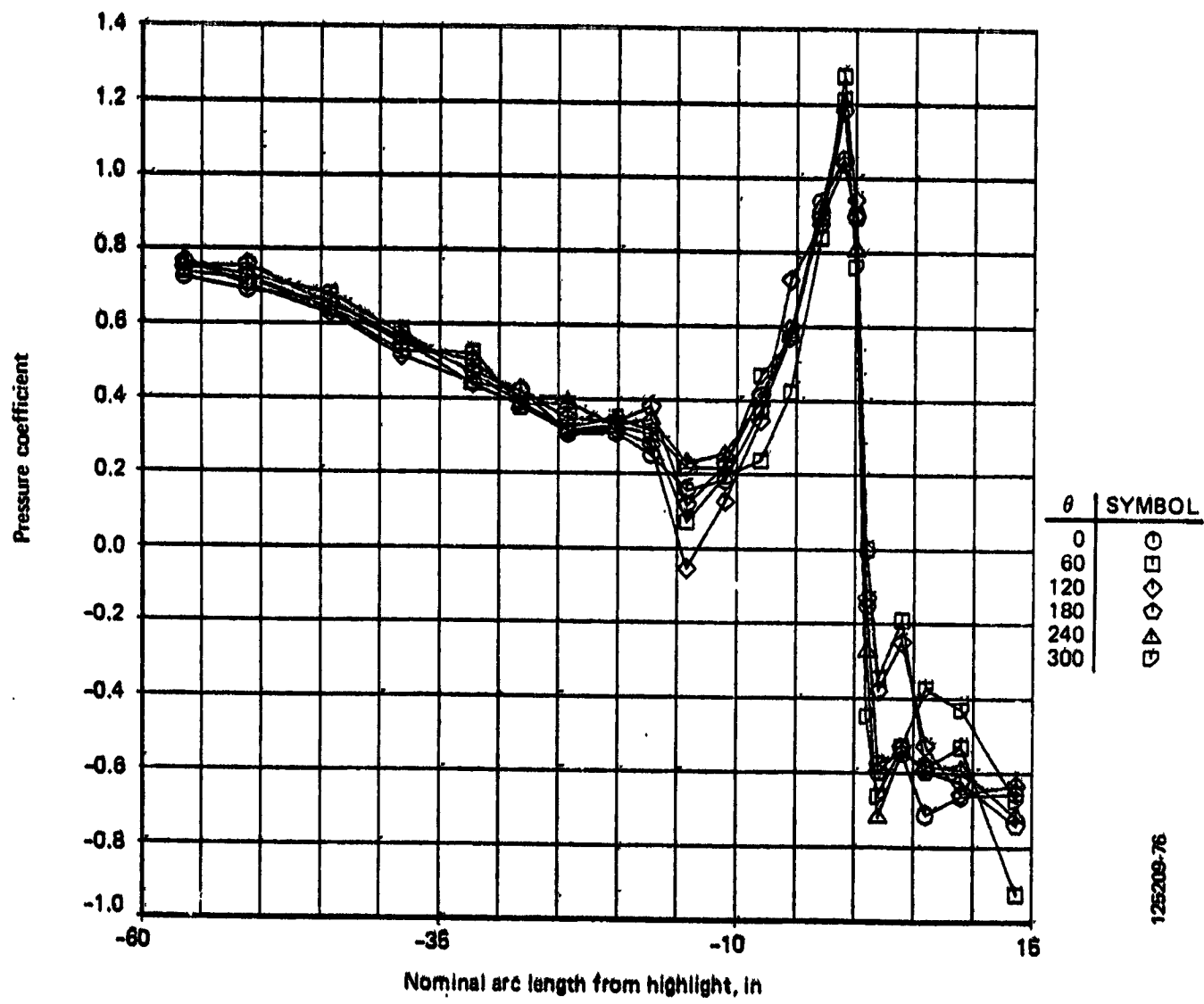


Figure A-18. Engine No. 3 Inlet Pressures, Condition 106, Maximum M

ORIGINAL PAGE IS  
OF POOR QUALITY

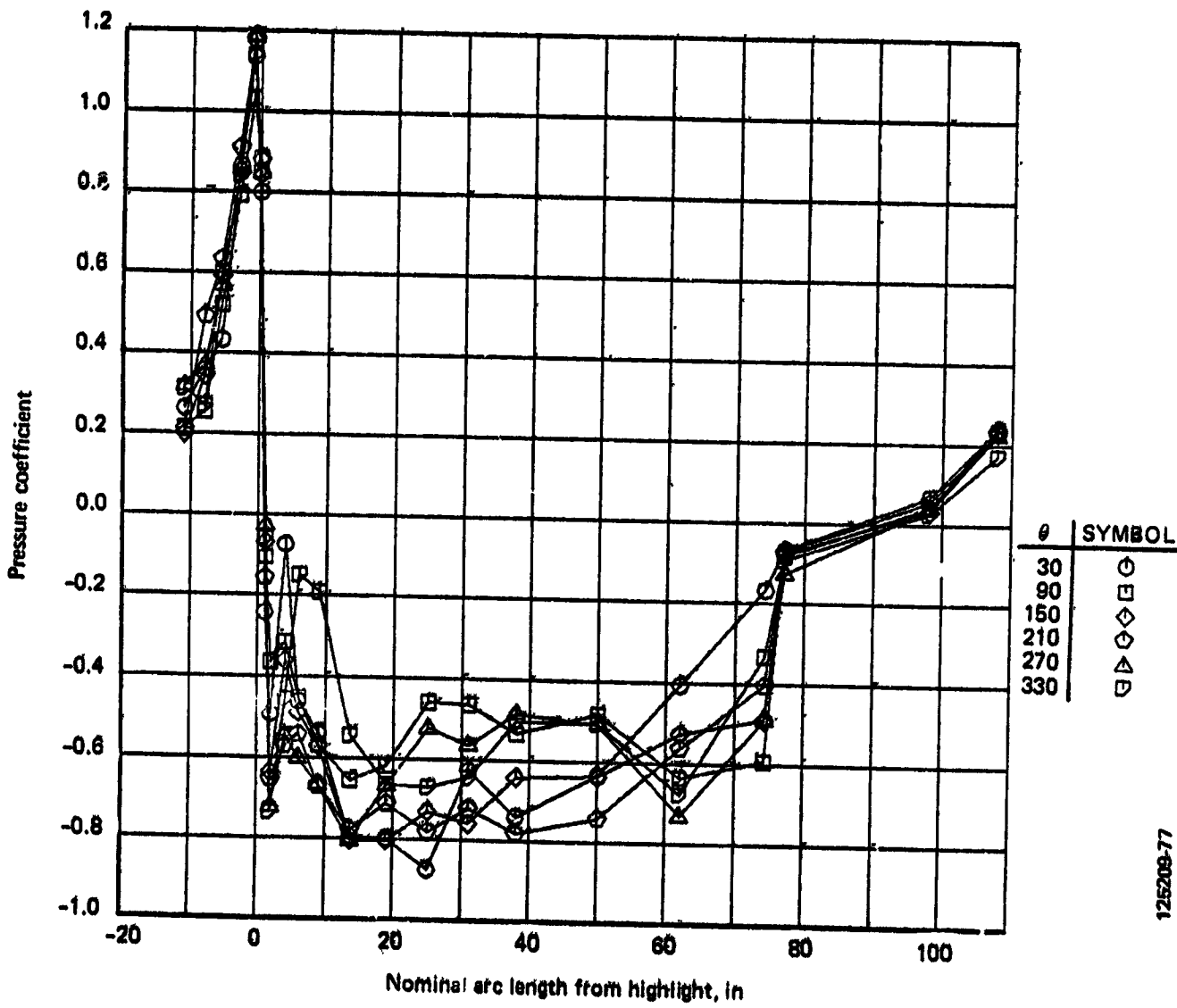


Figure A-19. Engine No. 3 Cowl Pressures, Condition 106, Maximum M

ORIGINAL PAGE IS  
OF POOR QUALITY

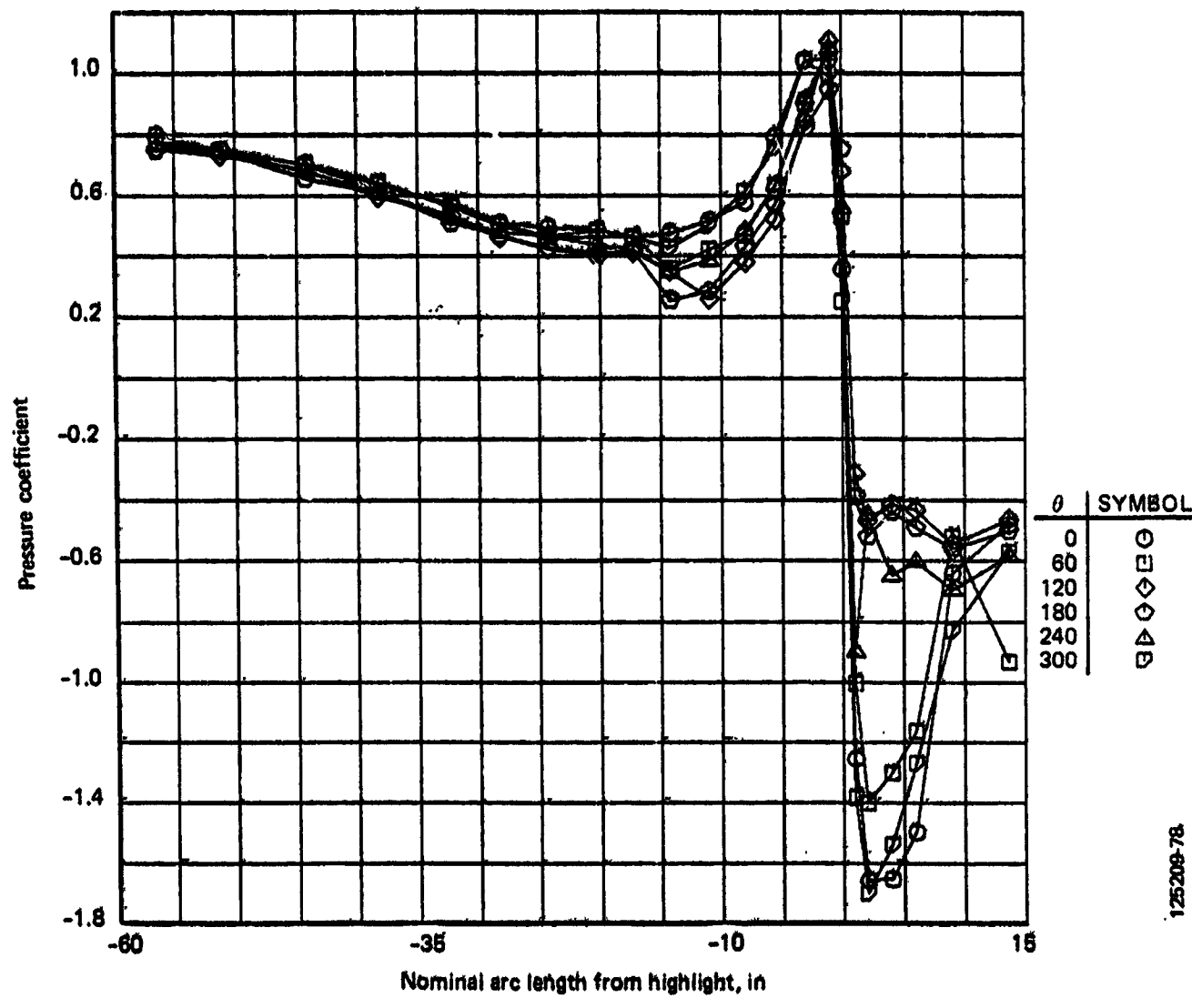


Figure A-20. Engine No. 3 Inlet Pressures, Condition 107, Inflight Relight



ORIGINAL PAGE IS  
OF POOR QUALITY

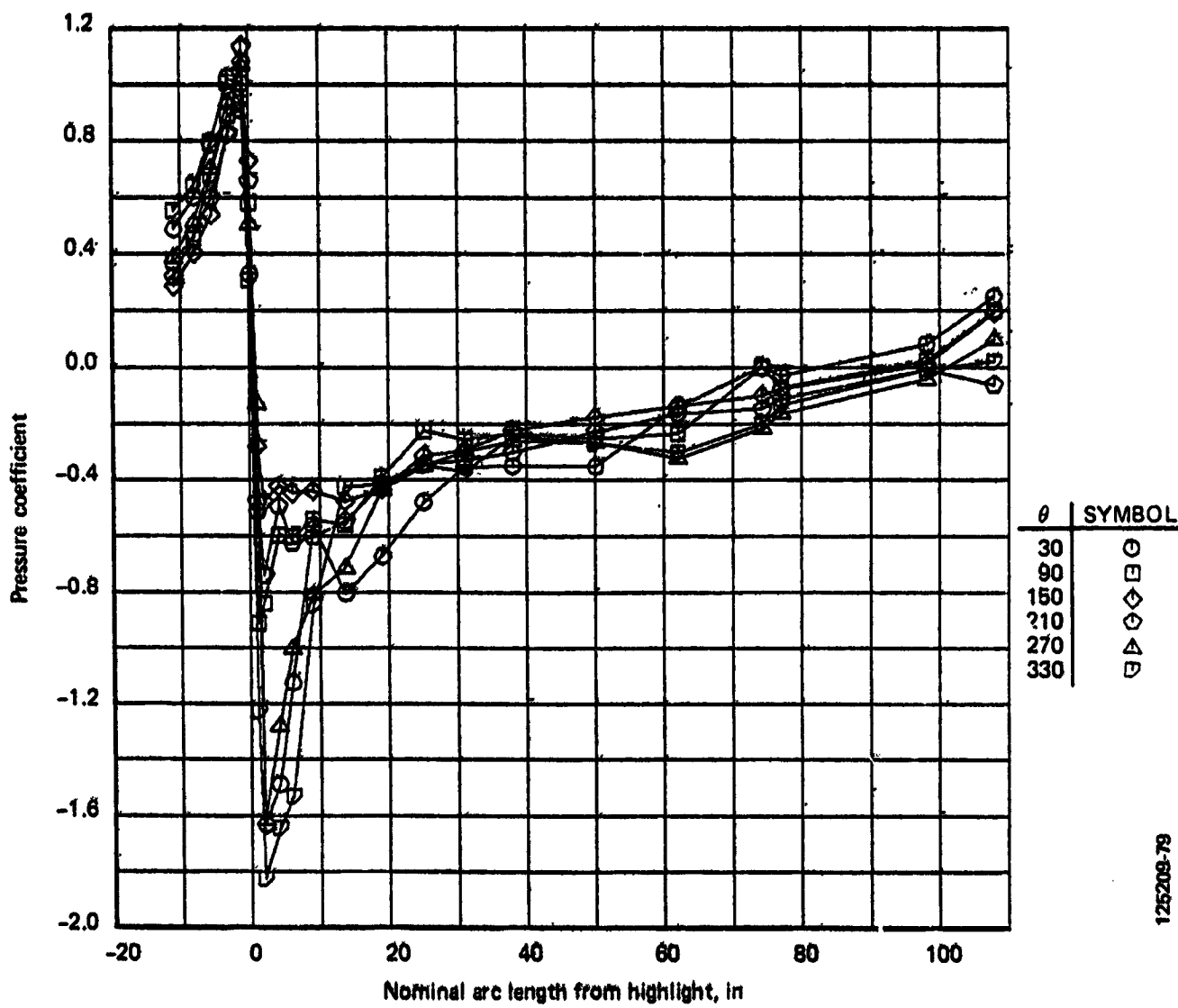


Figure A-21. Engine No. 3 Cowl Pressures, Condition 107, Inflight Relight

ORIGINAL PAGE IS  
OF POOR QUALITY

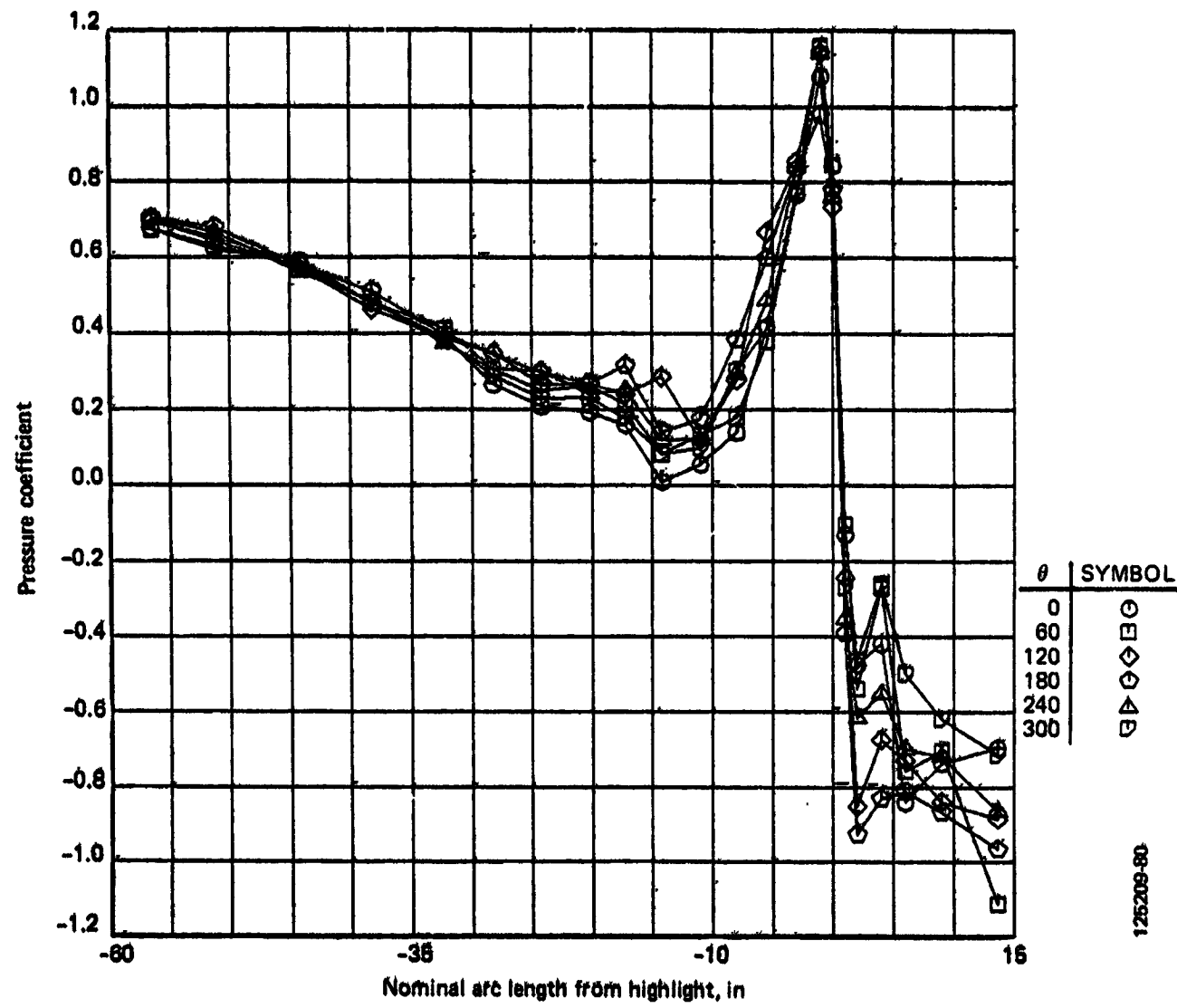


Figure A-22. Engine No. 3 Inlet Pressures, Condition 108, Maximum  $q$

ORIGINAL PAGE IS  
OF POOR QUALITY

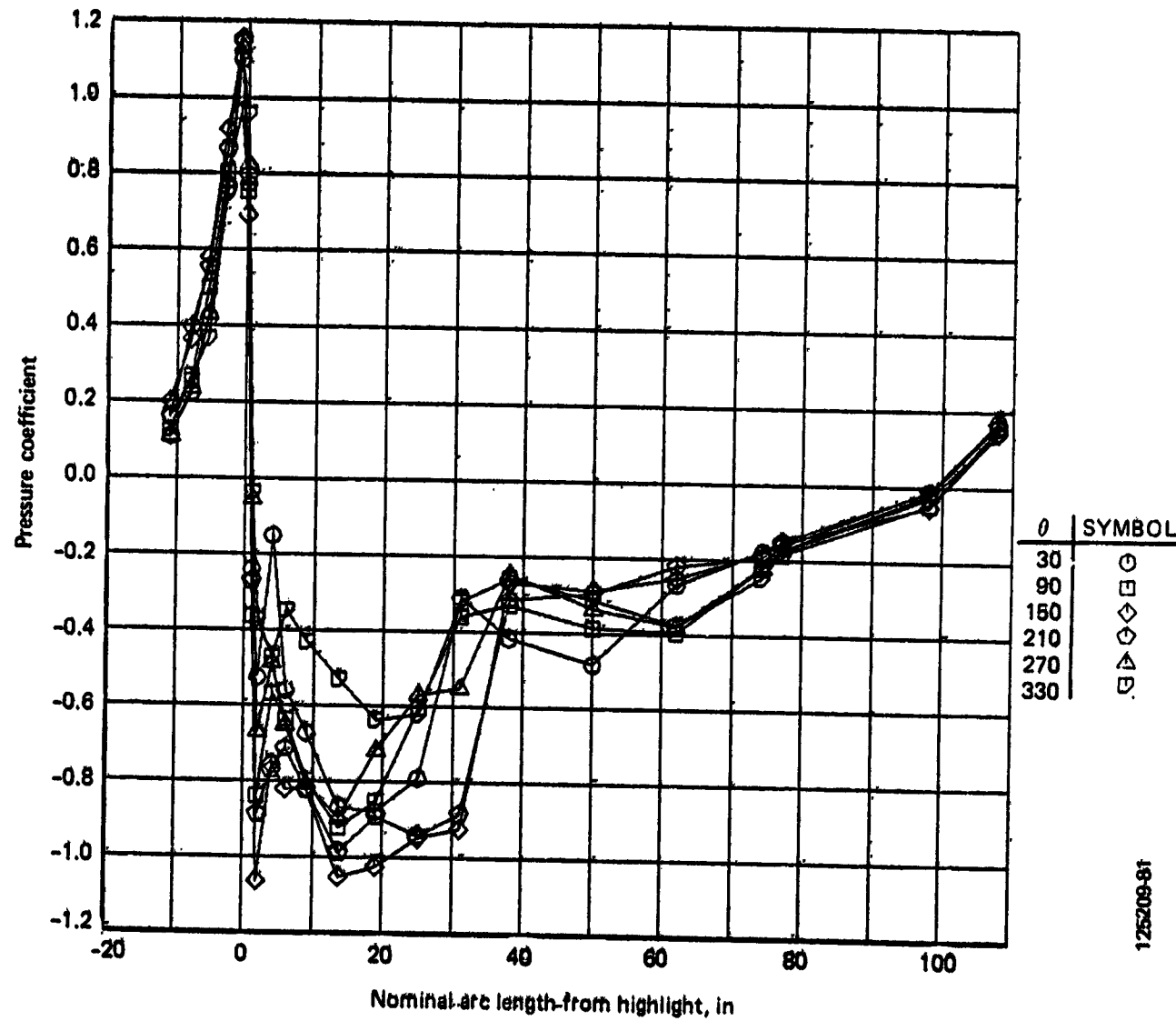


Figure A-23: Engine No. 3 Cowl Pressures, Condition 108, Maximum  $q$

ORIGINAL PAGE IS  
OF POOR QUALITY

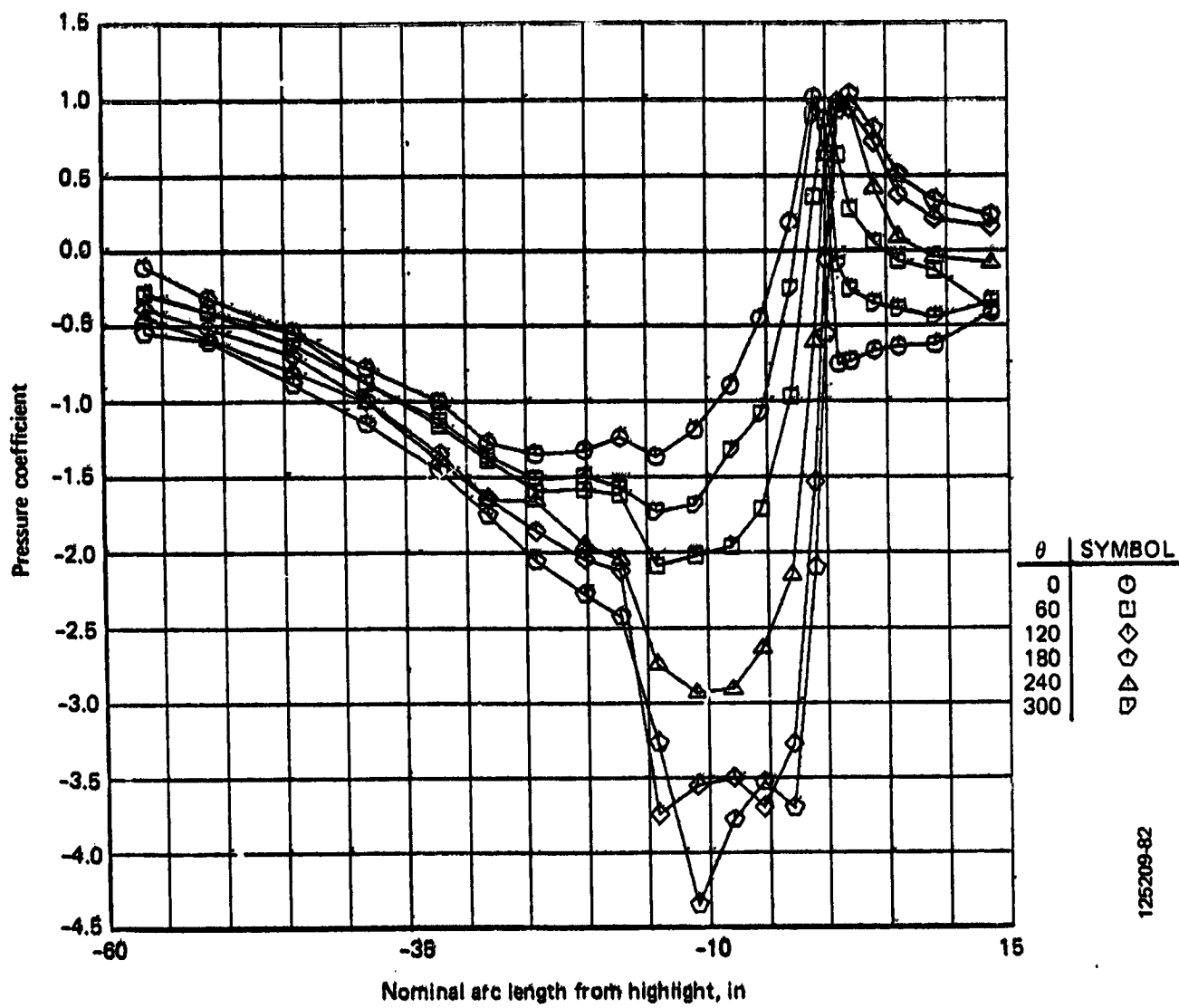


Figure A-24. Engine No. 3 Inlet Pressures, Condition 109, Stall Warning (Flaps Up)

ORIGINAL PAGE IS  
OF POOR QUALITY

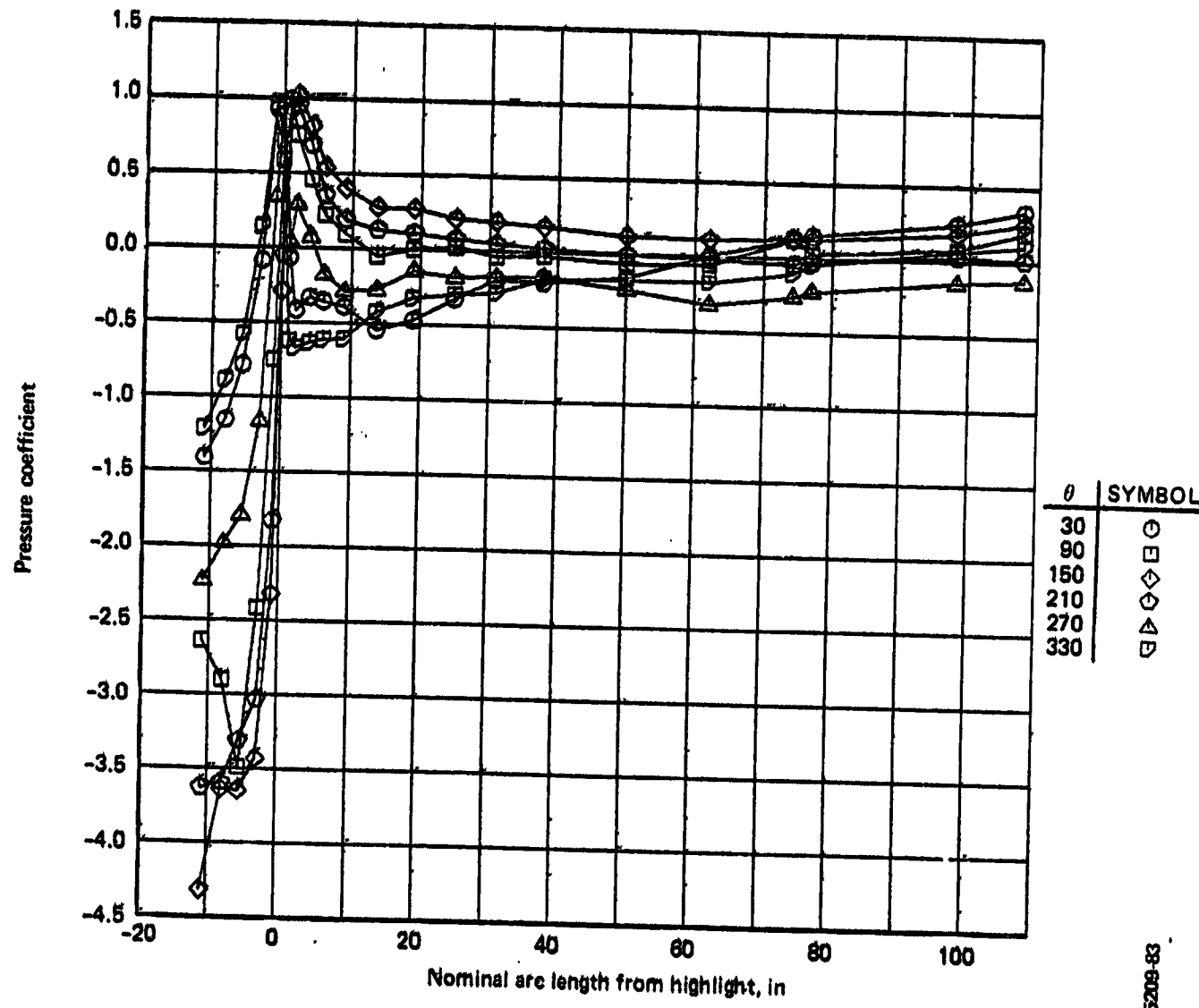


Figure A-25. Engine No. 3 Cowl Pressures, Condition 109, Stall Warning (Flaps Up)

ORIGINAL WORK  
OF POOR QUALITY

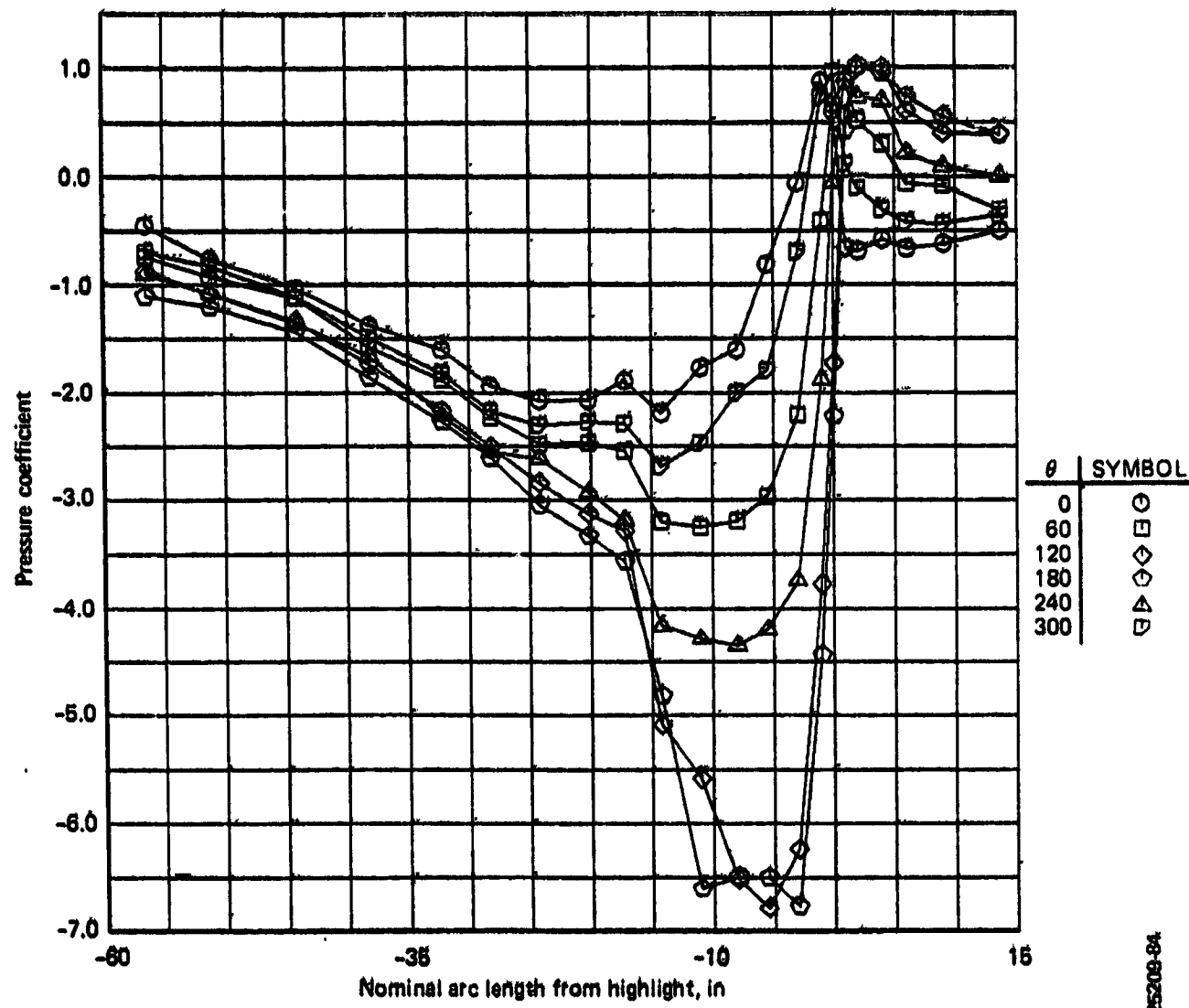


Figure A-26. Engine No. 3 Inlet Pressures, Condition 110, Stall Warning (Flaps 10)

ORIGINAL PAGE IS  
OF POOR QUALITY

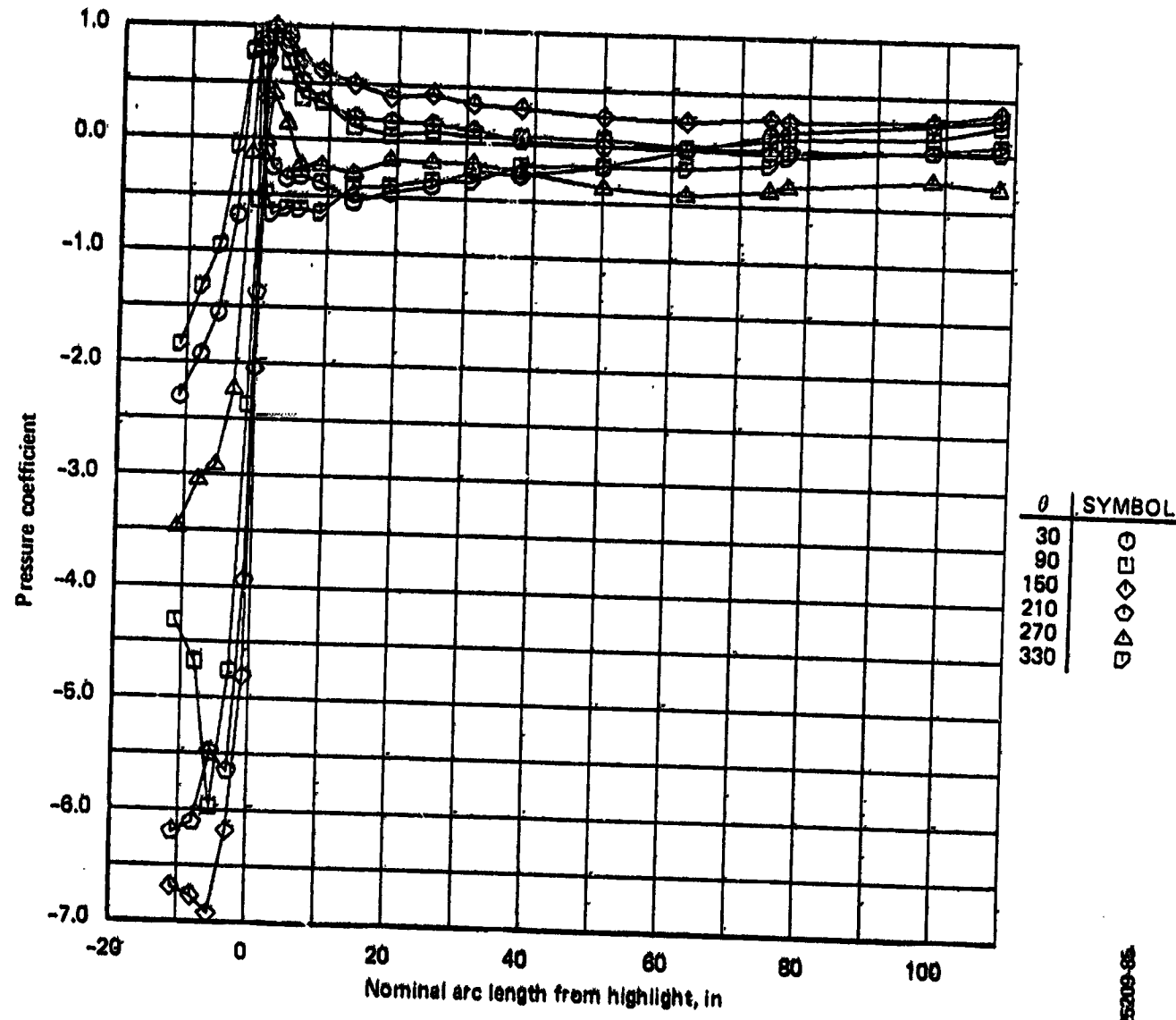


Figure A-27. Engine No. 3 Cowl Pressures, Condition 110, Stall Warning (Flaps 10)

ORIGINAL PAGE IS  
OF POOR QUALITY

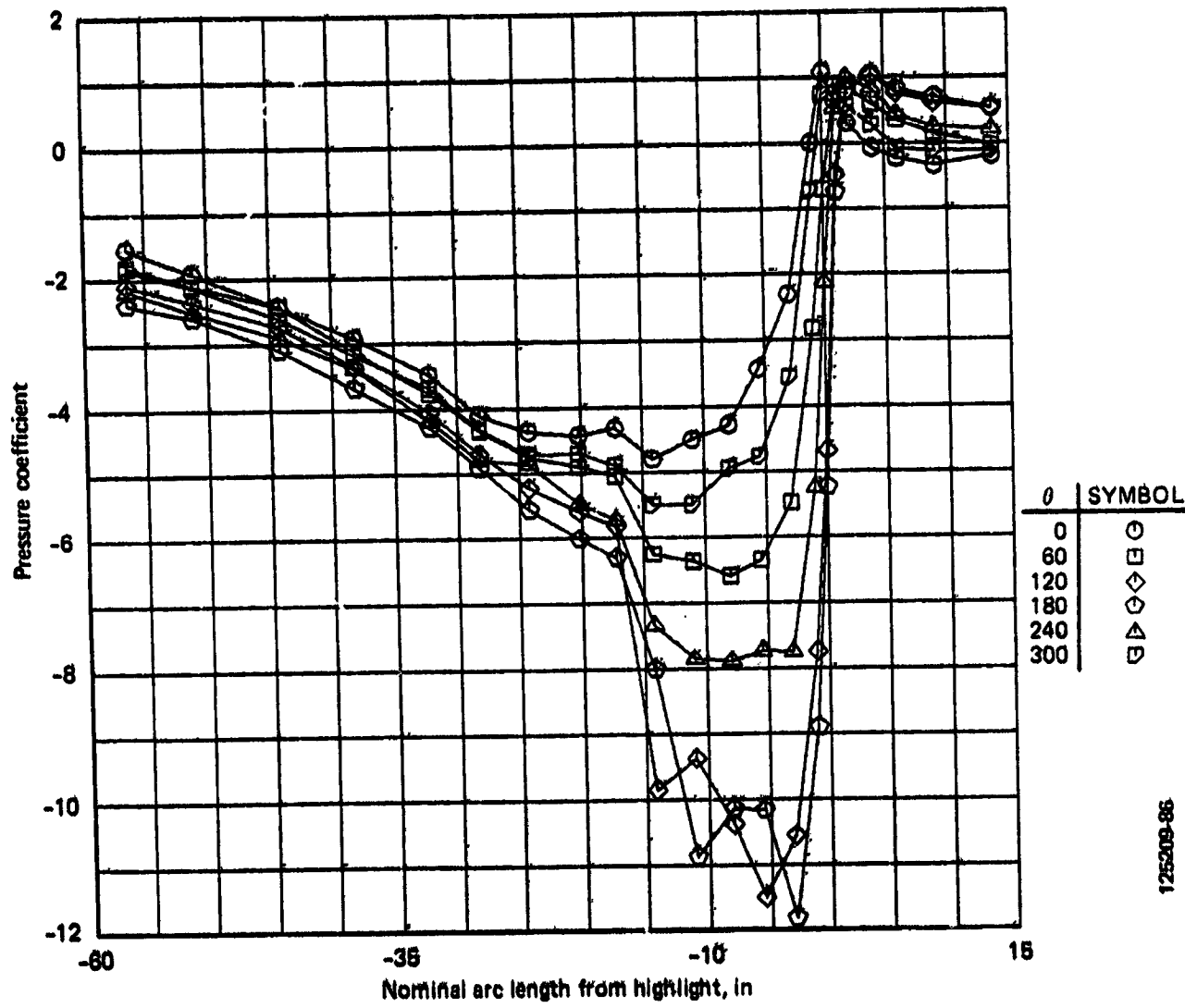


Figure A-28. Engine No. 3 Inlet Pressures, Condition 111, Stall Warning (Flaps 30)

ORIGINAL PAGE IS  
OF POOR QUALITY

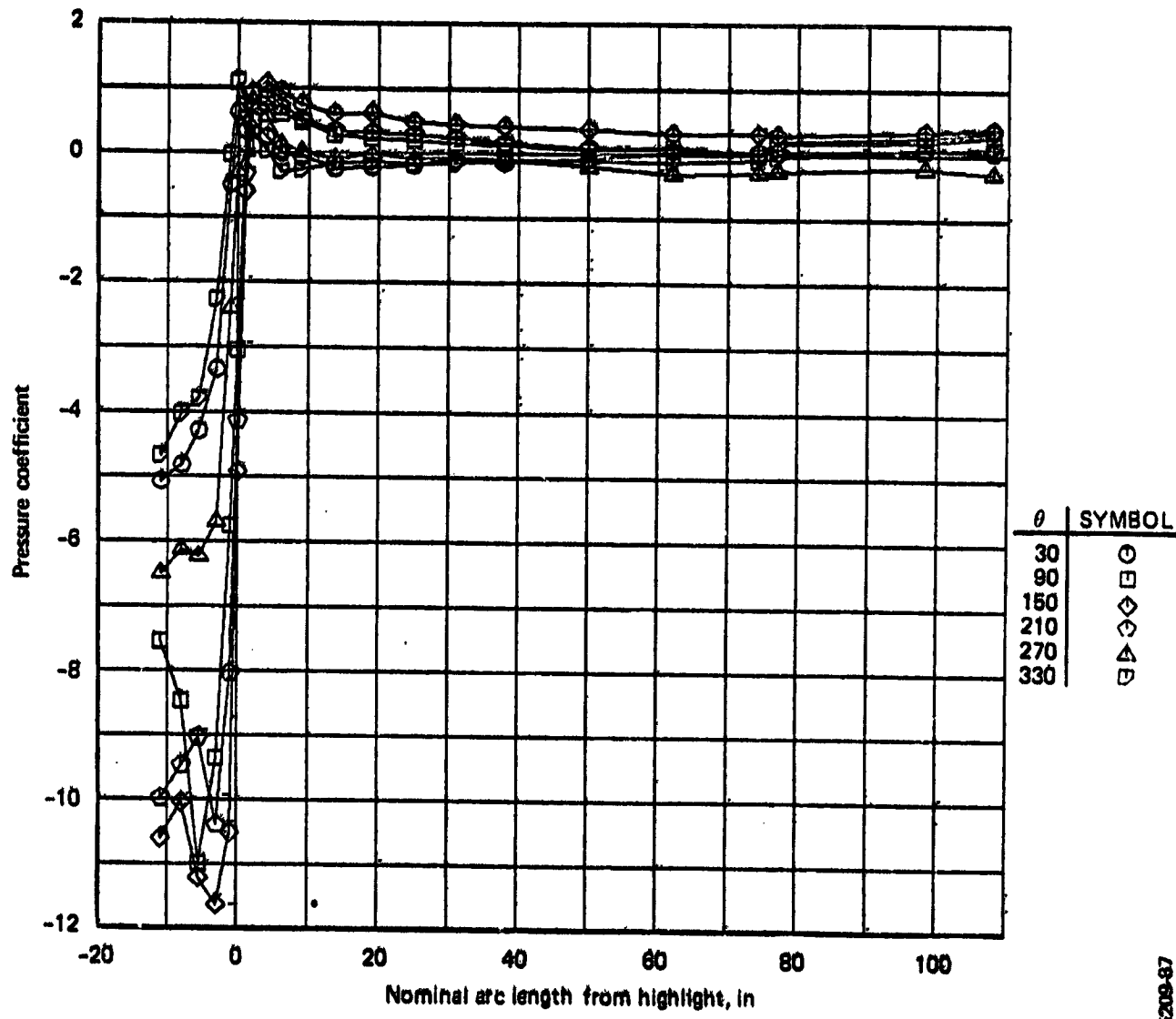


Figure A-29. Engine No. 3 Cowl Pressures, Condition 111, Stall Warning (Flaps 30)

125209-87

ORIGINAL PAGE IS  
OF POOR QUALITY

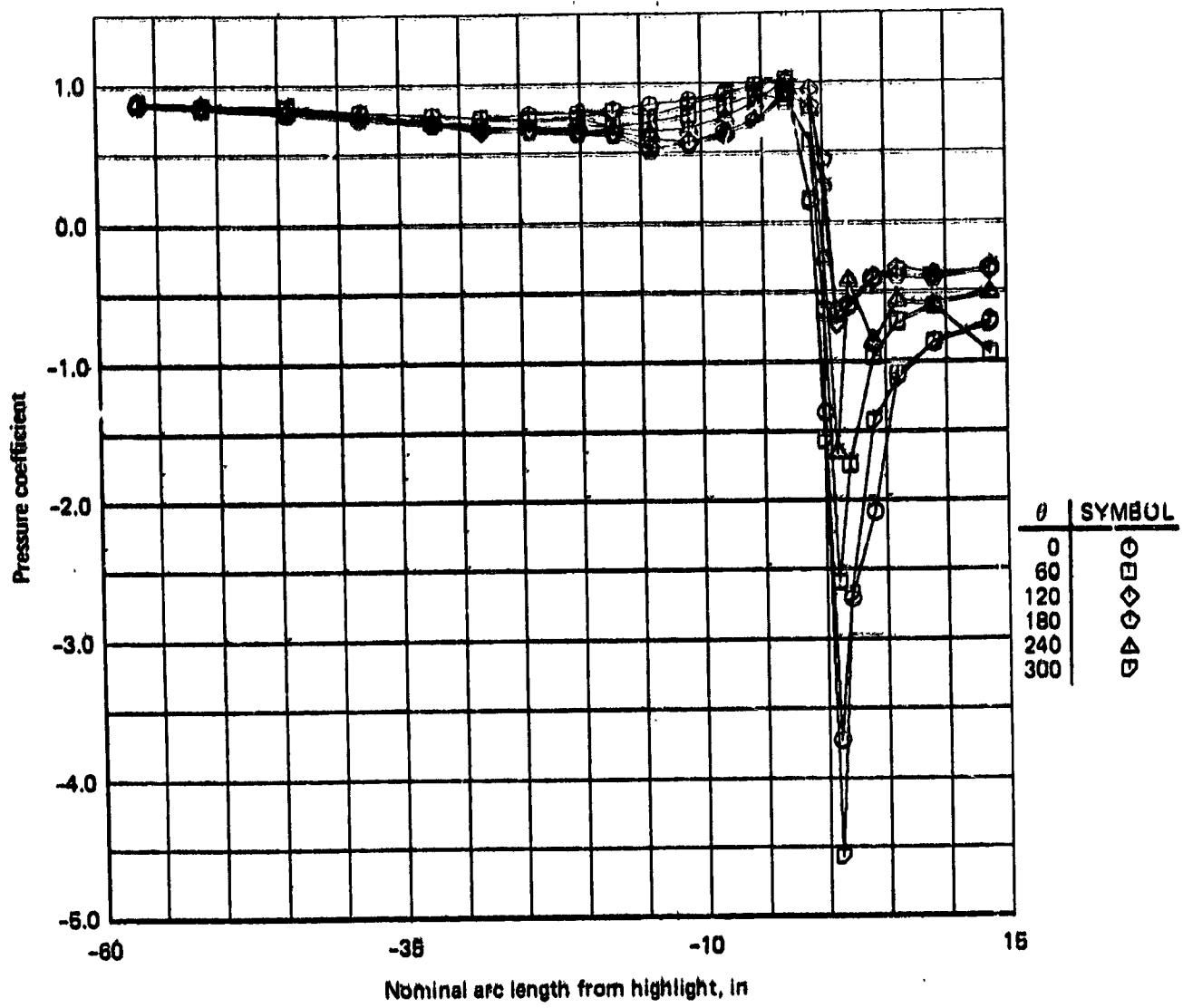


Figure A-30. Engine No. 3 Inlet Pressures, Condition 112, Idle Descent

ORIGINAL PAGE IS  
OF POOR QUALITY

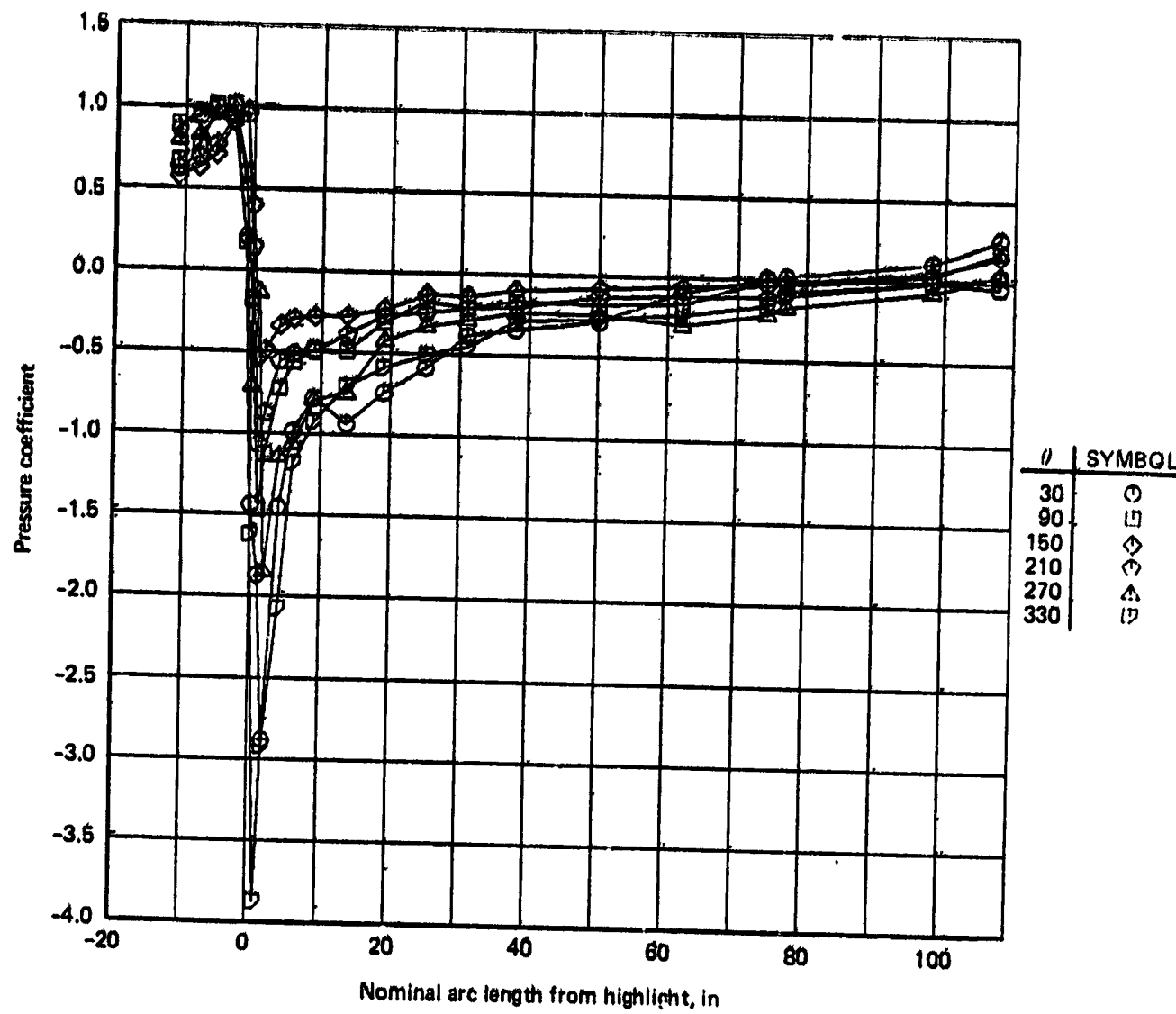


Figure A-31. Engine No. 3 Cowl Pressures, Condition 112, Idle Descent

125299-89

ORIGINAL PAGE IS  
OF POOR QUALITY

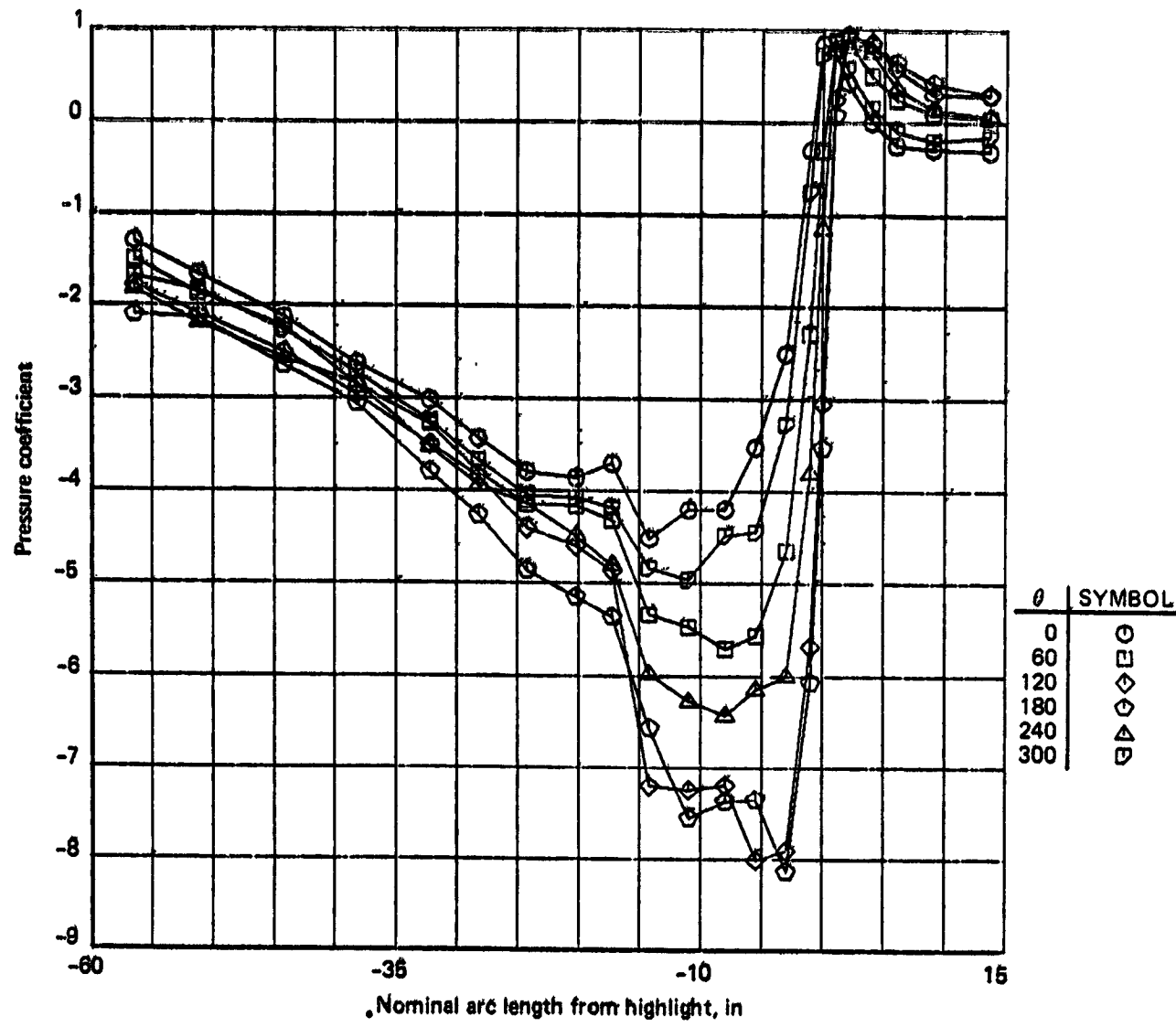


Figure A-32. Engine No. 3 Inlet Pressures, Condition 113, Approach

ORIGINAL PAGE IS  
OF POOR QUALITY

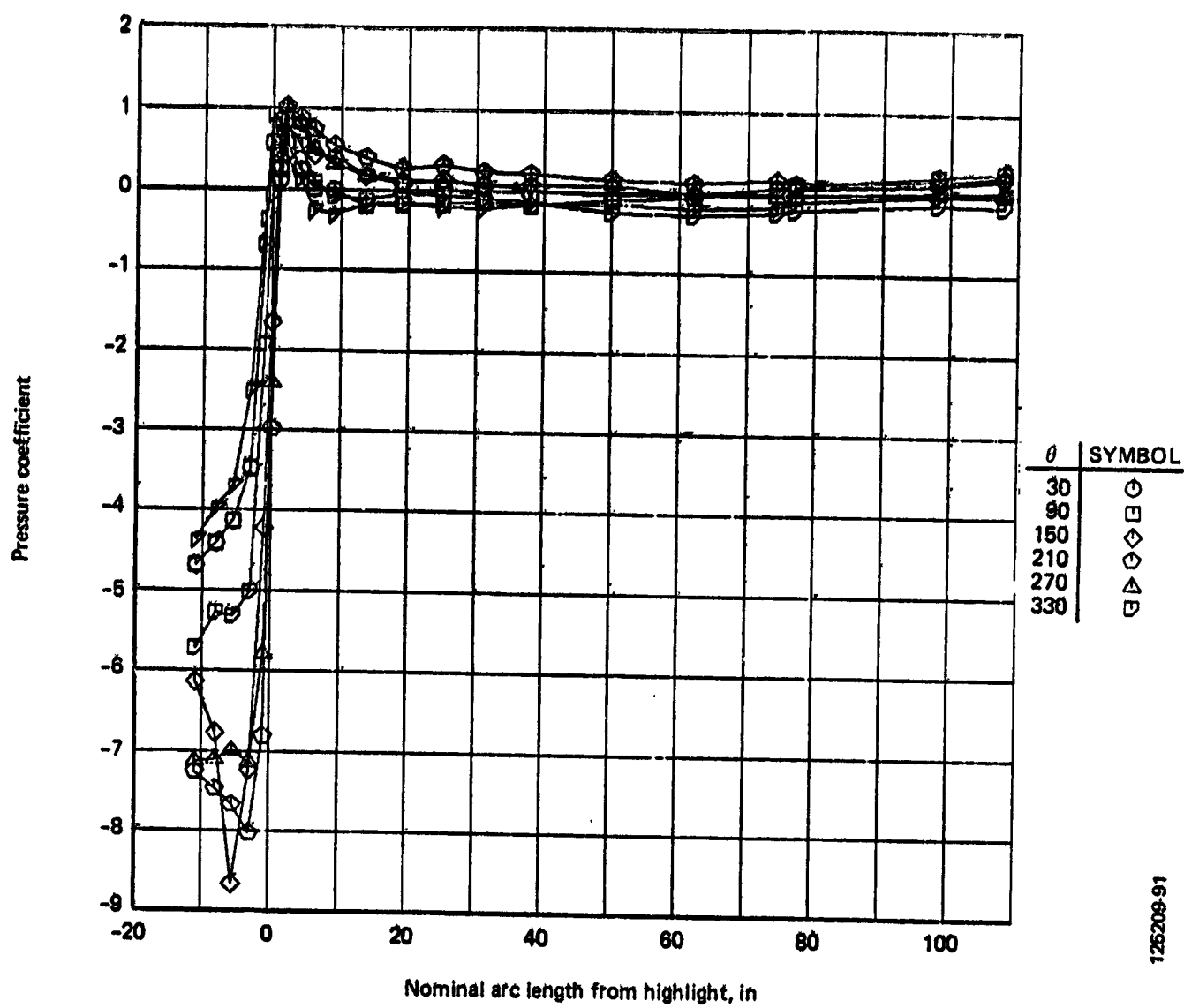


Figure A-33. Engine No. 3 Cowl Pressures, Condition 113, Approach

125209-91

ORIGINAL PAGE IS  
OF POOR QUALITY

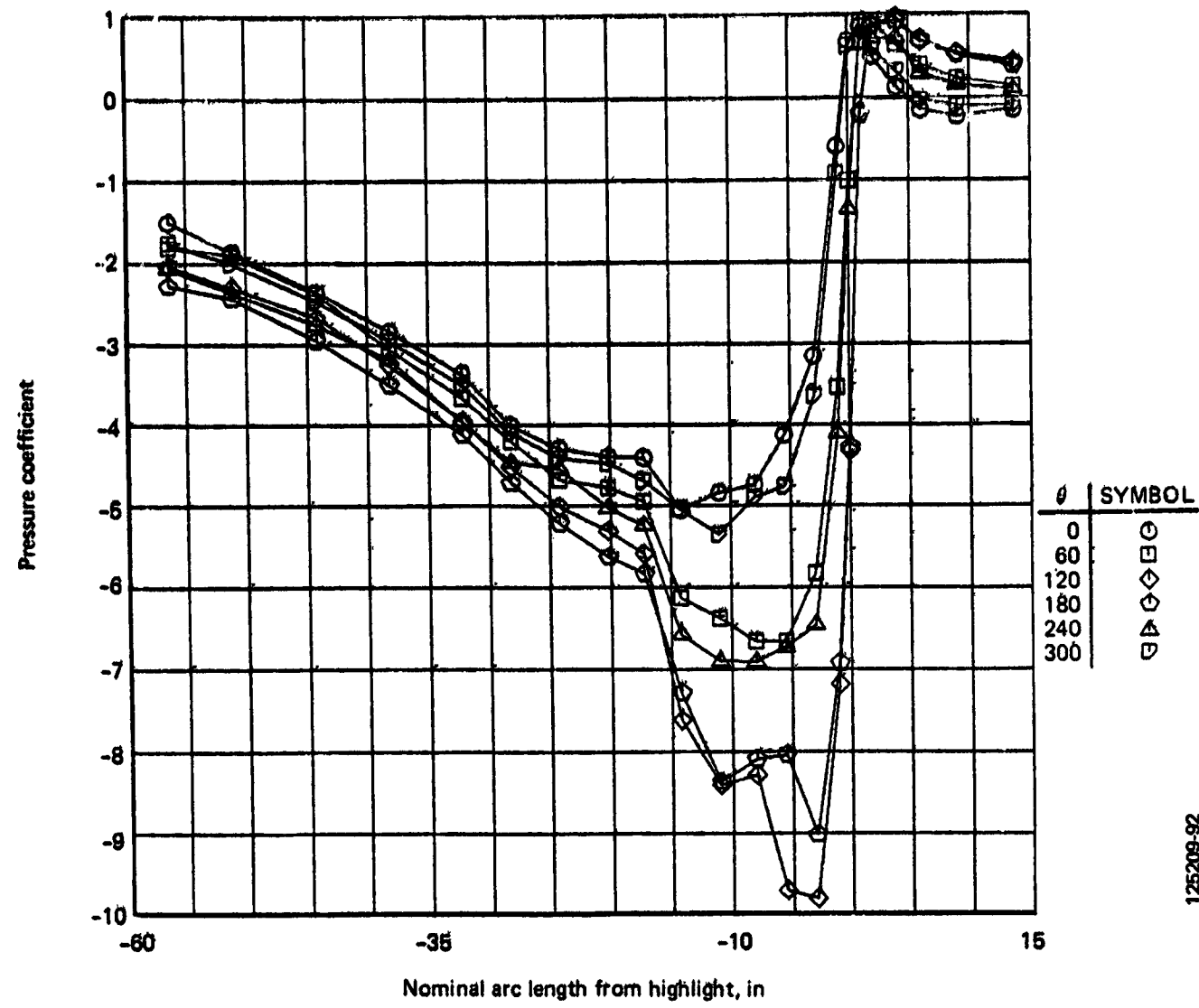


Figure A-34. Engine No. 3 Inlet Pressures, Condition 114, Touch and Go

ORIGINAL PAGE IS  
OF POOR QUALITY

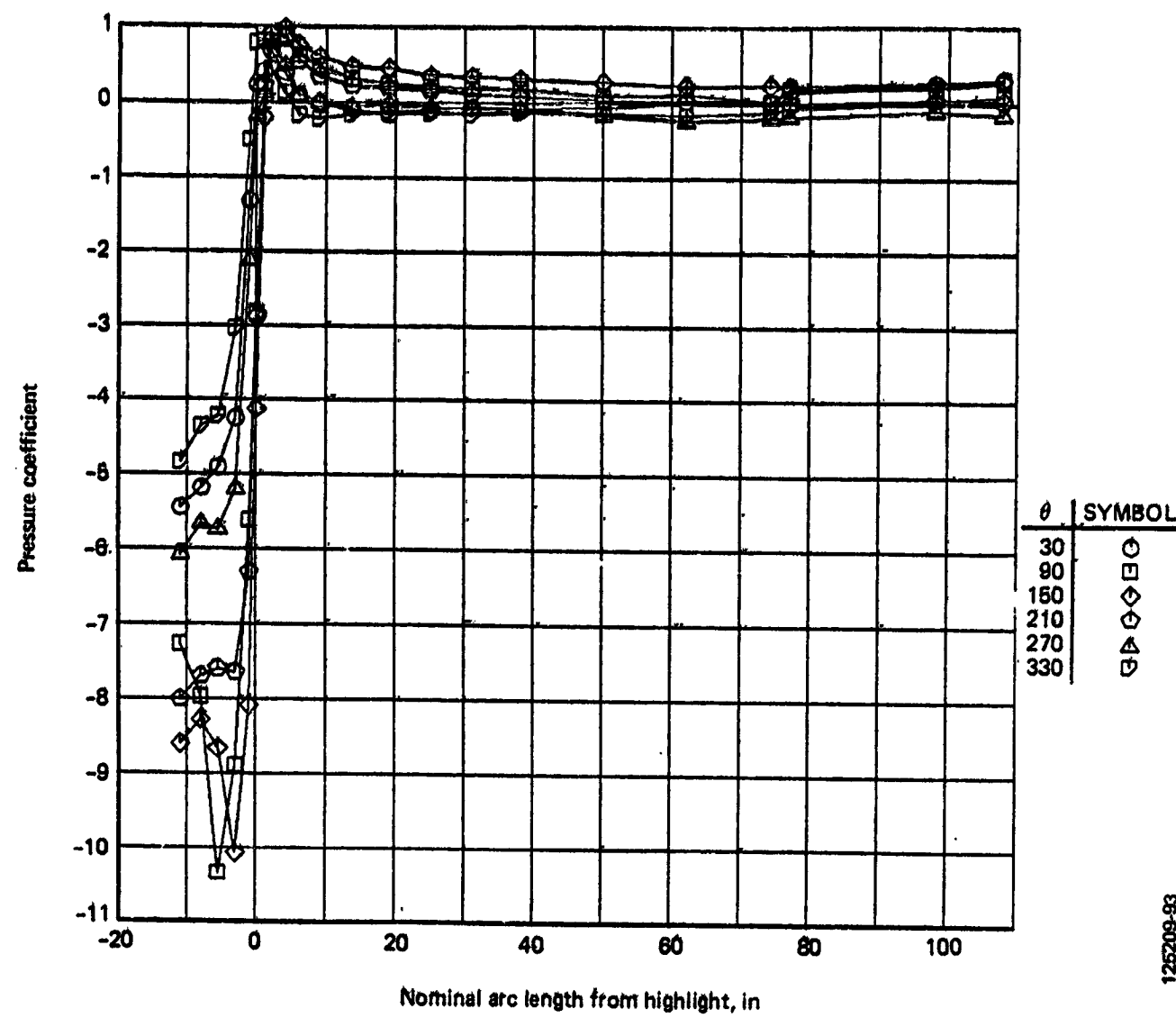


Figure A-35. Engine No. 3 Cowl Pressures, Condition 114, Touch and Go

ORIGINAL PAGE IS  
OF POOR QUALITY

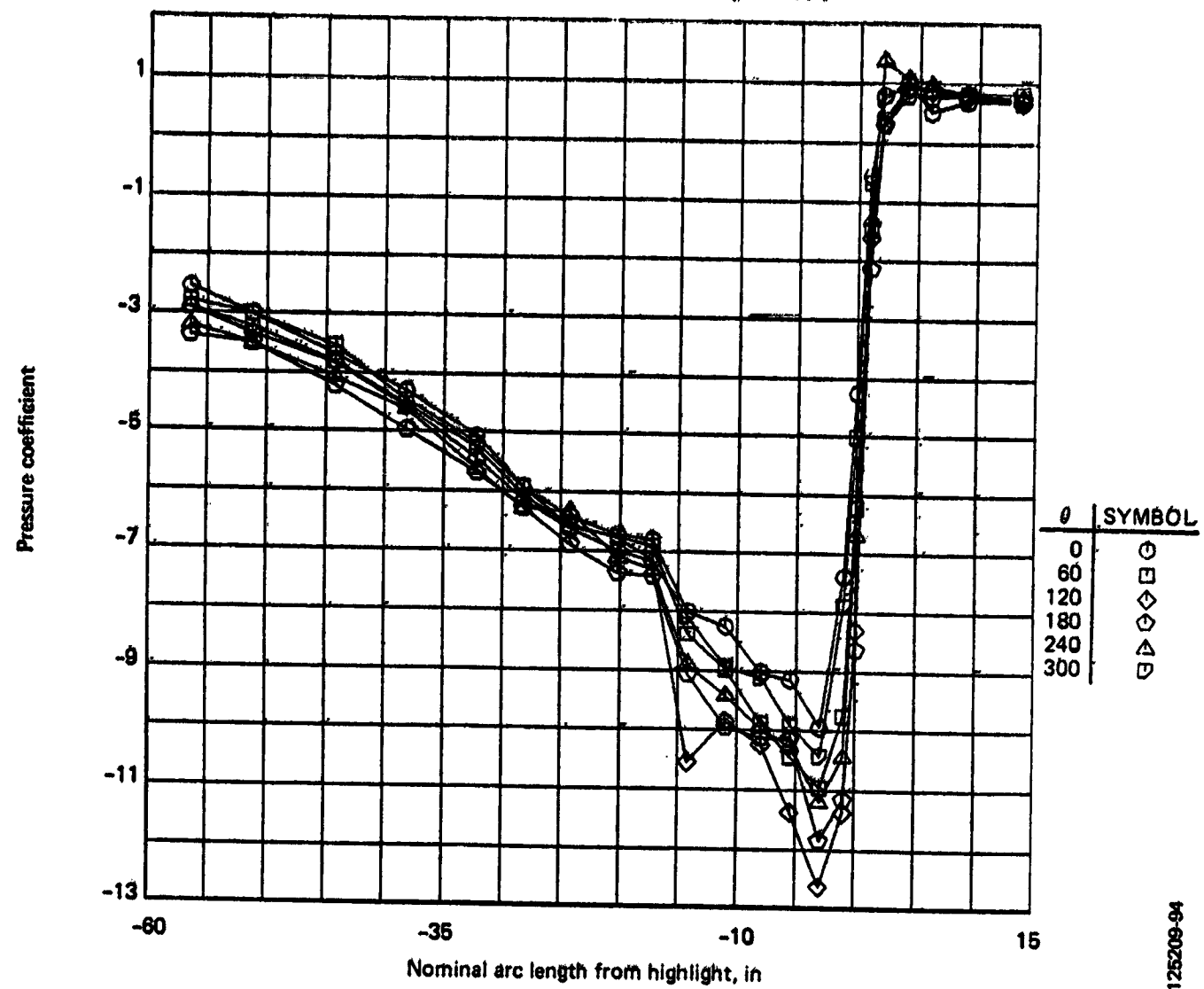


Figure A-36. Engine No. 3 Inlet Pressures, Condition 115, Thrust Reverse

125209-94

ORIGINAL PAGE IS  
OF POOR QUALITY

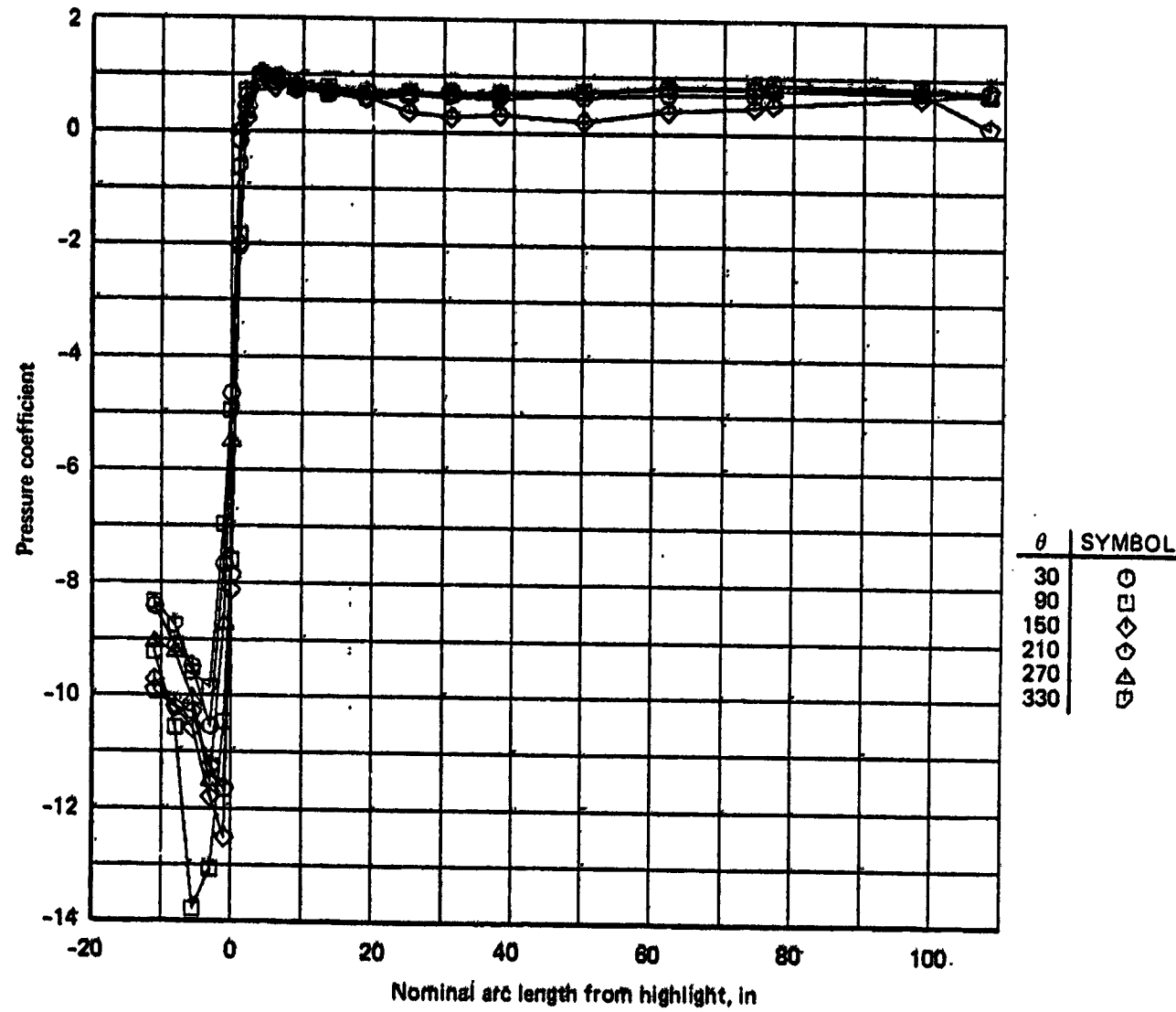


Figure A-37. Engine No. 3 Cowl Pressures, Condition 115, Thrust Reverse

125209-95

ORIGINAL PAGE IS  
OF POOR QUALITY

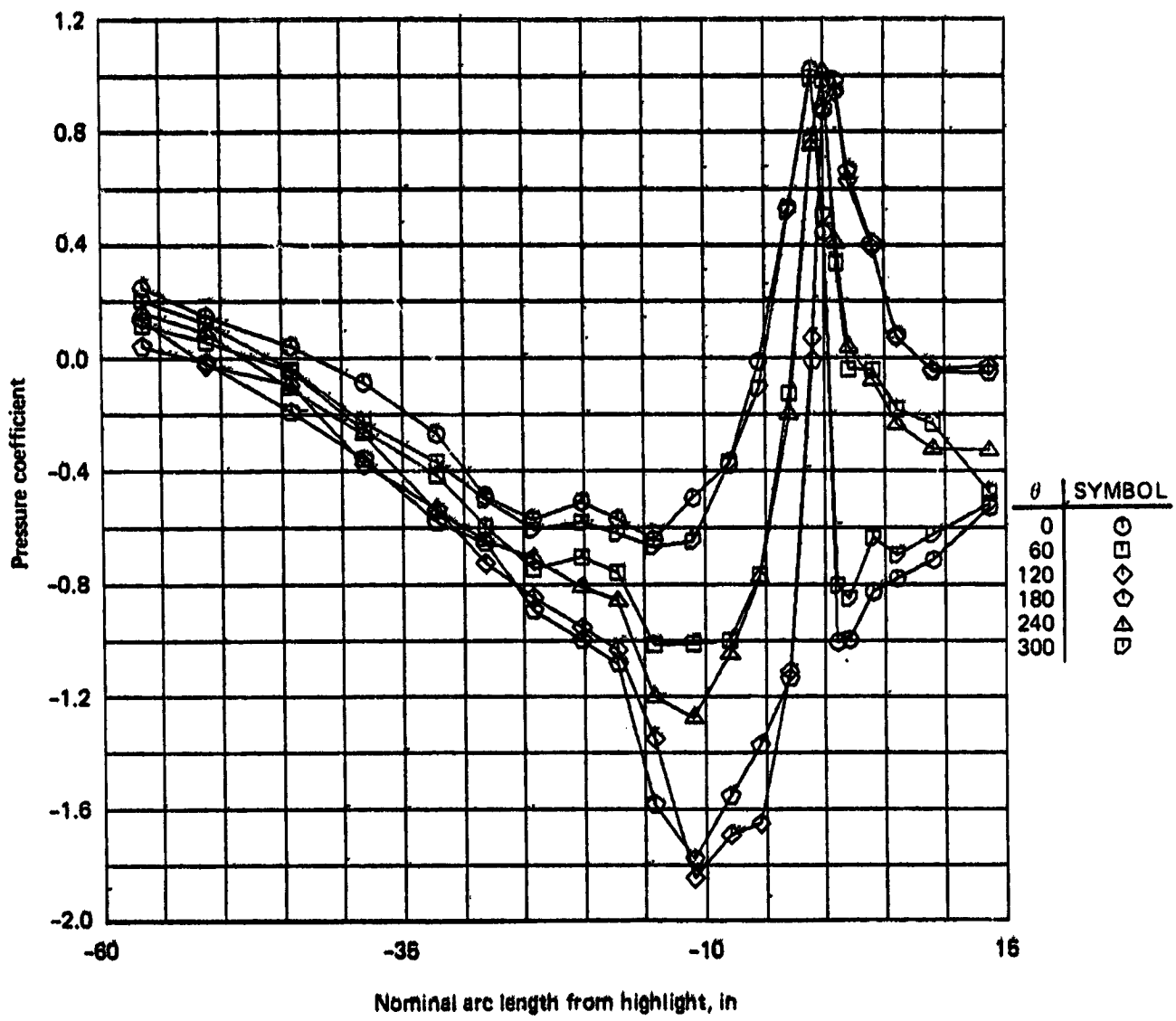


Figure A-38. Engine No. 3 Inlet Pressures, Condition 116, 2.0g Left Turn (Flaps Up)

ORIGINAL PAGE IS  
OF POOR QUALITY

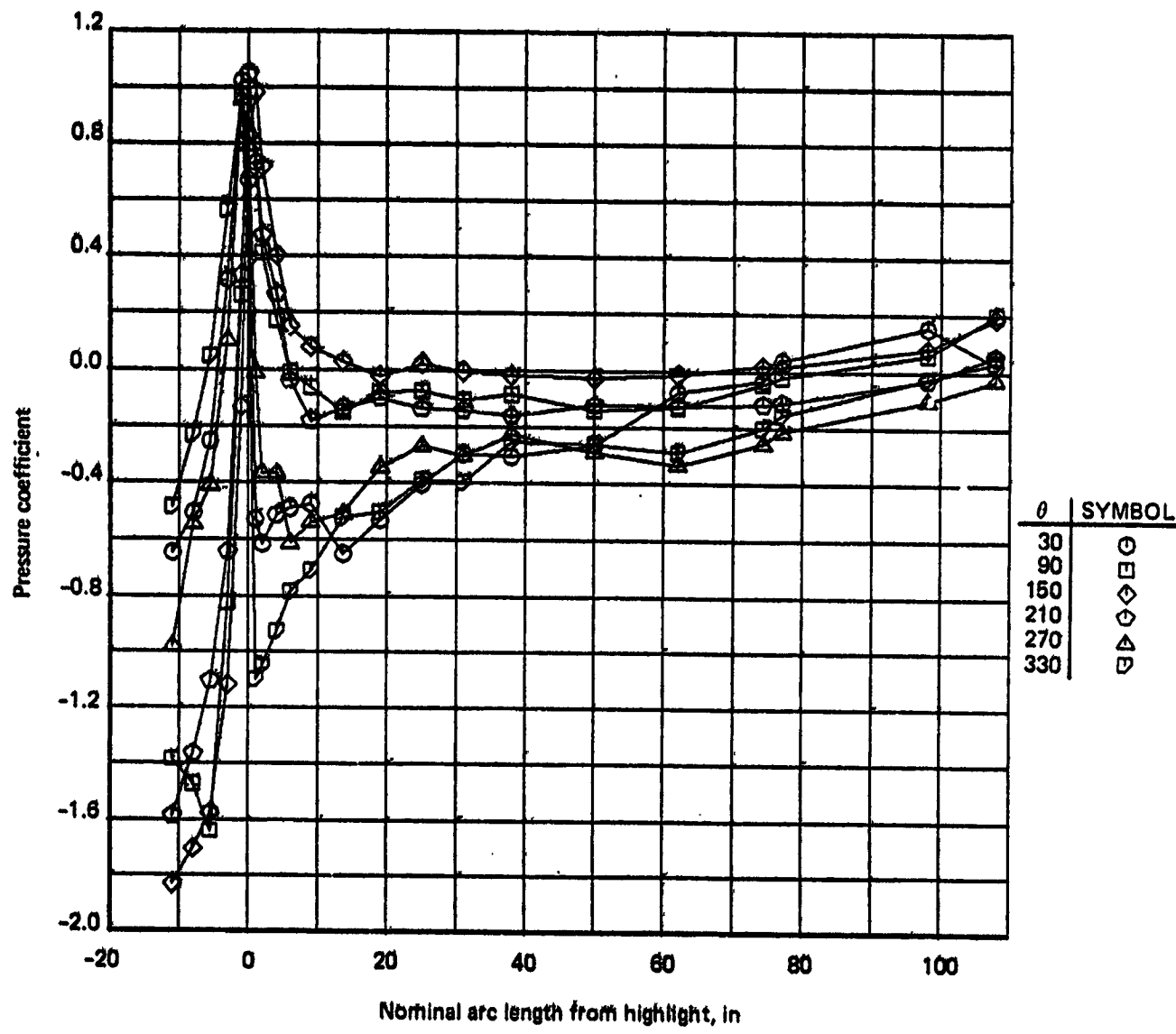


Figure A-39. Engine No. 3 Cowl Pressures, Condition 116, 2.0g Left Turn (Flaps Up)

125209-97

ORIGINAL PAGE IS  
OF POOR QUALITY

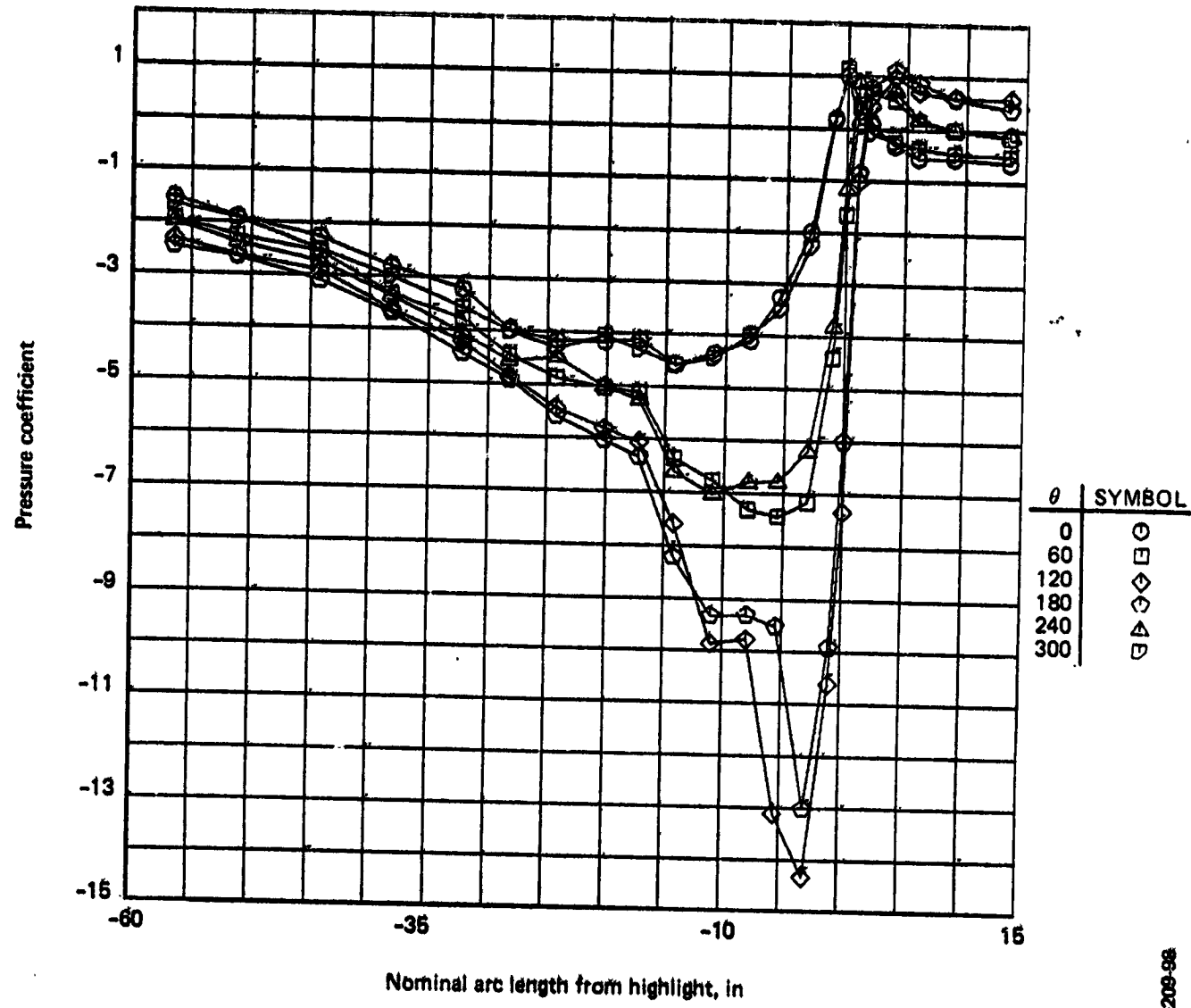


Figure A-40. Engine No. 3 Inlet Pressures, Condition 117, 1.6g Left Turn (Flaps 30)

ORIGINAL PAGE IS  
OF POOR QUALITY

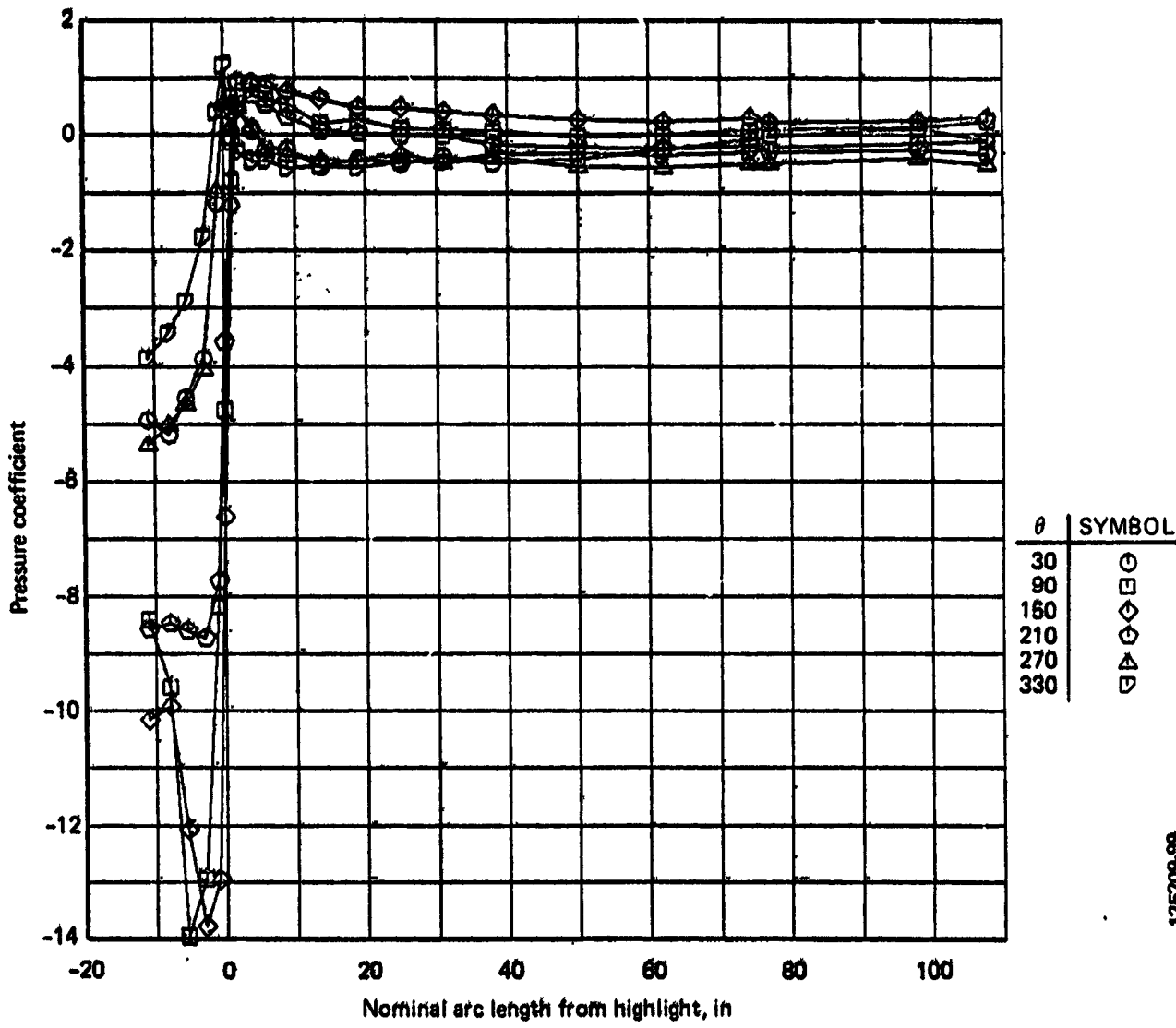


Figure A-41. Engine No. 3 Cowl Pressures, Condition 117, 1.8g Left Turn (Flaps 30)

ORIGINAL PAGE IS  
OF POOR QUALITY

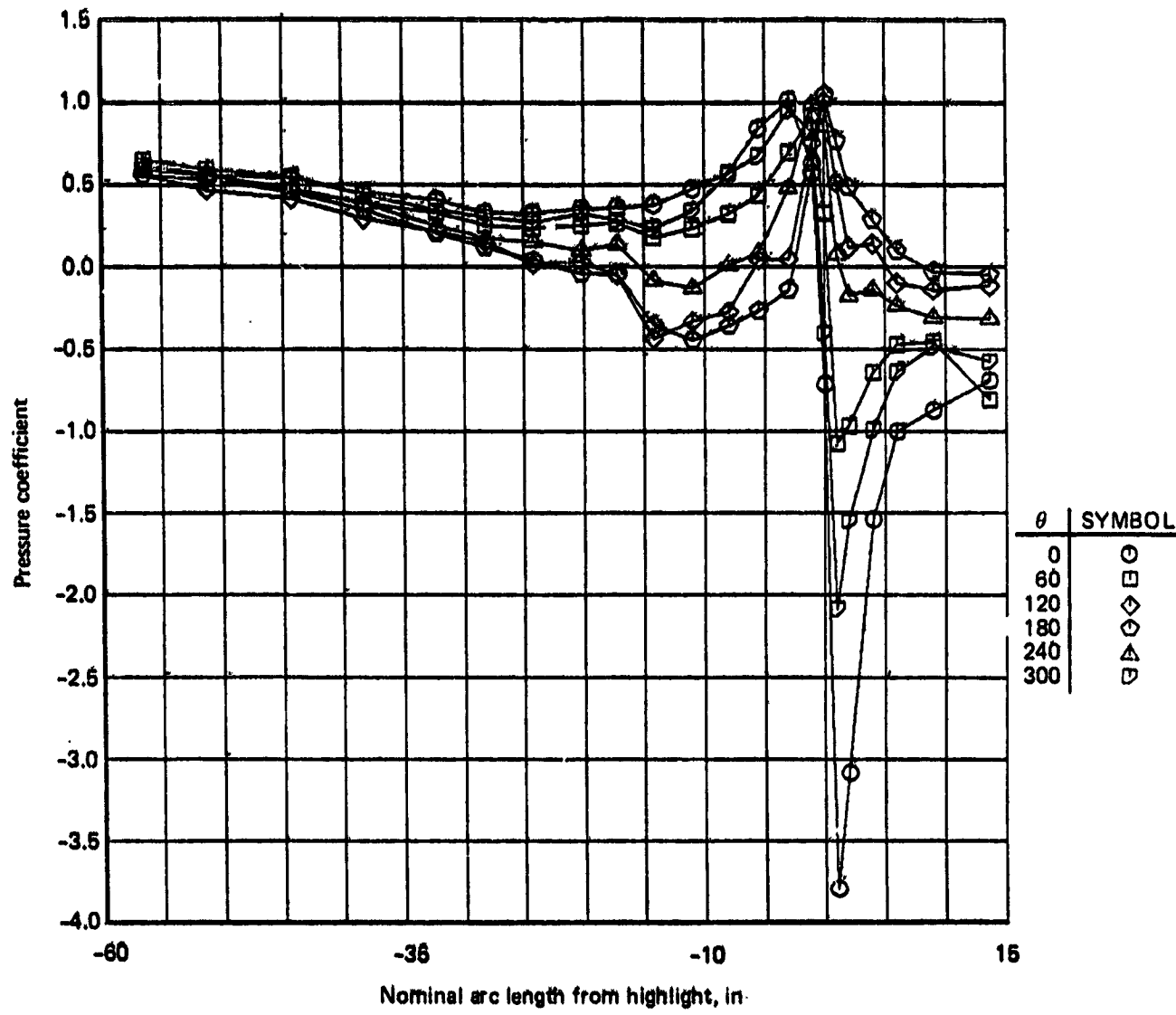


Figure A-42. Engine No. 3 Inlet Pressures, Condition 120, 2.0g Right Turn (Flaps Up)

126209-100

ORIGINAL PAGE IS  
OF POOR QUALITY

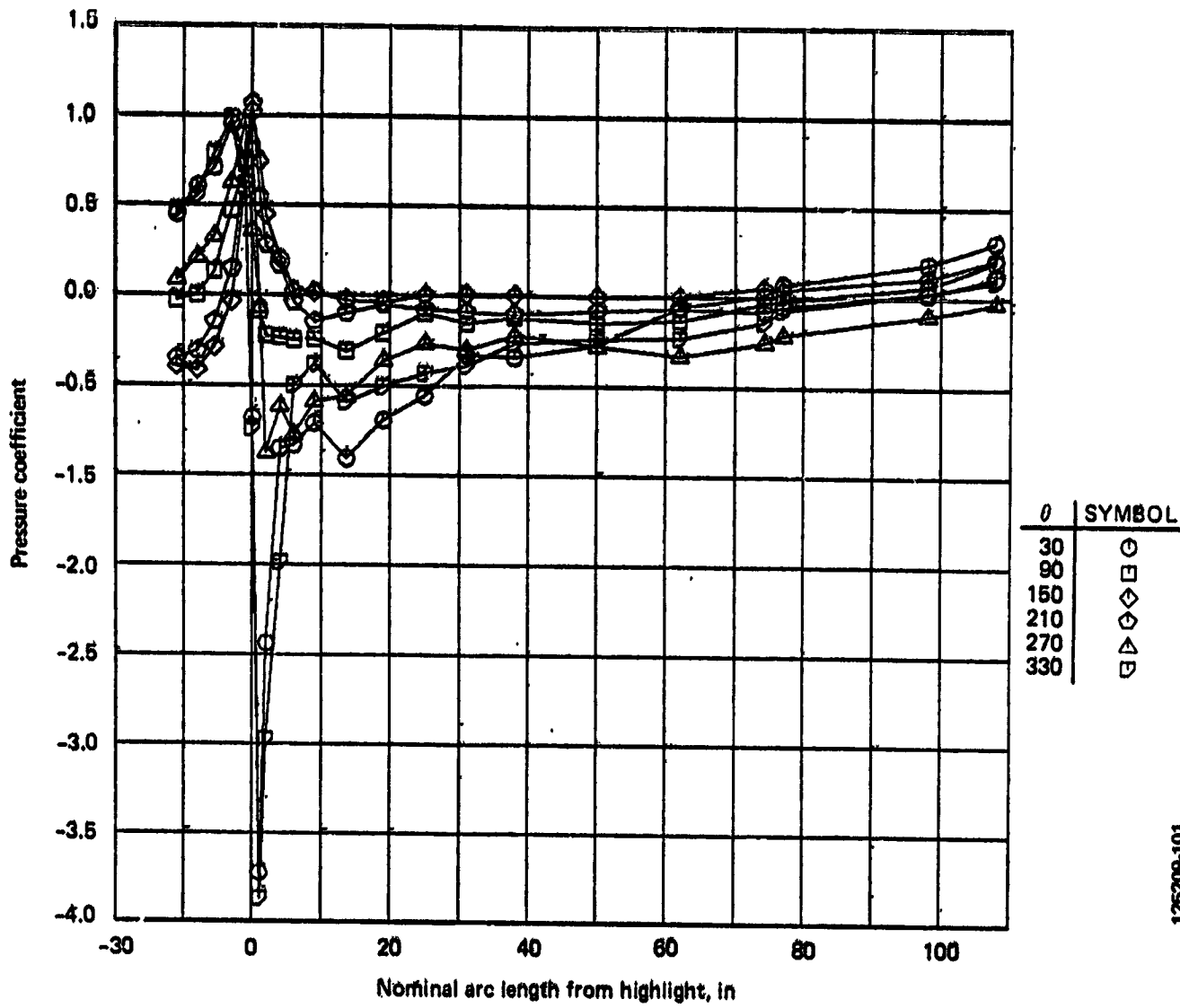


Figure A-43. Engine No. 3 Cowl Pressures, Condition 120, 2.0g Right Turn (Flaps Up)

ORIGINAL PAGE IS  
OF POOR QUALITY

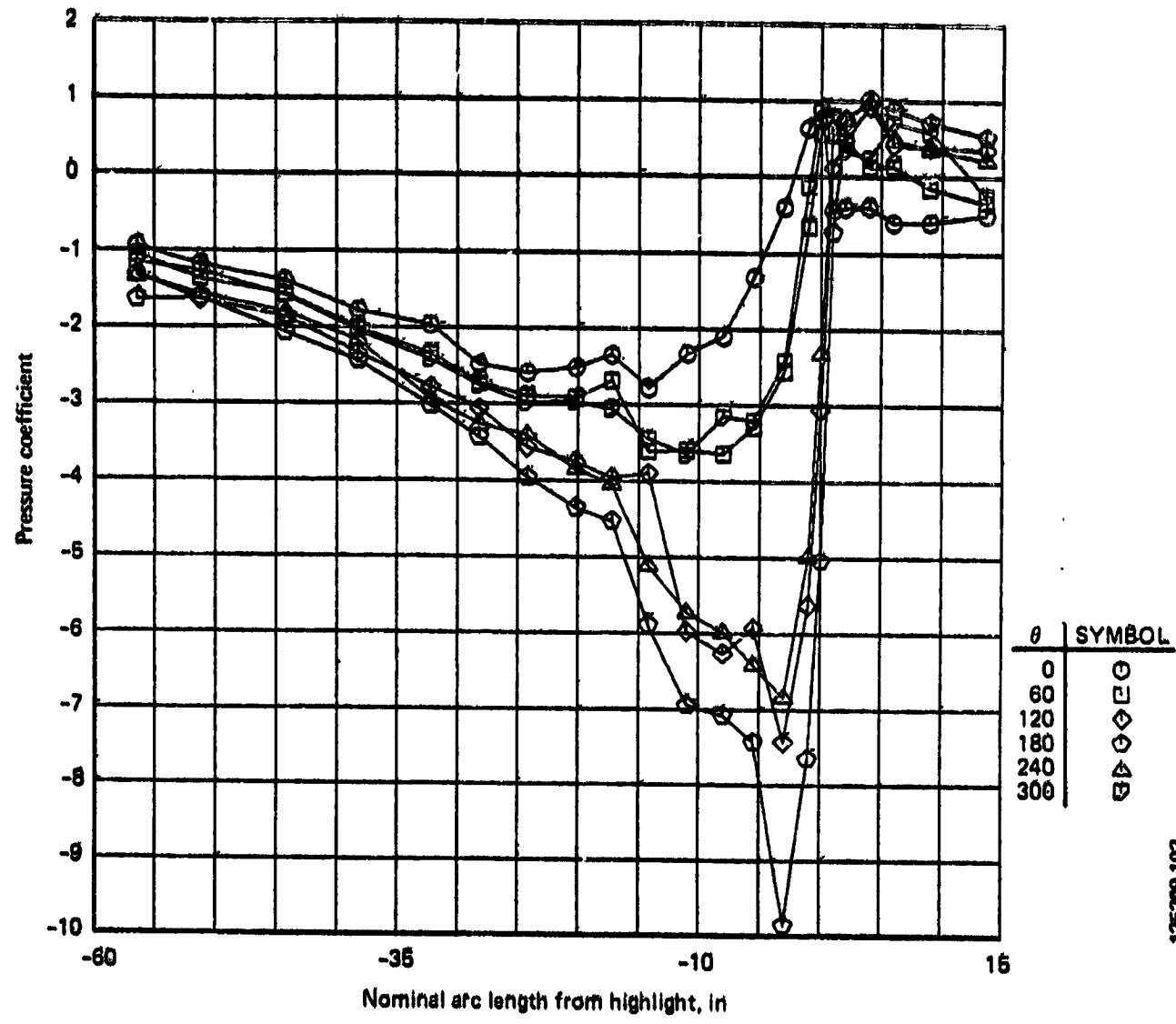


Figure A-44. Engine No. 3 Inlet Pressures, Condition 121, 1.6g Right Turn (Flaps 30)

ORIGINAL PAGE IS  
OF POOR QUALITY

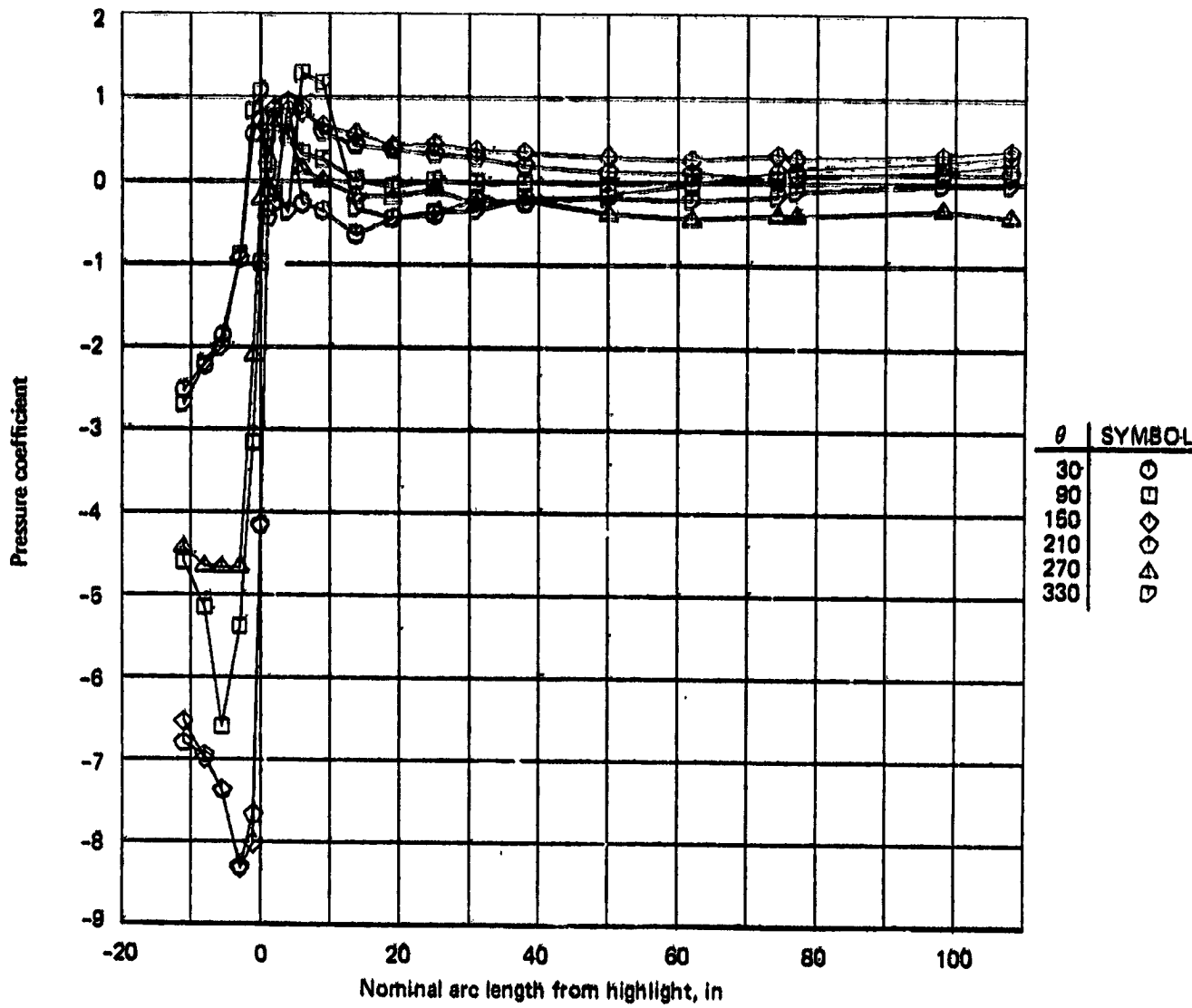
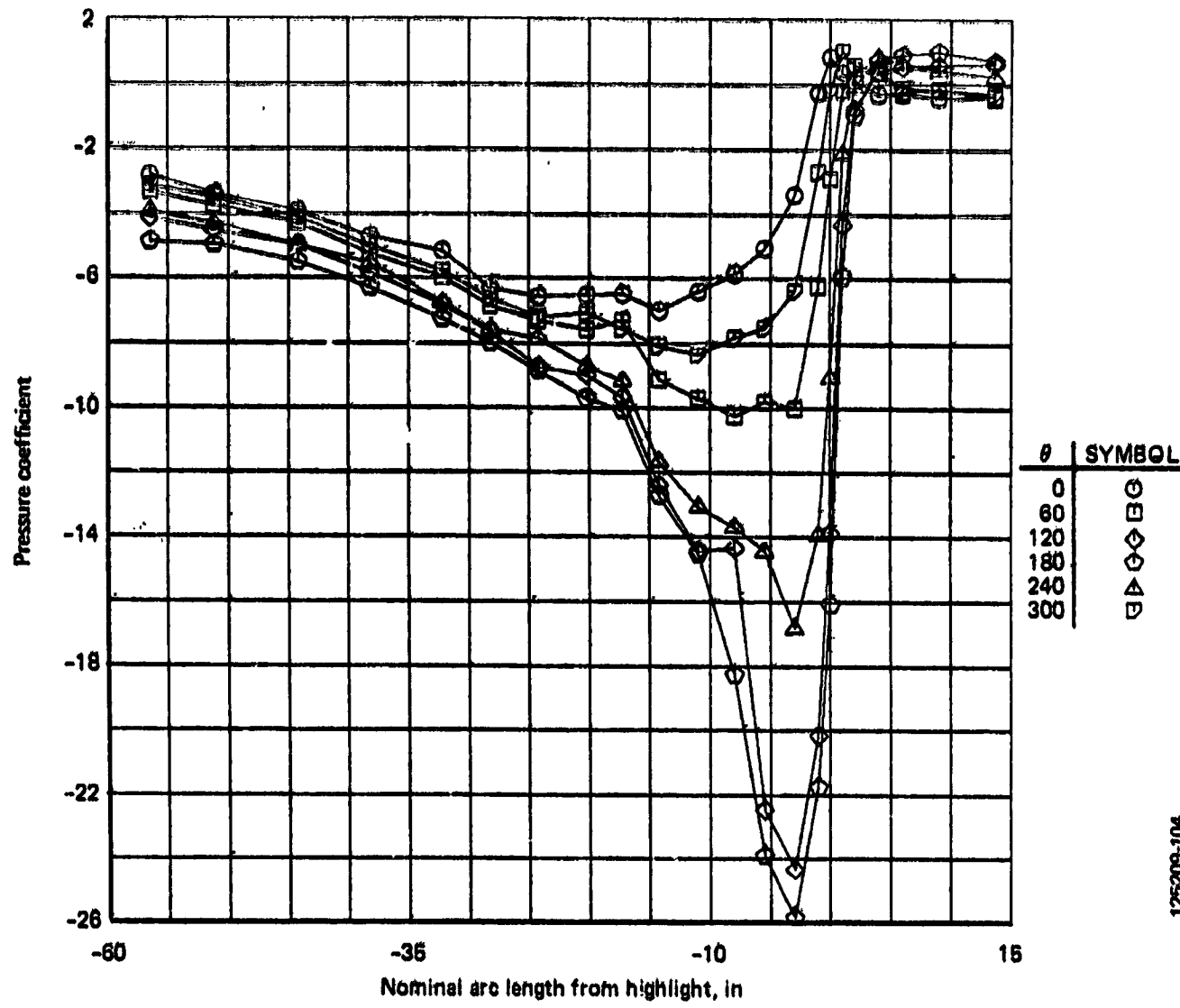


Figure A-45. Engine No. 3 Cowl Pressures, Condition 121, 1.6g Flight Turn (Flaps 30)

ORIGINAL PAGE IS  
OF POOR QUALITY



ORIGINAL PAGE IS  
OF POOR QUALITY

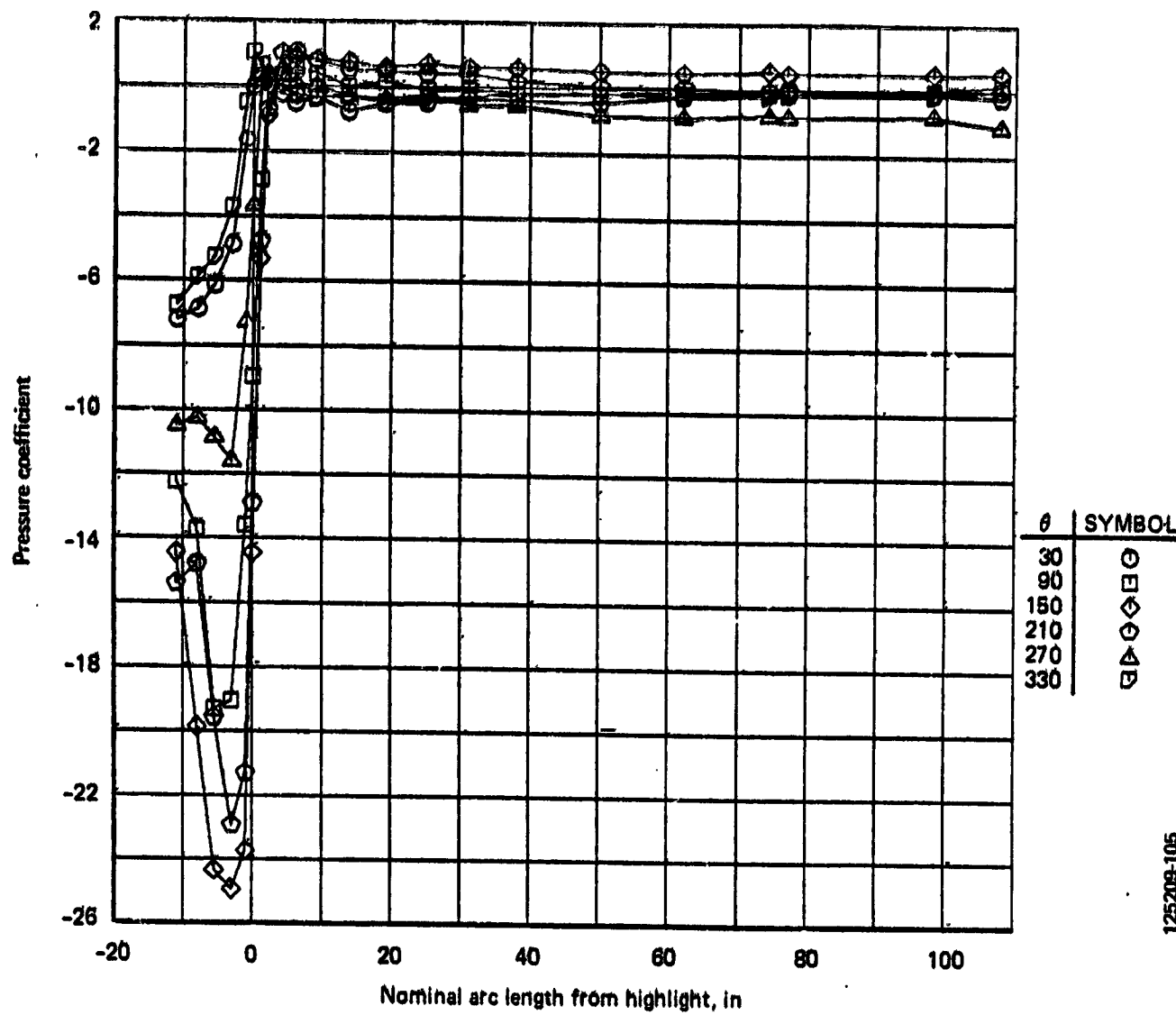


Figure A-47. Engine No. 3 Cowl Pressures, Condition 123, Airplane Stall

ORIGINAL PAGE IS  
OF POOR QUALITY

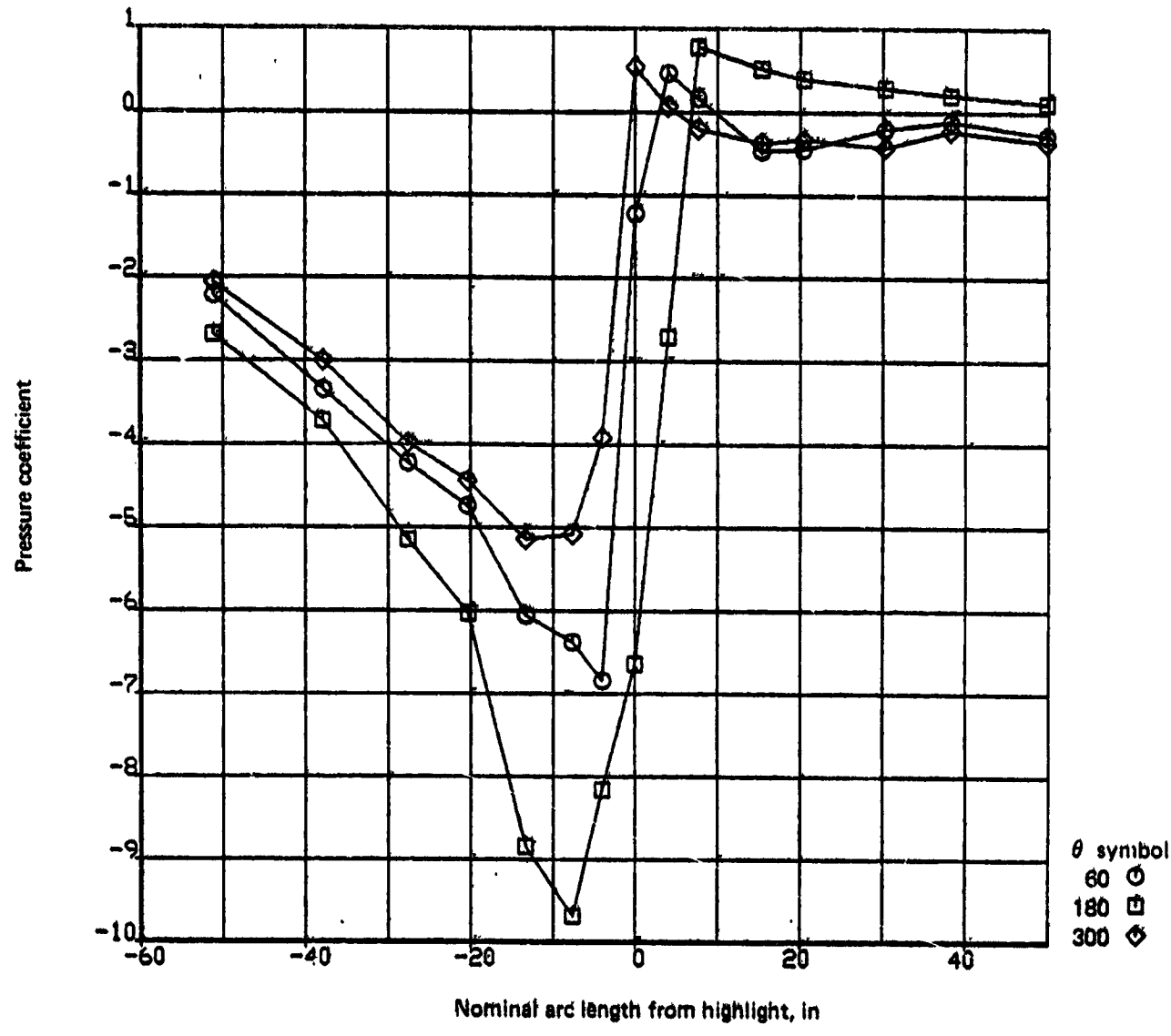


Figure A-48. Engine No. 4 Inlet Pressures, Condition 101, 612K Gross Weight Takeoff

125239-55-446

ORIGINAL PAGE IS  
OF POOR QUALITY

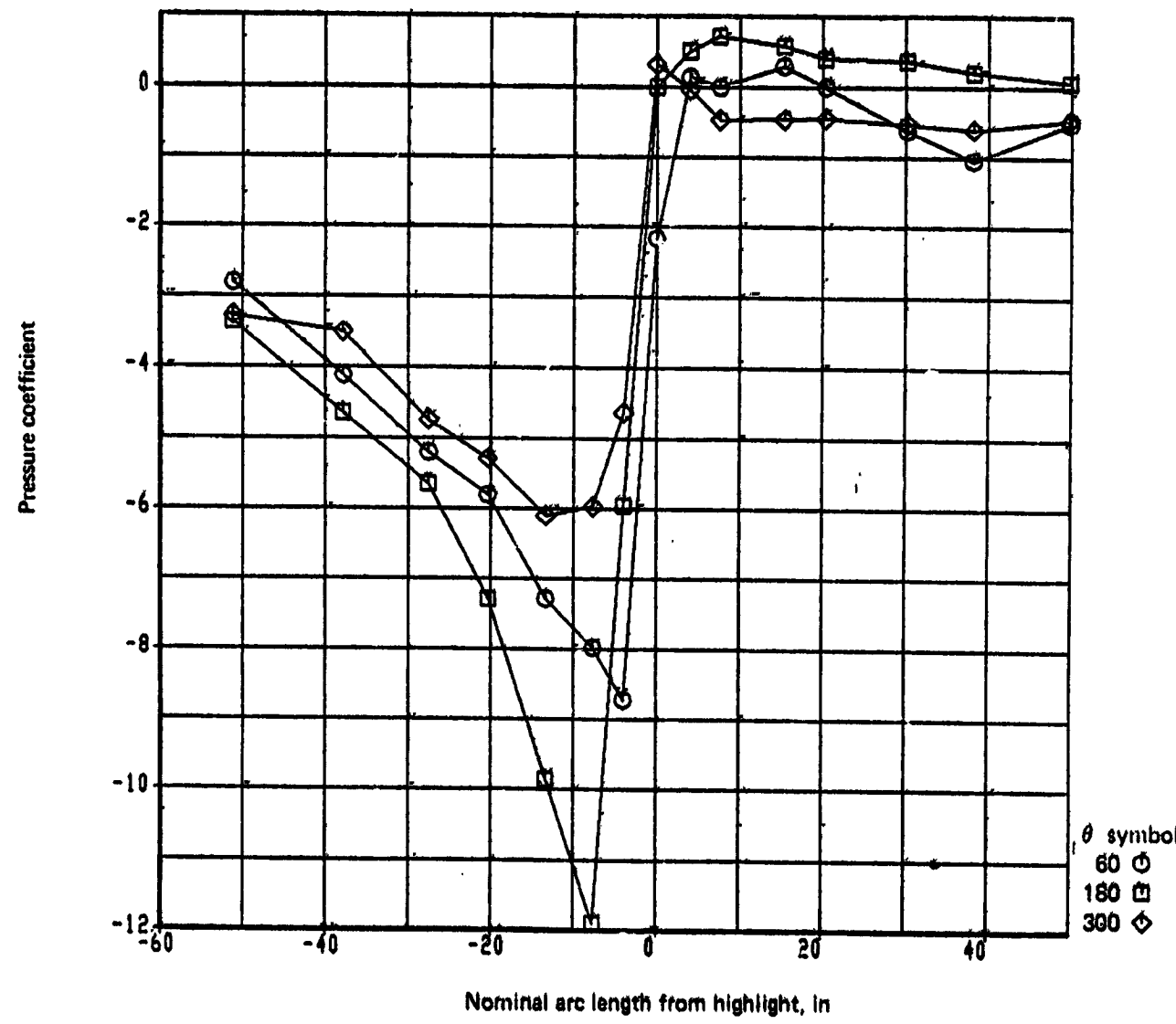


Figure A-49. Engine No. 4 Inlet Pressures, Condition 101, 538K Gross Weight Takeoff

125209-55-445

ORIGINAL PAGE IS  
OF POOR QUALITY

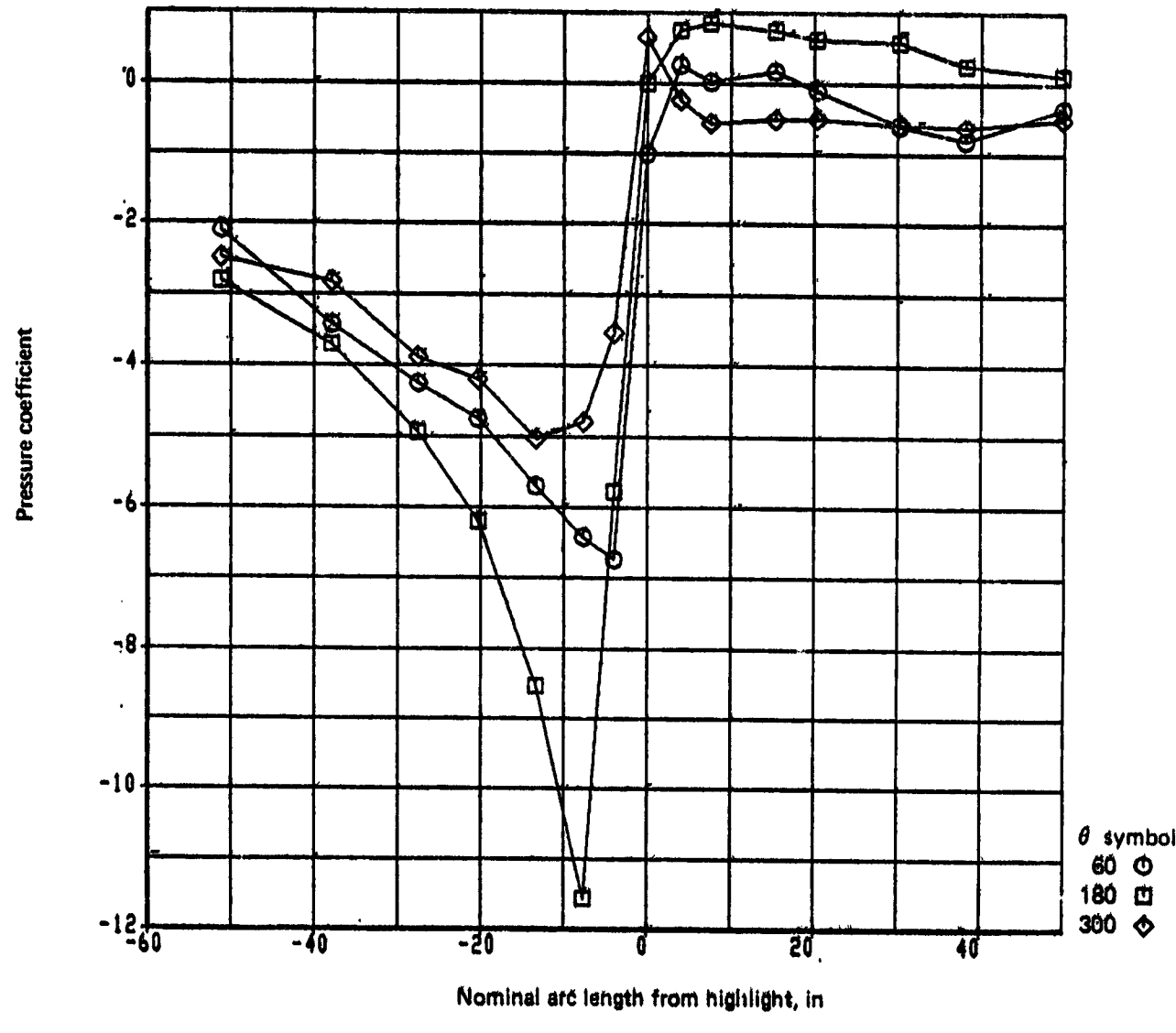


Figure A-50. Engine No. 4 Inlet Pressures, Condition 101, 647K Gross Weight Takeoff

1252009-55-444

ORIGINAL PAGE IS  
OF POOR QUALITY

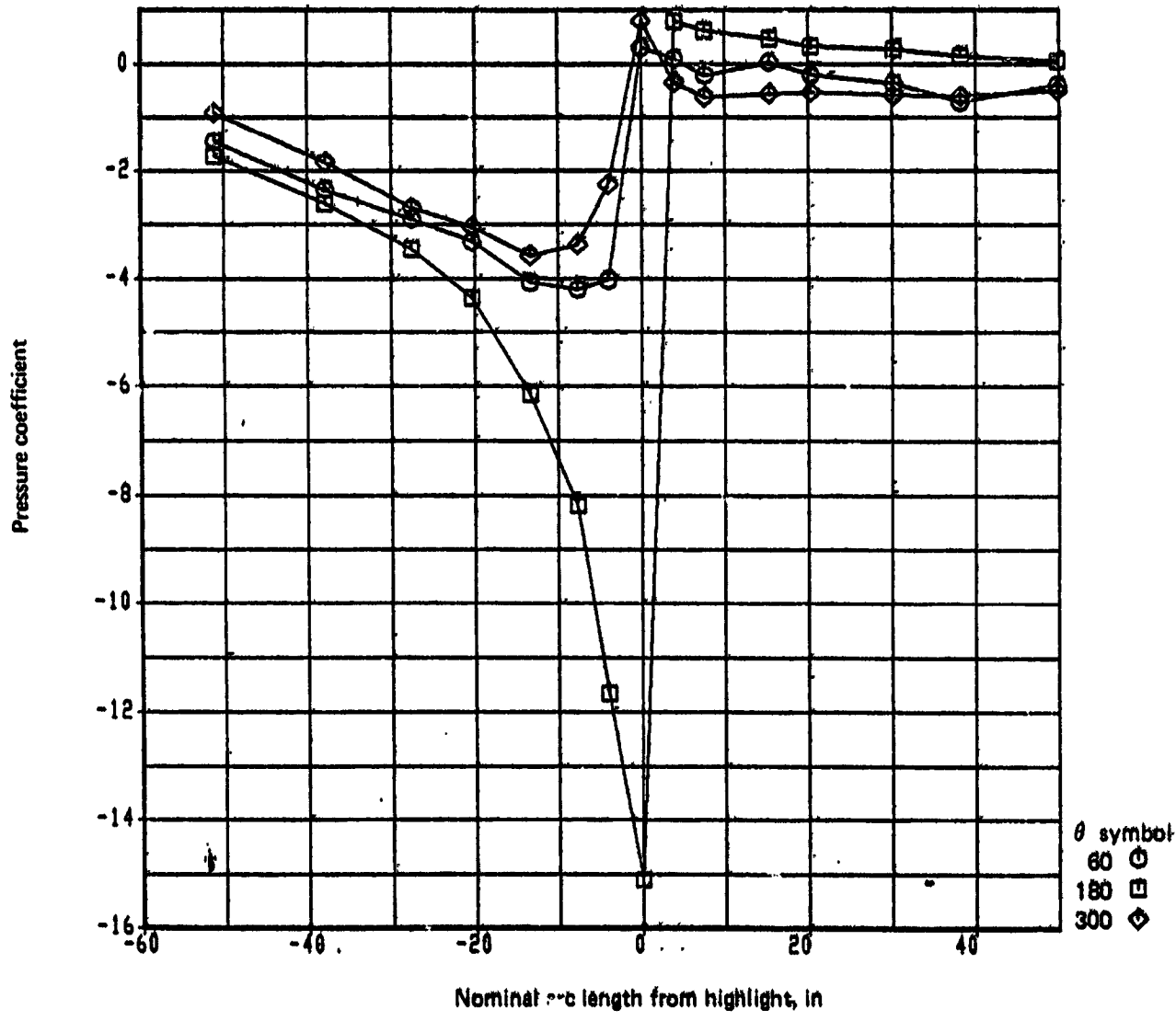


Figure A-51. Engine No. 4 Inlet Pressures, Condition 118, 780K Gross Weight Simulated Takeoff

12800-55442

ORIGINAL DRAWING  
OF POOR QUALITY

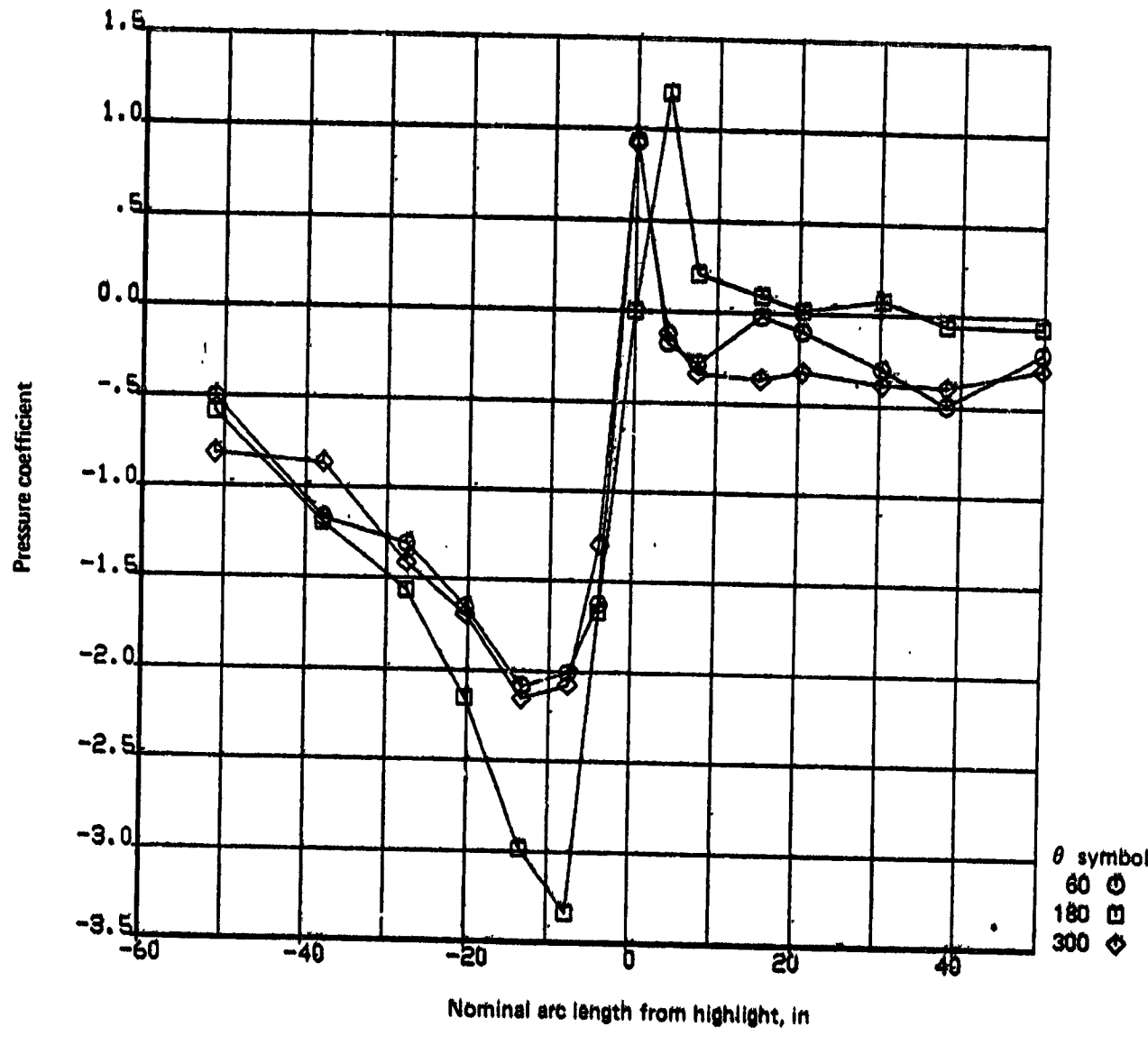


Figure A-52. Engine No. 4 Inlet Pressures, Condition 102, Low Climb

125309-55-442

ORIGINAL PAGE IS  
OF POOR QUALITY

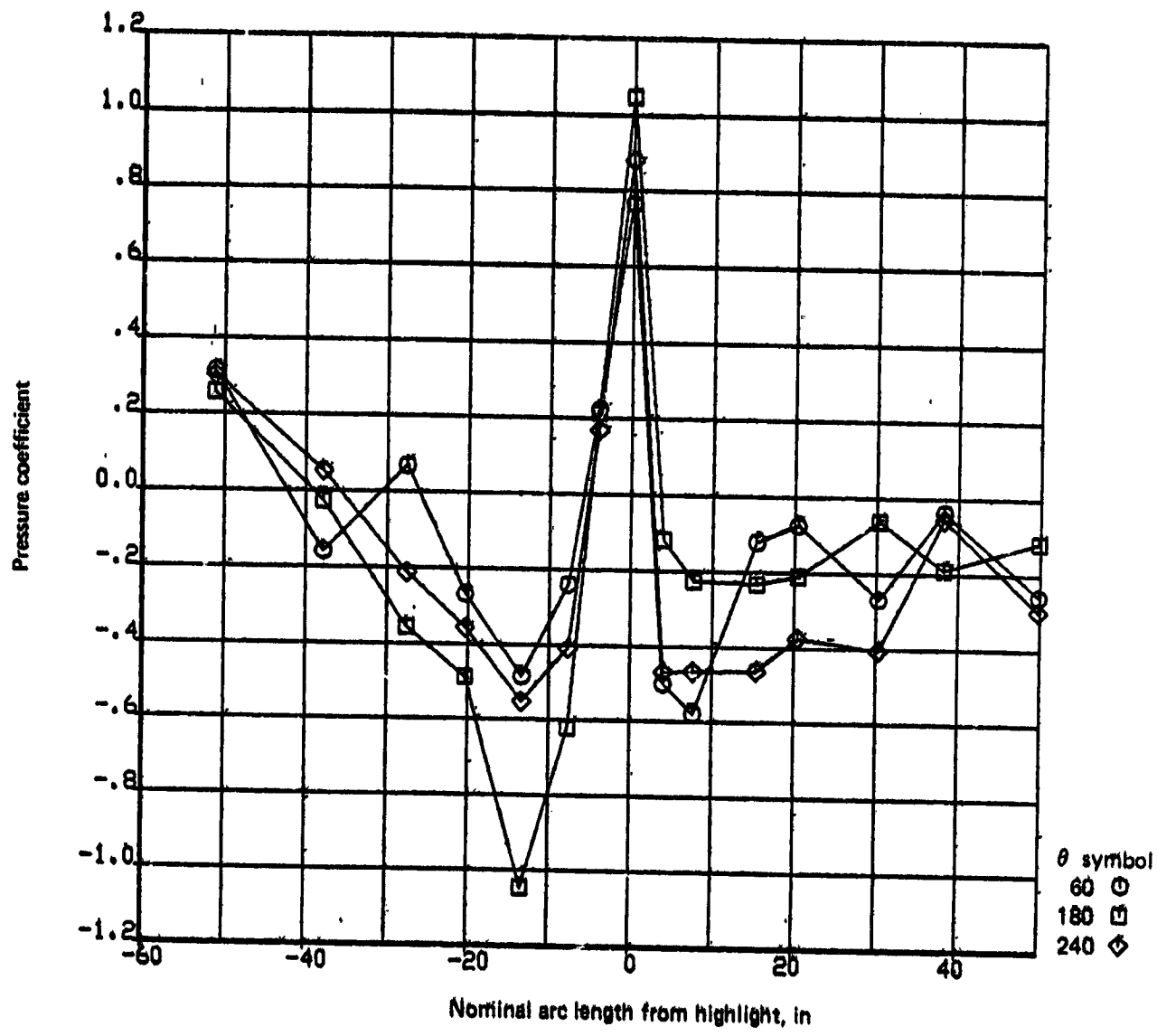


Figure A-53. Engine No. 4 Inlet Pressures, Condition 103, Mid Climb

125289-55-44

ORIGINAL PAGE IS  
OF POOR QUALITY

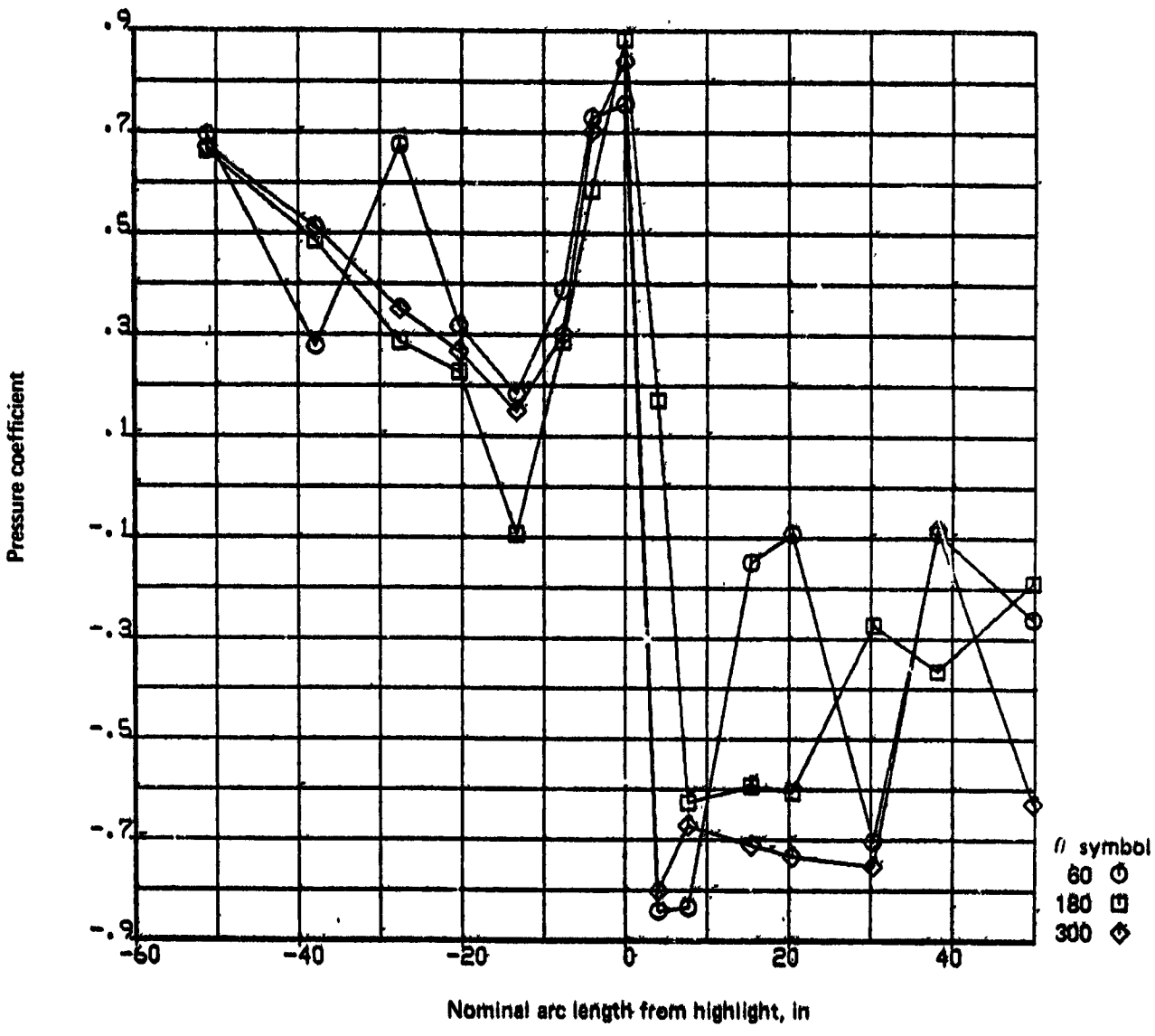


Figure A-54. Engine No. 4 Inlet Pressures, Condition 104, High M Cruise

125289-455-440

ORIGINAL PAGE IS  
OF POOR QUALITY

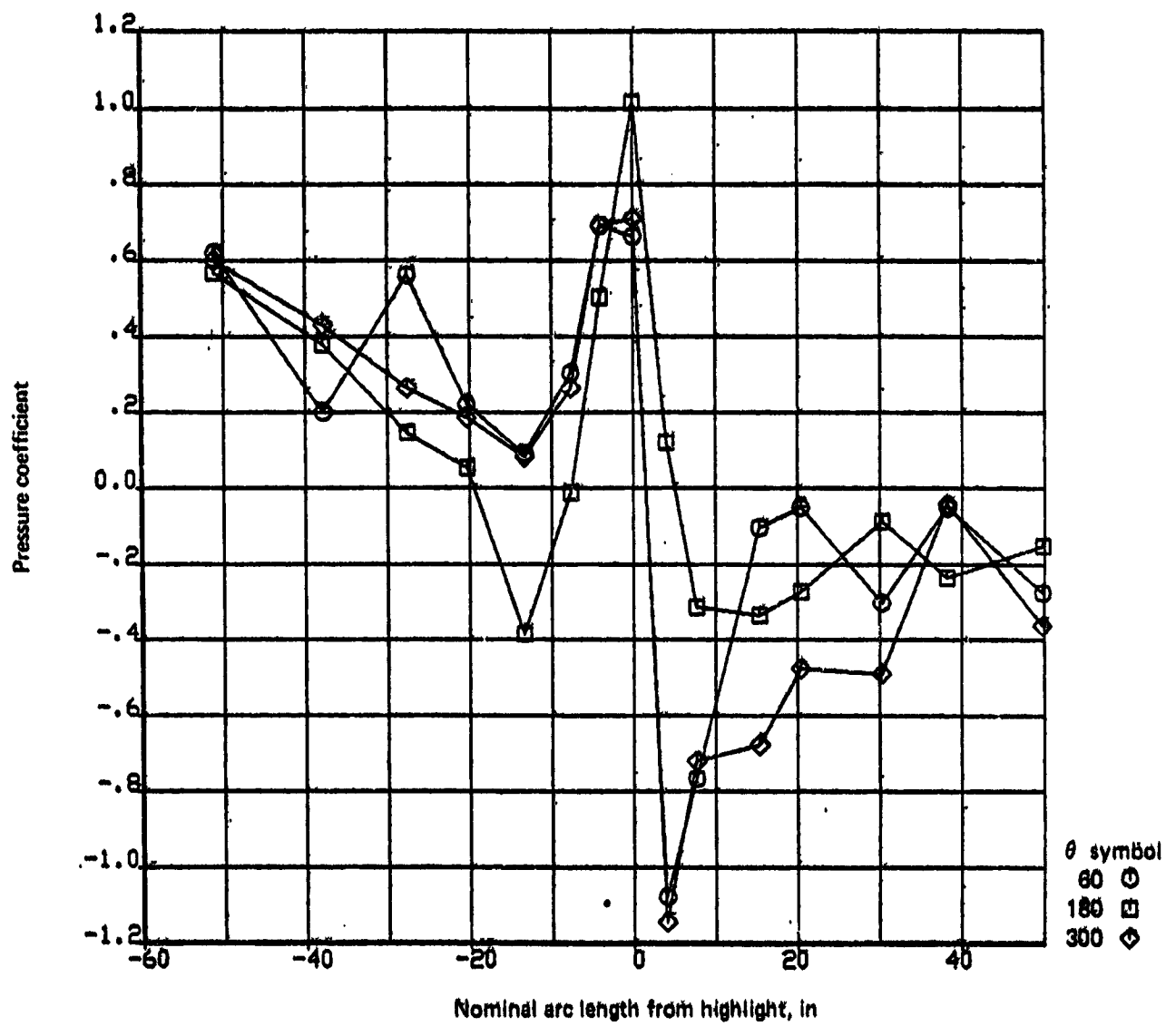


Figure A-55. Engine No. 4 Inlet Pressures, Condition 105, Low M Cruise

12209-55-43

ORIGINAL PAGE IS  
OF POOR QUALITY.

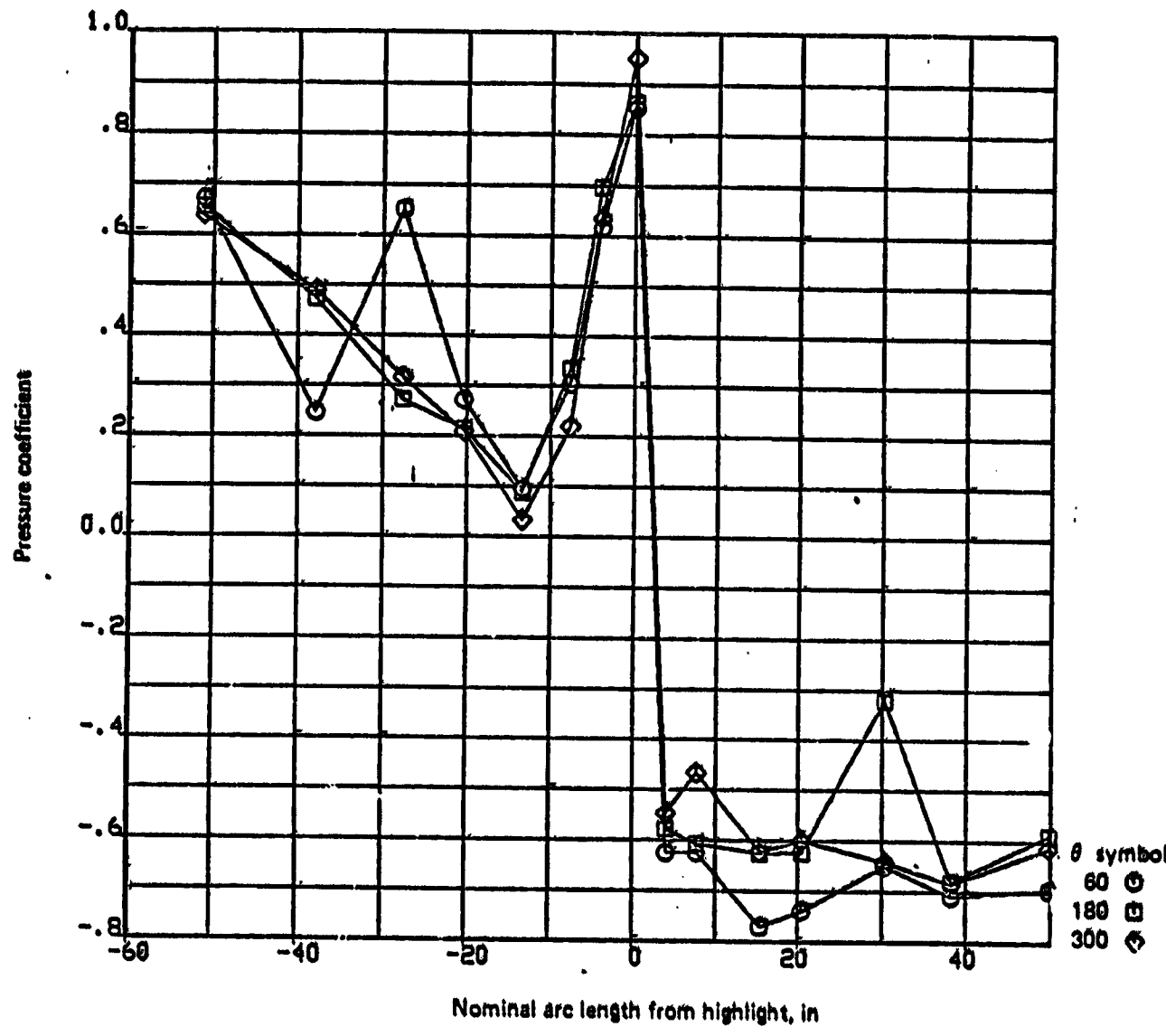


Figure A-56. Engine No. 4 Inlet Pressures, Condition 106, Maximum M

125209-65-438

ORIGINAL PAGE IS  
OF POOR QUALITY

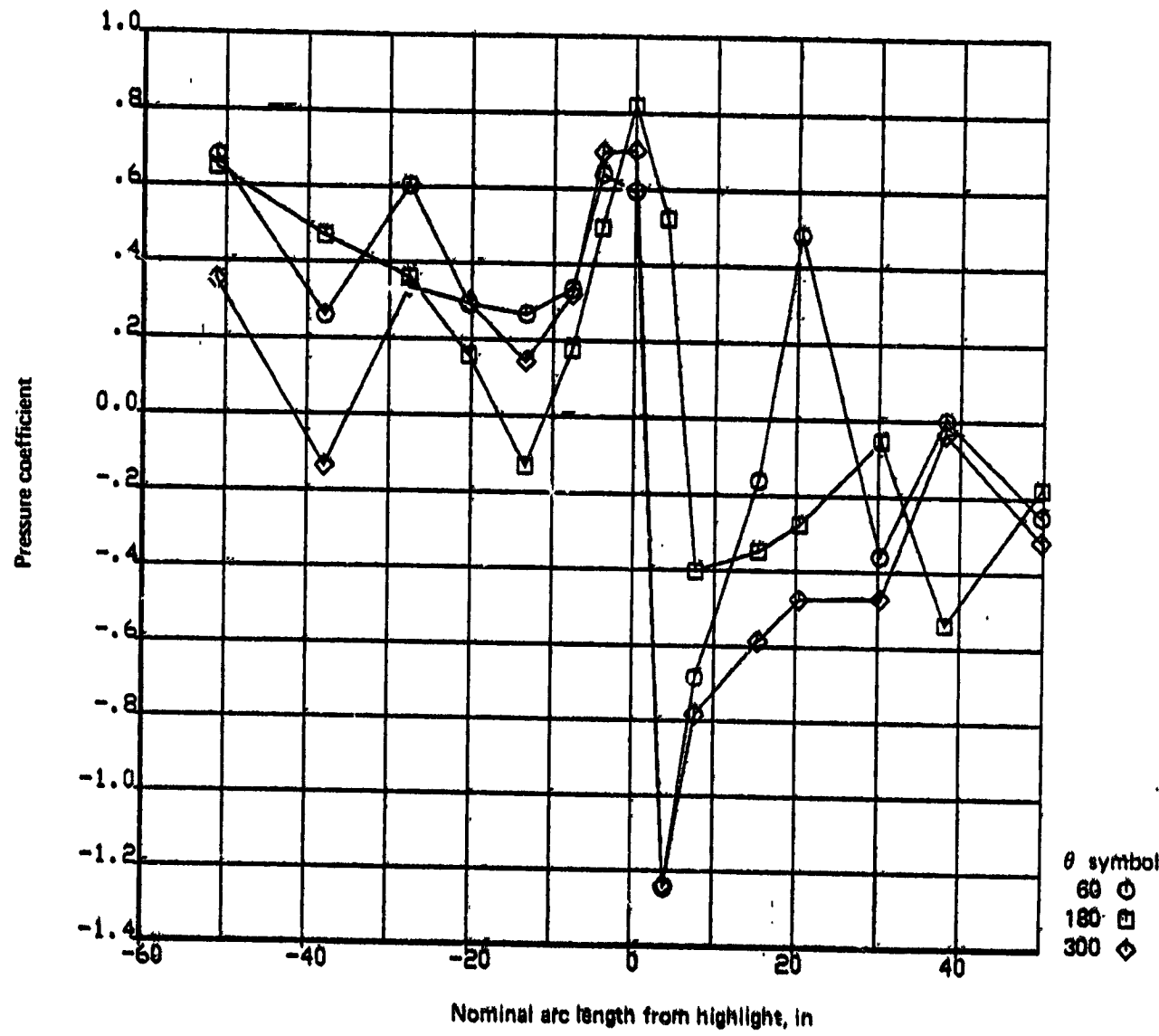


Figure A-57. Engine No. 4 Inlet Pressures, Condition 107, Intlight Relight

125009-55-437

ORIGINAL PRACTICE  
OF POOR QUALITY

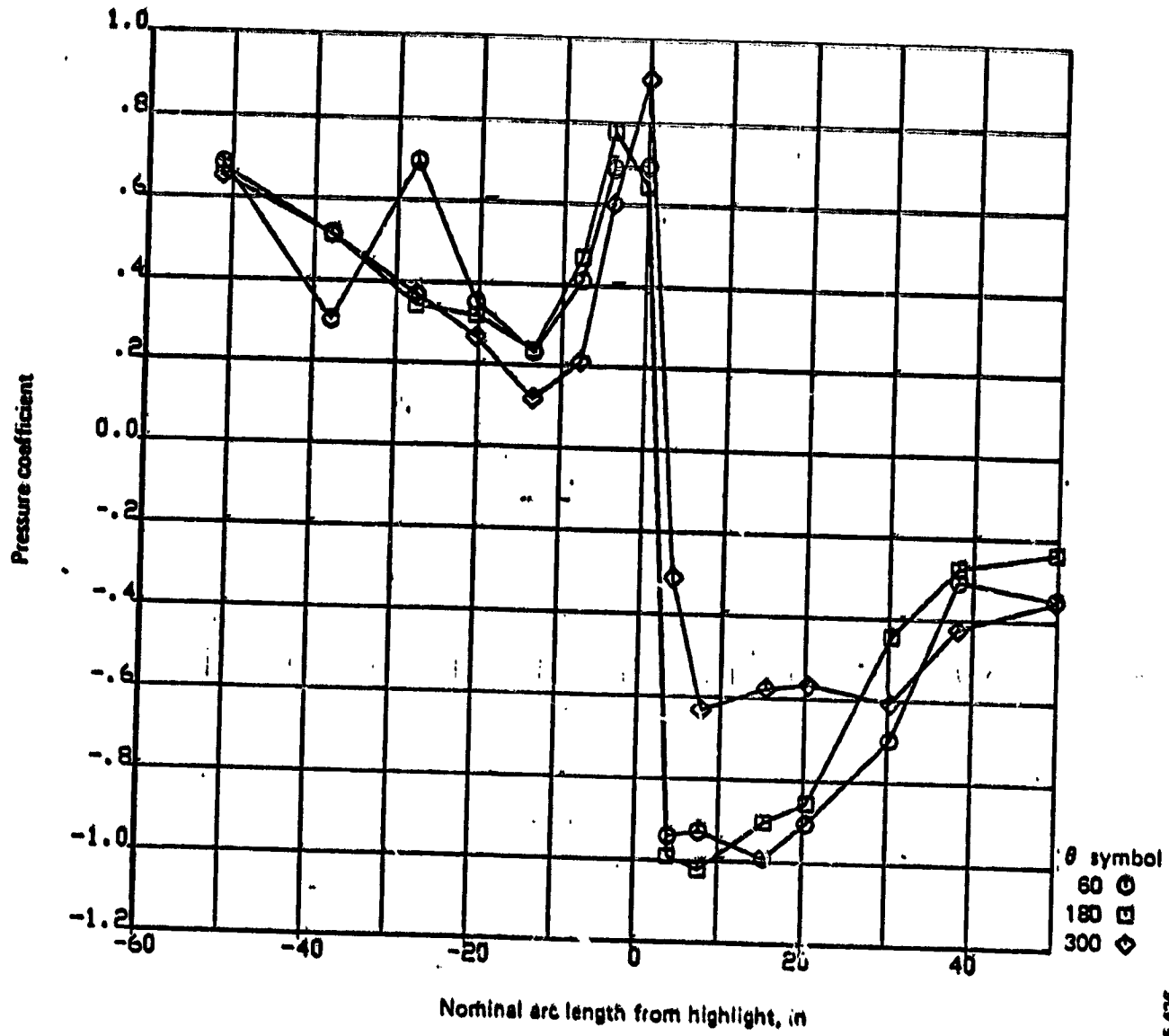


Figure A-58. Engine No. 4 Inlet Pressures, Condition 108, Maximum  $q$

126208-56-437

ORIGINAL PAGE IS  
OF POOR QUALITY

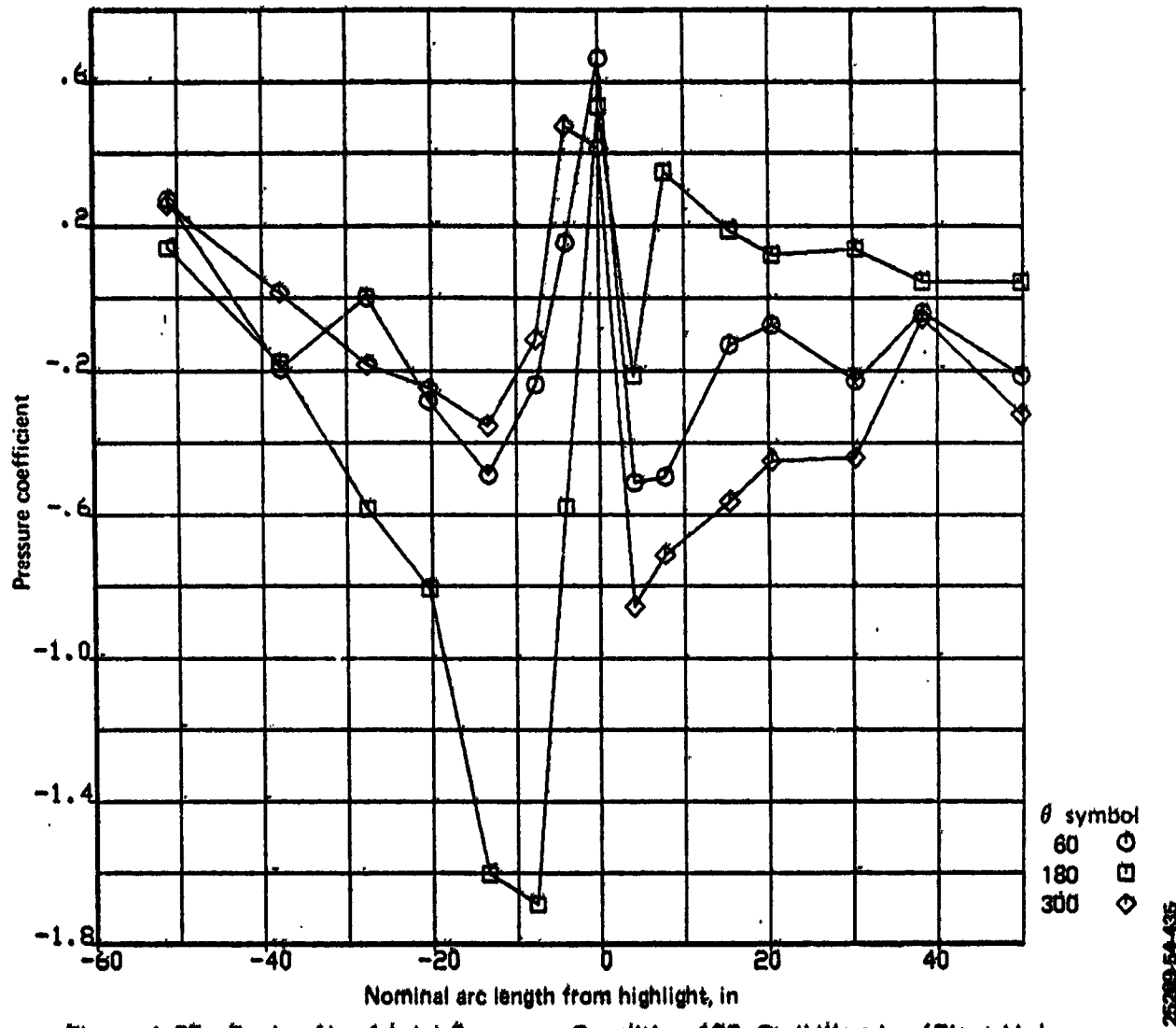


Figure A-59. Engine No. 4 Inlet Pressures, Condition 109, Stall Warning (Flaps Up)

ORIGINAL DESIGN  
OF POOR QUALITY

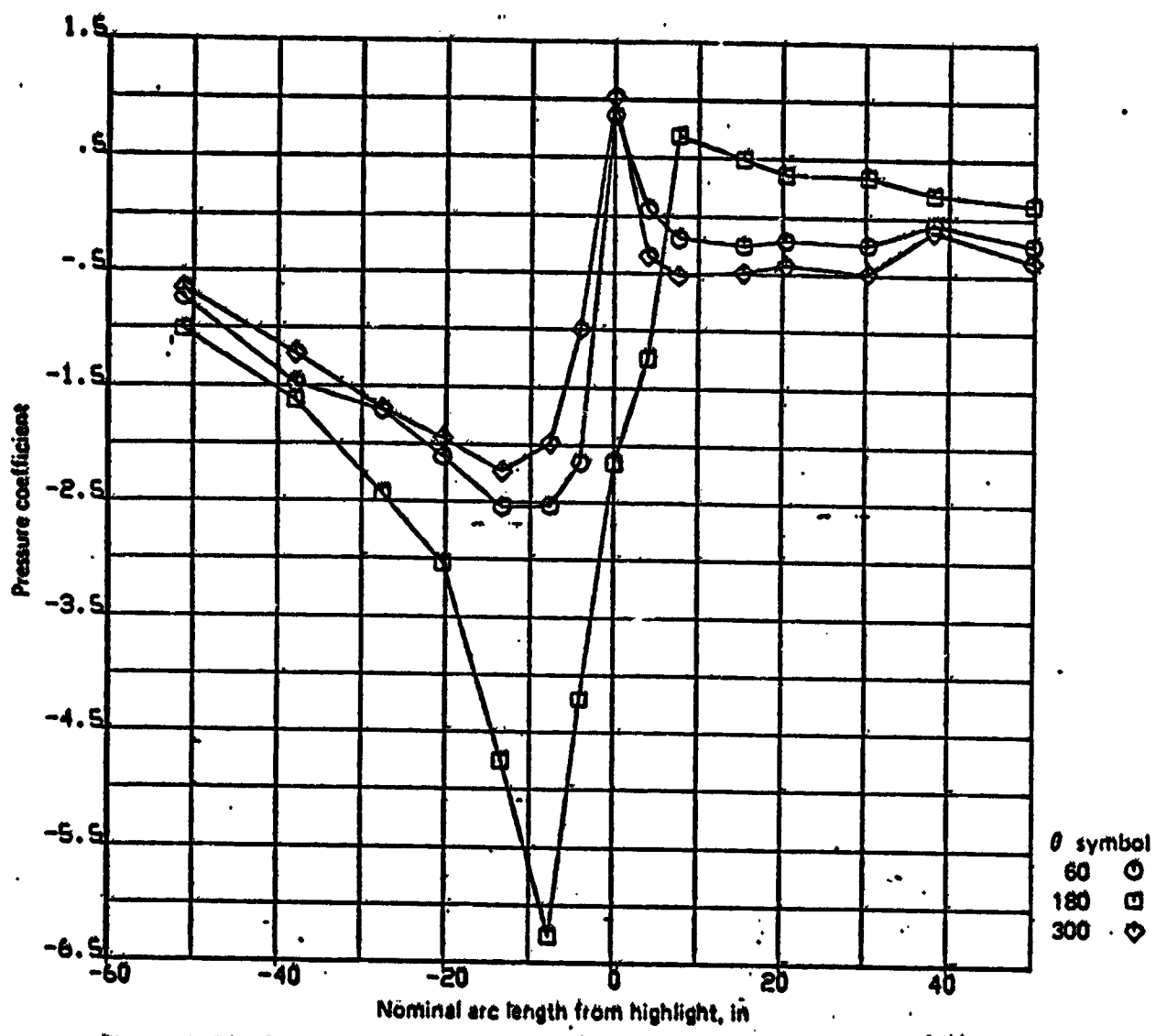


Figure A-80. Engine No. 4 Inlet Pressures, Condition 110, Stall Warning (Flaps 10)

125209-54-34

ORIGINAL PAGE IS  
OF POOR QUALITY

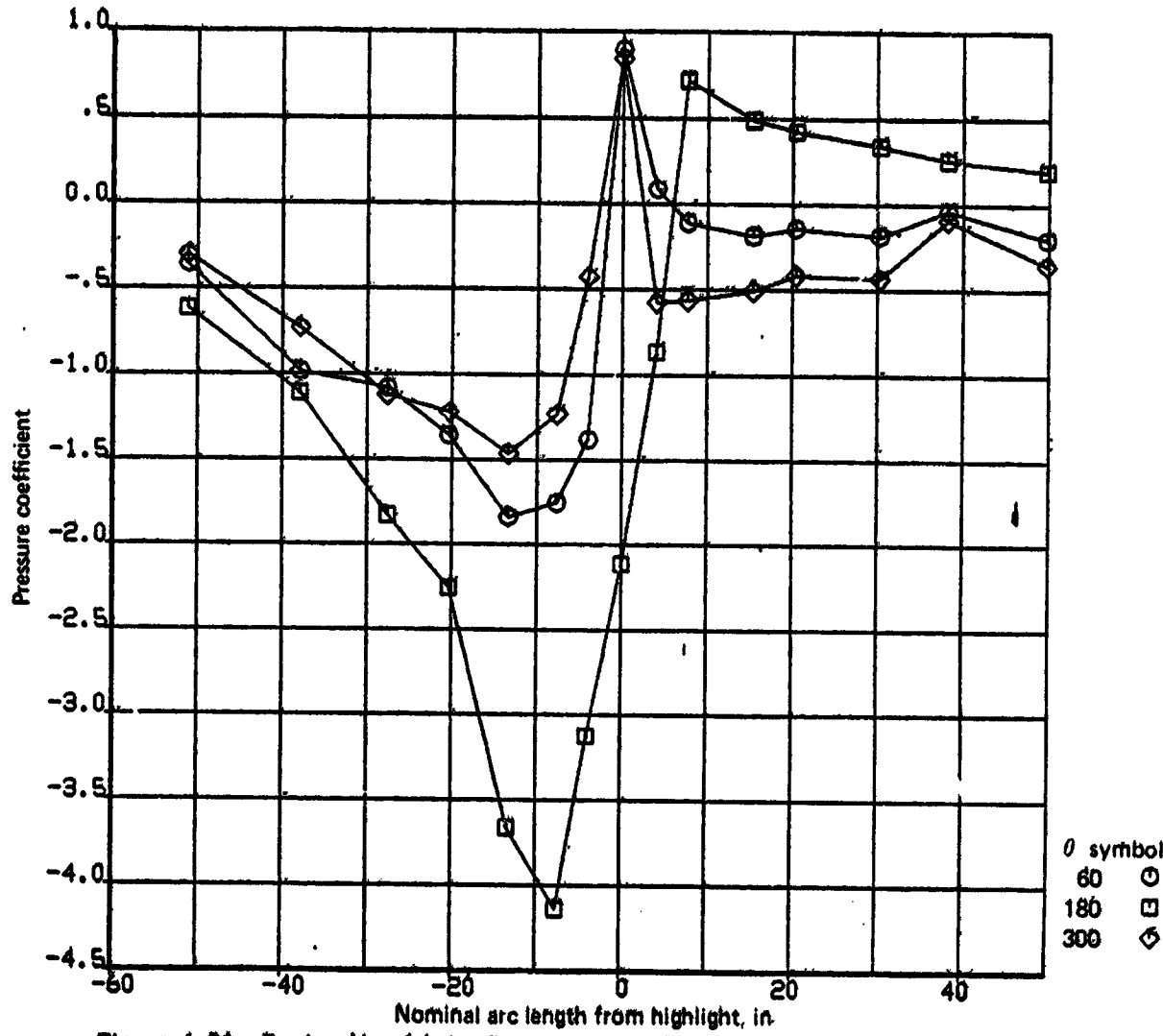


Figure A-61. Engine No. 4 Inlet Pressures, Condition 111, Stall Warning (Flaps 30)

12288-54-423

ORIGINAL PAGE IS  
OF POOR QUALITY

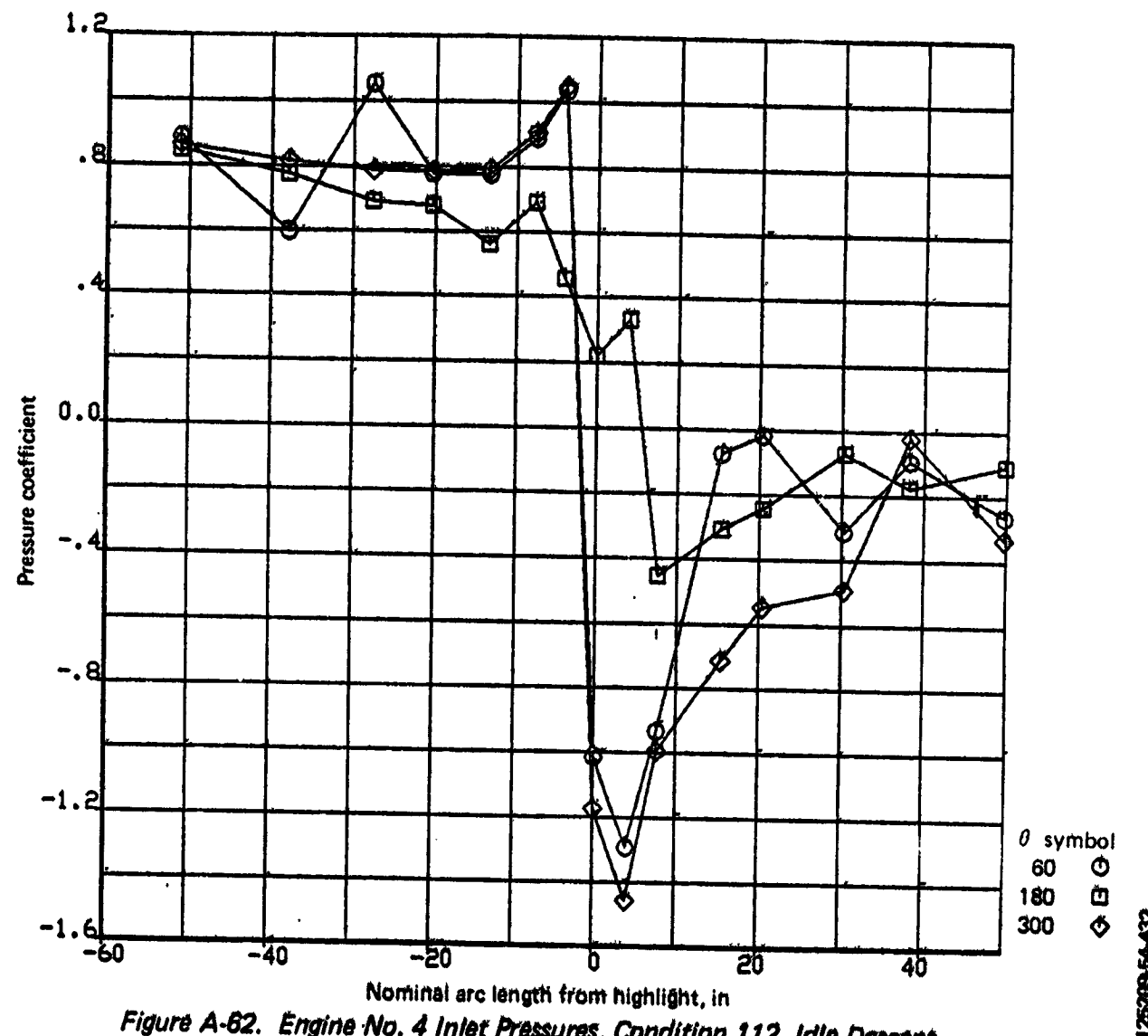


Figure A-62. Engine No. 4 Inlet Pressures, Condition 112, Idle Descent

125099-54-432

ORIGINAL PAGE IS  
OF POOR QUALITY

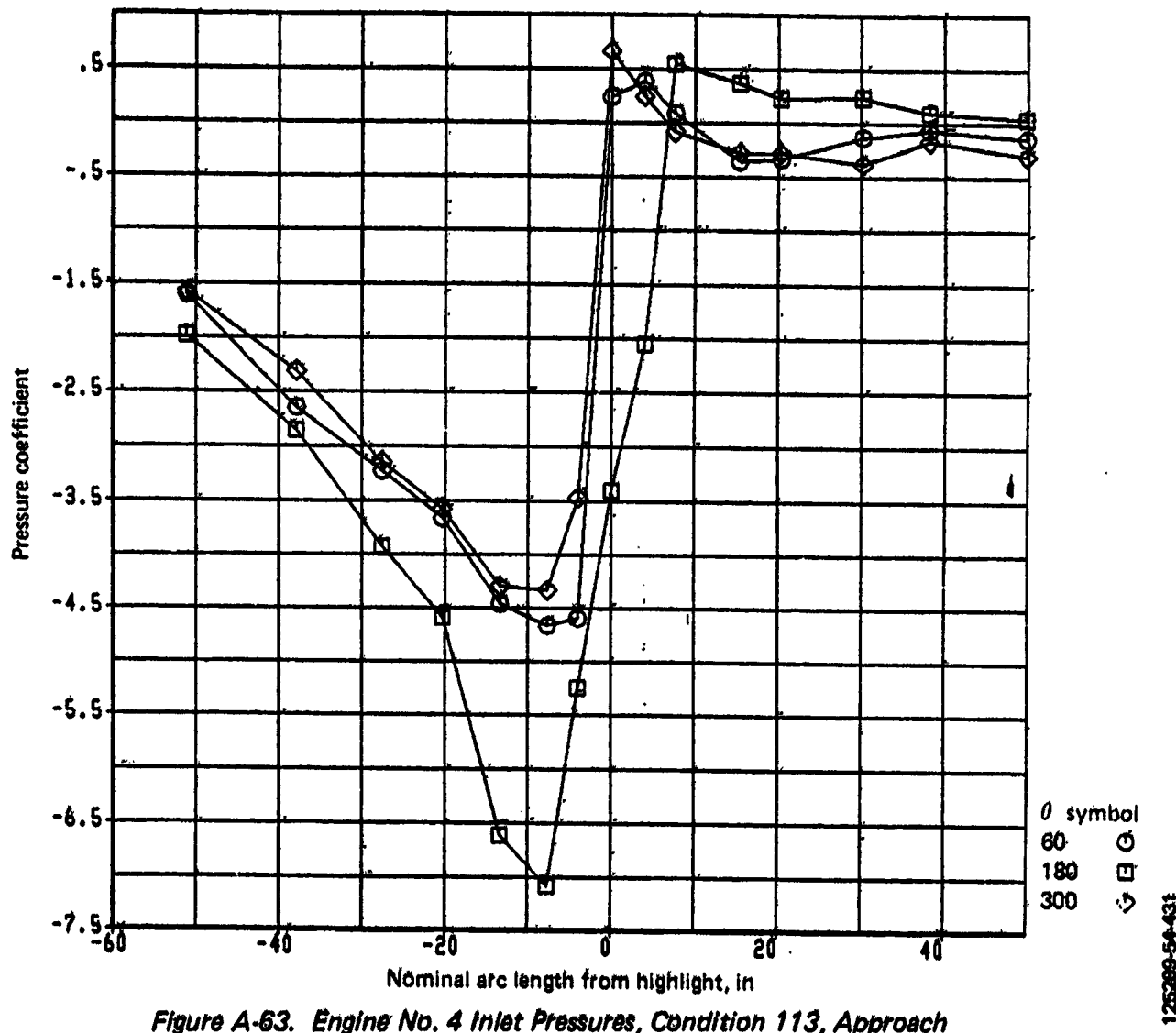


Figure A-63. Engine No. 4 Inlet Pressures, Condition 113, Approach

125289-54-431

ORIGINAL PAGE IS  
OF POOR QUALITY

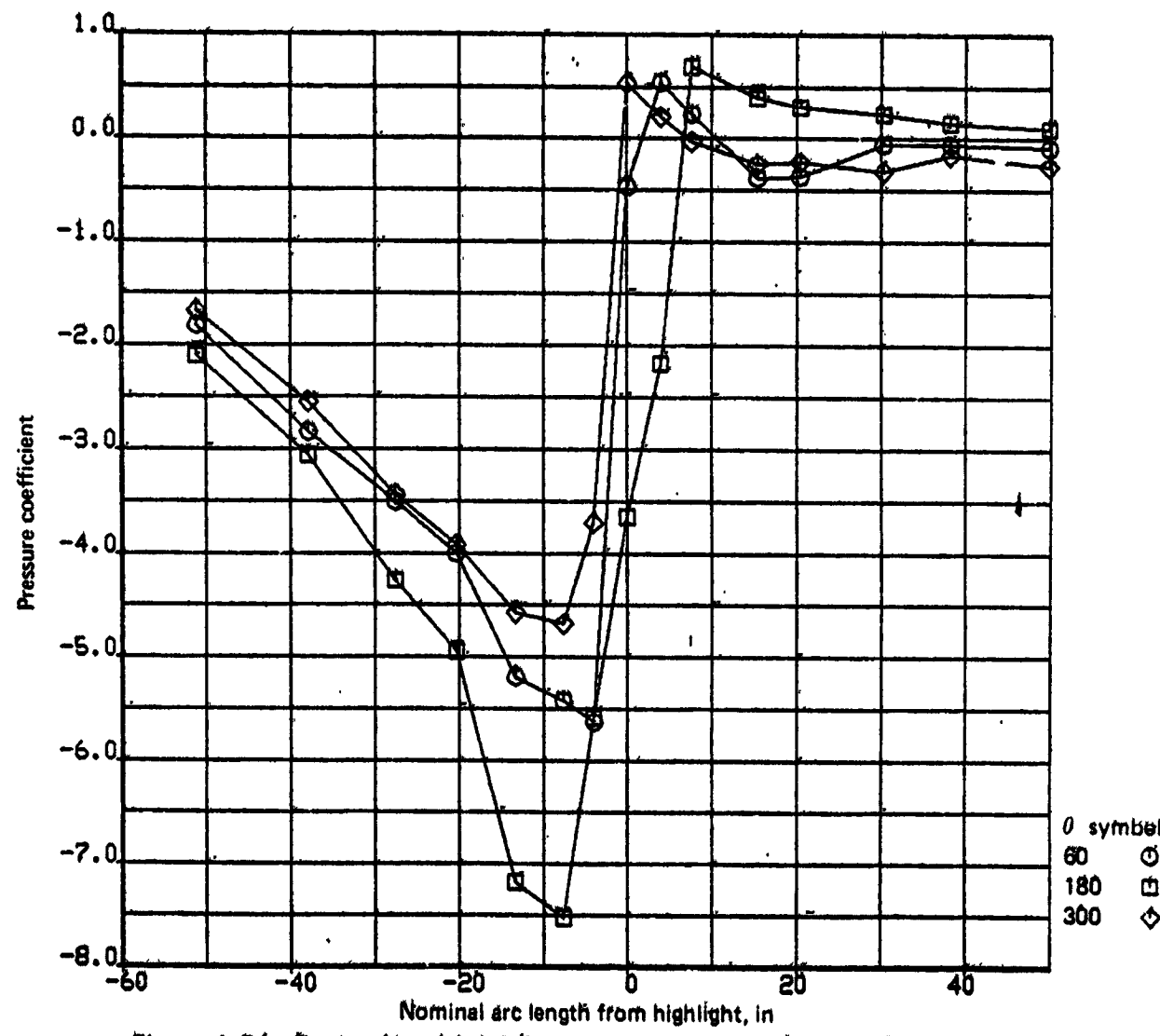


Figure A-84. Engine No. 4 Inlet Pressures, Condition 114, Touch and Go

125009-54430

2728

ORIGINAL PAGE IS  
OF POOR QUALITY

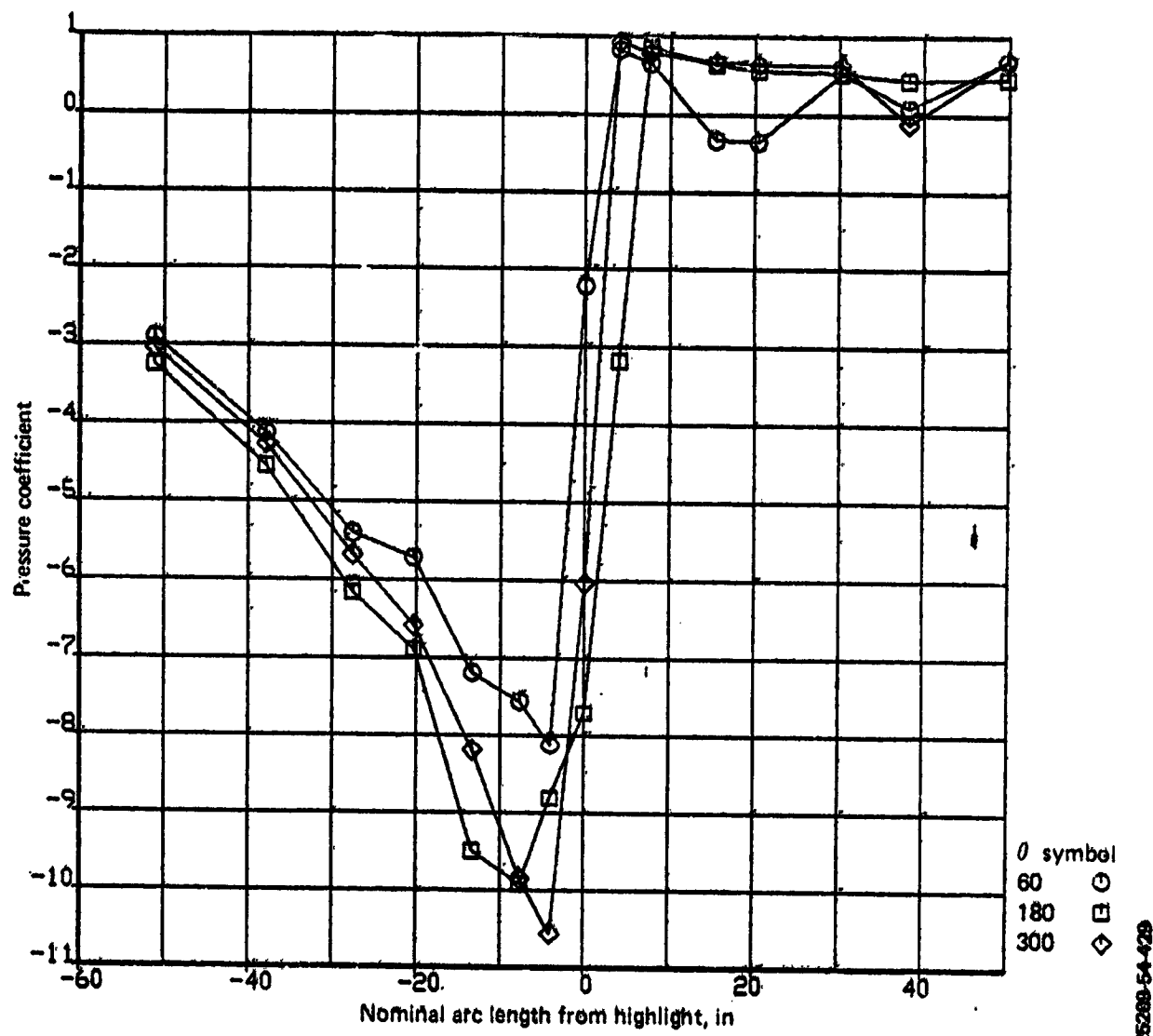


Figure A-65. Engine No. 4 Inlet Pressures, Condition 115, Thrust Reverse

126289-54-429

ORIGINAL PAGE IS  
OF POOR QUALITY

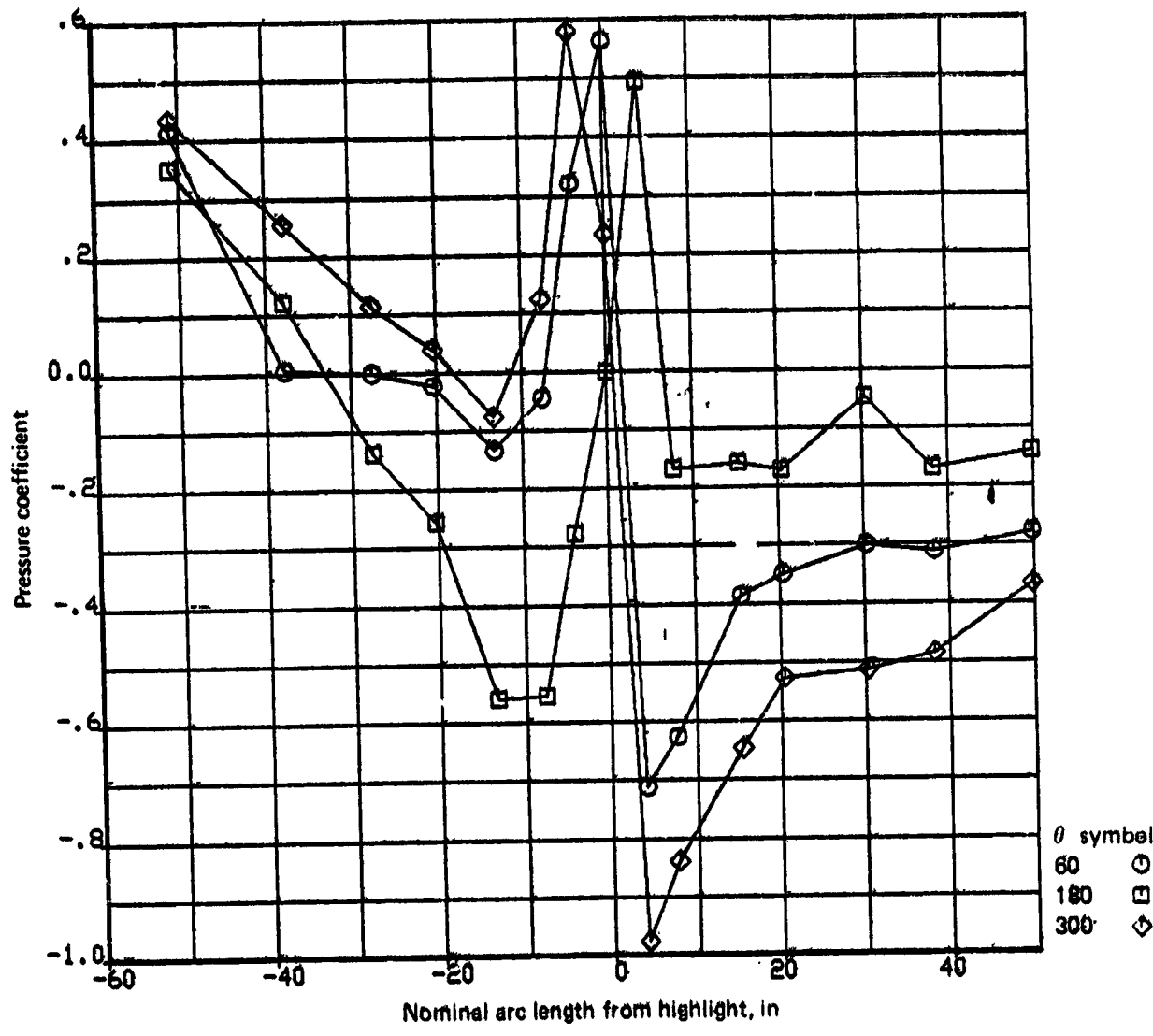
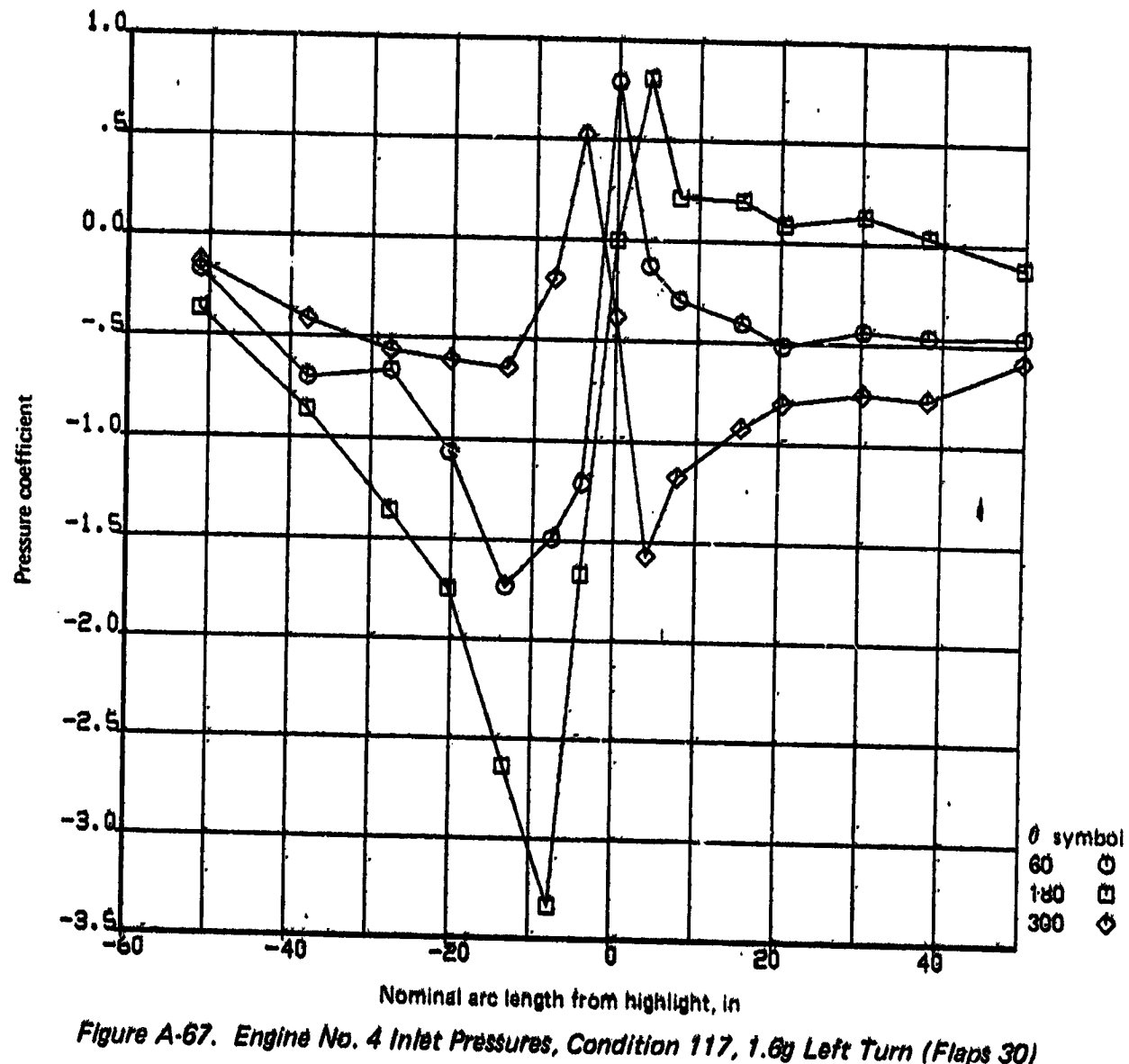


Figure A-86. Engine No. 4 Inlet Pressures, Condition 116, 2.0g Left Turn (Flaps Up)

126209-54-428

ORIGINAL PAGE IS  
OF POOR QUALITY



DATA FOR GOOD  
OR POOR QUALITY

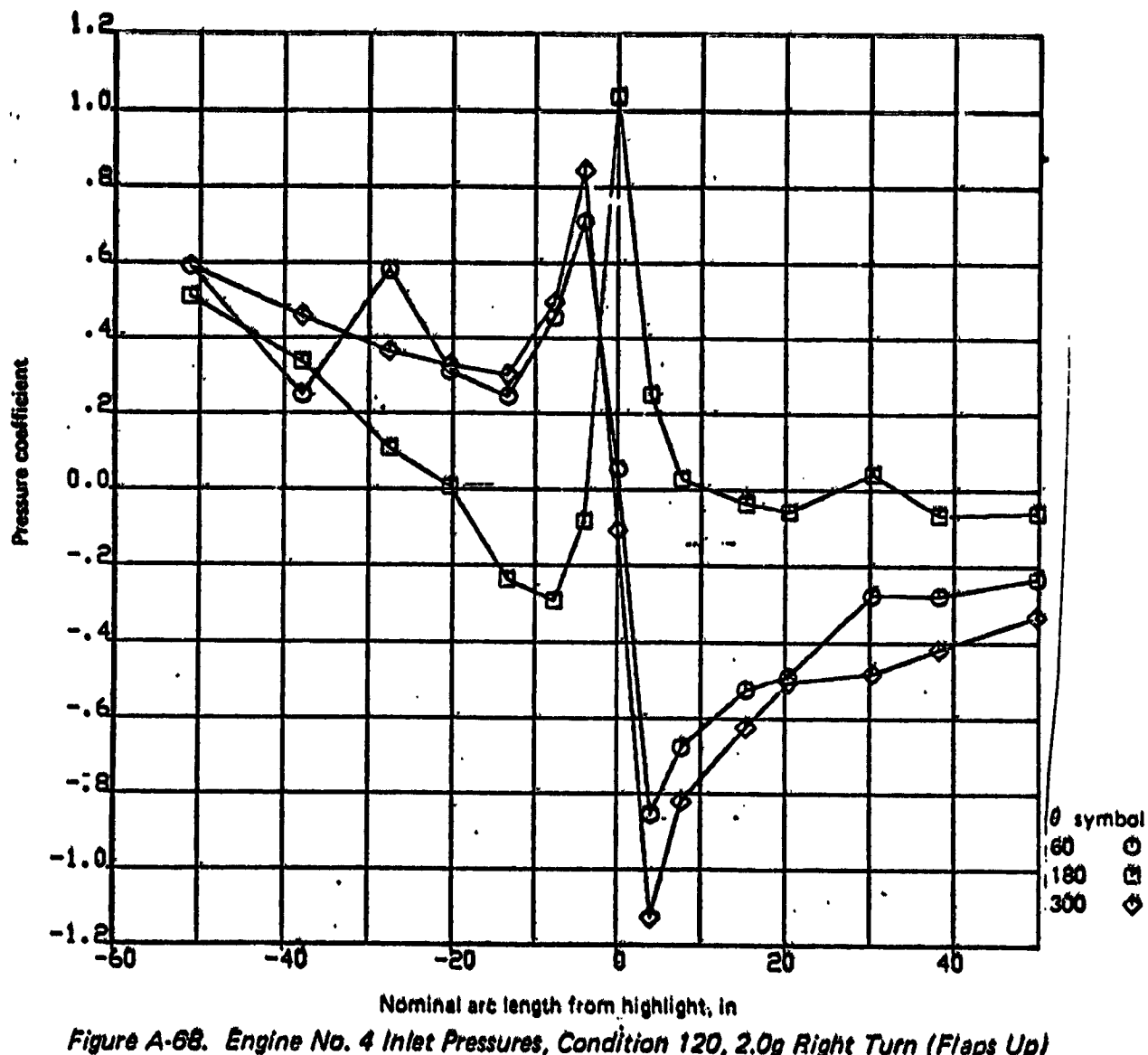


Figure A-68. Engine No. 4 Inlet Pressures, Condition 120, 2.0g Right Turn (Flaps Up)

126209-5A-426

WING SPAN, POSITION  
OF POUL. STATION

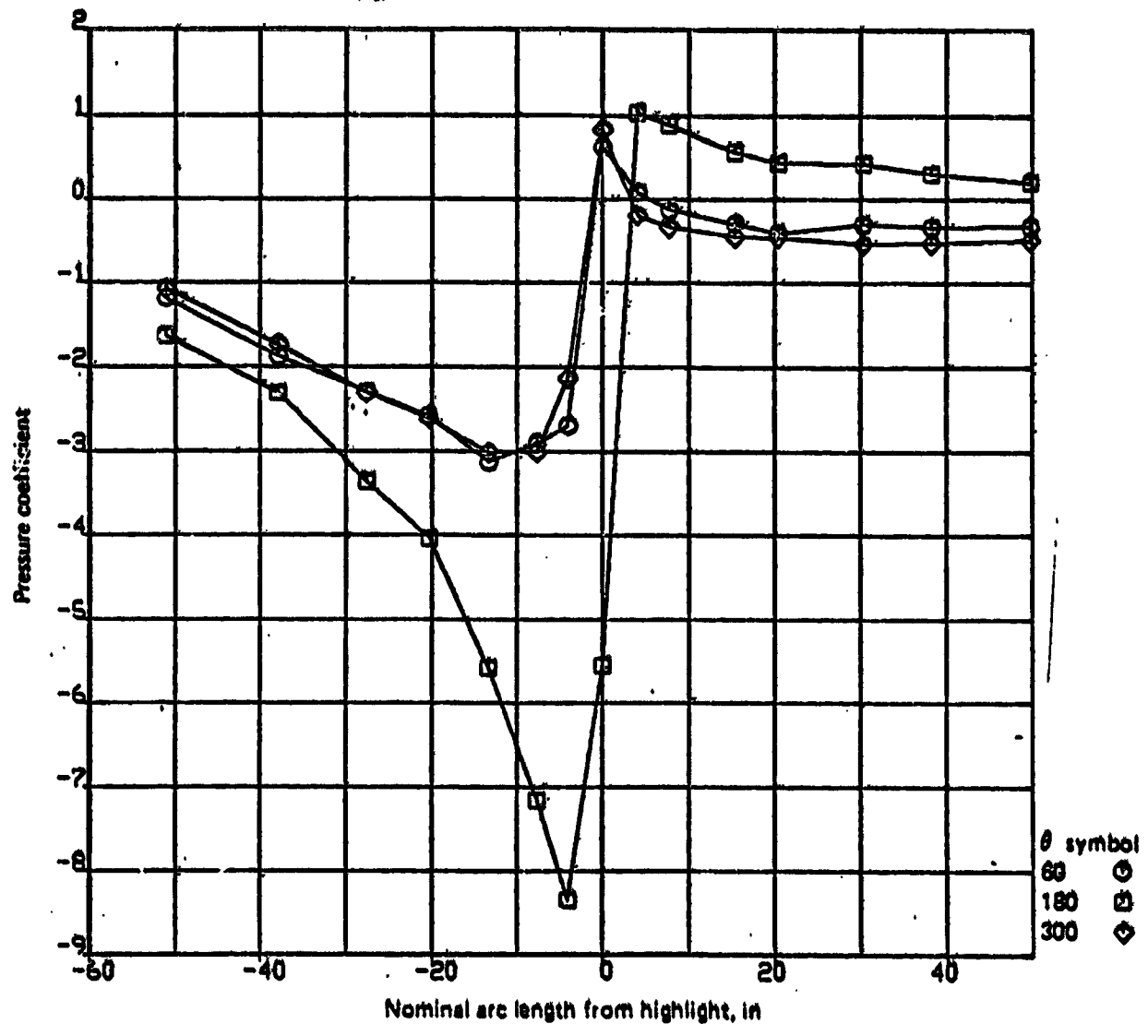


Figure A-69. Engine No. 4 Inlet Pressures, Condition 121, 1.6g Right Turn (Flaps 30)

125209-54-436

ORIGINAL PAGE IS  
OF POOR QUALITY

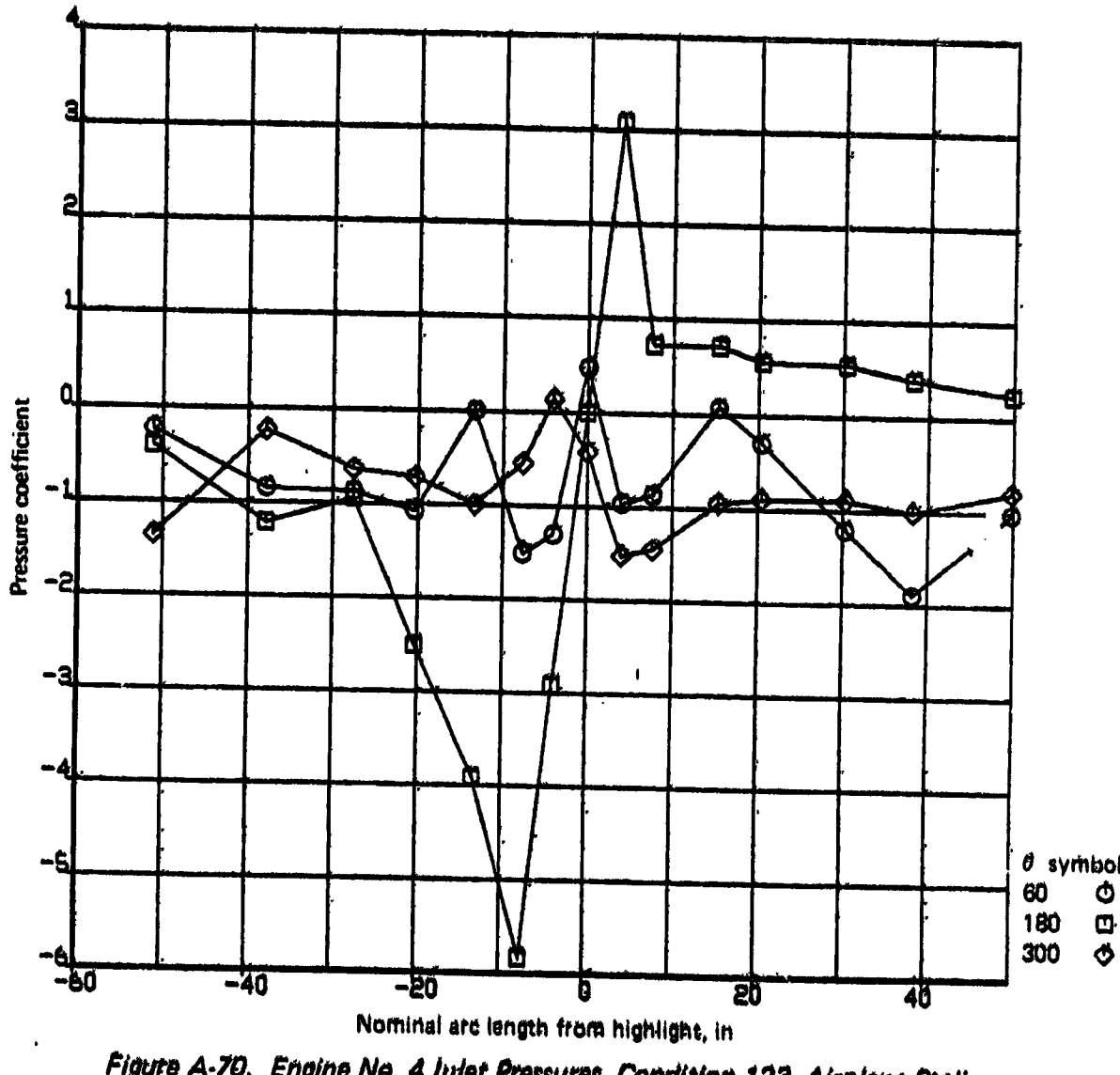


Figure A-70. Engine No. 4 Inlet Pressures, Condition 123, Airplane Stall

ORIGINAL PAGE IS  
OF POOR QUALITY

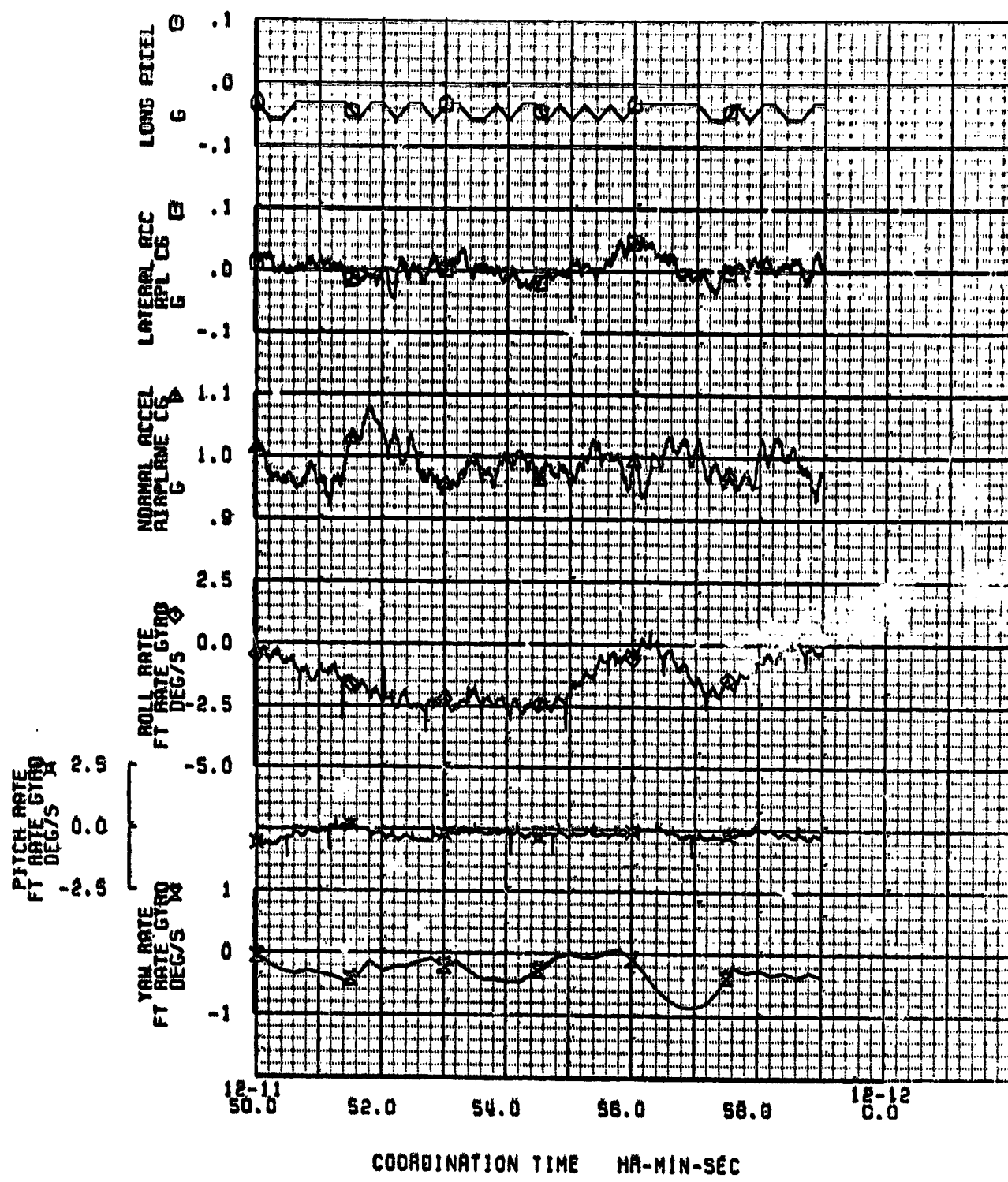


Figure A-71. Airplane Center-of-Gravity Accelerations, Mild Gust

120009-21-115

(4)

ORIGINAL PAGE IS  
OF POOR QUALITY

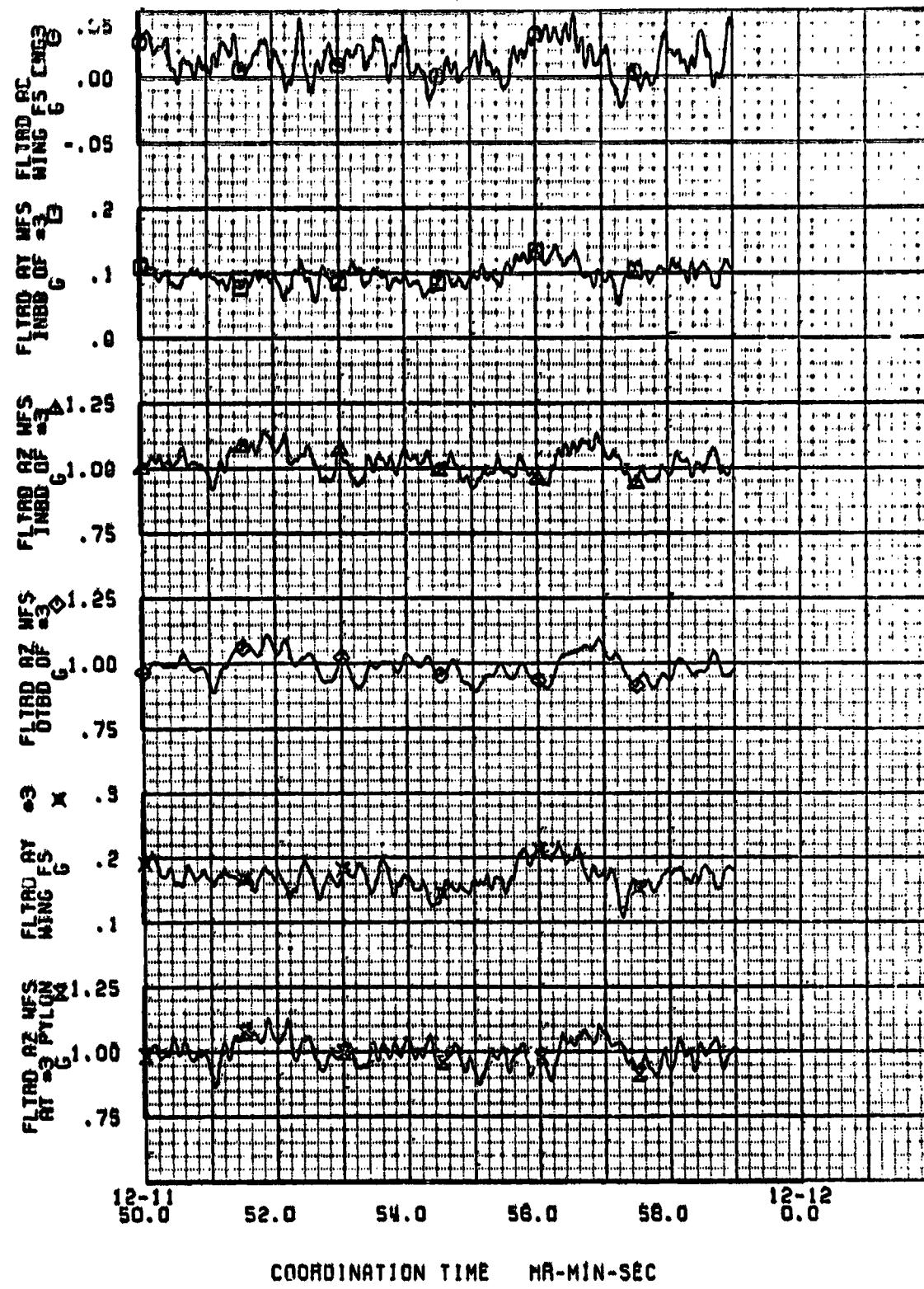
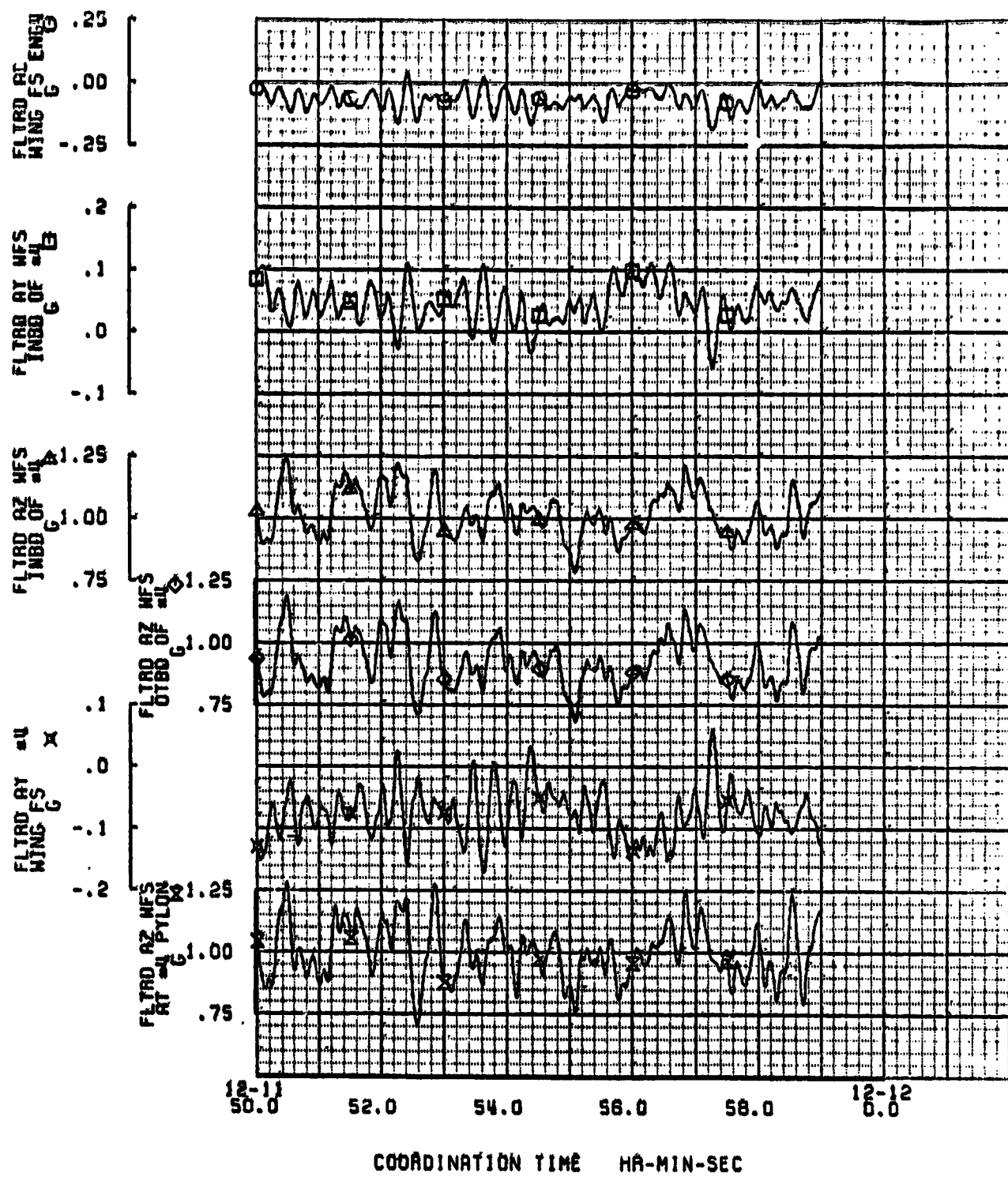


Figure A-72. Engine No. 3 Wing/Strut Accelerations, Mild Gust

ORIGINAL PAGE IS  
OF POOR QUALITY



125009-21-117

Figure A-73. Engine No. 4 Wing/Strut Accelerations, Mild Gust

ORIGINAL PAGE IS  
OF POOR QUALITY

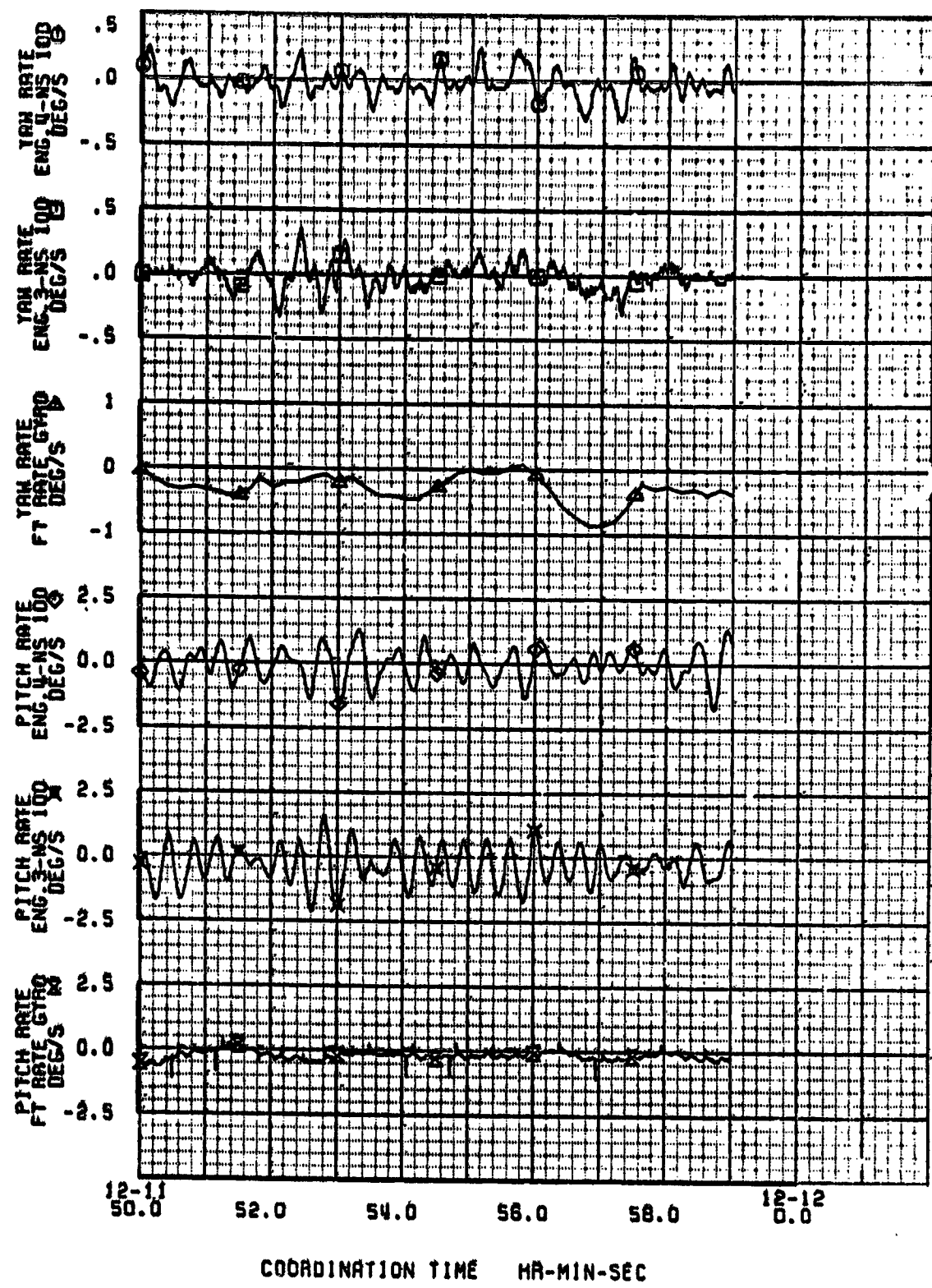


Figure A-74. Engine Angular Rates, Mild Gust

ORIGINAL PAGE IS  
OF POOR QUALITY

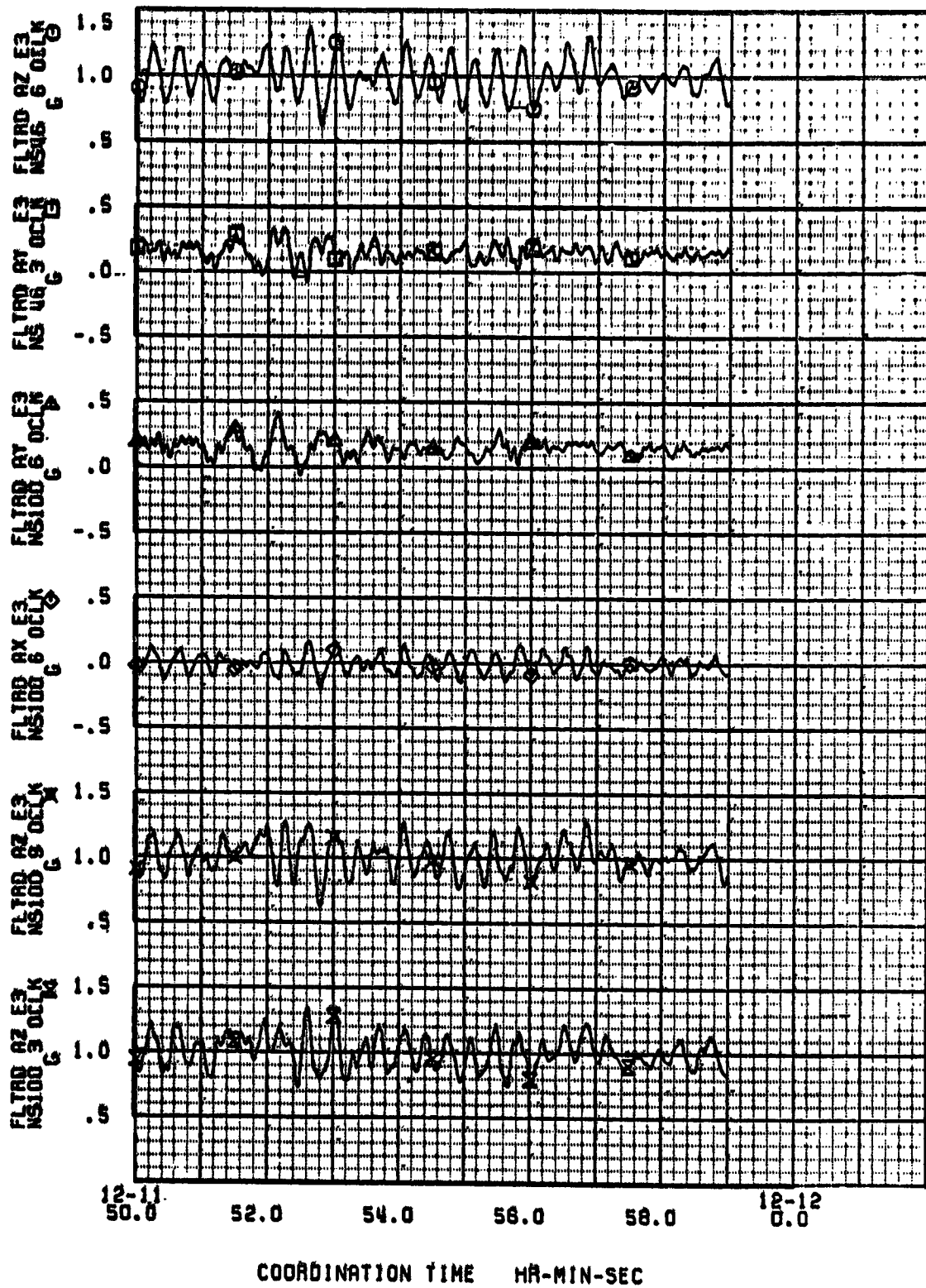
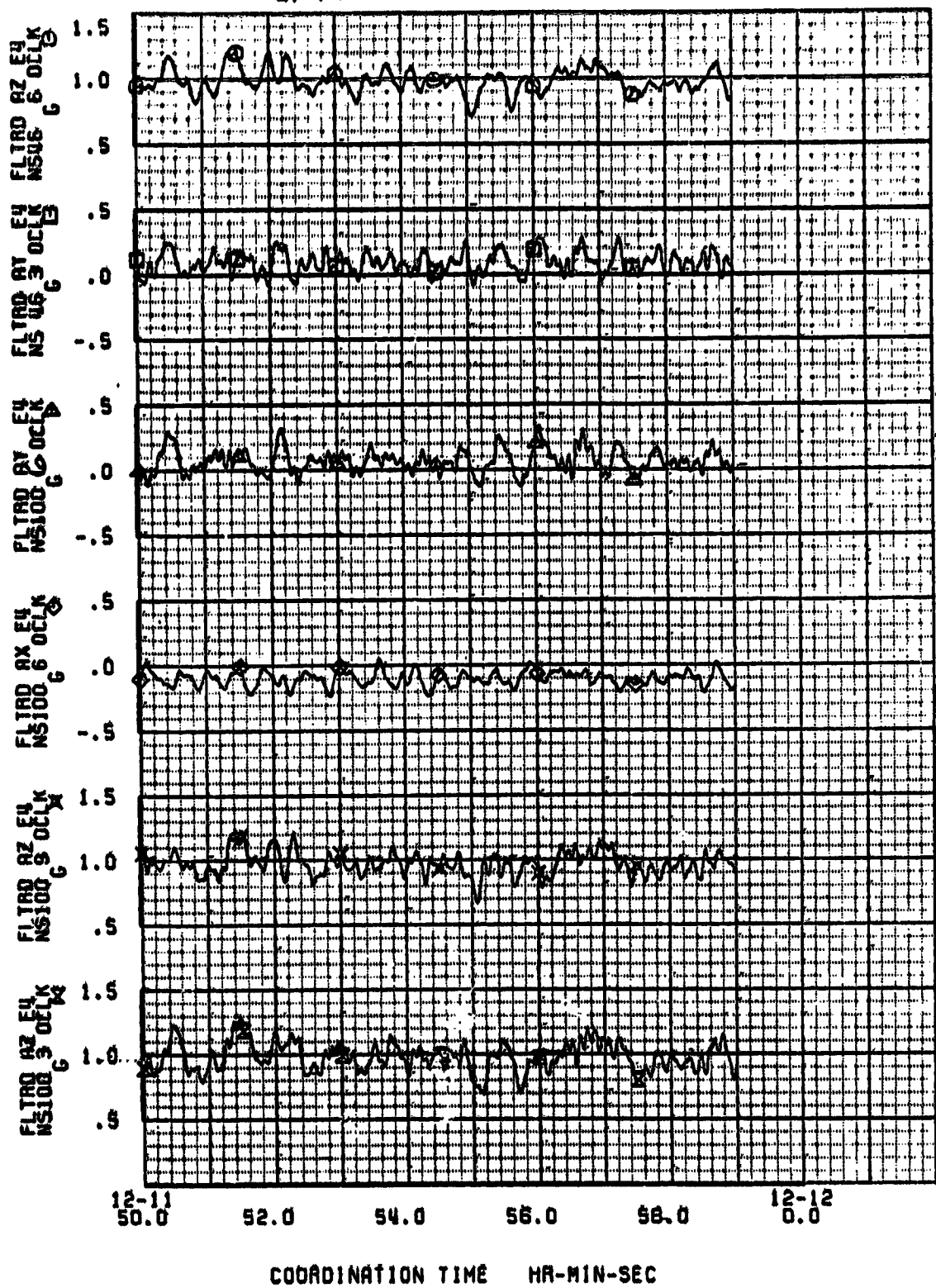


Figure A-75. Engine No. 3 Accelerations, Mild Gust

12500021-119

ORIGINAL PAGE IS  
OF POOR QUALITY



122009-21-120

Figure A-76. Engine No. 4 Accelerations, Mild Gust

ORIGINAL PAGE IS  
OF POOR QUALITY

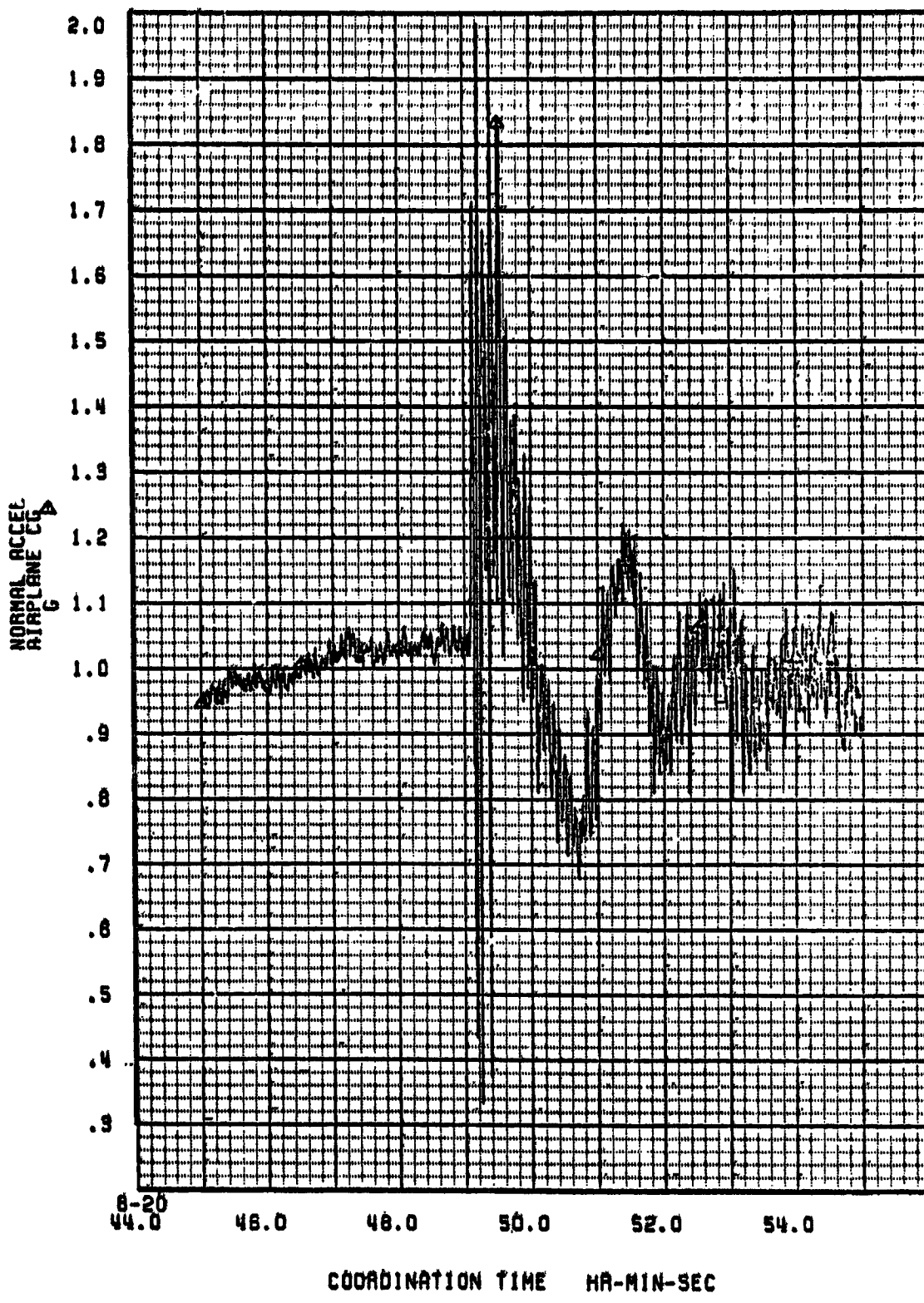


Figure A-77. Airplane Center-of-Gravity Normal Acceleration, Hard Landing

ORIGINAL PAGE IS  
OF POOR QUALITY

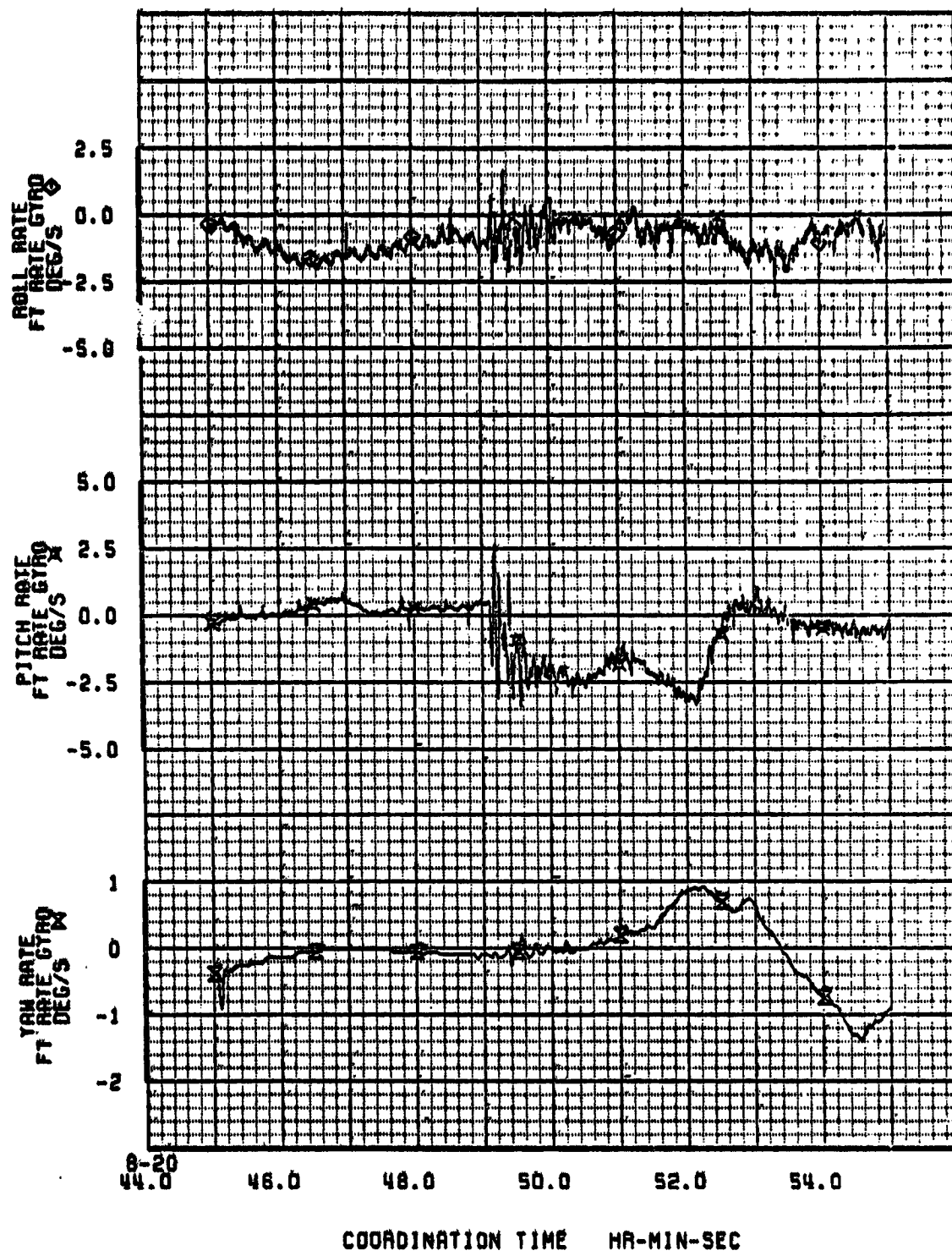


Figure A-78. Airplane Center-of-Gravity Angular Rates, Hard Landing

ORIGINAL PAGE IS  
OF POOR QUALITY

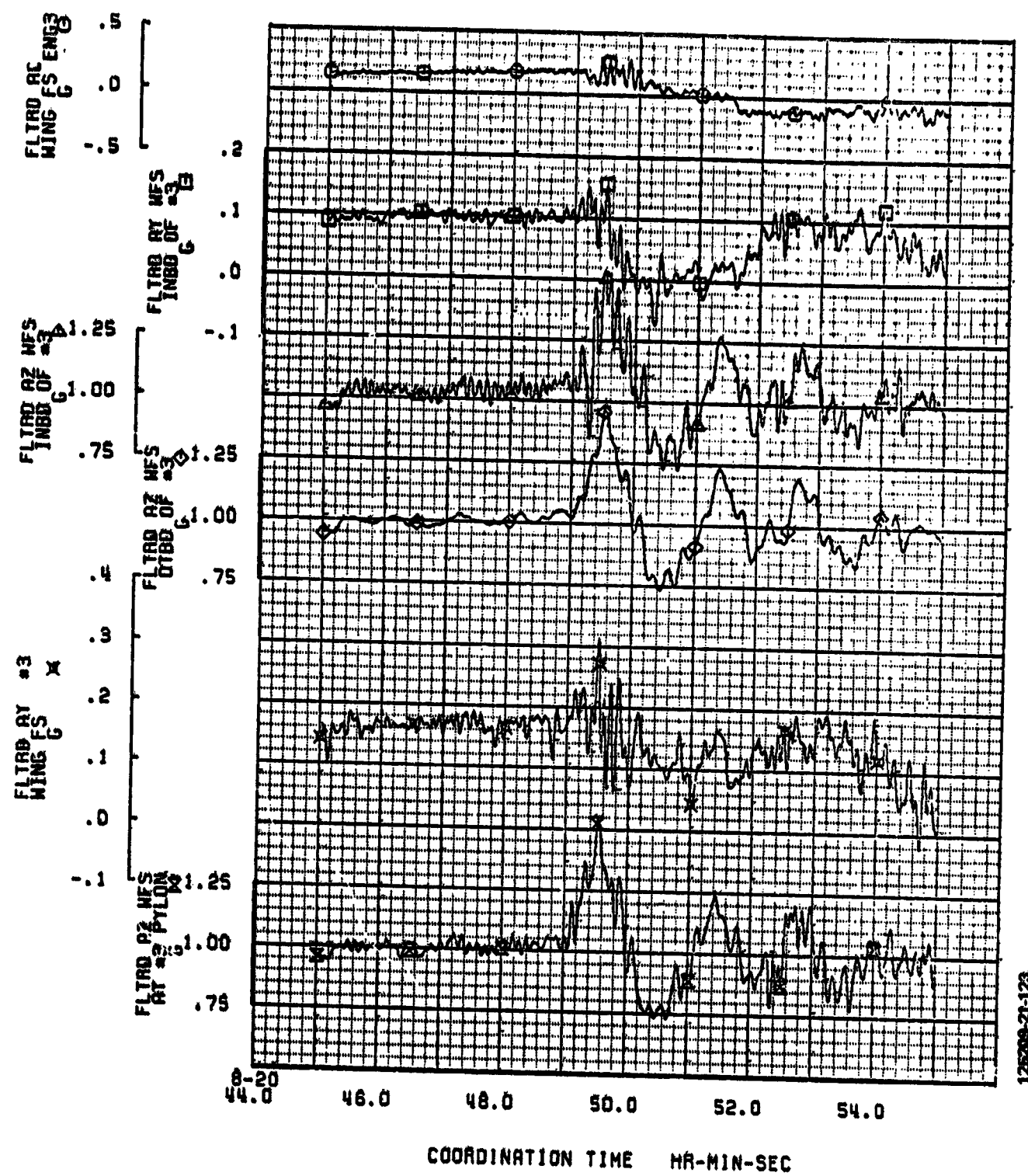


Figure A-79. Engine No. 3 Wing/Strut Accelerations, Hard Landing

ORIGINAL PAGE IS  
OF POOR QUALITY

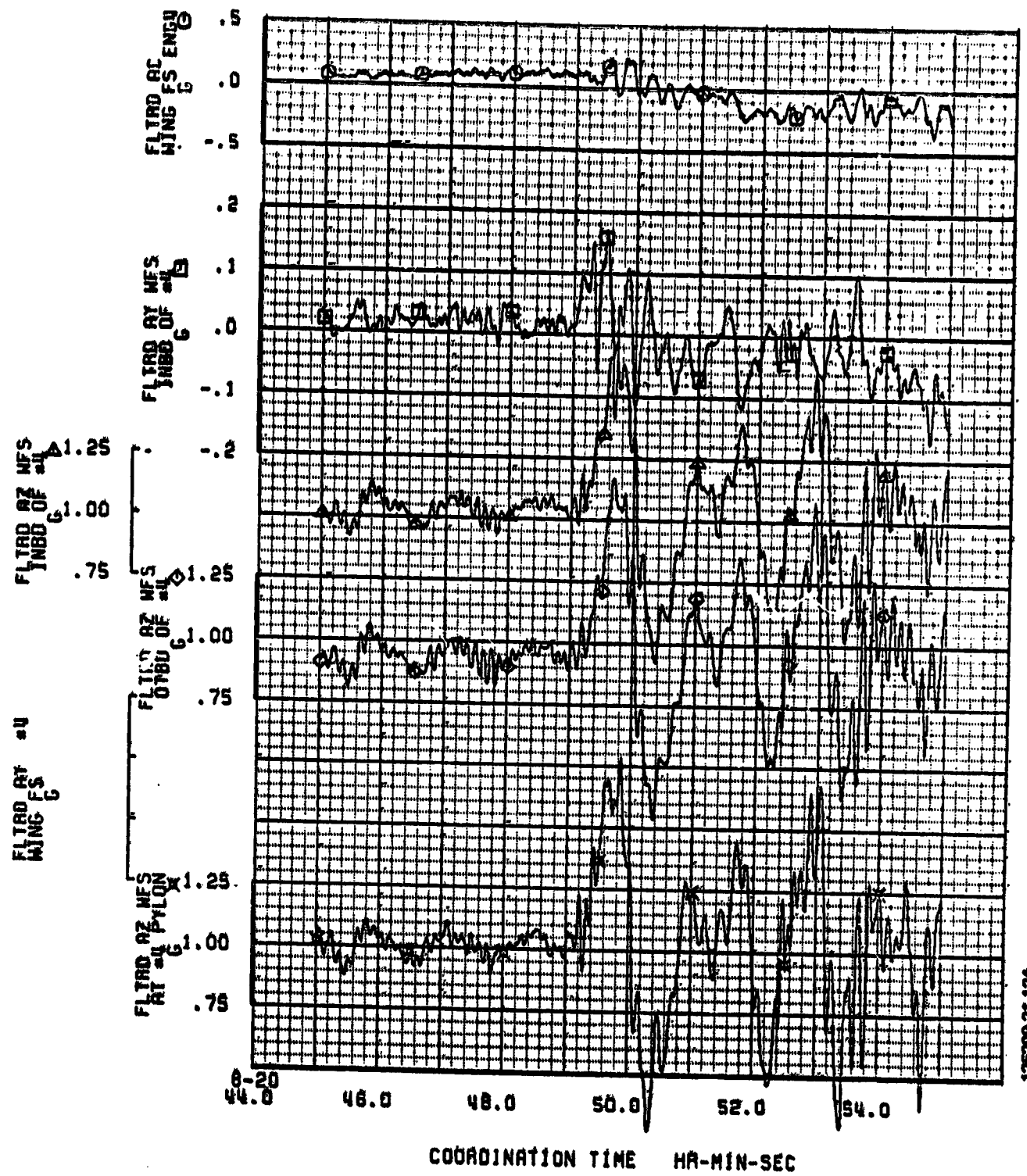
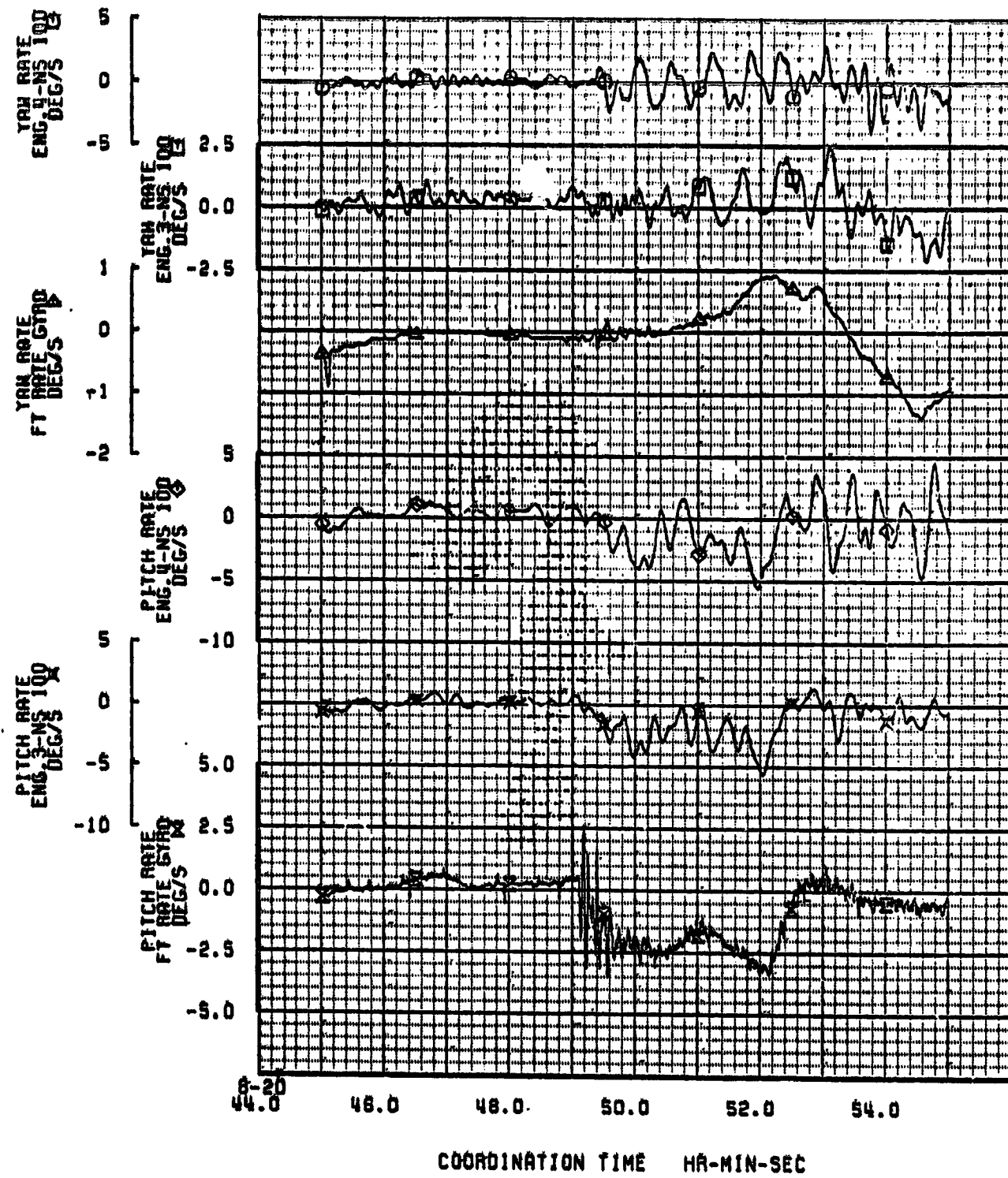


Figure A-80. Engine No. 4 Wing/Strut Accelerations, Hard Landing

ORIGINAL PAGE IS  
OF POOR QUALITY



12200-125

Figure A-81. Engine Angular Rates, Hard Landing

A-110

ORIGINAL PAGE IS  
OF POOR QUALITY

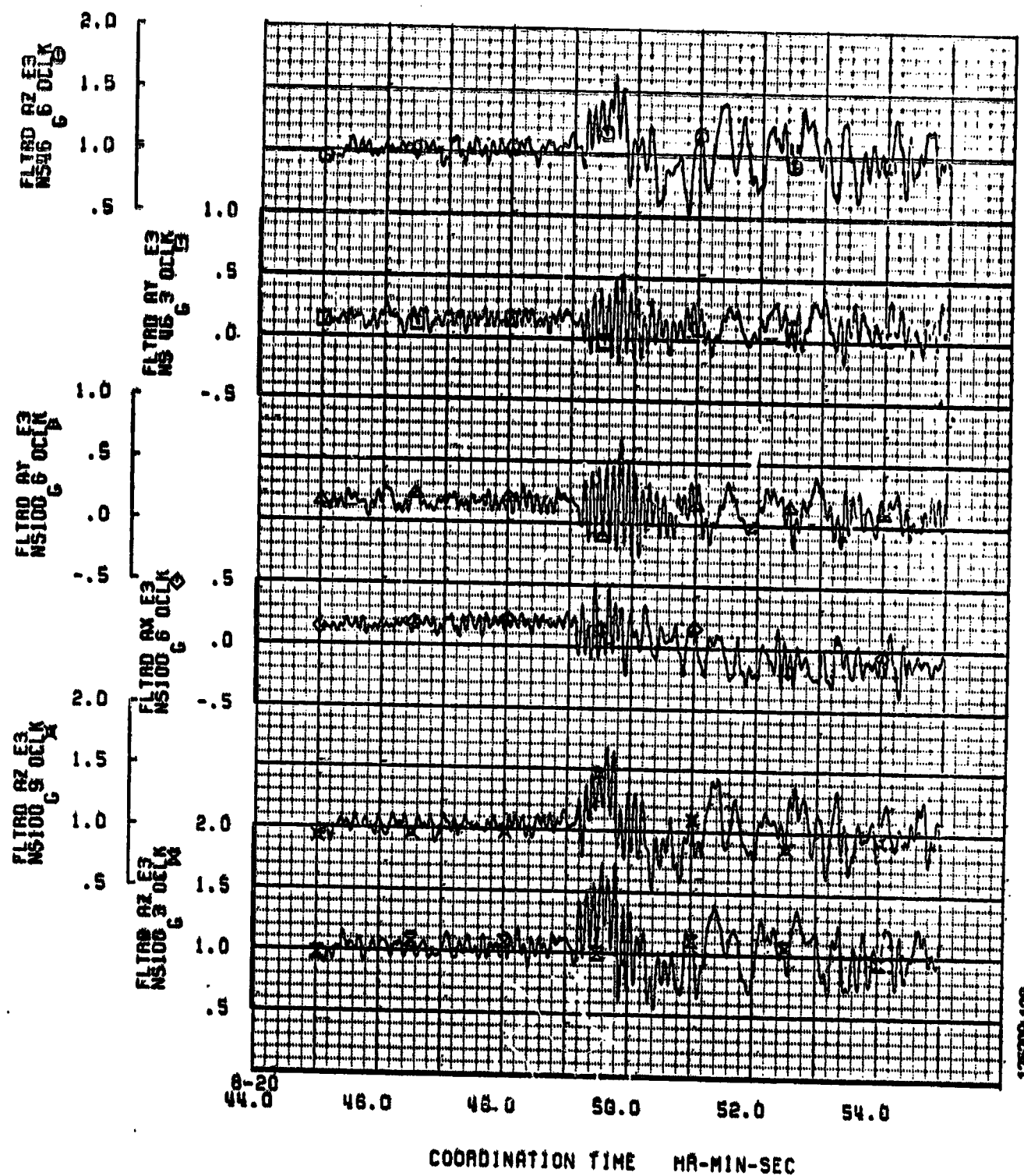


Figure A-82. Engine No. 3 Accelerations, Hard Landing

ORIGINAL PAGE IS  
OF POOR QUALITY

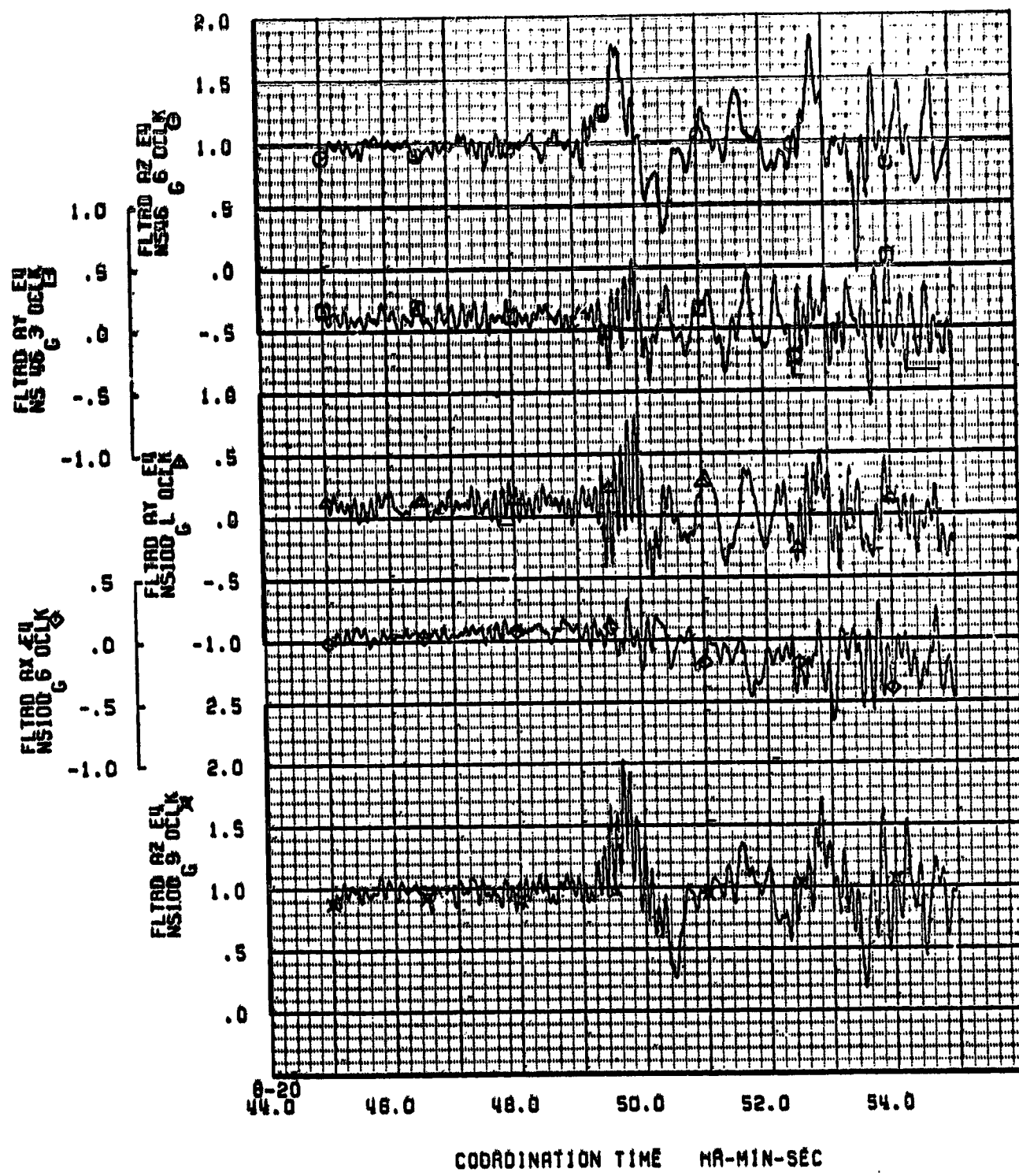


Figure A-83. Engine No. 4 Accelerations, Hard Landing

ORIGINAL PAGE IS  
OF POOR QUALITY

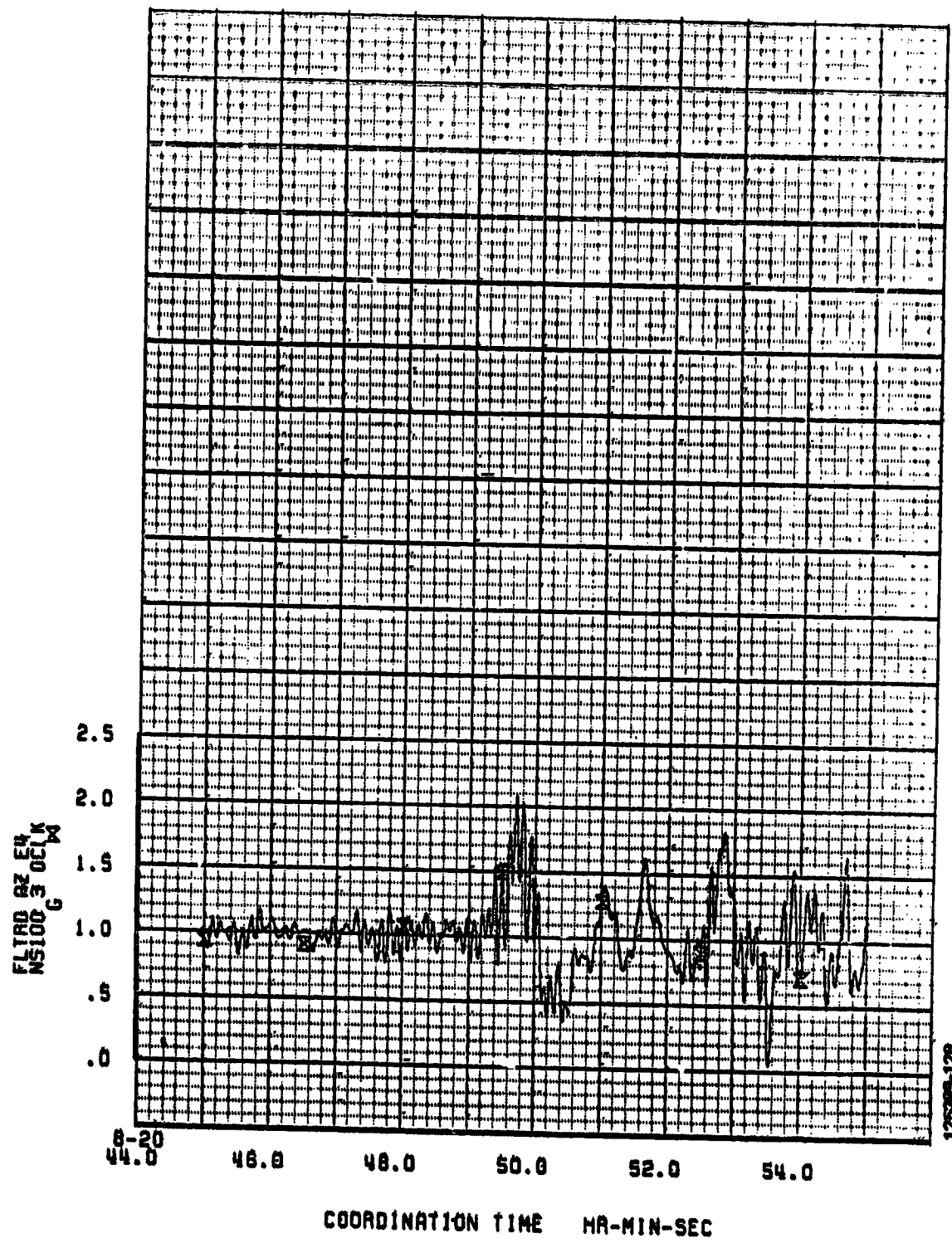


Figure A-83. Engine No. 4 Accelerations, Hard Landing (Concluded)

A-113 & A-114